Eidgenössische Technische Hochschule Zürich
Swiss Federal Institute of Technology Zurich

Identifying factors that conctribute to Phenotypic heterogeneity in melanoma progression

Daniel Simon Widmer

2012

Diss ETH No. 20537

DISS. ETH NO. 20537

IDENTIFYING FACTORS THAT CONTRIBUTE TO PHENOTYPIC HETEROGENEITY IN MELANOMA PROGRESSION

A dissertation submitted to

ETH ZURICH

for the degree of

Doctor of Sciences

presented by

Daniel Simon Widmer

Master of Science UZH
University of Zurich

born on February 26th 1982
citizen of Gränichen AG

accepted on the recommendation of

Professor Sabine Werner, examinor
Professor Reinhard Dummer, co-examinor
Professor Michael Detmar, co-examinor

2012

Contents

1. Zusammenfassung

Das Melanom, auch schwarzer Hautkrebs genannt, ist ein bösartiger Tumor, der sich aus melanozytären Zellen entwickelt. Es entsteht meistens auf der Haut, kann aber auch in anderen Geweben gefunden werden. Leider ist das Melanom die Krebsart mit der grössten Zunahme an Neuerkrankungen in der Schweiz. In einem weltweiten Vergleich liegt die Schweiz auf dem dritten Platz nach Australien und Neuseeland. Wenn ein Melanom Metastasen bildet, sinkt die Überlebenswahrscheinlichkeit dramatisch. Während der letzten Jahre wurden vielversprechende neue Therapien entwickelt, allerdings entwickeln sich in vielen Fällen Resistenzen.

Melanomläsionen sind sehr heterogen bezüglich Antigenexpression, Proliferation etc., was die Entwicklung einer Therapie erschwert. Die Unterschiede zwischen verschiedenen Melanomzellen werden deshalb in vielen Labors untersucht. Unsere Forschungsgruppe hat ein Modell beschrieben, welches die Heterogenität der Melanome zu erklären versucht. Kurz zusammengefasst geht es davon aus, dass Melanomzellen zwischen zwei Phänotypen hin- und her wechseln können, indem sie ihre Gen-Expressionsmuster ändern. Diese zwei Phänotypen weisen entweder proliferative oder invasive Eigenschaften auf. Ein möglicher Auslöser für den Wechsel von proliferativen zu invasiven Melanomzellen ist ein Mangel an Sauerstoff im Gewebe, Hypoxie genannt. Das Hauptziel dieser Arbeit war es, die Rolle der Hypoxie beim Fortschreiten des Melanoms zu untersuchen. Wir haben die Auswirkungen von Hypoxie auf die Genexpression und auf funktionelle Eigenschaften in Melanom Zellkulturen untersucht. Wir zeigen, dass Hypoxie einen invasiveren Phänotyp von Melanomzellen induzieren kann. Die Bestimmung des Zell-Phänotyps mittels der üblichen Methoden ist zeit- und kostenintensiv. Ein Ziel dieser Arbeit war daher die Entwicklung einer Methode, mit welcher der Phänotyp von Zellkulturen basierend auf Genexpressionsdaten bestimmt wird. Wir haben *in vitro* Eigenschaften von primären Melanom Zellkulturen bestimmt und diese mit Phänotypen verglichen, die mit Hilfe von Computerprogrammen vorhergesagt wurden. Das resultierende Hilfsprogramm (HOPP) ist frei im Internet

verfügbar und bietet der Melanom Forschungsgemeinde viele nützliche Anwendungsmöglichkeiten.

Resultate früherer Arbeiten aus unserem Labor haben darauf hingedeutet, dass die Wnt-Signalkaskade eine wichtige Rolle beim Wechsel der Phänotypen spielen könnte. Deshalb haben wir die Bedeutung von LEF/TCF Transkriptionsfaktoren genauer untersucht. Die hier vorgestellte Arbeit zeigt, dass der kanonische Wnt Signalweg via LEF1 die Expression von melanozytären Genen in den proliferativen Melanom Zellkulturen antreibt, während die Unterdrückung dieses Faktors in den invasiven Melanom Zellkulturen über den nicht kanonischen Wnt Signalweg die melanozytären Gene supprimiert und einen invasiven Phänotyp fördert. Die Hemmung von melanozytären Genen ist ein Zeichen von Dedifferenzierung, welche ein wichtiger Schritt in der Steigerung der Malignität darstellt. Der wichtigste melanozytäre Transkriptionsfaktor ist der „microphthalmia associated transcription factor“ (MITF). Die regulierenden Eigenschaften dieses Transkriptionsfaktors sind essentiell für die Biologie von Melanozyten und Melanomzellen. Da unser Labor einen Schwerpunkt in der Beschreibung von transkriptionellen Vorgängen hat und über grosse Erfahrung mit „high-throughput“ Methoden verfügt, war es ein Ziel dieser Arbeit, im Rahmen einer Kollaboration mit der Universität Island neue Zielgene von MITF zu entdecken, um eine bessere Einsicht in die biologischen Vorgänge im Melanom zu erhalten.

Die Behandlungsmöglichkeiten für metastasierendes Melanom sind immer noch sehr begrenzt trotz Fortschritte in der Immuntherapie und der Therapie mit Kinasen. Die Gründe für die tiefe Erfolgsrate sind weitgehend unbekannt. Deshalb wurden zwei Tyrosin-Kinase-Inhibitoren an Melanom Zellkulturen getestet. Diese Medikamente werden für die Behandlung von Melanomen verwendet, weil sie den MAPK Signalweg unterbrechen. Diese Arbeit hat gezeigt, dass eine Behandlung mit diesen Molekülen vor allem auf proliferative Melanomzellen wirkt, während invasive Zellen weitgehend resistent sind. Behandelte proliferative Zellen zeigen Anzeichen von einem Wechsel zum invasiven Phänotyp, was die häufige Resistenzbildung bei diesen Krebstherapien erklären könnte.

Leider können gewisse Fragen nicht mit Forschung an Zellkulturen beantwortet werden. Deshalb sind in der Krebsforschung weiterhin Tierversuche nötig. In der

Melanomforschung fehlte es bisher an einem *in vivo* Modell, welches die Untersuchung dieser Krankheit in einem vollständig humanisierten System ermöglicht hat. Durch Einbringung von Melanomzellen in ein System, welches ursprünglich für die Herstellung eines dermo-epidermalen Hautersatz-Präparates entwickelt wurde, haben wir ein neues *in vivo* Modell für das Melanom entwickelt.

Zusammengefasst führten die Resultate, welche in dieser Doktorarbeit präsentiert werden, zu neuen Erkenntnissen über den Vorgang des „phenotype-switching". Zudem wurden zahlreiche Werkzeuge für die weitere Erforschung des Melanoms bereitgestellt. Damit sind wir einen Schritt weiter auf dem langen Weg zu einer Therapie, welche die verschiedenen Aktivierungsmuster von Melanomzellen blockiert und die Krankheit des metastasierenden Melanoms langfristig behandelbar macht.

2. Summary

Melanoma is a malignant tumor originating from melanocytic cells that mostly develops in skin, but can also arise in other epithelia. Unfortunately, during the last decades, melanoma was the cancer with the largest increase in incidence in Switzerland. In a worldwide comparison only Australia and New Zealand have a higher incidence. When the disease becomes metastatic, the prognosis worsens rapidly. In the past few years, promising new treatments have been developed; unfortunately in almost all cases the tumor eventually becomes resistant.

The highly heterogeneous nature of melanoma makes it especially difficult to treat with the currently available anti-cancer therapies. The study of melanoma heterogeneity is currently the subject of investigation in many laboratories around the world. Recently, our group published a model for melanoma progression in which melanoma cells respond to changes in microenvironmental conditions by changing their transcriptional programs to switch back and forth between phenotypes of proliferation and invasion, thereby driving metastatic progression. A candidate microenvironmental condition proposed to be involved in phenotype switching is hypoxia. The principal aim of this PhD thesis was to investigate the role of hypoxia in melanoma progression by assessing the effects of normoxia and hypoxia on gene expression and functional characteristics in the different melanoma cell phenotypes. We found that hypoxia actually shifts the phenotype of melanoma cells to a more invasive state *in vitro*. These data suggest that tumor hypoxia serves as a possible trigger for the switch from a differentiated pigment-producing melanoma cell to a dedifferentiated, stem-like melanoma cell. With standard techniques, the characterisation of melanoma phenotypes is costly and time consuming. A goal of this thesis was to develop a method to predict the phenotype of a melanoma cell culture based on gene expression signatures obtained from DNA microarray analyses. We examined *in vitro* characteristics of melanoma cell cultures and commonly used melanoma cell lines and correlated these results to the features predicted by computer-based analyses of phenotype-specific microarray signatures. The resulting tool is available online and provides a number of useful features to the melanoma research community.

Earlier work in our group suggested an important role for Wnt-signalling in phenotype switching. Therefore, the role of LEF/TCF factors was investigated in more detail. This project showed that canonical Wnt signalling, via LEF1, drives the expression of melanocytic genes in proliferative phenotype melanoma cells, whereas the suppression of this factor via non-canonical Wnt signalling in the invasive phenotype cells shuts down the melanocytic genes to establish an invasive phenotype. The downregulation of melanocytic genes suggests a dedifferentiation of the melanoma cells and represents an important event in the process of disease progression. The most important of these melanocytic genes is the "microphthalmia associated transcription factor" (MITF). The regulatory functions of MITF are critical to both melanocyte and melanoma biology. Given our focus on transcription profiling and our expertise in high-throughput data analysis, one aim of this thesis was to participate in a collaborative program with the University of Iceland to uncover novel targets of MITF to gain further insight in the process of melanoma progression. Melanoma treatment is still quite ineffective, and the reason for this low efficacy is largely unknown, although thought to be due to extensive intratumor heterogeneity. Therefore, we tested the effects of two tyrosine kinase inhibitors on melanoma cell cultures. These reagents are used for melanoma treatment because of their inhibitory effect on the MAPK pathway. The study revealed that the treatment has an influence on proliferative phenotype melanoma cell cultures, but not on invasive phenotype cells. Treated proliferative cell cultures showed signs of a switch to the invasive phenotype, providing a possible explanation for the resistance observed in patients. Unfortunately, some questions cannot be answered by the use of *in vitro* models, and therefore, animal models are invaluable in cancer research for addressing those types of questions. In melanoma research, an *in vivo* model recapitulating initiation and progression of the disease in a humanized system has not yet been developed. Thus, we developed a new *in vivo* model for melanoma, by combining melanoma cells with a model originally developed to construct dermo-epidermal skin substitutes to close skin defects. This model is fully orthotopic and completely humanized. It allows studying initial incorporation of melanoma cells into their physiological environment as well as critical steps of human disease progression.

In summary, the results presented in this thesis provide further evidence for a role of the phenotype switching model in melanoma progression and offers multiple

opportunities for further studies. Specifically, discovering the microenvironmental cues and molecular mechanisms of phenotype determination and maintenance should provide a strong foundation for the development of a treatment strategy that affects all melanoma subtypes and for finally being able to cure metastatic melanoma or at least to delay its progression.

3. Introduction

3.1 Melanoma

3.1.1 Epidemiology

In Switzerland, 8600 men and 6900 women die of cancer every year, which is a third of all deaths among men and about a quarter of the deaths among women. In the male population at the age between 45 and 84 and in the female population between 45 and 64, cancer is the most frequent cause of death (Krebsstatistik Schweiz; Bundesamt für Statistik 2011). Breast cancer has the highest incidence in women, followed by colon cancer, lung cancer, and then melanoma. Also in men, melanoma is the fourth most common cancer, only surpassed by prostate, lung and colon cancer. Melanoma is responsible for 90% of the cutaneous tumor-associated deaths, even though it accounts for less than 5% of all skin cancer cases (cancer facts and figures 2011). Unfortunately, during the last decades, melanoma is the cancer with the largest increase in incidence in Switzerland. Surprisingly, among 40 European countries, Switzerland has the highest incidence for melanoma. In a worldwide comparison only Australia and New Zealand have higher rates (Krebsstatistik Schweiz; Bundesamt für Statistik 2011).

3.1.2 Definition

Melanoma is a malignant tumor that arises from melanocytic cells and primarily involves skin, but it can also arise in other epithelia, such as the eye, meninges and on mucosal surfaces. Although melanoma develops from pigment cells, it can also be amelanotic, which makes it particularly hard to detect at an early stage. A melanoma can be distinguished from nevi by applying the “ABCD rule”, which means that lesions are examined for Asymmetry, Border irregularities, Color heterogeneity and Dynamics (i.e. change of color or size over time). Diagnosis is based on a full-thickness biopsy of the suspicious lesion (Dummer et al., 2011a).

3.1.3 Risk factors

Little is known about the exact cause of melanoma. There is evidence that exposure to ultraviolet radiation is the main environmental risk factor. Especially during childhood, a history of sunburns increases the risk of developing melanoma by two fold (Elwood and Jopson, 1997). It was reported that multiple severe sunburns can increase the risk of developing melanoma by up to 6.8-fold (Cho et al., 2005b). In agreement with these findings there are certain phenotypic characteristics, such as grade of skin pigmentation, red hair, and freckles, which influence UV-radiation sensitivity and are associated with an increased risk of developing melanoma (Veierod et al., 2003). Surprisingly, a risk-reducing effect of sunscreen has not been demonstrated (Autier et al., 2000). However, the fact that melanoma can also develop on body sites that are not exposed to UV-radiation suggests that UV-radiation is not the only cause of melanoma. Next to factors associated with UV, the presence of a high number of melanocytic nevi is also associated with an increased risk of developing melanoma (Bauer and Garbe, 2003; Garbe et al., 1994; Grob et al., 1990; Holly et al., 1987). As in other cancers, there are genetic features that elevate the risk of getting melanoma. On that account the risk of developing a melanoma increases by two fold when a first-degree relative has a melanoma (Cho et al., 2005a).

3.1.4 Staging / Prognosis

Melanoma is staged according to the American Joint Committee on Cancer (AJCC) staging and classification system, which includes Breslow depth, Clark's level, ulceration and pathologic microstaging attributes (Balch et al., 2009). Breslow depth describes the thickness of a tumor in mm measured from the upper border of the epidermis. The thickness according to Breslow and ulceration of the primary lesion were found to be the most powerful predictors of survival. Patients with a thin primary melanoma (thickness <1mm without ulceration) have a five year survival rate of 95.3%, while patients with a thicker primary melanoma (more than 4mm) have a five year survival rate of 45.1% (Balch, Soong et al. 2001). When the melanoma has metastasized the prognosis worsens. In such cases, the

expected two year survival rate is 10 to 20% (Falkson et al., 1998; Middleton et al., 2000; Rusthoven et al., 1996).

3.1.5 Subtypes

Melanoma can be subdivided into several subtypes, which differ in incidence, visual and clinical appearance, prognosis, and other characteristics. There are four main subtypes of melanoma:

3.1.5.1 Superficial spreading melanoma (SSM)

This type of melanoma is with an occurrence of up to 70% the most common variant in Caucasians. There is a correlation with intermittent but not daily UV-exposure. The clinical appearance of SSM is irregular, with highly variable color distribution within the lesion. The border of the lesions is sharply demarcated, palpable and irregular (Dummer et al., 2011b).

3.1.5.2 Nodular malignant melanoma (NMM)

This type of melanoma grows vertically from the start. It is often symmetrically, well demarcated and can be poorly pigmented or even amelanotic which makes an early diagnosis difficult. The delayed recognition together with the rapid growth often leads to a poorer prognosis than of melanomas with a horizontal growth phase (Dummer et al., 2011b).

3.1.5.3 Lentigo maligna melanoma (LMM)

Lentigo Maligna (LM), a pigmentary, slow growing macule, usually arises on sun damaged skin of the face. After many years about half of the LM develop into LMM. It is the most common variant in elderly people. There is a correlation to cumulative UV-exposure much like in basal- and squamous-cell carcinomas (Dummer et al., 2011b).

3.1.5.4 Acrolentiginous melanoma (ALM)

Even though this is the most common variant in patients of Asian and African descent, overall the occurrence is less than 10%. Unlike with LMM or SMM there is no correlation with UV-exposure known. This subtype arises on hairless skin of

the palms of the hands and soles of the feet as well on the volar surface of the fingers and toes. Mucosal melanoma and ALM are similar in many respects which is why they are often considered to belong to the same type of melanoma. Because of the fast transition to the invasive growth phase and metastatic spreading, the prognosis of these subtypes is rather poor (Dummer et al., 2011b).

3.1.6 Familial predispositions

Some observations support a genetic cause of melanoma, for example the finding that up to 10% of the patients have a familial history of melanoma (Dummer et al., 2010). There are several genes known to be deleted in families with melanoma. The most important germ line mutations with a possible role in melanoma development are *CDKN2A*, *P14ARF* and *CDKN2B*, all coding for potential tumor suppressor genes (reviewed in (Nelson and Tsao, 2009)).

3.1.7 Somatic mutations

In melanoma, many mutations have been reported to have a tumor promoting potential, e.g. by activating oncogenes or inactivating tumor suppressor genes (Lin et al., 2008). In the past few years, the mitogen-activated protein kinase (MAPK) pathway has been the subject of many studies. It signals via RAS-RAF-MEK-ERK and is involved in numerous cellular processes, like growth, proliferation, survival, differentiation and transformation (Schreck and Rapp, 2006). Upstream of RAS are receptor tyrosine kinases (RTKs), such as c-KIT, which is commonly mutated in a subset of acrolentiginous melanomas, especially in melanomas from genital regions (Omholt et al., 2011). Rat sarcoma (*RAS*) was the first oncogene described in human cancer (Der et al., 1982). In melanoma as well as cancer in general, the human *RAS* isoforms *HRAS*, *NRAS* and *KRAS* are commonly mutated, which leads to a constitutively active protein. 20% of cutaneous melanomas have been found to harbor an activating mutation in *NRAS*. Downstream of RAS is the RAF family comprised of the ARAF, BRAF and CRAF proteins. A $BRAF^{V600E}$ mutation can be found in up to 60% of melanomas in skin without chronic sun damage (intermittently exposed to UV), leading to a

constitutive activation of this protein kinase (Davies et al., 2002). Interestingly, *NRAS* and *BRAF* mutations have been found, with few exceptions, to be mutually exclusive (Platz et al., 2008). Since the vast majority of the melanomas have a mutation in the MAPK signaling cascade, extracellular signal-regulated kinases (ERKs) are activated in 90% of human melanomas (Cohen et al., 2002), making it a very attractive target for therapy (Figure 1). Interestingly, *NRAS* and *BRAF* are also mutated in up to 81% of benign nevi (Kumar et al., 2004; Saldanha et al., 2004). In uveal melanomas *GNA11* or *GNAQ* genes are frequently mutated (Figure 1) (Onken et al., 2008; Van Raamsdonk et al., 2009; Van Raamsdonk et al., 2010).

3.1.8 Treatment options

The majority of patients (80%) are diagnosed with an early stage melanoma, which can be efficiently treated with surgery alone (Dummer et al., 2005). However, for patients with metastatic melanoma the prognosis is very poor. Until very recently, chemotherapy with dacarbazine (DTIC) was the standard treatment, which was associated with an objective response rate of, at most, 15% (Lui et al., 2007). Unfortunately, almost all these responses were only partial and there was no therapy available that improved overall survival. In March 2011 the U.S. Food and Drug Administration (FDA) approved ipilimumab (Yervoy®), a human IgG1 monoclonal antibody that augments T-cell activation and proliferation by blocking cytotoxic T lymphocyte-associated antigen 4 (CTLA-4), a negative regulator of T cells (Fong and Small, 2008; Melero et al., 2007; O'Day et al., 2007). As a monotherapy, this drug improved overall survival in a phase 2 study in patients with previously treated metastatic melanoma (Wolchok et al., 2010). It has also been tested in a phase 3 trial in combination with dacarbazine (DTIC), where it has been associated with a better overall survival than dacarbazine (DTIC) alone (Robert et al., 2011b). So far the only other treatment that increases overall survival in metastatic melanoma is vemurafenib (PLX4032, Zelboraf ®) which has been approved by the FDA in August 2011. Vemurafenib is an inhibitor of mutated $BRAF^{V600E}$ (Bollag et al., 2010) (Figure 1).

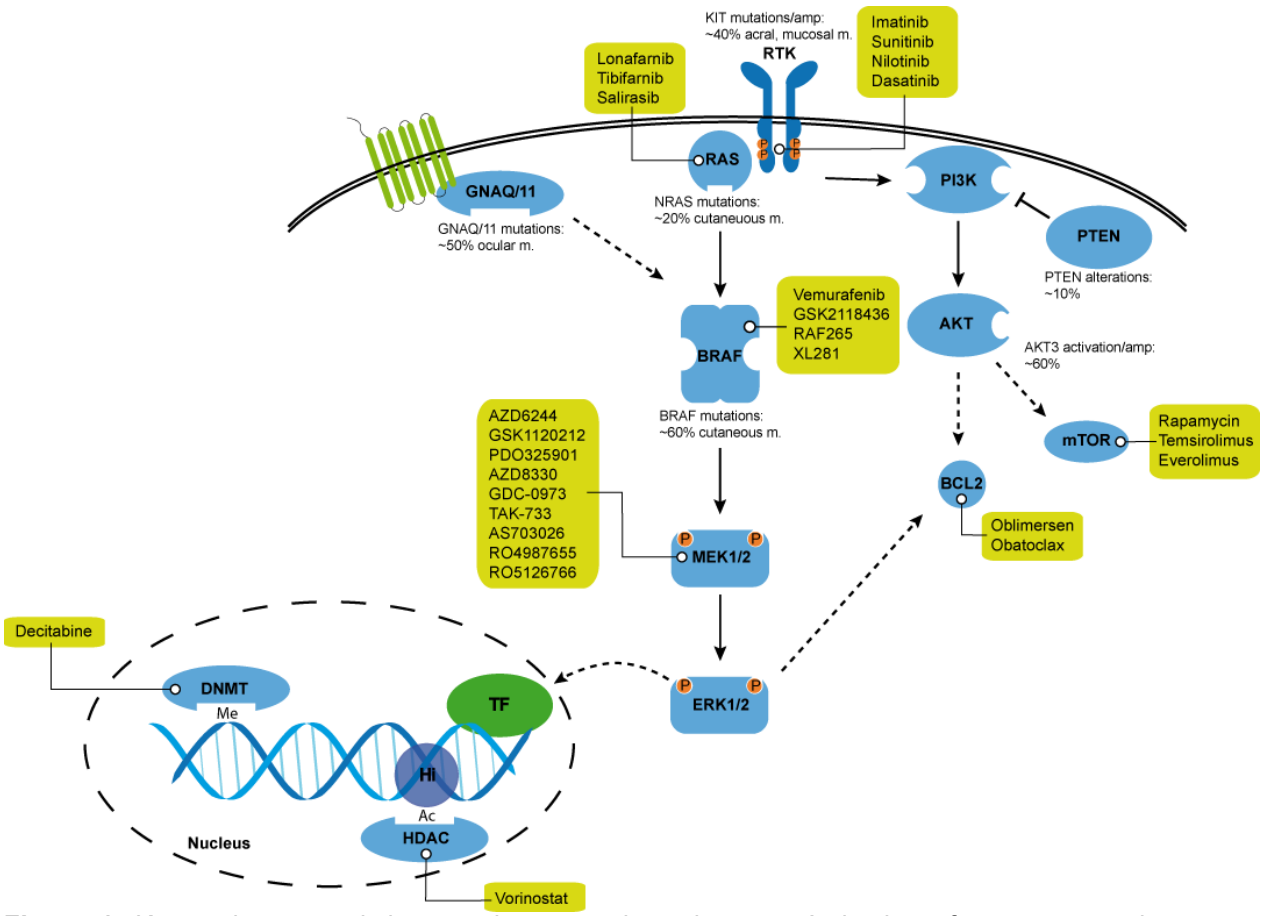

Figure 1: Key pathways and therapeutic targets in melanoma**.** Activation of receptor tyrosine kinases (RTK) and their downstream MAPK pathway is very important in most melanomas (m). Currently tested molecules (green boxes) for the treatment of melanoma affect the activity of proteins involved in MAPK- or PI3K/AKT signaling. The phosphatidylinositide 3-kinase (PI3K) pathway can be over-activated by either loss of PTEN or activation of AKT. DNA methylation (Me) and/or histone (Hi) acetylation (Ac) suppress transcription of tumor suppressor genes. DNA methyltransferase (DNMT), transcription factor (TF), histone deacetylase (HDAC). Adapted from (Nikolaou et al., 2012).

3.1.9 Resistance

The clinical responses of the patients with *BRAF*^{V600E} mutations that are treated with specific BRAF^{V600E} inhibitors are very promising, but unfortunately only relatively short lived (Bollag et al., 2010; Dummer and Flaherty, 2012; Flaherty et al., 2010). So far in almost every case tumor progression occurred through acquired resistance. In addition to the *BRAF* WT tumors, approximately 20% of the tumors with *BRAF* mutations do not show a response to the treatment at all

because of an intrinsic resistance (Flaherty et al., 2010; Søndergaard et al., 2010; Yang et al., 2010). Intrinsic resistance can be explained by tumor heterogeneity on the genetic and/or epigenetic level, leading to subgroups of melanoma cells with different responses to treatment (Paraiso et al., 2011; Shao and Aplin, 2010; Smalley et al., 2008). How acquired resistance develops is still unclear. It is suggested that a reactivation of the MAPK pathway is one major mechanism, however most likely a number of other possibilities exist (Garnett et al., 2005; Montagut et al., 2008; Nazarian et al., 2010; Paraiso et al., 2010; Paraiso et al., 2011; Poulikakos and Rosen, 2011; Solit and Sawyers, 2010; Villanueva et al., 2010).

Surprisingly, specific $BRAF^{V600E}$ inhibitors (PLX4720, PLX4032 and GDC-0879) have been found to increase MAPK pathway activation paradoxically in WT *BRAF* or *NRAS* mutant cells (Halaban et al., 2010; Hatzivassiliou et al., 2010; Heidorn et al., 2010; Joseph et al., 2010; Poulikakos et al., 2010). The exact mechanism of this activation is unclear, however it was suggested that a RAS-dependent heterodimerization of CRAF with WT BRAF and homodimerization of CRAF might lead to activation of CRAF and therefore increased MEK/ERK signaling (Garnett et al., 2005; Hatzivassiliou et al., 2010; Heidorn et al., 2010; Poulikakos et al., 2010). Interestingly, 31% of the patients treated with vemurafenib (PLX4032) developed Squamous Cell Carcinoma (SCC) after a median time of 8 weeks of treatment initiation (Flaherty and McArthur, 2010; Flaherty et al., 2010). It was speculated that the paradoxical activation of the MAPK pathway downstream of *BRAF* WT cells might be responsible for the development of these tumors (Flaherty et al., 2010; Robert et al., 2011a).

3.2 Models of melanoma progression

If melanoma is detected before metastatic spread, it is completely and easily curable by surgical removal of the lesion. This makes an early diagnosis essential, but the lethality of melanoma after it has metastasized also makes it very important to understand the propagation of melanoma from the primary benign lesion. There are multiple models that try to explain this fatal development from a proliferative melanocytic lesion to a metastatic disease.

3.2.1 Cancer Stem Cell model

The Cancer Stem Cell (CSC) model (Figure 2) proposes the presence of a small subset of cancer cells with higher tumorigenic potential than the vast majority of the cells in the tumor (Dick, 2008; Lobo et al., 2007; Reya et al., 2001). These cells give rise to more differentiated, less tumorigenic cancer cells, but are also able to renew their potential to initiate a tumor. CSCs are thought to be quiescent and therefore more resistant to treatment. These slow cycling cells are missed by traditional chemotherapy which is targeting proliferating cells (Ishikawa et al., 2007; Ito et al., 2008; Shachaf et al., 2004).

Cancer Stem Cells have been identified in numerous solid tumors by sorting for cell surface markers, which are only expressed by a rare, but highly tumorigenic subset of the cells. In breast cancer, CSCs were found in a $CD44^{+}CD24^{-/low}$ cell population (Al-Hajj et al., 2003), in brain (Singh et al., 2004), colorectal (O'Brien et al., 2007; Ricci-Vitiani et al., 2007) and pancreatic carcinoma (Hermann et al., 2007) CD133 was used as a marker for CSCs.

In melanoma, studies have shown that the expression of CD133 is associated with increased tumorigenicity, while cells lacking this marker were not able to produce tumors in immunocompromised NOD/SCID mice (Monzani et al., 2007). The multidrug transporter molecule ABCB5 was shown to be expressed by a melanoma cell subpopulation with increased frequency of tumorigenic cells (Schatton et al., 2008). Over time, many putative melanoma stem cell markers have been proposed. Recently this work has been challenged by contradictory

data showing a much higher proportion of cells being able to initiate a melanoma in a mouse model. In immunocompromised NOD/SCID IL2R$\gamma^{-/-}$(NSG) mice Quintana and coworkers could show that a very high proportion of melanoma cells (13%-70%) isolated from xenografted tumors can give rise to a new tumor (Quintana et al., 2008). Other groups have also found that a high proportion of melanoma cells are tumorigenic (Held et al., 2010; Prasmickaite et al., 2010; Zhong et al., 2010).

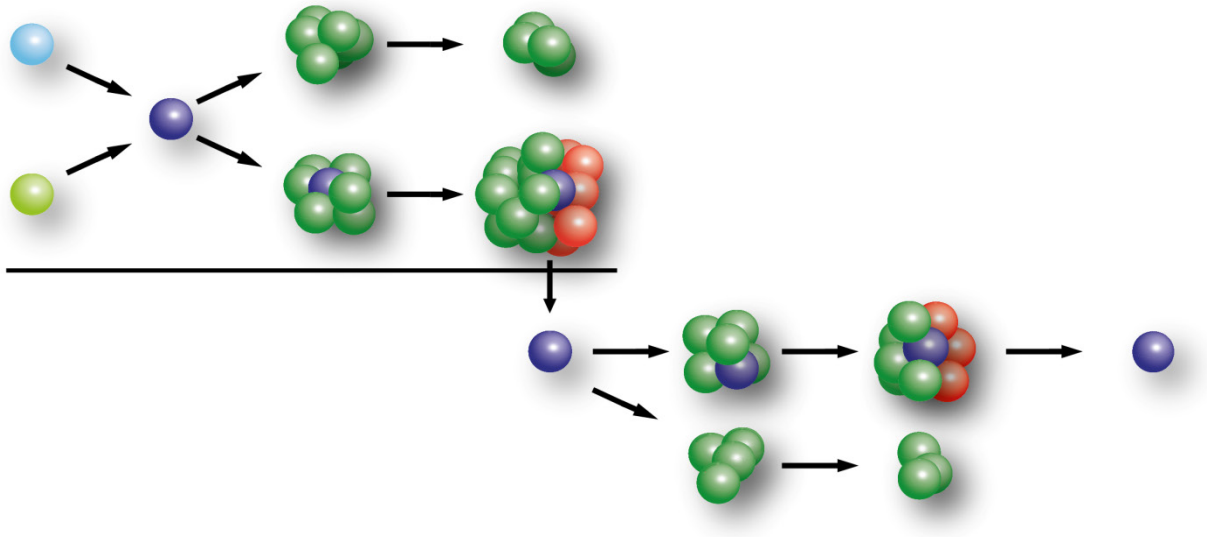

Figure 2: Cancer Stem Cell Model. From a melanocyte (light green) or melanocyte precursor cell (light blue) a melanoma cell (purple) develops by an unknown transformation event. Cancer stem cells are needed to maintain the tumor, when they are missing, the tumor will eventually regress (first and fourth row). Only the cancer stem cell is able to initiate a metastasis (down arrow).

3.2.2 Clonal evolution model

The clonal evolution model (Figure 3) suggests that cancer cells by time acquire additional mutations, which lead to a genetic intra- and intertumoral heterogeneity of tumor cells with different tumorigenic potential. These mutations lead to an advantage in survival, proliferation or metastasis and thereby drive cancer progression (Fearon and Vogelstein, 1990; Foulds, 1958; Greaves and Maley, 2012; Lengauer et al., 1998).

Clonal expansion has been reported in many cancers, often these highly proliferating clones have a mutation in *P53* as seen in brain cancer (Sidransky et al., 1992), kidney cancer (Bardeesy et al., 1995), stomach cancer (McDonald et al., 2008) and others. Also mutations in *p16* can lead to clonal expansions, which are observed in oral cancer (Braakhuis et al., 2004) and Barrett's esophagus (Maley et al., 2004), lung cancer (Franklin et al., 1997) as well as bladder cancer (Czerniak et al., 1999). A study recently published by Gerlinger et al. could show that in four tested renal cell carcinomas, every tumor had spatially separated heterogeneous somatic mutations and chromosomal imbalances. Thus, a tumor-biopsy only represents a minority of the genetic aberrations present in a tumor and should therefore not be interpreted as the genetic state of the whole lesion (Gerlinger et al., 2012). Shah et al. presented a study that demonstrated a very wide spectrum of mutational and clonal evolution in triple negative breast cancer samples, explaining at least in part why the response to current treatment of this cancer is so variable (Shah et al., 2012). In metastatic medulloblastoma it was shown that the metastases within an individual are very similar to each other, but very different from the matched primary lesion. Only a small subpopulation of the primary tumor exhibits the same genetic events that were found in the metastases presenting a possible barrier in the development of an effective therapy (Wu et al., 2012).

In melanoma the number of known mutations has accelerated greatly in recent years. The emerging paradigm and tools of personalized medicine, which involves targeting treatment to the specific mutations in a patient, as well as understanding the mechanisms of acquired drug resistance, have increased the interest in studying clonal heterogeneity in melanoma.

Interestingly, it was recently shown that circulating melanoma cells in the peripheral blood of patients are heterogeneous for mutations in *BRAF* and *KIT*. The sequences of these genes were inconsistent when compared to the autologous tumors in 3 out of 9 patients for *BRAF* and in 3 out of 4 patients for *KIT* (Sakaizawa et al., 2012). These results were confirmed in another study, where variable proportions of *BRAF* mutated and wild-type cells were found within individual melanoma tumors and among multiple lesions from individual patients (Yancovitz et al., 2012). These results provide at least one explanation for the high number of treatment resistant patients in specific $BRAF^{V600E}$ inhibitor therapy. Despite great effort and expenses invested into e.g. whole genome sequencing of melanoma patients, no case of melanoma has been detected where a single oncogenic event was considered to be responsible (Flaherty and Fisher, 2011). Taken together, many studies have shown that melanoma tumors exhibit high clonal heterogeneity, but yet these findings could not link genetic variation to tumor progression.

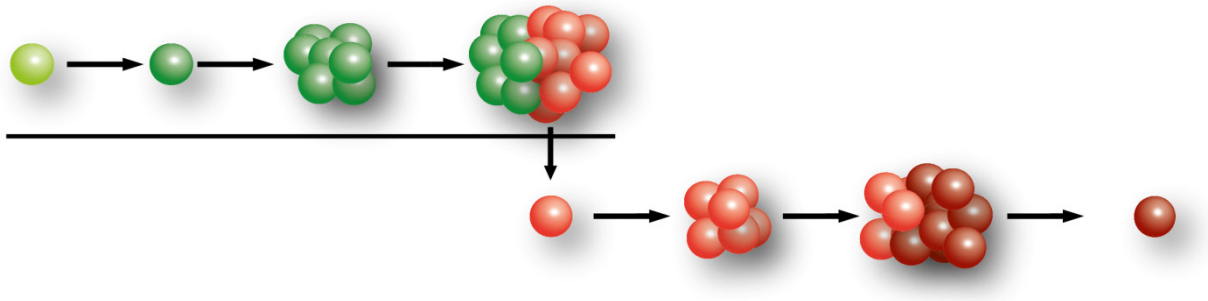

Figure 3: Clonal evolution model. Cancer cells gain an advantage over non-mutated cells by increased migratory capacity (red) or proliferation (dark red) by additional, mutations allowing progression and metastasis.

3.2.3 Phenotype switching model

The phenotype switching model (Figure 4) proposes that melanoma cells can reversibly switch between phenotypes of different malignant potential. Initially, our laboratory performed cDNA microarray analyses of short-term melanoma cell cultures that had been isolated from patient tumor samples in our clinic. Clustering analysis showed that the cell cultures could be grouped into two distinct cohorts based on their expression signatures (Hoek et al., 2006). Using these clusters, we generated a list of genes that discriminates between the two subgroups, and we created an online tool that predicts the phenotype of melanoma cell lines by their gene expression profiles (Widmer et al., 2012). Importantly, these cohorts could also be distinguished phenotypically by *in vitro* tests of proliferation, invasion, and growth factor resistance (Hoek et al., 2006). Due to the high proliferation rate of cells with one phenotype and the increased *in vitro* invasiveness of the second, we called them the proliferative phenotype and the invasive phenotype, respectively.

Immunohistochemistry of melanoma tumors for markers of the proliferative phenotype (e.g. MELANA, MITF) and the invasive phenotype (e.g. WNT5A) generally show heterogeneity for the two phenotypes (Eichhoff et al., 2010). To further characterize their tumorigenic potential, pure populations of each phenotype were separately injected subcutaneously into immunocompromised nude mice. Although proliferative phenotype melanoma cells formed tumors faster, both xenografts resulted in tumors, which were heterogeneous for both phenotypes (Hoek et al., 2008). These results suggest that both cohorts are able to form tumors and are able to switch between phenotypes, recapitulating tumor heterogeneity. Based on these data, we proposed the phenotype switching model for melanoma progression. It postulates that a melanoma tumor contains two genetically identical but phenotypically distinct populations of cells, one of which displays a proliferative phenotype and the other an invasive phenotype. It suggests that cell heterogeneity is driven by alterations in gene expression caused by the microenvironment rather than by an accumulation of genetic mutations. The oscillation between proliferative and quiescent, stem cell like states is more likely to be explained by microenvironmentally driven changes in transcription than by a series of genetic events that first suppress and then reactivate pro-proliferative signaling. We hypothesize that a stable, yet reversible molecular mechanism, such

as DNA methylation, is responsible for causing and maintaining the switch in melanoma cell phenotypes. Nevertheless, the phenotype switching model contains characteristics of the classical CSC and clonal evolution model, combining them with an explanation for the observed cell plasticity.

In recent years, the idea that cancer cell plasticity may explain cancer cell heterogeneity has become increasingly popular and interpreted in different ways (Hoek et al., 2006; Pinner et al., 2009; Roesch et al., 2010).

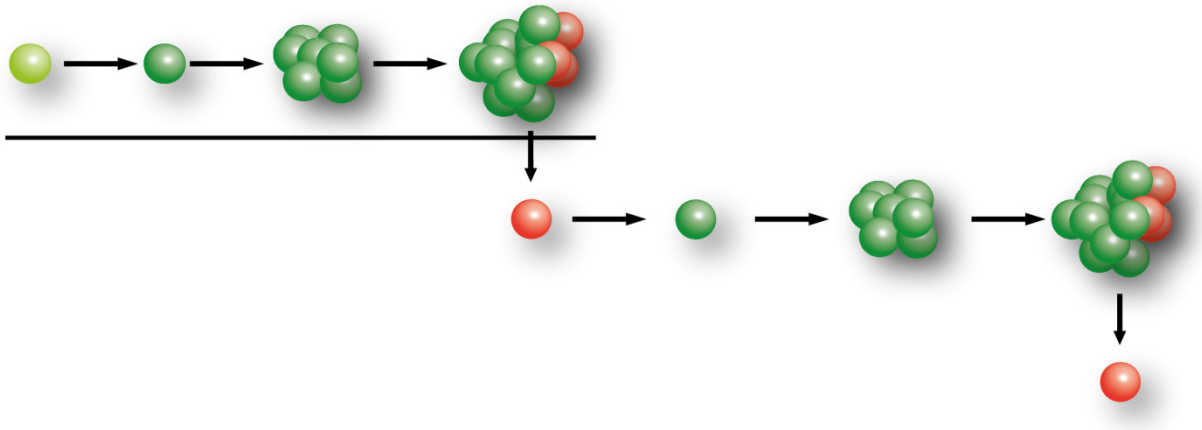

Figure 4: The phenotype switching model. Essentially every cell of a tumor can switch between proliferative and invasive phenotypes and thereby drive disease progression.

3.3 Hypoxia

As a common microenvironmental condition in cancer, hypoxia seemed like a reasonable trigger for the induction of a more aggressive subtype of melanoma cells, and a possible switch from proliferative to invasive states.

Hypoxia describes a reduced oxygen level in a tissue compared to normal conditions. This results from an imbalance of oxygen delivery and consumption and can lead to or is caused by a variety of diseases, ranging from vascular to pulmonary disorders to cancer. Since oxygen can only diffuse about 100-150 µm from a blood vessel to the tissue surrounding it, cells located outside of this area become hypoxic and eventually anoxic (Brown, 1990). Without compensatory genetic or epigenetic adaptations, a decreased oxygen tension as in a pathological state becomes toxic to cells.

The oxygen concentration in the skin has been measured and found to be about 10% in the dermis, 0.5-10% in the epidermis, and in hair follicles between 0.1 - 2.5% (Evans et al., 2006). The physiological oxygen levels of non-skin tissues range from roughly 2-3% in the brain, liver and heart to 9-10% in the spleen and up to 13-14% in the lung (Vaupel et al., 1989). Several cell-types, like melanocytes (Busca et al., 2005; Horikoshi et al., 1991), are adapted to hypoxic environments and can show increased proliferation or have an extended life span, like smooth muscle cells, when cultured in hypoxic culture conditions (Minamino et al., 2001). In addition, CNS precursor cells grown in 3% oxygen display a lower doubling time and a reduced rate of apoptosis (Studer et al., 2000).

Contrary to previous assumptions, oxygen sensing has been shown not to be restricted to specialized cells, but can be found in every nucleated cell in the body (Weir et al., 2005). The mechanism of oxygen sensing is mainly regulated by a basic-helix-loop-helix transcription factor, called Hypoxia-Inducible-Factor 1 (HIF1) (Semenza and Wang, 1992). This heterodimeric protein consists of an alpha subunit that senses oxygen levels and a constitutively expressed beta subunit called Aryl Hydrocarbon Receptor Nuclear Translocator (ARNT), also known as HIF1β (Wang et al., 1995). Next to HIF1α, two more alpha subunits are known: HIF2α (also called EPAS-1, MOP2, HLF and HRF) and HIF3α (Maynard et al.,

2003). Even though the role of HIF2 in cancer is still unclear, its expression was shown to correlate with poor patient outcome in hepatocellular, colorectal carcinoma, melanoma, ovarian and non-small cell lung cancers (Bangoura et al., 2007; Giatromanolaki et al., 2001; Giatromanolaki et al., 2003; Yoshimura et al., 2004).

At normal oxygen levels, two prolines of HIF1α are hydroxylated by prolyl hydroxylases (PHDs) and subsequently targeted for proteasomal degradation by the von Hippel-Lindau (VHL) tumor suppressor protein, pVHL (Cockman et al., 2000; Kamura et al., 2000; Maxwell et al., 1999). Transactivation of the HIF1α protein is regulated by the hydroxylation of an asparagine residue by an asparaginyl hydroxylase (FIH-1), inhibiting co-binding of the histone acetyltransferases p300/CBP, which abolishes transactivation (Mahon et al., 2001). Under hypoxia the reduced levels of oxygen lead to a lower activity of the PHDs and consequently to a stabilization and accumulation of HIF1α in the cytosol. After translocation to the nucleus, HIF1α dimerizes with ARNT (HIF1β) and then binds to Hypoxia Responsive Elements (HREs) located within the regulatory elements of HIF1 target genes (Wenger et al., 2005). Hundreds of HIF1 targets have been described with crucial roles in various biological processes (Semenza, 2007; Wenger et al., 2005). HIF1 is known to influence the regulation of angiogenesis, cytoskeletal structure, apoptosis, adhesion, migration and glucose metabolism (Pouyssegur et al., 2006; Semenza, 2003) (Figure 5).

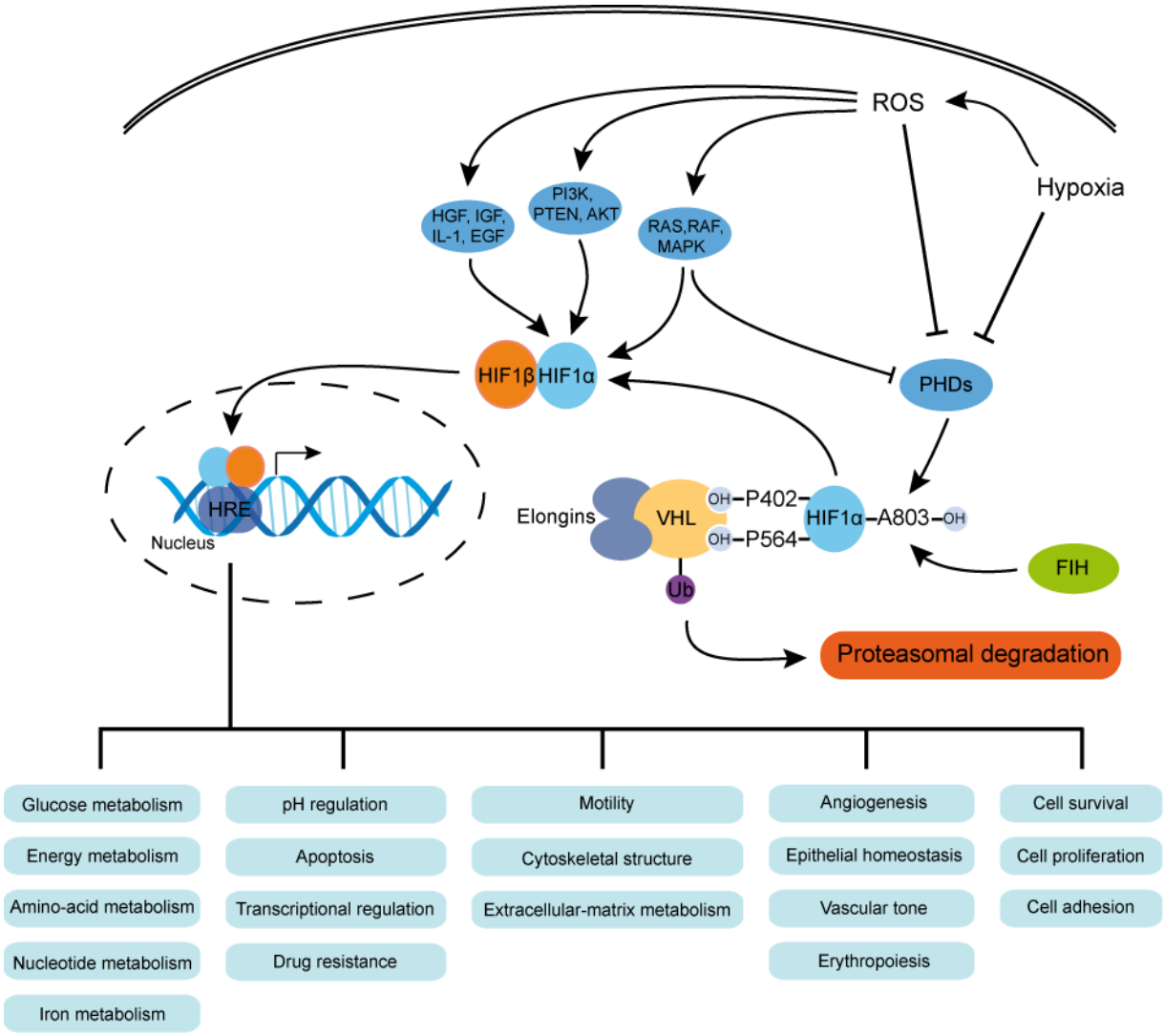

Figure 5: Mechanisms of hypoxia-inducible factor 1 alpha stabilization under different stimuli. HIF1α is regulated mainly on the protein level, but can also be upregulated on the mRNA level by multiple factors. Hypoxia-responsive elements (HRE), reactive oxygen species (ROS), hepatocyte growth factor (HGF), insulin growth factor (IGF), interleukin (IL), epidermal growth factor (EGF), phosphatidylinositide 3-kinase (PI3K), protein kinase B (AKT), mitogen-activated protein kinase (MAPK), hypoxia inducible factor 1α (HIF1α), hypoxia inducible factor 1β (HIF1β / ARNT), von Hippel Lindau protein (VHL), prolyl hydroxylases (PHDs). After (Rezvani et al., 2011) and (Papandreou et al., 2008)

3.3.1 The role of hypoxia in cancer

The role of hypoxia as a microenvironmental factor in cancer has been studied for many years (Chaplin et al., 1986; Hockel et al., 1999; Hockel and Vaupel, 2001). In various cancer types it has been shown that hypoxic regions within a tumor can serve as a marker for poor prognosis (Lartigau et al., 1997). Many of the target

genes of HIF1 are involved in processes of invasion and metastasis as well as in changes in glucose metabolism (Figure 6). A shift from aerobic to anaerobic metabolism, known as Warburg effect, allows cancer cells to increase their proliferation rate despite the lack of oxygen (Dang and Semenza, 1999; Pouyssegur et al., 2006; Semenza, 2003; Warburg, 1956). Hypoxia has been shown to increase the levels of reactive oxygen species (ROS), leading to DNA damage by causing single and double strand breaks and by impacting DNA repair pathways (Bindra and Glazer, 2005; Mihaylova et al., 2003). HIF1 also plays a role in immune evasion, radiation resistance and stem cell maintenance (Barnhart and Simon, 2007; Lukashev et al., 2007; Moeller et al., 2007). By regulating factors involved in epithelial to mesenchymal transition (EMT) (e.g. lysyl oxidase (LOX) and E-cadherin (CDH1)), HIF1 expression influences cancer metastasis. Furthermore, products of HIF1 target genes like UPAR (*PLAUR*) and *MMP2* affect invasion, pro-angiogenic factors such as VEGF, IL8 and ANGPT2 contribute to tumor angiogenesis and thereby to cancer progression (Bar-Eli, 1999; Erler et al., 2006; Evans et al., 2007; Hirota and Semenza, 2006; Karashima et al., 2003; Krishnamachary et al., 2003). Transient hypoxia, meaning alternating periods of hypoxia followed by reoxygenation as it appears in tumor microenvironments, can cause DNA damage and has been shown to increase the number of lung metastases in KHT fibrosarcoma bearing mice (Bindra and Glazer, 2005; Cairns et al., 2001).

The role of hypoxia in melanoma has been investigated more and more extensively in recent years. It has been shown that hypoxia influences migration and invasion of melanoma cells (Jeffs et al., 2009; Osawa et al., 2009) and increases their ability to form vasculogenic mimicry (Sun et al., 2007) as well as their metastatic potential (Rofstad et al., 2007).

Hypoxia may play a role in the malignant transformation of melanocytes in cooperation with oncogenic *BRAF* mutations and activation of the AKT signaling pathway (Bedogni et al., 2008; Bedogni et al., 2005). Also, in melanocytes with mutations in *KIT*, hypoxia or constitutively active HIF1α upregulate the activity of the MAPK pathway and increase proliferation (Monsel et al., 2010), possibly leading to malignant transformation. Interestingly, one study showed that the *V600E BRAF* mutation increases HIF1α expression in melanoma cells (Kumar et

al., 2007). It has been reported that HIF1α can also be increased in melanoma cells under normoxic (normal oxygen levels) conditions (Kuphal et al., 2010; Mills et al., 2009).

Research by Cheli and co-workers published in 2011 (Cheli et al., 2011) shows that hypoxia in melanoma cells leads to a decrease in MITF expression and that a deletion of MITF is sufficient to increase the metastatic potential of mouse and human melanoma cells. They identified BHLHE40 as the mediator of hypoxia/HIF1α dependent inhibitory effect on MITF, leading to a more aggressive melanoma phenotype.

In another study also published in 2011, Feige et al. (Feige et al., 2011) found the exact same gene *BHLHE40*, to be responsible for a hypoxia induced downregulation of MITF. Despite identical results from in vitro experiments, contrary outcomes from in vivo tests led to opposite conclusions about the effect of hypoxia on melanoma progression. Cheli et al. are proposing that hypoxia leads to an increase in tumorigenic and metastatic potential of melanoma cells, whereas Feige et al. suggest hypoxia having the opposing effect on melanoma.

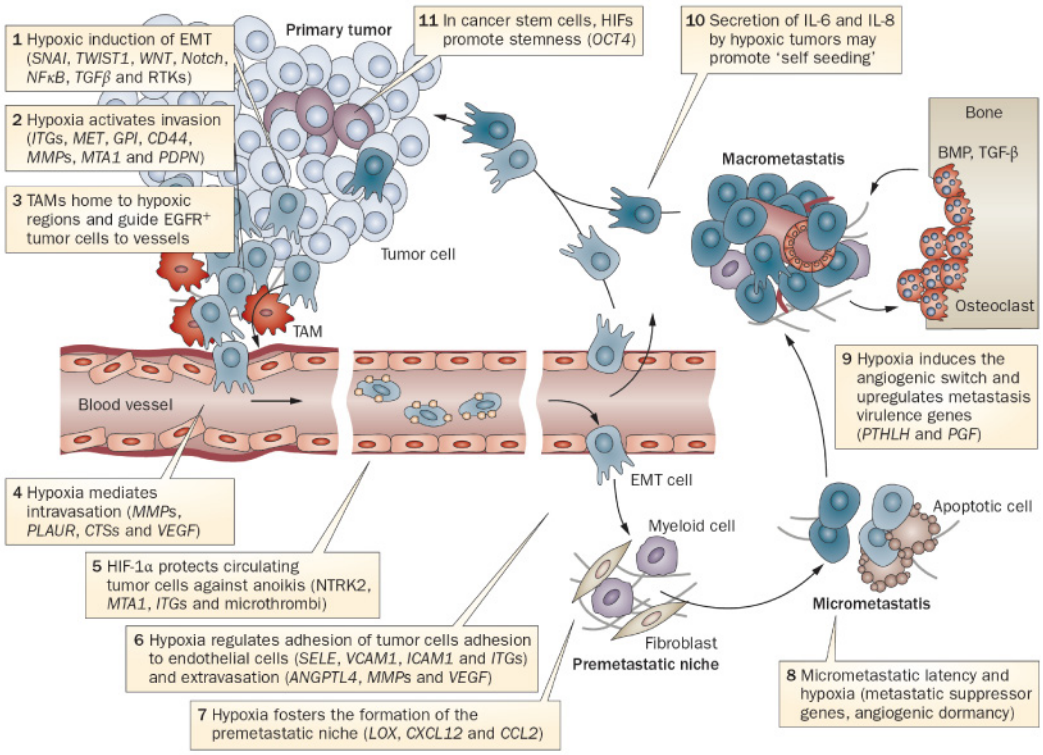

Figure 6: The regulation of the metastatic cascade by hypoxia. Almost every step in metastasis can be affected by hypoxia Bone-morphogenic protein (BMP), epithelial-mesenchymal transition (EMT), hypoxia-inducible factor 1α (HIF1α), interleukin (IL), matrix metalloproteinase (MMP), receptor tyrosine kinase (RTK), tumor-associated macrophages (TAM), transforming growth factor β (TGFβ) (De Bock et al., 2011).

3.4 Aim of the thesis

Melanoma is a heterogeneous disease on many levels, from clinical to molecular, although what this heterogeneity contributes to its biology is unknown. In exploring heterogeneity at the cellular and molecular levels our group recently described different expression signatures corresponding to different subtypes of melanoma cells. A model proposed by our group hypothesizes that cells, responding to changes in microenvironmental conditions, change their transcription programs to switch back and forth between proliferative and invasive phenotypes to drive metastatic progression. Candidate microenvironmental conditions proposed to be involved in phenotype switching include hypoxia. The principal aim of this PhD thesis was to investigate the role of hypoxia in melanoma progression by assessing the effects of normoxia and hypoxia on gene transcription in the

different melanoma cell phenotypes. The results of this study can be found in chapter 5.2.

Furthermore, with growing use of publically accessible transcription profiling databases there was an opportunity to challenge the phenotype switching model by re-examining widely used melanoma lines in the context of the gene expression profiles described above. The methodology for using DNA microarray data to predict phenotype had been relatively simplistic and was updated and formalized before being used to test the profiles of melanoma lines in common use. My goal was to develop a predictive expression analysis tool to characterize cell lines and display the distribution of the two phenotypes among melanoma cell lines and cultures. The results of this study are described in a publication presented in chapter 5.1.

Finally, the regulatory functions of the MITF transcription factor is critical to both melanocyte and melanoma biology. Given our focus on transcription profiling and high-throughput data analysis one aim of this thesis was to participate in a collaborative program (University of Iceland) designed to uncover novel targets of MITF. My contributions to this project and the resulting publication are presented in chapter 5.6.

3.5 References

Al-Hajj, M., Wicha, M. S., Benito-Hernandez, A., Morrison, S. J., and Clarke, M. F. (2003). Prospective identification of tumorigenic breast cancer cells. Proc Natl Acad Sci U S A *100*, 3983-3988.

Autier, P., Dore, J. F., Reis, A. C., Grivegnee, A., Ollivaud, L., Truchetet, F., Chamoun, E., Rotmensz, N., Severi, G., and Cesarini, J. P. (2000). Sunscreen use and intentional exposure to ultraviolet A and B radiation: a double blind randomized trial using personal dosimeters. Br J Cancer *83*, 1243-1248.

Balch, C. M., Gershenwald, J. E., Soong, S. J., Thompson, J. F., Atkins, M. B., Byrd, D. R., Buzaid, A. C., Cochran, A. J., Coit, D. G., Ding, S*., et al.* (2009). Final version of 2009 AJCC melanoma staging and classification. J Clin Oncol *27*, 6199-6206.

Bangoura, G., Liu, Z. S., Qian, Q., Jiang, C. Q., Yang, G. F., and Jing, S. (2007). Prognostic significance of HIF-2alpha/EPAS1 expression in hepatocellular carcinoma. World J Gastroenterol *13*, 3176-3182.

Bar-Eli, M. (1999). Role of interleukin-8 in tumor growth and metastasis of human melanoma. Pathobiology *67*, 12-18.

Bardeesy, N., Beckwith, J. B., and Pelletier, J. (1995). Clonal expansion and attenuated apoptosis in Wilms' tumors are associated with p53 gene mutations. Cancer Res *55*, 215-219.

Barnhart, B. C., and Simon, M. C. (2007). Metastasis and stem cell pathways. Cancer Metastasis Rev *26*, 261-271.

Bauer, J., and Garbe, C. (2003). Acquired melanocytic nevi as risk factor for melanoma development. A comprehensive review of epidemiological data. Pigment Cell Res *16*, 297-306.

Bedogni, B., Warneke, J. A., Nickoloff, B. J., Giaccia, A. J., and Powell, M. B. (2008). Notch1 is an effector of Akt and hypoxia in melanoma development. J Clin Invest *118*, 3660-3670.

Bedogni, B., Welford, S. M., Cassarino, D. S., Nickoloff, B. J., Giaccia, A. J., and Powell, M. B. (2005). The hypoxic microenvironment of the skin contributes to Akt-mediated melanocyte transformation. Cancer Cell *8*, 443-454.

Bindra, R. S., and Glazer, P. M. (2005). Genetic instability and the tumor microenvironment: towards the concept of microenvironment-induced mutagenesis. Mutat Res *569*, 75-85.

Bollag, G., Hirth, P., Tsai, J., Zhang, J., Ibrahim, P. N., Cho, H., Spevak, W., Zhang, C., Zhang, Y., Habets, G*., et al.* (2010). Clinical efficacy of a RAF inhibitor needs broad target blockade in BRAF-mutant melanoma. Nature *467*, 596-599.

Braakhuis, B. J., Leemans, C. R., and Brakenhoff, R. H. (2004). A genetic progression model of oral cancer: current evidence and clinical implications. J Oral Pathol Med *33*, 317-322.

Brown, J. M. (1990). Tumor hypoxia, drug resistance, and metastases. J Natl Cancer Inst *82*, 338-339.

Busca, R., Berra, E., Gaggioli, C., Khaled, M., Bille, K., Marchetti, B., Thyss, R., Fitsialos, G., Larribere, L., Bertolotto, C*., et al.* (2005). Hypoxia-inducible factor 1{alpha} is a new target of microphthalmia-associated transcription factor (MITF) in melanoma cells. J Cell Biol *170*, 49-59.

Cairns, R. A., Kalliomaki, T., and Hill, R. P. (2001). Acute (cyclic) hypoxia enhances spontaneous metastasis of KHT murine tumors. Cancer Res *61*, 8903-8908.

Chaplin, D. J., Durand, R. E., and Olive, P. L. (1986). Acute hypoxia in tumors: implications for modifiers of radiation effects. Int J Radiat Oncol Biol Phys *12*, 1279-1282.

Cheli, Y., Giuliano, S., Guiliano, S., Botton, T., Rocchi, S., Hofman, V., Hofman, P., Bahadoran, P., Bertolotto, C., and Ballotti, R. (2011). Mitf is the key molecular switch between mouse or human melanoma initiating cells and their differentiated progeny. Oncogene *30*, 2307-2318.

Cho, E., Rosner, B. A., and Colditz, G. A. (2005a). Risk factors for melanoma by body site. Cancer Epidemiol Biomarkers Prev *14*, 1241-1244.

Cho, E., Rosner, B. A., Feskanich, D., and Colditz, G. A. (2005b). Risk factors and individual probabilities of melanoma for whites. J Clin Oncol *23*, 2669-2675.

Cockman, M. E., Masson, N., Mole, D. R., Jaakkola, P., Chang, G. W., Clifford, S. C., Maher, E. R., Pugh, C. W., Ratcliffe, P. J., and Maxwell, P. H. (2000). Hypoxia inducible factor-alpha binding and ubiquitylation by the von Hippel-Lindau tumor suppressor protein. J Biol Chem *275*, 25733-25741.

Cohen, C., Zavala-Pompa, A., Sequeira, J. H., Shoji, M., Sexton, D. G., Cotsonis, G., Cerimele, F., Govindarajan, B., Macaron, N., and Arbiser, J. L. (2002). Mitogen-actived protein kinase activation is an early event in melanoma progression. Clin Cancer Res *8*, 3728-3733.

Czerniak, B., Chaturvedi, V., Li, L., Hodges, S., Johnston, D., Roy, J. Y., Luthra, R., Logothetis, C., Von Eschenbach, A. C., Grossman, H. B.*, et al.* (1999). Superimposed histologic and genetic mapping of chromosome 9 in progression of human urinary bladder neoplasia: implications for a genetic model of multistep urothelial carcinogenesis and early detection of urinary bladder cancer. Oncogene *18*, 1185-1196.

Dang, C. V., and Semenza, G. L. (1999). Oncogenic alterations of metabolism. Trends Biochem Sci *24*, 68-72.

Davies, H., Bignell, G. R., Cox, C., Stephens, P., Edkins, S., Clegg, S., Teague, J., Woffendin, H., Garnett, M. J., Bottomley, W.*, et al.* (2002). Mutations of the BRAF gene in human cancer. Nature *417*, 949-954.

De Bock, K., Mazzone, M., and Carmeliet, P. (2011). Antiangiogenic therapy, hypoxia, and metastasis: risky liaisons, or not? Nat Rev Clin Oncol *8*, 393-404.

Der, C. J., Krontiris, T. G., and Cooper, G. M. (1982). Transforming genes of human bladder and lung carcinoma cell lines are homologous to the ras genes of Harvey and Kirsten sarcoma viruses. Proc Natl Acad Sci U S A *79*, 3637-3640.

Dick, J. E. (2008). Stem cell concepts renew cancer research. Blood *112*, 4793-4807.

Dummer, R., and Flaherty, K. T. (2012). Resistance patterns with tyrosine kinase inhibitors in melanoma: new insights. Curr Opin Oncol *24*, 150-154.

Dummer, R., Guggenheim, M., Arnold, A. W., Braun, R., and von Moos, R. (2011a). Updated Swiss guidelines for the treatment and follow-up of cutaneous melanoma. Swiss Med Wkly *141*, w13320.

Dummer, R., Panizzon, R., Bloch, P. H., and Burg, G. (2005). Updated Swiss guidelines for the treatment and follow-up of cutaneous melanoma. Dermatology *210*, 39-44.

Dummer, R., Pittelkow, M., Iwatsuki, K., Green, A., and Elwan, N. (2010). Skin Cancer - A World Wide Perspective: Springer Verlag Berlin Heidelberg).

Dummer, R., Pittelkow, M., Iwatsuki, K., Green, A., and Elwan, N. (2011b). Skin Cancer - A World Wide Perspective. In Springer Verlag Berlin Heidelberg.

Eichhoff, O. M., Zipser, M. C., Xu, M., Weeraratna, A. T., Mihic, D., Dummer, R., and Hoek, K. S. (2010). The immunohistochemistry of invasive and proliferative phenotype switching in melanoma: a case report. Melanoma Res *20*, 349-355.

Elwood, J. M., and Jopson, J. (1997). Melanoma and sun exposure: an overview of published studies. Int J Cancer *73*, 198-203.

Erler, J. T., Bennewith, K. L., Nicolau, M., Dornhofer, N., Kong, C., Le, Q. T., Chi, J. T., Jeffrey, S. S., and Giaccia, A. J. (2006). Lysyl oxidase is essential for hypoxia-induced metastasis. Nature *440*, 1222-1226.

Evans, A. J., Russell, R. C., Roche, O., Burry, T. N., Fish, J. E., Chow, V. W., Kim, W. Y., Saravanan, A., Maynard, M. A., Gervais, M. L.*, et al.* (2007). VHL promotes E2 box-dependent E-cadherin transcription by HIF-mediated regulation of SIP1 and snail. Mol Cell Biol *27*, 157-169.

Evans, S. M., Schrlau, A. E., Chalian, A. A., Zhang, P., and Koch, C. J. (2006). Oxygen levels in normal and previously irradiated human skin as assessed by EF5 binding. J Invest Dermatol *126*, 2596-2606.

Falkson, C. I., Ibrahim, J., Kirkwood, J. M., Coates, A. S., Atkins, M. B., and Blum, R. H. (1998). Phase III trial of dacarbazine versus dacarbazine with interferon alpha-2b versus dacarbazine with tamoxifen versus dacarbazine with interferon alpha-2b and tamoxifen in patients with

metastatic malignant melanoma: an Eastern Cooperative Oncology Group study. J Clin Oncol *16*, 1743-1751.
Fearon, E. R., and Vogelstein, B. (1990). A genetic model for colorectal tumorigenesis. Cell *61*, 759-767.
Feige, E., Yokoyama, S., Levy, C., Khaled, M., Igras, V., Lin, R. J., Lee, S., Widlund, H. R., Granter, S. R., Kung, A. L., and Fisher, D. E. (2011). Hypoxia-induced transcriptional repression of the melanoma-associated oncogene MITF. Proc Natl Acad Sci U S A *108*, E924-933.
Flaherty, K. T., and Fisher, D. E. (2011). New strategies in metastatic melanoma: oncogene-defined taxonomy leads to therapeutic advances. Clin Cancer Res *17*, 4922-4928.
Flaherty, K. T., and McArthur, G. (2010). BRAF, a target in melanoma: implications for solid tumor drug development. Cancer *116*, 4902-4913.
Flaherty, K. T., Puzanov, I., Kim, K. B., Ribas, A., McArthur, G. A., Sosman, J. A., O'Dwyer, P. J., Lee, R. J., Grippo, J. F., Nolop, K., and Chapman, P. B. (2010). Inhibition of mutated, activated BRAF in metastatic melanoma. N Engl J Med *363*, 809-819.
Fong, L., and Small, E. J. (2008). Anti-cytotoxic T-lymphocyte antigen-4 antibody: the first in an emerging class of immunomodulatory antibodies for cancer treatment. J Clin Oncol *26*, 5275-5283.
Foulds, L. (1958). The natural history of cancer. J Chronic Dis *8*, 2-37.
Franklin, W. A., Gazdar, A. F., Haney, J., Wistuba, I. I., La Rosa, F. G., Kennedy, T., Ritchey, D. M., and Miller, Y. E. (1997). Widely dispersed p53 mutation in respiratory epithelium. A novel mechanism for field carcinogenesis. J Clin Invest *100*, 2133-2137.
Garbe, C., Buttner, P., Weiss, J., Soyer, H. P., Stocker, U., Kruger, S., Roser, M., Weckbecker, J., Panizzon, R., Bahmer, F., and et al. (1994). Associated factors in the prevalence of more than 50 common melanocytic nevi, atypical melanocytic nevi, and actinic lentigines: multicenter case-control study of the Central Malignant Melanoma Registry of the German Dermatological Society. J Invest Dermatol *102*, 700-705.
Garnett, M. J., Rana, S., Paterson, H., Barford, D., and Marais, R. (2005). Wild-type and mutant B-RAF activate C-RAF through distinct mechanisms involving heterodimerization. Mol Cell *20*, 963-969.
Gerlinger, M., Rowan, A. J., Horswell, S., Larkin, J., Endesfelder, D., Gronroos, E., Martinez, P., Matthews, N., Stewart, A., Tarpey, P.*, et al.* (2012). Intratumor heterogeneity and branched evolution revealed by multiregion sequencing. N Engl J Med *366*, 883-892.
Giatromanolaki, A., Koukourakis, M. I., Sivridis, E., Turley, H., Talks, K., Pezzella, F., Gatter, K. C., and Harris, A. L. (2001). Relation of hypoxia inducible factor 1 alpha and 2 alpha in operable non-small cell lung cancer to angiogenic/molecular profile of tumours and survival. Br J Cancer *85*, 881-890.
Giatromanolaki, A., Sivridis, E., Kouskoukis, C., Gatter, K. C., Harris, A. L., and Koukourakis, M. I. (2003). Hypoxia-inducible factors 1alpha and 2alpha are related to vascular endothelial growth factor expression and a poorer prognosis in nodular malignant melanomas of the skin. Melanoma Res *13*, 493-501.
Greaves, M., and Maley, C. C. (2012). Clonal evolution in cancer. Nature *481*, 306-313.
Grob, J. J., Gouvernet, J., Aymar, D., Mostaque, A., Romano, M. H., Collet, A. M., Noe, M. C., Diconstanzo, M. P., and Bonerandi, J. J. (1990). Count of benign melanocytic nevi as a major indicator of risk for nonfamilial nodular and superficial spreading melanoma. Cancer *66*, 387-395.
Halaban, R., Zhang, W., Bacchiocchi, A., Cheng, E., Parisi, F., Ariyan, S., Krauthammer, M., McCusker, J. P., Kluger, Y., and Sznol, M. (2010). PLX4032, a selective BRAF(V600E) kinase inhibitor, activates the ERK pathway and enhances cell migration and proliferation of BRAF melanoma cells. Pigment Cell Melanoma Res *23*, 190-200.
Hatzivassiliou, G., Song, K., Yen, I., Brandhuber, B. J., Anderson, D. J., Alvarado, R., Ludlam, M. J., Stokoe, D., Gloor, S. L., Vigers, G.*, et al.* (2010). RAF inhibitors prime wild-type RAF to activate the MAPK pathway and enhance growth. Nature *464*, 431-435.

Heidorn, S. J., Milagre, C., Whittaker, S., Nourry, A., Niculescu-Duvas, I., Dhomen, N., Hussain, J., Reis-Filho, J. S., Springer, C. J., Pritchard, C., and Marais, R. (2010). Kinase-dead BRAF and oncogenic RAS cooperate to drive tumor progression through CRAF. Cell *140*, 209-221.

Held, M. A., Curley, D. P., Dankort, D., McMahon, M., Muthusamy, V., and Bosenberg, M. W. (2010). Characterization of melanoma cells capable of propagating tumors from a single cell. Cancer Res *70*, 388-397.

Hermann, P. C., Huber, S. L., Herrler, T., Aicher, A., Ellwart, J. W., Guba, M., Bruns, C. J., and Heeschen, C. (2007). Distinct populations of cancer stem cells determine tumor growth and metastatic activity in human pancreatic cancer. Cell Stem Cell *1*, 313-323.

Hirota, K., and Semenza, G. L. (2006). Regulation of angiogenesis by hypoxia-inducible factor 1. Crit Rev Oncol Hematol *59*, 15-26.

Hockel, M., Schlenger, K., Hockel, S., and Vaupel, P. (1999). Hypoxic cervical cancers with low apoptotic index are highly aggressive. Cancer Res *59*, 4525-4528.

Hockel, M., and Vaupel, P. (2001). Tumor hypoxia: definitions and current clinical, biologic, and molecular aspects. J Natl Cancer Inst *93*, 266-276.

Hoek, K. S., Eichhoff, O. M., Schlegel, N. C., Dobbeling, U., Kobert, N., Schaerer, L., Hemmi, S., and Dummer, R. (2008). In vivo switching of human melanoma cells between proliferative and invasive states. Cancer Res *68*, 650-656.

Hoek, K. S., Schlegel, N. C., Brafford, P., Sucker, A., Ugurel, S., Kumar, R., Weber, B. L., Nathanson, K. L., Phillips, D. J., Herlyn, M.*, et al.* (2006). Metastatic potential of melanomas defined by specific gene expression profiles with no BRAF signature. Pigment Cell Res *19*, 290-302.

Holly, E. A., Kelly, J. W., Shpall, S. N., and Chiu, S. H. (1987). Number of melanocytic nevi as a major risk factor for malignant melanoma. J Am Acad Dermatol *17*, 459-468.

Horikoshi, T., Balin, A. K., and Carter, D. M. (1991). Effects of oxygen tension on the growth and pigmentation of normal human melanocytes. J Invest Dermatol *96*, 841-844.

Ishikawa, F., Yoshida, S., Saito, Y., Hijikata, A., Kitamura, H., Tanaka, S., Nakamura, R., Tanaka, T., Tomiyama, H., Saito, N.*, et al.* (2007). Chemotherapy-resistant human AML stem cells home to and engraft within the bone-marrow endosteal region. Nat Biotechnol *25*, 1315-1321.

Ito, K., Bernardi, R., Morotti, A., Matsuoka, S., Saglio, G., Ikeda, Y., Rosenblatt, J., Avigan, D. E., Teruya-Feldstein, J., and Pandolfi, P. P. (2008). PML targeting eradicates quiescent leukaemia-initiating cells. Nature *453*, 1072-1078.

Jeffs, A. R., Glover, A. C., Slobbe, L. J., Wang, L., He, S., Hazlett, J. A., Awasthi, A., Woolley, A. G., Marshall, E. S., Joseph, W. R.*, et al.* (2009). A gene expression signature of invasive potential in metastatic melanoma cells. PLoS One *4*, e8461.

Joseph, E. W., Pratilas, C. A., Poulikakos, P. I., Tadi, M., Wang, W., Taylor, B. S., Halilovic, E., Persaud, Y., Xing, F., Viale, A.*, et al.* (2010). The RAF inhibitor PLX4032 inhibits ERK signaling and tumor cell proliferation in a V600E BRAF-selective manner. Proc Natl Acad Sci U S A *107*, 14903-14908.

Kamura, T., Sato, S., Iwai, K., Czyzyk-Krzeska, M., Conaway, R. C., and Conaway, J. W. (2000). Activation of HIF1alpha ubiquitination by a reconstituted von Hippel-Lindau (VHL) tumor suppressor complex. Proc Natl Acad Sci U S A *97*, 10430-10435.

Karashima, T., Sweeney, P., Kamat, A., Huang, S., Kim, S. J., Bar-Eli, M., McConkey, D. J., and Dinney, C. P. (2003). Nuclear factor-kappaB mediates angiogenesis and metastasis of human bladder cancer through the regulation of interleukin-8. Clin Cancer Res *9*, 2786-2797.

Krishnamachary, B., Berg-Dixon, S., Kelly, B., Agani, F., Feldser, D., Ferreira, G., Iyer, N., LaRusch, J., Pak, B., Taghavi, P., and Semenza, G. L. (2003). Regulation of colon carcinoma cell invasion by hypoxia-inducible factor 1. Cancer Res *63*, 1138-1143.

Kumar, R., Angelini, S., Snellman, E., and Hemminki, K. (2004). BRAF mutations are common somatic events in melanocytic nevi. J Invest Dermatol *122*, 342-348.

Kumar, S. M., Yu, H., Edwards, R., Chen, L., Kazianis, S., Brafford, P., Acs, G., Herlyn, M., and Xu, X. (2007). Mutant V600E BRAF increases hypoxia inducible factor-1alpha expression in melanoma. Cancer Res *67*, 3177-3184.

Kuphal, S., Winklmeier, A., Warnecke, C., and Bosserhoff, A. K. (2010). Constitutive HIF-1 activity in malignant melanoma. Eur J Cancer *46*, 1159-1169.

Lartigau, E., Randrianarivelo, H., Avril, M. F., Margulis, A., Spatz, A., Eschwege, F., and Guichard, M. (1997). Intratumoral oxygen tension in metastatic melanoma. Melanoma Res *7*, 400-406.

Lengauer, C., Kinzler, K. W., and Vogelstein, B. (1998). Genetic instabilities in human cancers. Nature *396*, 643-649.

Lin, W. M., Baker, A. C., Beroukhim, R., Winckler, W., Feng, W., Marmion, J. M., Laine, E., Greulich, H., Tseng, H., Gates, C. *, et al.* (2008). Modeling genomic diversity and tumor dependency in malignant melanoma. Cancer Res *68*, 664-673.

Lobo, N. A., Shimono, Y., Qian, D., and Clarke, M. F. (2007). The biology of cancer stem cells. Annu Rev Cell Dev Biol *23*, 675-699.

Lui, P., Cashin, R., Machado, M., Hemels, M., Corey-Lisle, P. K., and Einarson, T. R. (2007). Treatments for metastatic melanoma: synthesis of evidence from randomized trials. Cancer Treat Rev *33*, 665-680.

Lukashev, D., Ohta, A., and Sitkovsky, M. (2007). Hypoxia-dependent anti-inflammatory pathways in protection of cancerous tissues. Cancer Metastasis Rev *26*, 273-279.

Mahon, P. C., Hirota, K., and Semenza, G. L. (2001). FIH-1: a novel protein that interacts with HIF-1alpha and VHL to mediate repression of HIF-1 transcriptional activity. Genes Dev *15*, 2675-2686.

Maley, C. C., Galipeau, P. C., Li, X., Sanchez, C. A., Paulson, T. G., and Reid, B. J. (2004). Selectively advantageous mutations and hitchhikers in neoplasms: p16 lesions are selected in Barrett's esophagus. Cancer Res *64*, 3414-3427.

Maxwell, P. H., Wiesener, M. S., Chang, G. W., Clifford, S. C., Vaux, E. C., Cockman, M. E., Wykoff, C. C., Pugh, C. W., Maher, E. R., and Ratcliffe, P. J. (1999). The tumour suppressor protein VHL targets hypoxia-inducible factors for oxygen-dependent proteolysis. Nature *399*, 271-275.

Maynard, M. A., Qi, H., Chung, J., Lee, E. H., Kondo, Y., Hara, S., Conaway, R. C., Conaway, J. W., and Ohh, M. (2003). Multiple splice variants of the human HIF-3 alpha locus are targets of the von Hippel-Lindau E3 ubiquitin ligase complex. J Biol Chem *278*, 11032-11040.

McDonald, S. A., Greaves, L. C., Gutierrez-Gonzalez, L., Rodriguez-Justo, M., Deheragoda, M., Leedham, S. J., Taylor, R. W., Lee, C. Y., Preston, S. L., Lovell, M. *, et al.* (2008). Mechanisms of field cancerization in the human stomach: the expansion and spread of mutated gastric stem cells. Gastroenterology *134*, 500-510.

Melero, I., Hervas-Stubbs, S., Glennie, M., Pardoll, D. M., and Chen, L. (2007). Immunostimulatory monoclonal antibodies for cancer therapy. Nat Rev Cancer *7*, 95-106.

Middleton, M. R., Grob, J. J., Aaronson, N., Fierlbeck, G., Tilgen, W., Seiter, S., Gore, M., Aamdal, S., Cebon, J., Coates, A. *, et al.* (2000). Randomized phase III study of temozolomide versus dacarbazine in the treatment of patients with advanced metastatic malignant melanoma. J Clin Oncol *18*, 158-166.

Mihaylova, V. T., Bindra, R. S., Yuan, J., Campisi, D., Narayanan, L., Jensen, R., Giordano, F., Johnson, R. S., Rockwell, S., and Glazer, P. M. (2003). Decreased expression of the DNA mismatch repair gene Mlh1 under hypoxic stress in mammalian cells. Mol Cell Biol *23*, 3265-3273.

Mills, C. N., Joshi, S. S., and Niles, R. M. (2009). Expression and function of hypoxia inducible factor-1 alpha in human melanoma under non-hypoxic conditions. Mol Cancer *8*, 104.

Minamino, T., Mitsialis, S. A., and Kourembanas, S. (2001). Hypoxia extends the life span of vascular smooth muscle cells through telomerase activation. Mol Cell Biol *21*, 3336-3342.

Moeller, B. J., Richardson, R. A., and Dewhirst, M. W. (2007). Hypoxia and radiotherapy: opportunities for improved outcomes in cancer treatment. Cancer Metastasis Rev *26*, 241-248.

Monsel, G., Ortonne, N., Bagot, M., Bensussan, A., and Dumaz, N. (2010). c-Kit mutants require hypoxia-inducible factor 1alpha to transform melanocytes. Oncogene *29*, 227-236.
Montagut, C., Sharma, S. V., Shioda, T., McDermott, U., Ulman, M., Ulkus, L. E., Dias-Santagata, D., Stubbs, H., Lee, D. Y., Singh, A.*, et al.* (2008). Elevated CRAF as a potential mechanism of acquired resistance to BRAF inhibition in melanoma. Cancer Res *68*, 4853-4861.
Monzani, E., Facchetti, F., Galmozzi, E., Corsini, E., Benetti, A., Cavazzin, C., Gritti, A., Piccinini, A., Porro, D., Santinami, M.*, et al.* (2007). Melanoma contains CD133 and ABCG2 positive cells with enhanced tumourigenic potential. Eur J Cancer *43*, 935-946.
Nazarian, R., Shi, H., Wang, Q., Kong, X., Koya, R. C., Lee, H., Chen, Z., Lee, M. K., Attar, N., Sazegar, H.*, et al.* (2010). Melanomas acquire resistance to B-RAF(V600E) inhibition by RTK or N-RAS upregulation. Nature *468*, 973-977.
Nelson, A. A., and Tsao, H. (2009). Melanoma and genetics. Clin Dermatol *27*, 46-52.
Nikolaou, V. A., Stratigos, A. J., Flaherty, K. T., and Tsao, H. (2012). Melanoma: new insights and new therapies. J Invest Dermatol *132*, 854-863.
O'Brien, C. A., Pollett, A., Gallinger, S., and Dick, J. E. (2007). A human colon cancer cell capable of initiating tumour growth in immunodeficient mice. Nature *445*, 106-110.
O'Day, S. J., Hamid, O., and Urba, W. J. (2007). Targeting cytotoxic T-lymphocyte antigen-4 (CTLA-4): a novel strategy for the treatment of melanoma and other malignancies. Cancer *110*, 2614-2627.
Omholt, K., Grafstrom, E., Kanter-Lewensohn, L., Hansson, J., and Ragnarsson-Olding, B. K. (2011). KIT pathway alterations in mucosal melanomas of the vulva and other sites. Clin Cancer Res *17*, 3933-3942.
Onken, M. D., Worley, L. A., Long, M. D., Duan, S., Council, M. L., Bowcock, A. M., and Harbour, J. W. (2008). Oncogenic mutations in GNAQ occur early in uveal melanoma. Invest Ophthalmol Vis Sci *49*, 5230-5234.
Osawa, T., Muramatsu, M., Watanabe, M., and Shibuya, M. (2009). Hypoxia and low-nutrition double stress induces aggressiveness in a murine model of melanoma. Cancer Sci *100*, 844-851.
Papandreou, I., Lim, A. L., Laderoute, K., and Denko, N. C. (2008). Hypoxia signals autophagy in tumor cells via AMPK activity, independent of HIF-1, BNIP3, and BNIP3L. Cell Death Differ.
Paraiso, K. H., Fedorenko, I. V., Cantini, L. P., Munko, A. C., Hall, M., Sondak, V. K., Messina, J. L., Flaherty, K. T., and Smalley, K. S. (2010). Recovery of phospho-ERK activity allows melanoma cells to escape from BRAF inhibitor therapy. Br J Cancer *102*, 1724-1730.
Paraiso, K. H., Xiang, Y., Rebecca, V. W., Abel, E. V., Chen, Y. A., Munko, A. C., Wood, E., Fedorenko, I. V., Sondak, V. K., Anderson, A. R.*, et al.* (2011). PTEN loss confers BRAF inhibitor resistance to melanoma cells through the suppression of BIM expression. Cancer Res *71*, 2750-2760.
Pinner, S., Jordan, P., Sharrock, K., Bazley, L., Collinson, L., Marais, R., Bonvin, E., Goding, C., and Sahai, E. (2009). Intravital imaging reveals transient changes in pigment production and Brn2 expression during metastatic melanoma dissemination. Cancer Res *69*, 7969-7977.
Platz, A., Egyhazi, S., Ringborg, U., and Hansson, J. (2008). Human cutaneous melanoma; a review of NRAS and BRAF mutation frequencies in relation to histogenetic subclass and body site. Mol Oncol *1*, 395-405.
Poulikakos, P. I., and Rosen, N. (2011). Mutant BRAF melanomas--dependence and resistance. Cancer Cell *19*, 11-15.
Poulikakos, P. I., Zhang, C., Bollag, G., Shokat, K. M., and Rosen, N. (2010). RAF inhibitors transactivate RAF dimers and ERK signalling in cells with wild-type BRAF. Nature *464*, 427-430.
Pouyssegur, J., Dayan, F., and Mazure, N. M. (2006). Hypoxia signalling in cancer and approaches to enforce tumour regression. Nature *441*, 437-443.
Prasmickaite, L., Skrbo, N., Hoifodt, H. K., Suo, Z., Engebraten, O., Gullestad, H. P., Aamdal, S., Fodstad, O., and Maelandsmo, G. M. (2010). Human malignant melanoma harbours a large fraction of highly clonogenic cells that do not express markers associated with cancer stem cells. Pigment Cell Melanoma Res *23*, 449-451.

Quintana, E., Shackleton, M., Sabel, M. S., Fullen, D. R., Johnson, T. M., and Morrison, S. J. (2008). Efficient tumour formation by single human melanoma cells. Nature *456*, 593-598.

Reya, T., Morrison, S. J., Clarke, M. F., and Weissman, I. L. (2001). Stem cells, cancer, and cancer stem cells. Nature *414*, 105-111.

Rezvani, H. R., Ali, N., Nissen, L. J., Harfouche, G., de Verneuil, H., Taieb, A., and Mazurier, F. (2011). HIF-1alpha in epidermis: oxygen sensing, cutaneous angiogenesis, cancer, and non-cancer disorders. J Invest Dermatol *131*, 1793-1805.

Ricci-Vitiani, L., Lombardi, D. G., Pilozzi, E., Biffoni, M., Todaro, M., Peschle, C., and De Maria, R. (2007). Identification and expansion of human colon-cancer-initiating cells. Nature *445*, 111-115.

Robert, C., Arnault, J. P., and Mateus, C. (2011a). RAF inhibition and induction of cutaneous squamous cell carcinoma. Curr Opin Oncol *23*, 177-182.

Robert, C., Thomas, L., Bondarenko, I., O'Day, S., M, D. J., Garbe, C., Lebbe, C., Baurain, J. F., Testori, A., Grob, J. J.*, et al.* (2011b). Ipilimumab plus dacarbazine for previously untreated metastatic melanoma. N Engl J Med *364*, 2517-2526.

Roesch, A., Fukunaga-Kalabis, M., Schmidt, E. C., Zabierowski, S. E., Brafford, P. A., Vultur, A., Basu, D., Gimotty, P., Vogt, T., and Herlyn, M. (2010). A temporarily distinct subpopulation of slow-cycling melanoma cells is required for continuous tumor growth. Cell *141*, 583-594.

Rofstad, E. K., Galappathi, K., Mathiesen, B., and Ruud, E. B. (2007). Fluctuating and diffusion-limited hypoxia in hypoxia-induced metastasis. Clin Cancer Res *13*, 1971-1978.

Rusthoven, J. J., Quirt, I. C., Iscoe, N. A., McCulloch, P. B., James, K. W., Lohmann, R. C., Jensen, J., Burdette-Radoux, S., Bodurtha, A. J., Silver, H. K.*, et al.* (1996). Randomized, double-blind, placebo-controlled trial comparing the response rates of carmustine, dacarbazine, and cisplatin with and without tamoxifen in patients with metastatic melanoma. National Cancer Institute of Canada Clinical Trials Group. J Clin Oncol *14*, 2083-2090.

Sakaizawa, K., Goto, Y., Kiniwa, Y., Uchiyama, A., Harada, K., Shimada, S., Saida, T., Ferrone, S., Takata, M., Uhara, H., and Okuyama, R. (2012). Mutation analysis of BRAF and KIT in circulating melanoma cells at the single cell level. Br J Cancer *106*, 939-946.

Saldanha, G., Purnell, D., Fletcher, A., Potter, L., Gillies, A., and Pringle, J. H. (2004). High BRAF mutation frequency does not characterize all melanocytic tumor types. Int J Cancer *111*, 705-710.

Schatton, T., Murphy, G. F., Frank, N. Y., Yamaura, K., Waaga-Gasser, A. M., Gasser, M., Zhan, Q., Jordan, S., Duncan, L. M., Weishaupt, C.*, et al.* (2008). Identification of cells initiating human melanomas. Nature *451*, 345-349.

Schreck, R., and Rapp, U. R. (2006). Raf kinases: oncogenesis and drug discovery. Int J Cancer *119*, 2261-2271.

Semenza, G. L. (2003). Targeting HIF-1 for cancer therapy. Nat Rev Cancer *3*, 721-732.

Semenza, G. L. (2007). Oxygen-dependent regulation of mitochondrial respiration by hypoxia-inducible factor 1. Biochem J *405*, 1-9.

Semenza, G. L., and Wang, G. L. (1992). A nuclear factor induced by hypoxia via de novo protein synthesis binds to the human erythropoietin gene enhancer at a site required for transcriptional activation. Mol Cell Biol *12*, 5447-5454.

Shachaf, C. M., Kopelman, A. M., Arvanitis, C., Karlsson, A., Beer, S., Mandl, S., Bachmann, M. H., Borowsky, A. D., Ruebner, B., Cardiff, R. D.*, et al.* (2004). MYC inactivation uncovers pluripotent differentiation and tumour dormancy in hepatocellular cancer. Nature *431*, 1112-1117.

Shah, S. P., Roth, A., Goya, R., Oloumi, A., Ha, G., Zhao, Y., Turashvili, G., Ding, J., Tse, K., Haffari, G.*, et al.* (2012). The clonal and mutational evolution spectrum of primary triple-negative breast cancers. Nature.

Shao, Y., and Aplin, A. E. (2010). Akt3-mediated resistance to apoptosis in B-RAF-targeted melanoma cells. Cancer Res *70*, 6670-6681.

Sidransky, D., Mikkelsen, T., Schwechheimer, K., Rosenblum, M. L., Cavanee, W., and Vogelstein, B. (1992). Clonal expansion of p53 mutant cells is associated with brain tumour progression. Nature *355*, 846-847.

Singh, S. K., Hawkins, C., Clarke, I. D., Squire, J. A., Bayani, J., Hide, T., Henkelman, R. M., Cusimano, M. D., and Dirks, P. B. (2004). Identification of human brain tumour initiating cells. Nature *432*, 396-401.

Smalley, K. S., Lioni, M., Dalla Palma, M., Xiao, M., Desai, B., Egyhazi, S., Hansson, J., Wu, H., King, A. J., Van Belle, P.*, et al.* (2008). Increased cyclin D1 expression can mediate BRAF inhibitor resistance in BRAF V600E-mutated melanomas. Mol Cancer Ther *7*, 2876-2883.

Solit, D., and Sawyers, C. L. (2010). Drug discovery: How melanomas bypass new therapy. Nature *468*, 902-903.

Studer, L., Csete, M., Lee, S. H., Kabbani, N., Walikonis, J., Wold, B., and McKay, R. (2000). Enhanced proliferation, survival, and dopaminergic differentiation of CNS precursors in lowered oxygen. J Neurosci *20*, 7377-7383.

Sun, B., Zhang, S., Zhang, D., Gu, Y., Zhang, W., and Zhao, X. (2007). The influence of different microenvironments on melanoma invasiveness and microcirculation patterns: an animal experiment study in the mouse model. J Cancer Res Clin Oncol *133*, 979-985.

Søndergaard, J. N., Nazarian, R., Wang, Q., Guo, D., Hsueh, T., Mok, S., Sazegar, H., MacConaill, L. E., Barretina, J. G., Kehoe, S. M.*, et al.* (2010). Differential sensitivity of melanoma cell lines with BRAFV600E mutation to the specific Raf inhibitor PLX4032. J Transl Med *8*, 39.

Van Raamsdonk, C. D., Bezrookove, V., Green, G., Bauer, J., Gaugler, L., O'Brien, J. M., Simpson, E. M., Barsh, G. S., and Bastian, B. C. (2009). Frequent somatic mutations of GNAQ in uveal melanoma and blue naevi. Nature *457*, 599-602.

Van Raamsdonk, C. D., Griewank, K. G., Crosby, M. B., Garrido, M. C., Vemula, S., Wiesner, T., Obenauf, A. C., Wackernagel, W., Green, G., Bouvier, N.*, et al.* (2010). Mutations in GNA11 in uveal melanoma. N Engl J Med *363*, 2191-2199.

Vaupel, P., Kallinowski, F., and Okunieff, P. (1989). Blood flow, oxygen and nutrient supply, and metabolic microenvironment of human tumors: a review. Cancer Res *49*, 6449-6465.

Veierod, M. B., Weiderpass, E., Thorn, M., Hansson, J., Lund, E., Armstrong, B., and Adami, H. O. (2003). A prospective study of pigmentation, sun exposure, and risk of cutaneous malignant melanoma in women. J Natl Cancer Inst *95*, 1530-1538.

Villanueva, J., Vultur, A., Lee, J. T., Somasundaram, R., Fukunaga-Kalabis, M., Cipolla, A. K., Wubbenhorst, B., Xu, X., Gimotty, P. A., Kee, D.*, et al.* (2010). Acquired resistance to BRAF inhibitors mediated by a RAF kinase switch in melanoma can be overcome by cotargeting MEK and IGF-1R/PI3K. Cancer Cell *18*, 683-695.

Wang, G. L., Jiang, B. H., Rue, E. A., and Semenza, G. L. (1995). Hypoxia-inducible factor 1 is a basic-helix-loop-helix-PAS heterodimer regulated by cellular O2 tension. Proc Natl Acad Sci U S A *92*, 5510-5514.

Warburg, O. (1956). On respiratory impairment in cancer cells. Science *124*, 269-270.

Weir, E. K., Lopez-Barneo, J., Buckler, K. J., and Archer, S. L. (2005). Acute oxygen-sensing mechanisms. N Engl J Med *353*, 2042-2055.

Wenger, R. H., Stiehl, D. P., and Camenisch, G. (2005). Integration of oxygen signaling at the consensus HRE. Sci STKE *2005*, re12.

Widmer, D. S., Cheng, P. F., Eichhoff, O. M., Belloni, B. C., Zipser, M. C., Schlegel, N. C., Javelaud, D., Mauviel, A., Dummer, R., and Hoek, K. S. (2012). Systematic classification of melanoma cells by phenotype-specific gene expression mapping. Pigment Cell Melanoma Res.

Wolchok, J. D., Neyns, B., Linette, G., Negrier, S., Lutzky, J., Thomas, L., Waterfield, W., Schadendorf, D., Smylie, M., Guthrie, T., Jr.*, et al.* (2010). Ipilimumab monotherapy in patients with pretreated advanced melanoma: a randomised, double-blind, multicentre, phase 2, dose-ranging study. Lancet Oncol *11*, 155-164.

Wu, X., Northcott, P. A., Dubuc, A., Dupuy, A. J., Shih, D. J., Witt, H., Croul, S., Bouffet, E., Fults, D. W., Eberhart, C. G.*, et al.* (2012). Clonal selection drives genetic divergence of metastatic medulloblastoma. Nature *482*, 529-533.

Yancovitz, M., Litterman, A., Yoon, J., Ng, E., Shapiro, R. L., Berman, R. S., Pavlick, A. C., Darvishian, F., Christos, P., Mazumdar, M.*, et al.* (2012). Intra- and inter-tumor heterogeneity of BRAF(V600E))mutations in primary and metastatic melanoma. PLoS One *7*, e29336.

Yang, H., Higgins, B., Kolinsky, K., Packman, K., Go, Z., Iyer, R., Kolis, S., Zhao, S., Lee, R., Grippo, J. F.*, et al.* (2010). RG7204 (PLX4032), a selective BRAFV600E inhibitor, displays potent antitumor activity in preclinical melanoma models. Cancer Res *70*, 5518-5527.

Yoshimura, H., Dhar, D. K., Kohno, H., Kubota, H., Fujii, T., Ueda, S., Kinugasa, S., Tachibana, M., and Nagasue, N. (2004). Prognostic impact of hypoxia-inducible factors 1alpha and 2alpha in colorectal cancer patients: correlation with tumor angiogenesis and cyclooxygenase-2 expression. Clin Cancer Res *10*, 8554-8560.

Zhong, Y., Guan, K., Zhou, C., Ma, W., Wang, D., Zhang, Y., and Zhang, S. (2010). Cancer stem cells sustaining the growth of mouse melanoma are not rare. Cancer Lett *292*, 17-23.

4. Material and methods

4.1 Chemicals and consumables

Acetone	Kantons-Apotheke, Zürich
Agarose	Eurobio AG (GEPA GA07-64)
Calcium chloride	Sigma
Cell culture flasks	BD Biosciences, Falcon
Cell culture inserts	Uncoated: BD Biosciences (353097)
	Coated: Biocoat BD Biosciences (354480)
Cell scraper	Thermo Scientific, Nunc (179693)
Chloroform	FLUKA Chemie AG
Cobalt(II)-chloride	Sigma (232696)
Cotton swabs	Migros, Zürich
DMSO	Sigma
dNTP	Applied Biosystems
DNA marker	Fermentas
Ethanol	FLUKA Chemie AG
Ethidium bromide	Invitrogen (15585-011)
Formaldehyde	Sigma
Glycerol	FLUKA Chemie AG
Glycine	FLUKA Chemie AG
HEPES	FLUKA Chemie AG
Hydrochloric acid	FLUKA Chemie AG
Isopropanol	Kantons-Apotheke, Zürich
Loading Dye	Fermentas
Matrigel	BD Biosciences (356234)
Magnesium chloride	Applied Biosystems
Methanol	Sigma
MTT	Thiazolyl Blue Tetrazolium Bromide Sigma (M2128)
NP-40	FLUKA Chemie AG
Paraffin	Paraplast, McCormick scientific (39501006)
Paraformaldehyde	FLUKA Chemie AG
Pertex	Bio-Systems (41-4012-00)

Potassium chloride	FLUKA Chemie AG
Protein marker	Invitrogen; Seeblue plus2 prestained standard (LC5925)
RNA marker	Fermentas
RNase inhibitor	Roche
Skimmed milk powder	Migros, Zürich
Slides superfrost	Thermo Scientific (J1810AMNZ)
Sodium azide	Sigma
Sodium chloride	Sigma
Sodium dodecyl sulfate (SDS)	Sigma
Trizma base	Sigma
TRIzol	Invitrogen
Tween	Sigma
Xylene	FLUKA Chemie AG

4.1.1 Transfection agents

INTERFERin	Polyplus, Chemie Brunschwig AG (409-50)
JetPEI	Polyplus, Chemie Brunschwig AG (101-40)

4.1.2 Enzymes

Collagenase-IA	Sigma (C2674)
Dispase	Dispase II; Roche (04942078001)
DNase	RNase-Free DNase Set; Qiagen (79254)
DNA polymerases	FastStart Universal SYBR Green Master (ROX); Roche (04913914001)
	AmpliTaq Gold 360 DNA polymerase; Applied Biosystems (4398823)
Proteinase K	DAKO (S3020)
Trypsin/EDTA	Biochrom AG (L2143)

4.1.3 Cell isolation and culture reagents

254 Melanocyte Medium	GIBCO (M254-500)

Calcium solution	50mM $CaCl_2$
DMEM	GIBCO (41966-029)
FBS heat inactivated	GIBCO (10500)
L-Glutamate	Biochrom AG (k0282)
PBS Dulbecco	Biochrom AG (L1825)
RPMI 1640	GIBCO (31870-025)
Sodium pyruvate	GIBCO (11360)
Stop-solution	50mM Tris Base 150mM NaCl 10mM EDTA pH 7.4

4.1.4 Growth factors, cytokines and drugs

Recombinant Human Transforming Growth Factor-beta1; GIBCO (PHG9202)
YC-1 (3-(5'-Hydroxymethyl-2'-furyl)-1-benylindazole; Calbiochem (688100)
Vemurafenib; Roche (PLX4032)

4.1.5 Antibiotics

Antibiotic/Antimycotic	GIBCO; Anti-Anti (15240-096)
Echinomycin Streptomyces sp.	Calbiochem (330175)

4.1.6 Kits

DNA Cleanup Kit:	MinElute Reaction Cleanup Kit; Qiagen (28204) Qiaquick PCR Purification Kit; Qiagen (28104)
DNA isolation:	QIAmp DNA Blood Mini Kit; Qiagen (51104) NucleoSpin Tissue XS KIT; Machery-Nagel (740901.50)
Diff-Quick staining kit	Medion Diagnostics (130832)
ELISA	DuoSet ELISA for human VEGF; R&D Systems (DY293B)
Maxi-prep	EndoFree Plasmid Maxi Kit; Qiagen (136254507)
Microarrays:	MessageAmp II-Biotin Enhanced (AM1791)

	Nugen applause WT-Amp Plus ST-System (5510-24)
	Nugen FL-Ovation cDNA Biotin Module V2 (4200-12)
Protein conc. Assay	Dc Protein Assay; BioRad (500-0114)
qRT-PCR:	RT2-HT First Strand Kit; Qiagen (330411)
	Reverse Transcription System; Promega (A3500)
RNA:	RNeasy Mini; Qiagen (74104)

4.1.7 Arrays and plates

Microarray:	GeneChip Human Genome U133 Plus 2.0 Array
	GeneChip Human Exon 1.0 ST Array
qRT-PCR plates:	MicroAmp Fast Optical 96-well Reaction Plate; Applied Biosystems (4346906)
	MicroAmp Optical 384-well Reaction Plate with Barcode; Applied Biosystems (4309849)
qRT-PCR arrays:	Custom RT2 Profiler PCR Array; Qiagen (CAH10586E-6)
	RT2 Profiler PCR Array Human Cancer Drug Targets; Qiagen (PAHS-507E-4)

4.1.8 Standard buffers

TAE

40mM Trizma base

1mM EDTA

TBE

89mM Tris

89mM Boric Acid

2mM EDTA, pH 8.0

TBS

20mM Trizma base

137mM NaCl

Ph 7.6

TBST

20mM Trizma base

137mM NaCl

pH 7.6

0.1% TWEEN 20

RIPA

20mM Tris-HCl, pH 7.5

150mM NaCl

5mM EDTA

1% Triton-X100

1mM Na_3VO_4

1 tablet protease inhibitor cocktail per 100ml total buffer solution; Roche

1ml phosphatase inhibitor cocktail 1 per 100ml total buffer solution; Sigma

Stripping buffer for reprobing western blots

(mild, www.abcam.com/technical)

15g glycine

1g SDS

10ml Tween 20

Adjust pH to 2.2

Bring volume up to 1l with ultrapure water

Buffers to obtain nuclear and cytosolic protein extracts

Buffer A:

10 mM HEPES (pH 7.9)

10 mM KCl

1.5 mM $MgCl_2$

0.625% NP-40

protease and phosphatase inhibitors; Roche

Buffer B:

20 mM HEPES (pH 7.9)

1.5 mM $MgCl_2$

420 mM NaCl

25% glycerol
protease and phosphatase inhibitors; Roche

4.1.9 Lentiviral particles

pBlasti_GFP in lentivirus

4.1.10 Oligonucleotides

4.1.10.1 Plasmids

IPAS:	pFLAG-CMV-2_IPAS
GFP	pMax_GFP
LAC-Z	pCMV3.1_lacZ

4.1.10.2 Primers for genotyping

NRAS_exon_2	5'-AACCTAAAACCAACTCTTCCCA-3' and
	5'-CCCCTTACCCTCCACAC-3'
BRAF_exon_15	5'-CTAAGAGGAAAGATGAAGTACTATG-3' and
	5'-CTAGTAACTCAGCAGCATCTCAG-3'

4.1.10.3 Primers for qRT-PCR

18s-RNA:	5'-AAACGGCTACCACATCCA AG-3' and
	5'-CCTCCAATGGATCCTCGTTA-3'
WNT5A:	5'-AGGGCTCCTACGAGAGTGCT-3' and
	5'-GACACCCCATGGCACTTG-3'
RPS13:	5'-GCTGTTCGAAAGCATCTTGA-3' and
	5'-AGGGCAGAGGCTGTAGATGA-3'
RPL28:	5'-GCAATTGGTTCCGCTACAAC-3' and
	5'-TGTTCTTGCGGATCATGTGT-3'
TYR:	5'-ACAACAGCCATCAGTCT-3' and

5’-CCTGTACCTGGGACATT3’

GAPDH: 5’-GGTGAAGGTCGGAGTCAACGG-3’ and
5’-GGTCATGAGTCCTTCCACGATACC-3’

β-Actin: 5’-CGACAACGGCTCCGGCATGTGC-3’ and
5’-CGTCACCGGAGTCCATCACGATGC-3’

Hs_EPAS1_1_SG (QT00069587, QuantiTect Primer, Qiagen)
Hs_HIF1A_1_SG (QT00083664, QuantiText Primer, Qiagen)
Hs_MLANA_1_SG (QT00028364, QuantiText Primer, Qiagen)
Hs_MITF_1_SG (QT00037737, QuantiText Primer, Qiagen)
Hs_IRF4_1_SG (QT00065716, QuantiText Primer, Qiagen)
Hs_PDGFC_1_SG (QT00026551, QuantiText Primer, Qiagen)
Hs_ANGPTL4_1_SG (QT00003661, QuantiText Primer, Qiagen)
Hs_B2M_1_SG (QT00088935, QuantiText Primer, Qiagen)
Hs_TUBB_1_SG (QT00089775, QuantiText Primer, Qiagen)
Hs_PPIA_1_SG (QT01866137, QuantiText Primer, Qiagen)
Hs_SERPINE1_1_SG (QT00062496, QuantiText Primer, Qiagen)
Hs_PLAUR_1_SG (QT00076447, QuantiText Primer, Qiagen)
Hs_LOX_1_SG (QT00017311, QuantiText Primer, Qiagen)
Hs_CTGF_1_SG (QT00052899, QuantiText Primer, Qiagen)
Hs_VEGFA_1_SG (QT01682072, QuantiText Primer, Qiagen)
Hs_DKK1_1_SG (QT00009093, QuantiText Primer, Qiagen)

4.1.10.4 siRNAs

All Stars negative control siRNA (1027280, Qiagen)
Hs_EPAS1_4 (NM_001430, S100380226, Qiagen FlexiTube)
Hs_EPAS1_5 (NM_001430; S1002663038, Qiagen FlexiTube)
Hs_HIF1A_5 (NM_001530; S102664053, Qiagen FlexiTube)
Hs_HIF1A_6 (NM_001530; S102664431, Qiagen FlexiTube)
Hs_ANGPTL4_5 (NM_001039667; S103057691, Qiagen FlexiTube)
Hs_ANGPTL4_6 (NM_001039667; S103065734, Qiagen FlexiTube)

4.1.11 Antibodies

4.1.11.1 Western blot Antibodies

Mouse monoclonal anti-MITF 1:500, 2 h at RT in 5% milk, 1% BSA, 55kDa (ab13703, Abcam)

Mouse monoclonal anti-MelanA 1:1000, 2 h at RT in 5% milk, 1% BSA, 18kDa (ab3168, Abcam)

Rabbit anti-PKC 1:300, 2 h at RT in 5% milk, 1% BSA, 82kDa (ab19031, Abcam)

Goat polyclonal anti-Actin 1:1000, 2 h at RT in 5% milk, 1% BSA, 43kDa (sc-1616, Santa Cruz Biotechnology Inc.)

Rabbit polyclonal anti-Cu/Zn-SOD 1:375, 2 h at RT in 5% milk, 1% BSA, 23kDa (SPC-113C/D, StressMarq)

Goat anti-ANGPTL4 1:1000; 2 h at RT in 5% milk, 1% BSA; 50kDa (AF3485, R&D Systems)

Mouse monoclonal anti-Tyrosinase 1:1000; 2 h at RT in 5% milk, 1% BSA; 60kDa (ab58284; Abcam)

Rabbit polyclonal anti-Hif1alpha 1:1000; overnight at 4°C. in 5% BSA; 120kDa (3716; Cell Signaling)

Mouse monoclonal anti-HIF1alpha 1:1000; overnight at 4°C. in 5% BSA; 120kDa (610959; BD Biosciences)

Mouse monoclonal anti-HIF2alpha 1:500; overnight at 4°C. in 5% BSA; 120kDa (NB100-132; Novus Biologicals)

Goat anti-WNT5A 1:500, overnight at 4°C. in 5% BSA, 42kDa (R&D)

anti phospho-PKC (pan) 1:1000; overnight at 4°C. in 5% BSA, (Cell Signalling),

Goat polyclonal anti-GAPDH 1:1000; 2 h at RT in 5% milk, 1% BSA; 37kDa (Abcam)

Rabbit polyclonal anti-TGFbeta 1:1000; overnight at 4°C. in 5% BSA; 12, 25, 45-65kDa (3711, Cell Signaling)

Rabbit monoclonal anti-Phospho-p44/42 MAPK (Erk1/2) (Thr202/Tyr204) 1:2000; overnight at 4°C. in 5% BSA; 42,44kDa (4370; Cell Signaling)

Rabbit monoclonal anti- p44/42 MAPK (Erk1/2) 1:1000; overnight at 4°C. in 5% BSA; 42,44kDa (4695; Cell Signaling)

4.1.11.2 Secondary Antibodies

Goat anti-rabbit IgG-HRP (170-6515, Bio-Rad, Hercules, CA)
Rabbit polyclonal anti mouse IgG-HRP (ab97046, Abcam)
Rabbit anti-goat IgG-HRP (sc-2768, Abcam Cambridge)

4.1.11.3 Immunohistochemistry Antibodies

HIF1alpha (ab16066; Abcam; 1:200)
Phospho-p44/42 MAPK (Erk1/2) (Thr202/Tyr204), (4370; Cell Signaling; 1:400)
p44/42 MAPK (Erk1/2) (4695; Cell Signaling; 1:250)
MelanA (Novocastra; NCL-L-MelanA; EDTA; 1:50)
Glut1 (Cell Marque; 355A-16; EDTA; 1:100)
Ki67 (DAKO; N1633; TRS 6,0; pH 6; ready to use)
Wnt5a (R&D Systems, BAF645; MN1:50)
D2-40 (DAKO; M3619; TRS 6.0; pH 6.0; 1:100)
CD31 (DAKO; M0823; Proteinkinase K; 1:40)
Mitf (Zytomed; 513-6164; TRS9.0; pH9.0;1:200)

4.1.12 Custom RT2 Profiler PCR Array (CAH10586E-6; Qiagen)

Gene Symbol	Refseq #	Official Full Name
ACP5	NM_001611	Acid phosphatase 5, tartrate resistant
ADAM12	NM_003474	ADAM metallopeptidase domain 12
ADCY2	NM_020546	Adenylate cyclase 2 (brain)
APOE	NM_000041	Apolipoprotein E
ASAH1	NM_004315	N-acylsphingosine amidohydrolase (acid ceramidase) 1
AXL	NM_001699	AXL receptor tyrosine kinase
BIRC3	NM_001165	Baculoviral IAP repeat-containing 3
BIRC7	NM_022161	Baculoviral IAP repeat-containing 7
CAPN3	NM_173090	Calpain 3, (p94)
CDH1	NM_004360	Cadherin 1, type 1, E-cadherin (epithelial)
CDH13	NM_001257	Cadherin 13, H-cadherin (heart)
CDK2	NM_001798	Cyclin-dependent kinase 2
CDK5R1	NM_003885	Cyclin-dependent kinase 5, regulatory subunit 1 (p35)
CEACAM1	NM_001712	Carcinoembryonic antigen-related cell adhesion molecule 1 (biliary glycoprotein)
COL13A1	NM_080815	Collagen, type XIII, alpha 1
CRIM1	NM_016441	Cysteine rich transmembrane BMP regulator 1 (chordin-like)
CRISPLD2	NM_031476	Cysteine-rich secretory protein LCCL domain containing 2
CYR61	NM_001554	Cysteine-rich, angiogenic inducer, 61
DAPK1	NM_004938	Death-associated protein kinase 1
DCT	NM_001922	Dopachrome tautomerase (dopachrome delta-isomerase, tyrosine-related protein 2)
DPYD	NM_000110	Dihydropyrimidine dehydrogenase
EFEMP1	NM_004105	EGF-containing fibulin-like extracellular matrix protein 1
EGFR	NM_005228	Epidermal growth factor receptor (erythroblastic leukemia viral (v-erb-b) oncogene homolog, avian)
EIF2C2	NM_012154	Eukaryotic translation initiation factor 2C, 2
F2RL1	NM_005242	Coagulation factor II (thrombin) receptor-like 1
FAM174B	NM_207446	Family with sequence similarity 174, member B
MYOF	NM_013451	Myoferlin
FGF2	NM_002006	Fibroblast growth factor 2 (basic)

FLNB	NM_001457	Filamin B, beta (actin binding protein 278)
FOXD1	NM_004472	Forkhead box D1
FST	NM_006350	Follistatin
FZD2	NM_001466	Frizzled homolog 2 (Drosophila)
GALNT3	NM_004482	UDP-N-acetyl-alpha-D-galactosamine:polypeptide N-acetylgalactosaminyltransferase 3 (GalNAc-T3)
GPM6B	NM_005278	Glycoprotein M6B
GPR143	NM_000273	G protein-coupled receptor 143
GPRC5B	NM_016235	G protein-coupled receptor, family C, group 5, member B
GYG2	NM_003918	Glycogenin 2
HEG1	NM_020733	HEG homolog 1 (zebrafish)
NTM	NM_016522	Neurotrimin
HPS4	NM_022081	Hermansky-Pudlak syndrome 4
HS3ST3A1	NM_006042	Heparan sulfate (glucosamine) 3-O-sulfotransferase 3A1
INPP4B	NM_003866	Inositol polyphosphate-4-phosphatase, type II, 105kDa
IRF4	NM_002460	Interferon regulatory factor 4
ITGA2	NM_002203	Integrin, alpha 2 (CD49B, alpha 2 subunit of VLA-2 receptor)
ITGA3	NM_002204	Integrin, alpha 3 (antigen CD49C, alpha 3 subunit of VLA-3 receptor)
KCNMA1	NM_002247	Potassium large conductance calcium-activated channel, subfamily M, alpha member 1
RP1-21O18.1	NM_001018000	Kazrin
LOXL2	NM_002318	Lysyl oxidase-like 2
MBP	NM_002385	Myelin basic protein
MITF	NM_000248	Microphthalmia-associated transcription factor
MLANA	NM_005511	Melan-A
MYO1D	NM_015194	Myosin ID
NR4A3	NM_006981	Nuclear receptor subfamily 4, group A, member 3
NRP1	NM_003873	Neuropilin 1
NUAK1	NM_014840	NUAK family, SNF1-like kinase, 1
OCA2	NM_000275	Oculocutaneous albinism II
OSMR	NM_003999	Oncostatin M receptor
PDGFC	NM_016205	Platelet derived growth factor C

PHACTR1	NM_030948	Phosphatase and actin regulator 1
PIR	NM_003662	Pirin (iron-binding nuclear protein)
PLXNC1	NM_005761	Plexin C1
PODXL	NM_005397	Podocalyxin-like
SIRPA	NM_080792	Signal-regulatory protein alpha
RAB27A	NM_183236	RAB27A, member RAS oncogene family
RAB38	NM_022337	RAB38, member RAS oncogene family
RHOQ	NM_012249	Ras homolog gene family, member Q
RRAGD	NM_021244	Ras-related GTP binding D
S100A2	NM_005978	S100 calcium binding protein A2
SEMA6A	NM_020796	Sema domain, transmembrane domain (TM), and cytoplasmic domain, (semaphorin) 6A
SILV	NM_006928	Silver homolog (mouse)
SLC22A4	NM_003059	Solute carrier family 22 (organic cation/ergothioneine transporter), member 4
SLC45A2	NM_016180	Solute carrier family 45, member 2
SLIT2	NM_004787	Slit homolog 2 (Drosophila)
ST3GAL6	NM_006100	ST3 beta-galactoside alpha-2,3-sialyltransferase 6
SYNJ2	NM_003898	Synaptojanin 2
TCF7L2	NM_030756	Transcription factor 7-like 2 (T-cell specific, HMG-box)
THBS1	NM_003246	Thrombospondin 1
TLE4	NM_007005	Transducin-like enhancer of split 4 (E(sp1) homolog, Drosophila)
TNFRSF11B	NM_002546	Tumor necrosis factor receptor superfamily, member 11b
TNFRSF14	NM_003820	Tumor necrosis factor receptor superfamily, member 14 (herpesvirus entry mediator)
TPBG	NM_006670	Trophoblast glycoprotein
TPM1	NM_000366	Tropomyosin 1 (alpha)
TRPM1	NM_002420	Transient receptor potential cation channel, subfamily M, member 1
TYR	NM_000372	Tyrosinase (oculocutaneous albinism IA)
TYRP1	NM_000550	Tyrosinase-related protein 1
WNT5A	NM_003392	Wingless-type MMTV integration site family, member 5A
ZEB1	NM_030751	Zinc finger E-box binding homeobox 1

ZFYVE16	NM_014733	Zinc finger, FYVE domain containing 16
TRAM2	NM_012288	Translocation associated membrane protein 2
AMOTL2	NM_016201	Angiomotin like 2
B2M	NM_004048	Beta-2-microglobulin
RPL13A	NM_012423	Ribosomal protein L13a
ACTB	NM_001101	Actin, beta
HGDC	SA_00105	Human Genomic DNA Contamination
RTC	SA_00104	Reverse Transcription Control
PPC	SA_00103	Positive PCR Control

4.2 Devices

qRT-PCR:	VIIA7; Applied Biosystems
	Roche; Lightcycler
Pipetting robot	Qiagen; Qiagility
Sequencer	Applied Biosystems/HITACHI; 3500
	Genetic Analyzer
Cell counter	Casy cell counter, Innovatis AG
Thermocycler:	Biometra; T1
	Biometra; T-Gradient
Optical density reader:	Anthos HTII microplate reader
	BIORAD Model 550 microplate reader

4.3 Methods

4.3.1 DNA methods

4.3.1.1 Isolation

DNA was extracted using the QIAamp DNA Mini kit (Qiagen). DNA from paraffin-embedded tumor punches were extracted using the NucleoSpin Tissue XS KIT (Machery-Nagel, Switzerland).

4.3.1.2 BigDye 3.1 Sequencing

Template Type

Template	Quantity
PCR Product:	
100-200 bp	1-3 ng
200-500 bp	3-10 ng
500-1000 bp	5-20 ng
1000-2000 bp	10-40 ng
>2000 bp	20-50 ng
Single-stranded	25-50 ng
Double-stranded	150-300 ng
Cosmid, BAC	0.5 – 1.0 μg
Bacterial genomic DNA	2-3 μg

Reaction Mix

Reagent	Volume
Ready Reaction Premix	2 μl
5X Sequencing Buffer	1 μl
Primer (1 uM)	3 μl
Template	4 μl
Total	10 μl

PCR Protocol

Temperature	Time	Cycles
96ºC	60 s	1
96ºC 50ºC 60ºC	10 s 5 s 240 s	50
4ºC	long-term	

Big Dye Xterminator Purification

Reagent	Volume/Well	Volume/Plate
SAM solution	49.5 μl	4752 μl
XTerminator	11 μl	1056 μl

Add 55 μl of this mix into each well. Vortex plate on IKA MS3 Vortexer at 2000 rpm for 30 min.

Mutation status was analyzed by variant reporter (AB Biosciences)

4.3.2 RNA methods

4.3.2.1 Isolation

Total RNA was extracted from melanoma cell cultures using TRIzol (Invitrogen). The medium was removed from the cells and the cell culture flask was placed on ice immediately. 1 ml of TRIzol was added to a T75 cell culture flask (when using other sizes of flasks the volume of all reagents were adjusted accordingly) and incubated for 5 min at RT. The samples were either frozen at -80°C for RNA isolation at a later stage or 200 µl of chloroform was added followed by 15 s shaking of the samples and 2-3 minutes incubation at RT. After a centrifugation step for 15 min at 12000 g at 4°C the upper phase (aqueous) was transferred to a new tube followed by adding 0.5 ml isopropyl alcohol, inverting 6 times and incubation for 10 min at 2-8°C. By centrifugation for 10 min at 12000 g at 4°C, the RNA was pelleted. The supernatant was discarded. The pellet was washed by adding 1 ml of 75% EtOH, vortexing and then centrifuging for 5 min at 7500 g at 2-8°C. After air drying the pellet for 10 minutes, the RNA was resolved in 20 µl RNase free water.

4.3.2.2 cDNA synthesis

Total RNA was used for cDNA synthesis using Promega's Reverse Transcription System according to the supplied protocol (Promega, Madison, WI, USA).

4.3.2.3 qRT-PCR

Gene expression was quantified using the Light Cycler DNA Master SYBR Green Kit (Roche, Basel, Switzerland) on 1 µg of template cDNA with Roche's Light Cycler 4.0 instrument. Alternatively, we used the FastStart Universal SYBR Green Master (ROX); 04913914001, Roche) with the Viia7 system from Applied Biosystems. The following amplification program was used: 95°C., 10 sec; 58°C., 30 sec., ~40 cycles.

Messenger RNA levels were compared against standard curves and normalized to a housekeeping gene.

4.3.2.4 siRNA

Silencing RNA (siRNA) transfection of melanoma cells was carried out using INTERFERin transfection solution according to the manufacturer's protocol (Polyplus-transfection, Illkirch, France). Cells were transfected with 10 nM of siRNA (Qiagen) for 24h, 48h or 72 h before RNA or protein was extracted. As control siRNA the All-Star negative siRNA sequence (Qiagen) was used.

4.3.2.5 Plasmid transfection

Transfection of melanoma cells with plasmids was done using JetPEI transfection reagent according to the manufacturer's protocol (Polyplus-transfection, Illkirch, France).

4.3.3 Protein methods

4.3.3.1 Preparation of whole cell protein extracts

Cells were washed twice with cold PBS and lysed at 4^{o}C in RIPA protein lysis buffer. After pulse vortexing, the samples were centrifuged at maximal speed for 20 minutes in a microfuge and the supernatant was transferred to a new tube. Here, the samples were either frozen in -80°C or processed further.

4.3.3.2 Isolation of nuclear and cytosolic protein extracts

To obtain protein lysates from cytosolic and nuclear fractions, cells were lysed in protein lysis buffer A. After incubation at 4^{o}C for 10 min, nuclei were pelleted by centrifugation at 5000 rpm for 5 min and the supernatant was kept as the cytoplasmic fraction (which was further centrifuged another three times to remove remaining particulates). Pelleted nuclei were washed three times in protein lysis buffer A, resuspended in protein lysis buffer B and rotated for 1 h at 4^{o}C. After centrifugation at 16000 rpm for 20 min at 4^{o}C the supernatant was used as the nuclear fraction.

4.3.3.3 Measurement of protein concentration

For the measurement of the protein concentration, the BioRad Dc Protein Assay (500-0114) was used according to manufacturer's protocol. The absorbance was measured at 690 nm in an Anthos HT-II microplate reader.

4.3.3.4 SDS- PAGE

Proteins were separated by SDS-PAGE using the NuPAGE SDS-PAGE Gel System (Invitrogen) under reducing conditions. 10-40 μg of protein was mixed with 9 µl of NuPage LDS sample buffer (4x) (Invitrogen, NP0007), 3.6 µl of NUPAGE Sample Reducing (Invitrogen, NP0009) and filled up to 36 µl with RIPA buffer. This mixture was incubated at 85°C. for 10 minutes while shaking at 900 rpm. Depending on the size of the protein, the samples were loaded on precast gels from Invitrogen.

Gels NUPAGE 4-12% BT GEL 1.5 mm 10 W (Invitrogen, NP0335BOX)

NUPAGE 10% BT GEL 1.5 mm 10 W (Invitrogen, NP0315BOX)

NUPAGE Novex 3-8% Tris-Acetate GEL 1.0 mm 10 W (Invitrogen, EA0375BOX)

SDS-Page running buffer

760 ml H_2O

40 ml of NP MOPS SDS Running buffer 20x (Invitrogen, NP0001) or

NP MES SDS Running buffer 20x (Invitrogen, NP0002)

500 μl NUPAGE Antioxidant (Invitrogen, NP0005) was added to 200 ml of the running buffer, which was added to the inner buffer chamber, the rest of the running buffer was filled in the outer buffer chamber. Next to the protein samples, also a Seeblue Plus2 protein marker (Invitrogen, LC5925) was loaded onto the gel. Electrophoresis was carried out in vertical direction at 160 V until the marker reached the end of the gel.

4.3.3.5 Western blot

For the transfer, the gel was taken out of the cassette and placed in the transfer cell, covered with a nitrocellulose membrane and sandwiched by filter papers (Invitrogen, LC2001). The inner transfer chamber was filled with transfer buffer and the outer chamber was filled with ice-cold water. The transfer was carried out in vertical direction at 30 V for 80 to120 minutes.

Transfer buffer

50 ml NP Transfer buffer 20x (Invitrogen, NP00061)

200 ml methanol

750 ml H_2O

After transfer the membranes were washed with TBST followed by blocking with blocking solution (5% milk 1%BSA in TBST) for 2 h at RT. The membranes were probed with primary antibodies, followed by incubation with secondary antibodies which were horseradish peroxidase-conjugated. Bound antibodies were detected using ECL Western Blotting Detection Reagent (28906836, GE Healthcare).

Stripping for reprobing Western blot membranes

The membrane was incubated with stripping buffer for 5-10 minutes at RT, using a volume that covered the membrane. Buffer was discarded and the membrane was washed twice with PBS for 10 minutes, followed by washing twice with TBST for 5 minutes. Now the membrane is ready for the blocking stage. (www.abcam.com/technical)

4.3.3.6 ELIsA

ELISA for VEGF was carried out with the DuoSet ELISA Development System (DY293B; R&D Systems) according to manufacturer's protocol. In short, a 96-well plate was coated with capture antibody and incubated overnight at room

temperature. After several washing-steps the plate with the capture antibody was blocked for a minimum of one hour and washed again. Then the sample was added and incubated for 2 h at RT. After washing, the detection antibody was added followed by a washing step. The streptavidin-HRP solution was added to each well and after an incubation time of 20 minutes, substrate solution and after another 20 minutes stop solution was added. Finally, optical density was determined at 450 nm.

4.3.4 Cell culture

4.3.4.1 Melanoma cells

Melanoma cell cultures were established from surplus material from cutaneous melanoma and melanoma metastases removed by surgery. Written informed consent was approved by the local IRB (EK647 and EK800). Clinical diagnosis was confirmed by histology and immunohistochemistry. Melanoma tumors were cut into small pieces and incubated in dispase mixed with medium in a ratio of 1:1 for 1-4 h at 37°C. After centrifugation at 1500 g for 5 min, the supernatant was discarded. In a second digestion step, the pellet was incubated in 1% collagenase and 10% calcium-solution (50mM $CaCl_2$) in TBS for 1-3 h at 37°C under constant stirring. After centrifugation at 1500 g for 5 min the supernatant was discarded and stop solution (1/10 of the pellet volume) was added. Finally the pellet was washed two times with RPMI and the cells were seeded in a cell culture flask. If necessary, Antibiotic/Antimycotic (GIBCO; Anti-Anti; 15240-096) was added to the medium during the first two or three passages. Melanoma cell cultures were maintained in RPMI (Invitrogen, Carlsbad, CA, USA) supplemented with 5 mM glutamine, 1 mM sodium pyruvate and 10% heat-inactivated fetal calf serum, and they were grown at 37°C and 5% CO_2.

4.3.4.2 Melanocytes

Melanocytes were isolated from normal healthy skin or foreskin. The skin was cut into small pieces and incubated in 1% dispase dissolved in melanocyte culture medium for 15-18 h at 2-8°C. Then the epidermis was manually separated from

dermis and placed on a drop of Trypsin/EDTA for about 15 minutes. Finally, the cells were released from the epidermis by gently scraping with a cell scraper and seeded in a cell culture flask. The melanocyte cell cultures were maintained in 254 Melanocyte Medium (GIBCO; M254-500) with supplement (HMGS-2, S-016-5). If necessary, 1% Antibiotic/Antimycotic (GIBCO; Anti-Anti; 15240-096) was added to the medium during the first two or three passages.

4.3.4.3 HLA-testing of patient material

Patient origin was confirmed through genotyping of patient-derived paraffin-embedded tissues or peripheral blood mononuclear cells using 11 different gene loci (AmpFISTR SGM Plus PCR Amplification Kit, Applied Biosystems).

4.3.5 Histology

4.3.5.1 Immunohistochemistry

All tissue used for immunohistochemistry was fixed in 4% paraformaldehyde and embedded in paraffin. Sections were deparaffinized in xylene and rehydrated. Epitope retrieval was performed in antibody specific buffers. Staining was performed using kits supplied by Ventana or Dako REAL Detection System (kit 5005). Antigen-specific antibodies were applied and visualized with either the iVIEW DAB detection kit (Ventana) or the Chem- Mate detection kit (Dako). Slides were counterstained with haematoxylin. Melanin was visualized using the Masson-Fontana technique with nuclear fast red as counterstain.

4.3.5.2 Image acquisition and analysis

Stained slides were imaged at 0.25 mm per pixel resolution using a ScanScope XT (Aperio, Vista, California, USA) Full-slide scans were captured as high-resolution (0.21 microns/pixel) two-dimensional vector graphic files and selected regions were extracted using ImageScope software (Aperio).

4.3.6 Phenotypic characterization of melanoma cells

4.3.6.1 Matrigel assay

48-well plates were coated with Matrigel™ (356234, BD Biosciences) and 2 x 10^4 and 4 x 10^4 melanoma cells in 400 ml of RPMI complete medium were seeded on them. After incubation for 24 h at 37°C cell morphology and growth patterns were assessed using microscopy.

4.3.6.2 Proliferation assay

Doubling times were assessed by using a Casy cell counter (Roche, Basel, Switzerland) or by manual counting with a Neubauer chamber (hemocytometer).

4.3.6.3 Cell viability assay (MTT)

To assess cell proliferation and viability during treatment with chemicals or hypoxia, melanoma cells were seeded at a minimum density of 2 x10^4 cells in each well of a twenty-four-well plate. After 72 hours the medium was removed and 20 µl of MTT was added to each well. After an incubation of 1 h at 37°C the MTT solution was removed and 200 µl of solution A (95% isopropanol, 5% formic acid) and 200 µl of solution B (10% SDS in PBS) were added. The plate was incubated for 5 min at 37°C, followed by resuspending by pipetting. Then 200 µl of the samples from each well was transferred into a 96 well plate and the optical density was measured at both 595 nm and 620 nm (reference).

4.3.6.4 Motility and Invasion assay

To assess the invasive potential of melanoma cells in vitro, melanoma cells were seeded 48 h prior to the assay at a density of approximately 60% for the proliferative and about 80% for the invasive phenotype cells. The next morning the medium was changed to RPMI complete (3% FBS) and the cells were starved for 48 h. For motility assay, inserts were rehydrated for 2 h at 37°C in starving

medium (without any supplements). Cells were trypsinized, washed twice with PBS and resuspended in starving medium. Then, $5x10^4$ cells in 500 µl starving medium were seeded onto uncoated cell culture inserts with a pore size of 8 µm (BD Biosciences 353097). After incubation at 37°C for 22 hours the membranes of the inserts were fixed, stained, cut out, and mounted on a glass slide. The number of cells, which had moved through the pores to the other side of the membrane, was assessed by microscopy.

For invasion assay the procedure was the same, but the cells were seeded on 8 µm PET membrane with a layer of BD Matrigel™ basement membrane matrix (BD Biosciences, 354480). RPMI containing 10% FCS was used as chemoattractant. Invasion values were calculated by dividing the number of cells migrating through matrix-coated inserts by the number of cells migrating through uncoated inserts.

4.3.6.5 Drug treatment of cells

Melanoma cell cultures were treated with different concentrations of vemurafenib (10 nM, 50 nM, 100 nM, 250 nM, 500 nM, 1 µM) for 72 h under normoxic or hypoxic conditions. After this incubation the effect of the drug treatment and the drug-hypoxia treatment was assessed by doing an MTT or proliferation assay.

4.3.7 Hypoxia

Cells were cultured in a Modular Incubator Chamber (MIC-101, Billups-Rothenberg inc.), flushed with 20 liters/minute (flow meter; RMA-23-SSV; Dwyer) with certified premixed gas including 1% O_2 , 5% CO_2 and 94% N_2 purchased at CARBAGAS. The O_2 concentration inside the chamber was measured with an oxygen sensor (VTI-122, Disposable Polarographic Oxygen Cell; 100122, Vascular Technology). The hypoxia chamber was placed in an incubater at 37°C. Medium exchange and splitting of the cells was performed outside the hypoxic environment.

To stabilize Hif1a expression in melanoma cells under normoxic conditions, cells were treated with 100 μM $CoCl_2$ for 24 h, 48 h or 72 h.

To inhibit expression or stabilization of Hif1a in melanoma cells under hypoxic conditions, cells were treated with 60 μM YC-1, 5 nM of Echinomycin Streptomyces sp. or with 10 nM of siRNA against HIF1a for 24 h, 48 h or 72 h.

4.3.8 DNA Microarray analysis

Total RNA was isolated from melanoma cell cultures using TRIzol according to the manufacturer's instructions (Invitrogen). Total RNA was amplified and biotin-labeled using the "Message Amp II-Biotin Enhanced aRNA Amplification" Kit (Ambion). Biotin-labeled RNA was hybridized to Affymetrix HG-U133 plus 2.0 oligonucleotide microarrays following the manufacturer's protocol (Affymetrix). After hybridization, microarrays were washed and stained using a GeneChip Fluidics Station 450 (Affymetrix), and then scanned using a GeneChip Scanner 7G (Affymetrix). Raw data were processed by Genespring GX 7.3 (RMA) to obtain signal intensity measures for each probeset.

4.3.8.1 Exon chips

Total RNA was isolated from melanoma cell cultures using TRIzol according to the manufacturer's instructions (Invitrogen). Total RNA was amplified with the Nugen applause WT-Amp Plus ST-System (5510-24) and biotin-labeled using the Nugen FL-Ovation cDNA Biotin Module V2 (4200-12). Biotin-labeled RNA was hybridized to Affymetrix GeneChip Human Exon 1.0 ST Array following the manufacturer's protocol (Affymetrix). After hybridization, microarrays were washed and stained using a GeneChip Fluidics Station 450 (Affymetrix), and then scanned using a GeneChip Scanner 7G (Affymetrix). Raw data was processed by Genespring GX 10 to obtain signal intensity measures for all probesets.

4.3.8.2 Identifying genes with phenotype-specific expression pattern

Gene expression data sets were extracted from the NCBI Gene Expression Omnibus database (http://www.ncbi.nlm.nih.gov/geo/) using the accession numbers GSE4840 (Zürich), GSE4841 Philadelphia), GSE4843 (Mannheim), GSE7127 (Johansson), GSE8332 (Wagner) and GSE10916 (Augustine). Each data set was separately normalized and assessed using Genespring GX 7.3 (Agilent Technologies). For normalization, each probe-set value was divided by the 50th percentile of all measurements within a sample and then divided by the median of its values across all samples. To identify genes that are differentially expressed between subgroups of melanoma cell cultures, we applied a modified version of the method previously used to identify phenotype groups (Hoek et al., 2006). Pools of probesets were generated by using each sample as a denominator for fold-change comparison against every other sample, retaining only the probesets that demonstrated a >2-fold difference in at least 25% of comparisons. Each probeset pool (one per sample) generated in this way was used to hierarchically cluster (Pearson correlation) the samples. A bootstrapping analysis was applied to calculate confidence levels and to determine stable cluster memberships (Kerr and Churchill, 2001), which classified each sample into one of the three groups. Two groups each represented samples that always clustered together. Previous studies have established that samples with these type of expression signatures corresponded with in vitro characteristics of proliferation and invasion. Therefore, these samples are referred to as having proliferative or invasive phenotype signatures, respectively. To determine the genes, whose expression patterns are responsible for the difference between stable groups, we performed ANOVA and adjusted P-values via multiple-testing-correction using the Benjamini and Yekutieli (2001) false discovery rate. Probe-sets for which the corrected probability of erroneously identifying differential expression was >0.05, or which showed a differential expression <2-fold, or which met these criteria in less than five of six data sets were discarded.

4.3.8.3 Phenotype-specific gene expression mapping

We calculated two median signal intensity values for every probeset of the MPSE gene list, one for the proliferative phenotype samples and one for the invasive phenotype samples. These two gene expression signatures represented the standards against which other samples were compared. Data from individual samples were correlated against the standards using the Pearson correlation algorithm and the two resulting correlation coefficients were then plotted against each other (Widmer plot). Consequently, samples with a similar phenotype signature will tend to group together on the plot nearer the standard with which they most closely correlate. The significance of a given correlation coefficient to a given standard is calculated using the Fisher transformation as has been previously described by us (Hoek et al., 2008b). We refer to this procedure as phenotype-specific gene expression mapping.

4.3.8.4 Kernel density estimation

To graphically represent the probability distribution of HOPP plot data, we used the R “np” package. Specifically, we employed the “npudens” function to estimate the joint density over a second-order Gaussian kernel, which was then plotted as a 3D surface. These figures help to show that samples tend to concentrate near one or the other of the phenotype standard signatures.

4.3.8.5 HOPP user guide

The HOPP tool predicts the phenotype of a test sample by comparing input microarray data against standard phenotype signatures. One can either upload raw data in the form of an appropriately formatted tab-delimited text file or you can analyze publicly available sample data by entering NCBI GEO accession numbers (e.g. GSM700746) for up to 15 samples at a time. The program will extract the necessary probe-set data and use it to predict phenotype. Presently, HOPP analysis is restricted to the platforms listed on the homepage. The resulting table includes some sample information and the correlation coefficients as calculated against the proliferative and invasive standards. The data are also graphically

represented with a Widmer plot (Pro (r) versus Inv (r)). We use the term 'heuristic' to preface the name of the HOPP algorithm, because it is based on our prior experience with a limited number of data sets, which we used to solve the problem of what constituted standard expression signatures for each phenotype. Therefore, as more data become available, it will be possible to refine the standards; though, it is probable that changes brought by further refinement will be negligible. Furthermore, these standard signatures are not meant to describe real examples of melanoma cells (though these may, and probably do, exist within specific tolerances of measurement). Rather they describe set-states which may be considered as being akin to mathematical attractors to which real examples of melanoma cells are (to varying degrees) associated. Because our attractor signatures are built upon the performance of a large number of different genes for whom expression is nominally fixed in terms of state (phenotype) and certainly dynamic in terms of process (phenotype switching), they can be regarded being as similar to strange attractors derived from the study of ostensibly chaotic dynamical systems. In our case, the nature of phenotype switching, because we do not yet understand the conditions required for switching, is an effectively unpredictable process and may therefore be considered a species of a chaotic dynamical system. Within this system, our strange attractors (the phenotypes) impose complex, yet specific rules of gene expression to which the phenotype switching process likely adheres.

4.3.8.6 Discovery of MITF target genes by correlation analysis

For the correlation analyses, seven different sets of DNA microarray data were extracted from various databases for the purpose of comparing Mitf expression with that of potential target genes. The criteria for data set selection were that each had to comprise at least ten different samples and use a common platform. These included melanoma cell line data from GSE8332 , GSE7127 , GSE4843, GSE4841, and GSE4840 (33, 35, 36) extracted from the NCBI Gene Expression Omnibus (http://www.ncbi.nlm.nih.gov/projects/geo/), melanoma cell line data published by Ryu and co-workers (37) extracted from the Public Library of Science (http://www.plosone.org), and melanocyte culture data published by Magnoni and co-workers (38). All data sets derive from experiments using HG-U133 series

microarrays (Affymetrix, Santa Clara, CA, USA). Each data set was normalized as previously described and analyzed separately using GeneSpring GS 7.3 (Agilent Technologies) and identical protocols. To identify gene expression patterns which correlated with that of MITF, the expression patterns of all probe sets were individually compared with the MITF probe set 207233_s_at by performing a Pearson correlation and selecting probe sets with correlation coefficients greater than 0.5. Probe sets which failed to pass this filter in all seven data sets were discarded and for each remaining probe set the median correlation coefficient was calculated.

4.3.8.7 Anti-correlation analysis

To identify gene expression patterns, which anti-correlated with that of *MITF*, and thus identify potential candidates for transcriptional inhibition, an identical comparison protocol was followed, except that probe sets with correlation coefficients less than -0.5 were selected. As before, probe sets, which failed to pass this filter in all seven data sets, were discarded and for each remaining probe set the median correlation coefficient was calculated.

4.3.8.8 Target identification

The probe sets identified by assessing gene expression change resulting from transformation of SK-MEL-28 with a MITF-expressing vector were combined with results of the correlation and anti-correlation studies. Probe sets, which correlated or anti-correlated with *MITF* expression, but showed no significant change in expression on MITF-induction were considered to be co-regulated genes (i.e. responding to the same transcriptional signals as MITF, but not governed by MITF). Probesets, which strongly correlated or anti-correlated with *MITF* expression and showed significant change in expression on MITF-induction, were considered to be candidate targets for regulation by MITF.

5. Results

5.1 Systematic classification of melanoma cells by phenotype-specific gene expression mapping.

AUTHORS

Daniel S. Widmer[1], Phil F. Cheng[1], Ossia M. Eichhoff[1], Benedetta C. Belloni[1], Marie C. Zipser[1], Natalie C. Schlegel[2], Delphine Javelaud[3], Alain Mauviel[3], Reinhard Dummer[1], and Keith S. Hoek[1].

AFFILIATIONS

[1]Department of Dermatology, University Hospital of Zurich, Zurich, Switzerland.

[2]Department of Biomedicine, Institute of Biochemistry and Genetics, University of Basel, Basel, Switzerland.

[3]Institute Curie, INSERM U1021/CNRS UMR3347, University Center, Building 110, 91400 Orsay, France.

CORRESPONDENCE ADDRESS

Keith Hoek, Department of Dermatology, University Hospital of Zürich, Gloriastrasse 31, CH-8091 Zürich, Switzerland (keith.hoek@usz.ch).

WORD COUNT

6172

5.1.1 Summary

There is growing evidence that the metastatic spread of melanoma is driven not by a linear increase in tumorigenic aggressiveness, but rather by switching back-and-forth between two different phenotypes of metastatic potential. *In vitro* these phenotypes are respectively defined by the characteristics of strong proliferation/weak invasiveness and weak proliferation/strong invasiveness. Melanoma cell phenotype is tightly linked to gene expression. Taking advantage of this we have developed a gene expression-based tool for predicting phenotype called Heuristic Online Phenotype Prediction (HOPP). We demonstrate the predictive utility of this tool by comparing phenotype-specific signatures with measurements of characteristics of melanoma phenotype-specific biology in different melanoma cell lines and short-term cultures. We further show that 86% of 536 tested melanoma lines and short-term cultures are significantly associated with the phenotypes we describe. These findings reinforce the concept that a two-state system, as described by the phenotype switching model, underlies melanoma progression.

5.1.2 Significance

A recent model for melanoma progression suggests that melanoma cells switch back-and-forth between states of proliferation and invasion to drive disease progression. We describe the use of a new online expression-analysis tool which shows that melanoma cell expression signatures are divided into distinct groups correlating with behavioural phenotypes of proliferation or invasion. Using this tool we also show evidence suggesting that short term cultures, rather than cell lines, may be a more relevant model system for *in vitro* studies of melanoma.

KEYWORDS

Melanoma, Expression, Phenotype, Classification, Prediction, HOPP

RUNNING TITLE

Melanoma phenotype-specific expression mapping

5.1.3 Introduction

Cutaneous melanoma is an aggressively dangerous disease and median patient survival after metastases are diagnosed is only 6-9 months (Klimek et al., 2000). While recent clinical trials have shown some improvements in overall survival for patients undergoing nonspecific immune or kinase inhibitor therapies, median survival rates remain dismal (Hodi et al., 2010, Flaherty et al., 2010, Chapman et al., 2011). Therefore gaining a comprehensive cellular and molecular understanding of metastatic spread continues to be critically important. A major focus of study is the phenomenon of melanoma cell heterogeneity. That there can be significant molecular differences between melanoma cells from the same lesion is widely appreciated, though what this means for disease progression remains the subject of debate (Shackleton and Quintana, 2010, Hoek and Goding, 2010, Roesch et al., 2010).

Pursuing *in vitro* studies into melanoma heterogeneity, we and others have identified two subgroups of cultured melanoma cells which are clearly distinguishable by how they express specific genes (Bittner et al., 2000, Hoek et al., 2006, Jeffs et al., 2009, Alexaki et al., 2010, Javelaud et al., 2011). *In vitro* experiments have identified one subgroup as a *proliferative* phenotype and the other as an *invasive* phenotype, and immunohistochemical testing has shown that individual primary and metastatic lesions typically include cells of both phenotypes (Eichhoff et al., 2010, Eichhoff et al., 2011). Their co-presence in lesions is likely explained by experiments which have shown that melanoma cells can switch between phenotypes *in vivo* (Hoek et al., 2008a). Together these findings prompted what has become the phenotype switching model for melanoma progression, in which melanoma cells respond to changing microenvironmental signals by reprogramming their gene expression to switch between states of proliferation and invasion (Hoek et al., 2008a, Pinner et al., 2009, Hoek and Goding, 2010). In addition to providing a mechanism for the metastatic cascade and explaining heterogeneity within a lesion, phenotype switching may also underlie targeted therapy escape. For example, slow-cycling invasive phenotype melanoma cells would be less susceptible to standard chemotherapies and such survivors could later switch to a proliferative state (Fukunaga-Kalabis et al., 2011). Furthermore, cultures of invasive and proliferative phenotype cells have been shown to differentially express melanocytic markers, suggesting that subverting the immune response to specifically target melanocytic cells may be similarly defeated (Hoek et al., 2006). Finally, we have shown that while proliferative phenotype cells respond to MAPK inhibitors, invasive phenotype cells do not and may provide a pool from which resistant cells emerge (Zipser et al., 2011).

Most recently, our group showed that microenvironmentally-induced changes in the expression patterns of specific LEF/TCF family transcription factors may be important for the phenotype switching mechanism (Eichhoff et al., 2011). That the microenvironment is involved in phenotype switching is corroborated by the results of other groups who have explored its influence on melanoma gene expression and metastatic potential (Seftor et al., 2006, Folberg et al., 2006, Postovit et al., 2008). Several laboratories have considered the phenotype switching model and reported data supporting a relationship between factors expressed in a phenotype-specific manner and disease progression (Carreira et al., 2006, Almanzar et al., 2009, Orgaz et al., 2009, O'Connell et al., 2009, Alexaki et al., 2010). These studies contrast those which purport to identify melanoma stem cells (or melanoma initiating cells) by the identification of stem-cell markers (Fang et al., 2005, Schatton et al., 2008). While the melanoma stem cell paradigm also seeks to explain intralesional heterogeneity and therapy escape, several lines of research indicate that stem cell markers are not an exclusive or even necessary prerogative of cells propagating metastatic disease (Quintana et al., 2008, Roesch et al., 2010, Cheli et al., 2011). The inference is that “stemness” is a reversible phenotype to be adopted or shed by melanoma cells in response to microenvironmental signalling (Hoek and Goding, 2010). The reversible nature of stem cell marker expression closely mirrors the concept of phenotype switching, and we have argued that invasive phenotype melanoma cells themselves fit multiple criteria for cancer stem cells (Hoek and Goding, 2010). Thus it is critical that researchers working with melanoma cells are both aware of and can account for the phenotypes as they study various aspects of melanoma biology.

We have designed a gene expression analysis algorithm, termed Heuristic Online Phenotype Prediction (HOPP), which uses archetypes of proliferative and invasive phenotype signatures to identify and predict the phenotypes of melanoma cell lines and cultures. We tested its utility by carrying out proliferation and invasion experiments on both short-term melanoma cultures and widely-used melanoma cell lines. We also used HOPP to carry out a phenotyping survey of several hundred published expression profiling experiments which showed that, contrary to the expectation that samples may be uniformly distributed throughout the “expression space” between phenotypes, more than 80% of samples cluster with either the proliferative or the invasive phenotype.

5.1.4 Results

5.1.4.1 Melanoma phenotype specific gene expression

For high throughput studies of melanoma gene expression, the most frequently employed platform remains the HG-U133 series produced by Affymetrix (Hoek, 2007). In our experience this platform has proven to be a robust tool for genome-wide expression studies (Hoek et al., 2006, Zipser et al., 2011). Therefore the current study sources datasets produced using HG-U133 series platforms. We used six different datasets (including a total of 218 melanoma lines and cultures) to derive the phenotype signature standards. For each dataset we performed a class-discovery analysis following methods previously described (Hoek et al., 2006), with the modification that we used bootstrapped confidence estimates for determining phenotype membership based on sample clustering (Kerr and Churchill, 2001). From this we identified 100 samples in one subgroup and 92 samples in a second subgroup (Appendix; Table S1). A further 26 samples did not show 100% stability in their cluster memberships and were therefore not used to identify genes with subgroup-specific expression patterns. With the subgroup assignments we used ANOVA to identify a set of 97 genes expressed differentially between the two subgroups (Appendix; Table S2). Reference to earlier works with similar expression signatures derived from smaller datasets indicated that the first subgroup are characterized by a proliferative phenotype signature and the other by an invasive phenotype signature (Hoek et al., 2006, Jeffs et al., 2009). The identified list of genes is thus referred to as the Melanoma Phenotype-Specific Expression (MPSE) list.

5.1.4.2 Generating MPSE correlation data

Normalization of high throughput data across samples within a dataset is principally designed to account for dataset-specific sources of technical variation. However, different datasets do not necessarily share equivalent characteristics of variation and it is impractical to expect that analyses of combined datasets would not be susceptible to these differences. Our aim was to devise a method for predicting phenotype from gene expression data for single-sample experiments (where cross-sample normalization procedures do not apply) as well as for multi-sample experiments (considering each sample independently). We extracted the raw signal intensities for 134 probe-sets corresponding to the 97 MPSE genes from 192 samples (the control set) representing 100 proliferative and 92 invasive phenotype signatures (Appendix; Table S1). For each phenotype we then calculated the median cross-sample values for every probe-set. This

yielded two phenotype-specific standard signatures (Appendix; Table S2). An online algorithm, Heuristic Online Phenotype Prediction (HOPP, http://www.jurmo.ch/hopp), was written to perform Pearson's correlation analyses comparing data from each phenotype-assigned sample against both the invasive and the proliferative standards, yielding two correlation coefficients per sample. We graph the function of the two correlation coefficients on a simple cartesian coordinate system where the x-axis describes correlation with the proliferative phenotype signature standard, and the y-axis describes correlation with the invasive phenotype signature standard, referring to this particular arrangement as a "Widmer plot".

Plotting of sample correlation coefficients showed group-specific clustering of proliferative and the invasive phenotype samples (Figure 1A; Appendix; Table S3). We used this data to calculate the probability density distribution, which also showed group-specific clustering of the samples and indicated a strong peak near the proliferative standard (Figure 1B). We acquired DNA microarray data for an additional 318 *in vitro* melanoma gene expression profiling experiments from the NCBI GEO database (http://www.ncbi.nlm.nih.gov/geo/) and used HOPP to also calculate and plot their sample correlation coefficients. This revealed a distribution closely similar to that of the control set (Figure 1C; Appendix; Table S4). Calculating the probability density distribution reveals similar results as obtained with the control set (Figure 1D). Including the highly stringent Bonferroni multiple testing correction adjustment, we calculate the significance of a Pearson's correlation (r) of 0.4 to be $P < 0.001$. This shows that 81% of samples have expression signatures which are closely correlated ($r > 0.4$) to only one standard. In comparison, 1% of samples were closely correlated to both and 18% were not correlated to either. It should be appreciated that, because of the high number of samples being examined (the panels in Figure 1 describe the results obtained from a total of 536 profiling experiments) there is a high likelihood that some of these apparent outliers are the result of technical fault. For example, common faults that may be expected to affect the outcome on a Widmer plot include the use of degraded RNA samples to perform gene profiling experiments, or using samples which are contaminated with additional cells from other sources.

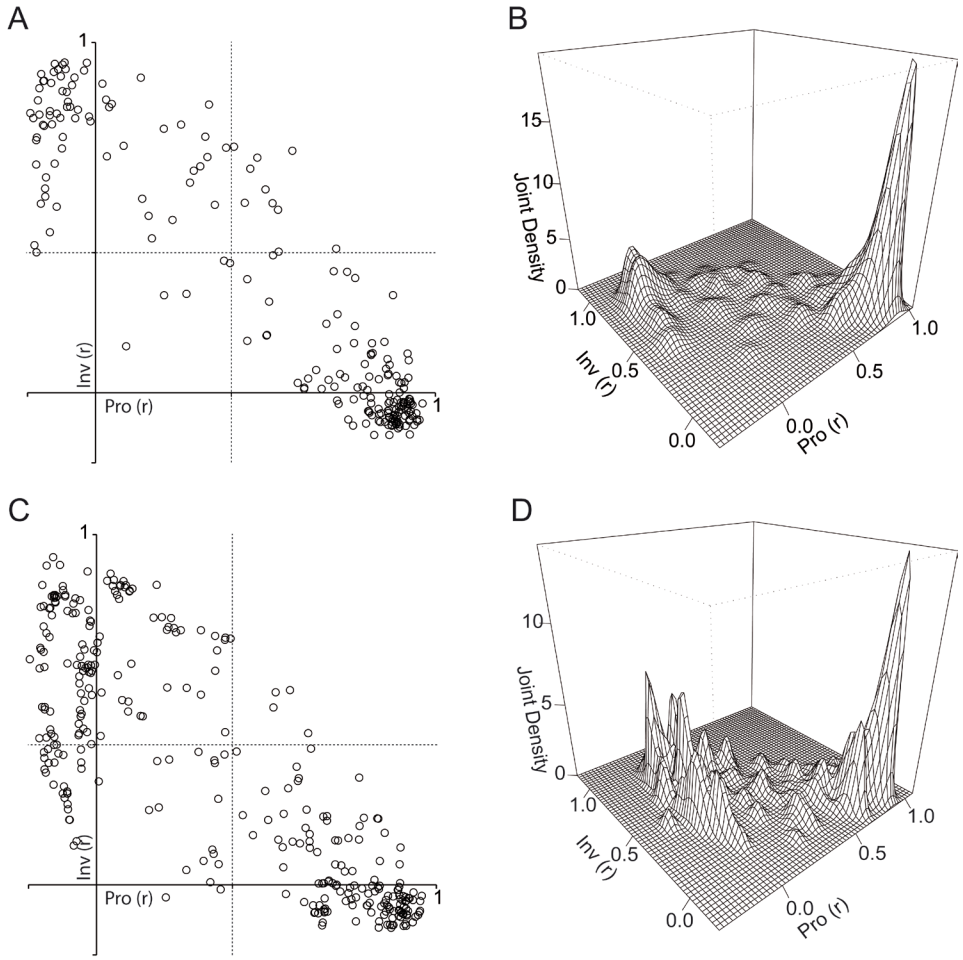

FIGURE 1. *MPSE correlation plots.* Sample gene expression data for the MPSE gene set was used to calculate, via HOPP, correlation coefficients (r values) against the proliferative and invasive standard signatures. (A) Widmer plot (proliferative (x-axis) *versus* invasive (y-axis) correlation coefficients) of the control data. This shows that 93.2% of samples yielded r > 0.4 for one phenotype only, 4.5% yielded r > 0.4 for both phenotypes and 2.3% yielded r > 0.4 for neither. (B) The kernel density estimation of the probability distribution for control data shows distinct sample concentrations near each phenotype standard. (C) Widmer plot of 318 test samples. This shows that 81.4% of samples yielded r > 0.4 for one phenotype only, 1.2% yielded r > 0.4 for both phenotypes and 17.4% yielded r > 0.4 for neither. (D) The kernel density estimation of the probability distribution for the test samples also shows distinct sample concentrations near the phenotype standards.

5.1.4.3 Assessing phenotype prediction for melanoma cultures and cell lines

We performed DNA microarray gene expression profiling on twelve additional short-term melanoma cell cultures and used HOPP to predict their phenotypes (Figure 2A). We then tested their *in vitro* characteristics of proliferation and invasion. Under standard culturing conditions the six proliferative signature samples had an average population doubling time

of 42.9 h, while the six invasive signature samples had an average population doubling time of 131.3 h (Figure 2C). In invasion assays the proliferative signature samples showed an average invasive index of 3.2%, while the invasive signature samples had an average invasive index of 30.3% (Figure 2E). These differences in proliferation and invasion were significant ($P < 0.002$ and $P < 0.004$, respectively). Culturing of these cells on Matrigel, as described previously (Zipser et al., 2011), yields surface organization patterns which are phenotype specific. Proliferative phenotype melanoma cells adopt an organization of small and isolated clusters, while invasive phenotype cells form connected networks (Appendix; Figure S1). Culturing short-term melanoma cell cultures on Matrigel confirmed phenotype-specific surface organization patterns (Table 1).

Table 1. Combined summary data for melanoma cell cultures.

Cell cultures	Accession	Correlation Pro (r)	Correlation Inv (r)	Doubling time (h)	Invasion (%)	Matrigel[a]
M080423	GSM700746	0.831	-0.122	70.9	5.3	isolated
M000921	GSM700745	0.550	0.050	42.4	7.8	isolated
M010817	GSM700743	0.734	-0.046	42.9	0.9	isolated
M980513	GSM700742	0.891	-0.074	37.1	0.0	isolated
M050829	GSM700744	0.618	0.215	33.3	3.0	isolated
M000907	GSM108375	0.511	0.260	30.5	2.4	isolated
M060125	GSM700750	-0.121	0.806	184.0	30.4	connected
M061103	GSM700749	-0.131	0.769	164.9	42.1	connected
M081008	GSM700752	-0.147	0.718	73.6	11.8	connected
M080310	GSM833481	-0.154	0.773	159.8	13.6	connected
M080201	GSM833482	-0.187	0.685	145.9	20.8	connected
M080214	GSM833483	-0.178	0.774	59.3	63.4	connected

[a] see Figure S1 for explanatory examples.

Table 2. Combined summary data for melanoma cell lines

Cell line	Accession	Correlation Pro (r)	Correlation Inv (r)	Doubling time (h)	Invasion (%)	Matrigel[a]
888mel	GSM206439	0.802	-0.052	27.8	8.8	isolated
WM983A	GSM109047	0.878	-0.027	46.7	2.8	isolated
WM983B	GSM109048	0.860	-0.052	49.0	0.9	isolated
501mel	GSM555120	0.831	-0.012	22.8	7.8	connected
SK-MEL-28	GSM206543	0.947	-0.082	24.5	1.6	connected
WM793B	GSM109043	-0.119	0.939	39.0	20.0	connected
WM852	GSM109044	-0.134	0.804	41.0	15.9	connected
1205Lu	GSM109021	-0.088	0.924	24.2	5.4	connected

[a] see Figure S1 for explanatory examples.

We compared the short-term culture results with a similar analysis of eight widely-used melanoma lines (SK-MEL-28, 501mel, 888mel, WM793, WM852, WM983A, WM983B and 1205Lu). Each of these has already been subject to microarray expression profiling by other researchers and this data is available on the NCBI GEO database. However, we performed additional DNA microarray expression profiling experiments on these lines and used HOPP to predict their phenotypes (Figure 2B). This showed close agreement between the published data and our experiments, where five are proliferative signature lines (888mel, WM983A, WM983B, 501mel, SK-MEL-28) and three are invasive signature lines (WM793B, WM852, 1205Lu). Then we assessed their *in vitro* proliferative and invasive characteristics. We found for these cell lines that while there was no significant difference in population doubling times between proliferative (34.1 h) and invasive (34.7 h) signature lines (Figure 2D), there was a significant difference ($P < 0.026$) in invasiveness, with proliferative signature lines showing an invasive index of 4.4% and invasive signature lines showing an invasive index of 13.8% (Figure 2F) in line with previous observations (Alexaki et al., 2010). However, culturing of cell lines on Matrigel yielded inconsistent results, with two (501mel, SK-MEL-28) yielding outcomes which were contra to HOPP prediction (Table 2, Appendix; Figure S1).

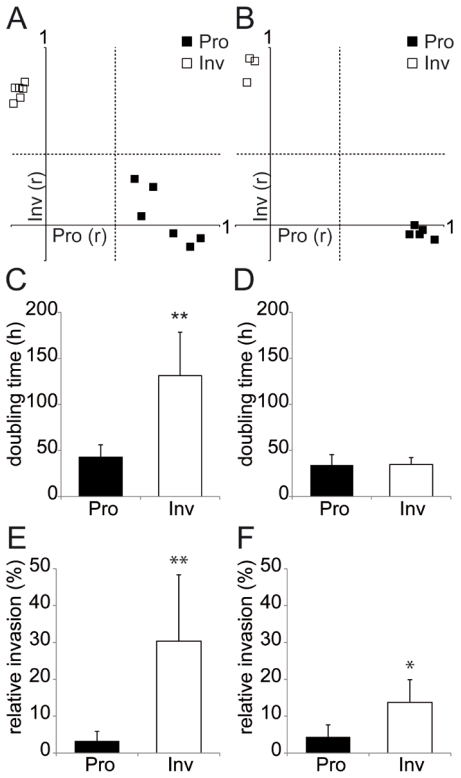

FIGURE 2. Phenotype prediction of *in vitro* behaviours. (A) Widmer plot of HOPP data from short-term cultures of melanoma cells. (B) Widmer plot of HOPP data from melanoma cell lines. (C) *In vitro* doubling time (h) of short-term cultures of melanoma cells. (D) *In vitro* doubling time (h) of melanoma cell lines. (E) *In vitro* invasive indices of short-term cultures of melanoma cells. (F) *In*

vitro invasive indices of melanoma cell lines (*P < 0.05, **P <0.01). Dotted lines in the Widmer plots indicate r = 0.4.

5.1.4.4 Phenotype is independent of BRAF mutation status

The $BRAF^{V600E}$ mutation is a frequent occurrence in melanoma, being present in more than half of all samples tested (Davies et al., 2002). The involvement of this mutation in disease progression has shown BRAF to be a promising target molecule in therapeutic trials (Flaherty et al., 2010, Bollag et al., 2010). We therefore explored whether the BRAF mutation had any relationship with the proliferative and invasive phenotype signatures. Four different datasets (GSE10916, GSE4841, GSE4843 and GSE7127) supply genotyping information concerning the mutation status of BRAF. HOPP analyses of these show there is no significant association between the HOPP result and BRAF mutation status (Figure 3). This indicates that BRAF mutation status has no relationship with phenotype-specific gene expression.

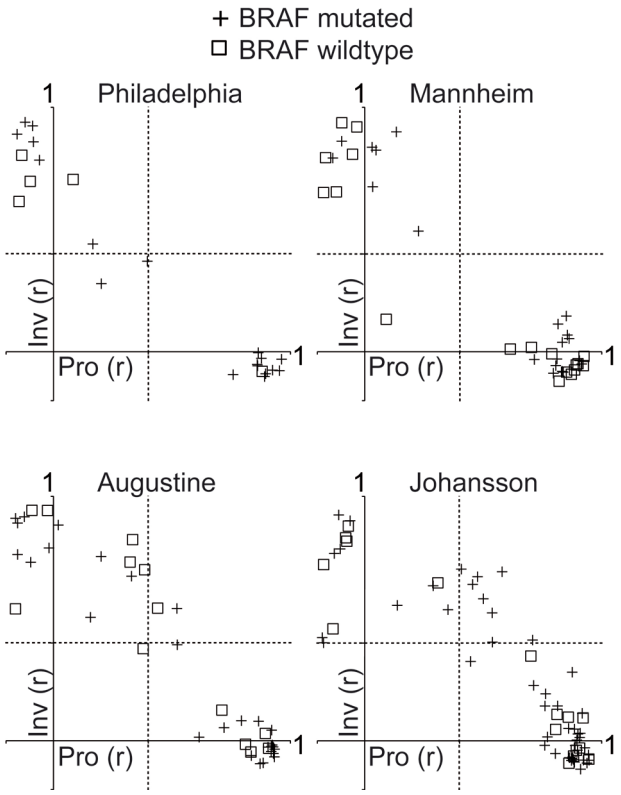

FIGURE 3. Phenotype and BRAF mutation. Datasets for which BRAF mutation status data was available were subjected to HOPP analysis and the distributions of BRAF wild-type versus

BRAFV600E were assessed. Widmer plots of four different datasets reveals no significant relationship between BRAF mutation status and HOPP outcome. Dotted lines indicate r = 0.4.

5.1.4.5 Melanoma cell phenotypes in vivo

In vitro, melanoma cell phenotype is assumed to be relatively homogenous and it is supposed that nearly all cells in a given culture share a uniform level of gene expression. In contrast to this, *in vivo* observation of melanoma tumors reveal a heterogeneous distribution of many markers as tumors typically include an irregularly distributed composition of tumor, stromal and infiltrating immune cells. The distribution of marker genes specific to invasive or proliferative phenotypes suggest that tumors, and the biopsies taken from them, also include cells of both phenotypes in proportions which are difficult to predict. Subsequently, while the measurement of the expression of any given gene is its mean among all cells in a biopsy, it does not necessarily follow that this is representative of the entire lesion. Thus tumor heterogeneity, with its irregular distribution of cell phenotypes, likely complicates the drawing of clinically relevant conclusions from expression data obtained from either biopsies or derived cell cultures. We therefore examined data obtained from melanoma tissue samples and used HOPP to perform Pearson correlation analyses against the proliferative and invasive standards. For example, Riker and co-workers published a study in which, among other things, they compared primary melanomas against metastatic lesions (Riker et al., 2008). We found that HOPP analysis does not separate these sample classes, with both primaries and metastases being similarly spread between proliferative and invasive phenotype signatures (Figure 4A). This supports earlier data which indicated that primary and metastatic lesions are composed of irregular distributions of both phenotypes (Hoek et al., 2006, Eichhoff et al., 2011).

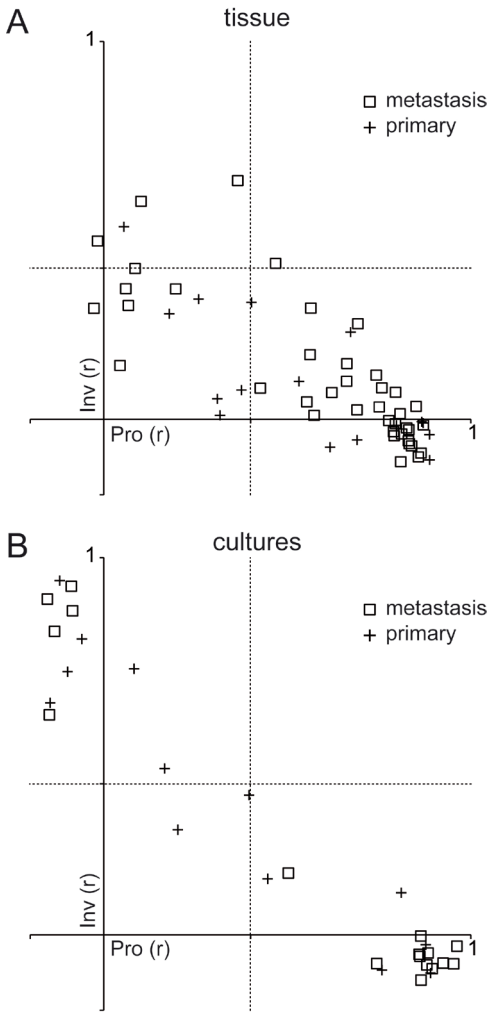

FIGURE 4. Primary versus metastatic melanoma tissues and cultures. (A) The Riker dataset (GSE7553) was assessed with HOPP and is shown here as a Widmer plot with samples identified according to whether they are primary melanoma tissue (crosses) or metastatic melanoma tissue (squares). (B) The Philadelphia dataset (GSE4841) was assessed with HOPP and the results are displayed here as a Widmer plot with samples identified according to whether they are primary melanoma cells (crosses) or metastatic melanoma cells (squares). Neither primary nor metastatic melanoma samples reveal a significant association with the phenotype signatures. Dotted lines indicate r = 0.4.

5.1.4.6 Comparison with hierarchical clustering

Freedman and co-workers profiled gene expression in cultures of primary and metastatic melanoma lesions and categorized them according to unsupervised hierarchical clustering (Freedman et al., 2011). Re-analysis of this data using HOPP shows that their M1 and M3 subclasses fit discretely into the proliferative and invasive phenotype signatures, respectively (Figure 5).

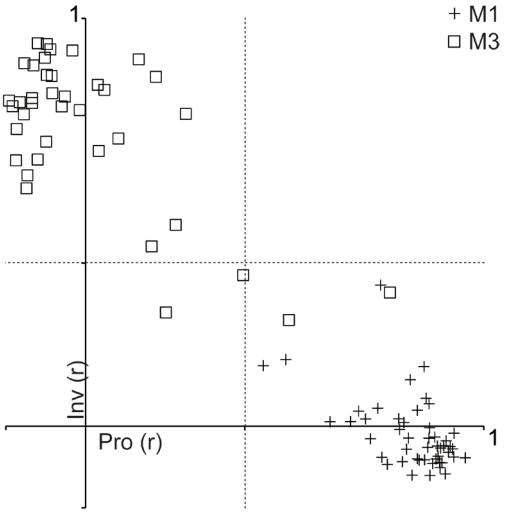

FIGURE 5. Hierarchical clustering versus HOPP. The Freedman data was assessed with HOPP and the results are displayed here as a Widmer plot with cultured samples identified according to the M1 (crosses) and M3 (squares) clustering results obtained by Freedman and co-workers. Dotted lines indicate r = 0.4.

5.1.4.7 Interlaboratory phenotype signature consistency

We compared HOPP analyses for nine different cell lines where for which were at least three independent sources of expression profiling data. Widmer plots of the results showed that four cell lines (WM35, MDA435, A2058 and A375) demonstrated inconsistent phenotype signatures. In contrast, five cell lines (SK-MEL-28, C8161, MALME-3M, SK-MEL-19 and SK-MEL-5) showed consistent phenotype signatures (Figure 6).

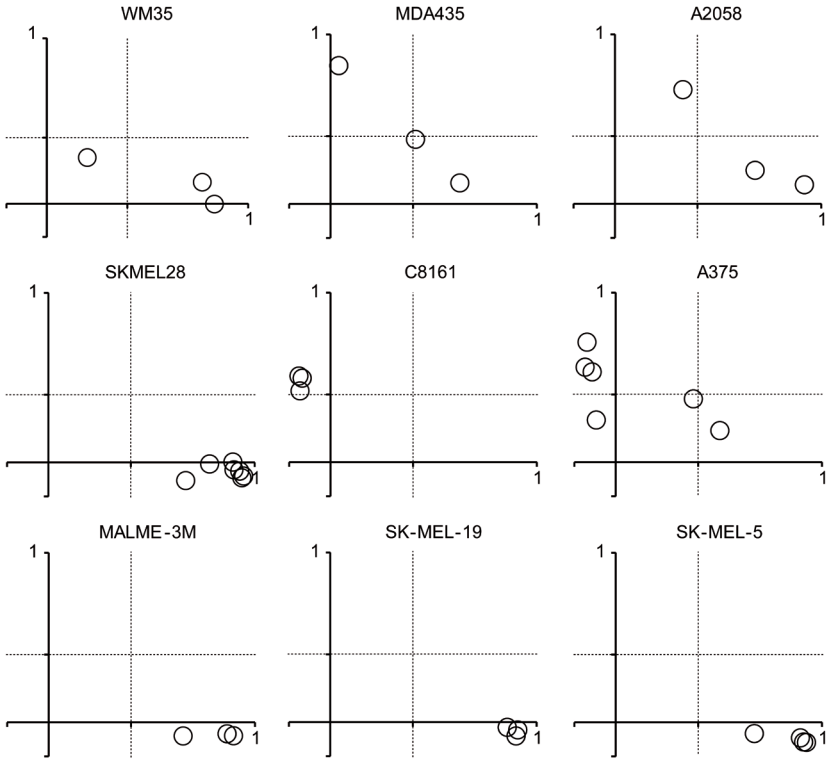

FIGURE 6. Melanoma cell line expression signature inconsistencies. The results of HOPP analyses of data taken from four different cell lines in wide use, each of which was expression profiled by at least three different laboratories, are shown here as Widmer plots. These data show that melanoma lines WM35, MDA435 and A2058 show little inter-laboratory consistency in their gene signatures. On the other hand, seven different laboratories yielded SK-Mel-28 expression data which showed a strongly consistent proliferative phenotype signature. Dotted lines indicate r=0.4.

5.1.5 Discussion

Previous studies which identified two phenotypes of melanoma cell yielded some clues concerning the molecular nature of phenotype switching (Hoek et al., 2006, Carreira et al., 2006). However, it was not clear if there were distinct intermediate stages between the proliferative and invasive archetypes. We show here that a large majority of gene expression profiles derived from melanoma *in vitro* cluster very closely to one or the other phenotype standard. This argues against the idea that melanoma cells adopt clear intermediate states during phenotype switching and counters an earlier suggestion that melanoma cells may inhabit a “continuum” in the expression space between phenotype standards (Hoek et al., 2008a).

We tested the ability of HOPP to predict *in vitro* behaviours in a dozen short-term cultures of melanoma cells and eight widely-used melanoma cell lines (Figure 2). We found close correlation between HOPP clustering and the *in vitro* proliferative and invasive characteristics of short-term cultures. This showed a close association between specific gene expression patterns and *in vitro* biological activities of short-term cultures of melanoma cells, meaning that HOPP may be used with confidence to predict their characteristics. Similarly, our *in vitro* characterization of cell lines showed that *in vitro* invasiveness correlated closely with phenotype specific expression patterns. However, we found no such significant signature-specific difference between cell lines' rates of proliferation. Overall, cell lines of both phenotypes proliferated significantly faster than invasive phenotype cell cultures, and were at least as fast as proliferative phenotype cell cultures. Why cell lines proliferate so well may be explained by the effects of somatic changes and experimenter selection. Cells in culture likely remain subject to additional somatic changes which could contribute towards the selection of faster growing clones. For example, such changes may influence proliferation-critical processes such as cyclin degradation, where it has been shown that truncation of cyclin genes abrogates normal processes nuclear expulsion and cytosolic degradation (Van Dross et al., 2006). Furthermore, cells which did not proliferate well in culture were routinely discarded on the basis that they were probably not cancer cells. This is understandable with a clonal evolution model in which cancer cells are thought to increase characteristics of both proliferation and invasion as the disease progresses (Miller and Mihm, 2006). The differences between short-term cultures and cell lines, in which the phenotypic behaviours of cell lines are less correlated with their expression signatures, suggest that over the long period of time cell lines have been in circulation they may have deviated from their original characteristics and been selected for by researchers' expectations of what constituted good *in vitro* models.

Many melanoma researchers use cell lines or cultures to study the disease. As mentioned earlier, a fundamentally important assumption had been that melanoma cells may be differentiated by their potential to drive metastatic progression. The language used to convey the extent or degree of this potential in a given cell line or culture is varied. Descriptors are sometimes determined by the clinical stage of the lesions from which cells are derived. This can influence conclusions drawn on the basis that differences between lines are significantly correlated with interpretations in which clinical stage reflects aggressiveness. For example, Pochec and co-workers use the fact that A375 comes from a metastasis and WM35 comes from a primary to make the claim that differences in how these cells glycosylate an integrin is significant for the acquisition of invasiveness (Pochec et al., 2003). Similarly, the Wistar Institute Melanoma Research Center maintains a

collection of melanoma cell lines which are explicitly characterized according to clinical stages of the patient lesions from which they are derived (http://www.wistar.org/lab/meenhard-herlyn-dvm-dsc/page/resources). However, our previously published analyses (Hoek et al., 2006) found no gene expression pattern correlating with stage progression in these lines and HOPP analysis confirms that their distribution is not phenotype specific. Alternatively, descriptors may be derived experimentally, for example cells may be described as “metastatic” or “non-metastatic” according to their performance in animal models (de Wit et al., 2005). In either context, differences between “metastatic” and “non-metastatic” are frequently interpreted in the same way as being intrinsic to disease progression. However, this is problematic because a cell line derived from a metastasis may not necessarily produce metastases in an animal model.

A significant consequence of a paradigm in which the existence of two distinct phenotypes of melanoma cell goes unrecognized is the likelihood of large-scale study bias towards one or another phenotype. For example, scientists studying DNA methylation patterns in melanoma examined eleven different cell cultures (Bonazzi et al., 2011). Of these, we note (from Table S1) that nine have clear proliferative phenotype signatures and one has a clear invasive phenotype signature. It is probable that the reason for this is simply because proliferative phenotype signature melanoma cultures grow faster and are thus more amenable to *in vitro* research than slower-growing invasive phenotype cultures. The results of these researchers’ experiments are therefore biased toward proliferative phenotype cells. Considering our probability density calculations it is clear that a large majority of experiments have been conducted on proliferative phenotype cultures, suggesting that this bias is wide-spread.

Interestingly, other workers have performed expression profiling analyses and clustering experiments which yielded distributions of data strikingly similar to the partition described by phenotype switching. For example, Freedman and co-workers profiled gene expression in cultures of primary and metastatic melanoma lesions and categorized them according to unsupervised hierarchical clustering (Freedman et al., 2011). Our analysis of this data showed that their M1 and M3 subclasses fit into the proliferative and invasive phenotype signatures, respectively. By gene enrichment analyses and pathway activity analyses these researchers identified distinct patterns of pathway activation. The M1 subclass exhibited stronger activity of the β-catenin, EGFR and ER pathways while the M3 subclass showed higher activity of SRC and STAT3 pathways. STAT3 signalling is known to induce expression of MMP2 and VEGF, genes which are highly upregulated in the invasive phenotype (Niu et al., 2002, Wei et al., 2003, Xie et al., 2004). Interestingly, due

to the activation of STAT3 in the M3 subclass and the reported importance of STAT3 activation for the formation of metastases in a mouse model (Xie et al., 2004), Freedman and co-workers suggested that the M3 subclass is a more aggressive subset. This is important because it relates to how the meaning of a term like “aggressive” is contextually nuanced. For example, it is implied that the M1 subset, which shows higher EGFR pathway activity, is less aggressive. This interpretation contrasts with other studies which report that EGFR pathway activation is critical for promoting tumor growth and metastasis, and which conclude that EGFR pathway activation is characteristic of aggressive cells (Ueno et al., 2008, Schartl et al., 2010). Our own interpretation is that these results are not in conflict because they are likely dealing with different phenotypic states. In this context, STAT3 signalling is important for driving invasiveness, while EGFR signalling is critical for proliferation. As both phenotypes are required for metastatic spread it is understandable that suppression of either pathway would retard the aspects of disease progression to which they respectively apply.

In a previous study we examined the effects of MAP kinase inhibition on proliferative and invasive phenotype melanoma cells (Zipser et al., 2011). While this showed that response to MAP kinase inhibition was phenotype-specific, we also saw evidence for the involvement of MAP kinase activity in phenotype regulation. Specifically, we noted that MAP kinase inhibition of proliferative phenotype cells induced the acquisition of invasive phenotype characteristics, which would revert upon removal of the inhibitor. Though expression profiling was performed on these samples, we found that MAP kinase inhibition induced no significant change in gene expression and analysis by HOPP confirmed this (data not shown). The transience of the induced changes seen suggests how melanoma cells *in vitro* maintain their phenotype. Under standard culturing conditions neither proliferative phenotype cells nor invasive phenotype cells have been observed to undergo phenotype change (Hoek et al., 2006). This may seem inconsistent with a phenotype switching model which holds that microenvironmental influence is key to phenotype change (Hoek et al., 2008a). However, we suggest that the particular microenvironmental influences required for phenotype change are absent under standard culturing conditions, allowing different phenotypes to persist (Eichhoff et al., 2011).

Scientists have been culturing cancer cells (including melanoma) from patient materials for a century (Losee and Ebeling, 1914) and immortalized cancer cell lines have been available for sixty years (Gey et al., 1952). Accordingly, there are many human melanoma cell lines which have been in common use for decades. For example, SK-Mel-28 and A375 are widely recognized examples of “standard” melanoma lines that have been in circulation since the 1970s. While it is a general assumption that any given aliquot is

representative of a cell line, passage through the years (and many hands) can lead to confusion. Accordingly, we have found that distinct batches of a cell line can yield inconsistent results when examined using the HOPP algorithm. It is important that these results show that many cell lines are consistent in their phenotype signature, and while this doesn't prove the identity of a cell line, it is circumstantial evidence to that effect and at the very least indicates that it the phenotype it is supposed to be. For cell lines where there is little agreement in HOPP results (e.g. A375) one is left to wonder which are the exemplars and which have become compromised.

Finally, the principles of HOPP can be readily applied to any system where a pair of standard signatures may be used in the analysis of single samples. So long as the standards were generated with sufficient samples to establish signatures with statistical confidence, then subsequent samples may be measured against such standards in the same way as we have described here for melanoma cells. While the MPSE standards for proliferative and invasive melanoma cell phenotypes are the default for HOPP, users may upload their own standards instead.

5.1.6 Acknowledgements

Funding was provided by the Swiss National Science Foundation (Project number 320030-119989, KSH and RD), the Gottfried und Julia Bangerter Rhyner Stiftung (RD) and the Georg und Bertha Schwyzer-Winiker Stiftung (RD). We thank the Cancer Biology PhD Program of the University/ETH Zürich for support.

5.1.7 References

Alexaki, V.I., Javelaud, D., Van, K., L.C., Mohammad, K.S., Dennler, S., Luciani, F., Hoek, K.S., Juàrez, P., Goydos, J.S., Fournier, P.J. *et al.* (2010) GLI2-mediated melanoma invasion and metastasis. J Natl Cancer Inst*, 102***,** 1148-1159.

Almanzar, G., Olkhanud, P.B., Bodogai, M., Dell'agnola, C., Baatar, D., Hewitt, S., Ghimenton, C., Tummala, M.K., Weeraratna, A.T., Hoek, K.S. *et al.* (2009) Sperm-derived SPANX-B is a clinically relevant tumor antigen that is expressed in human tumors and readily recognized by human CD4+ and CD8+ T cells. Clin Cancer Res*, 15***,** 1954-1963.

Benjamini, Y. and Yekutieli, D. (2001) The control of the false discovery rate in multiple testing under dependence. Ann Statist*, 29***,** 1165-1188.

Bittner, M., Meltzer, P., Chen, Y., Jiang, Y., Seftor, E., Hendrix, M., Radmacher, M., Simon, R., Yakhini, Z., Ben-Dor, A. *et al.* (2000) Molecular classification of cutaneous malignant melanoma by gene expression profiling. Nature*, 406***,** 536-540.

Bollag, G., Hirth, P., Tsai, J., Zhang, J., Ibrahim, P.N., Cho, H., Spevak, W., Zhang, C., Zhang, Y., Habets, G. *et al.* (2010) Clinical efficacy of a RAF inhibitor needs broad target blockade in BRAF-mutant melanoma. Nature*, 467***,** 596-599.

Bonazzi, V.F., Nancarrow, D.J., Stark, M.S., Moser, R.J., Boyle, G.M., Aoude, L.G., Schmidt, C. and Hayward, N.K. (2011) Cross-Platform Array Screening Identifies COL1A2, THBS1, TNFRSF10D and UCHL1as Genes Frequently Silenced by Methylation in Melanoma. PLoS One*, 6***,** e26121.

Carreira, S., Goodall, J., Denat, L., Rodriguez, M., Nuciforo, P., Hoek, K.S., Testori, A., Larue, L. and Goding, C.R. (2006) Mitf regulation of Dia1 controls melanoma proliferation and invasiveness. Genes Dev*, 20***,** 3426-3439.

Chapman, P.B., Hauschild, A., Robert, C., Haanen, J.B., Ascierto, P., Larkin, J., Dummer, R., Garbe, C., Testori, A., Maio, M. *et al.* (2011) Improved survival with vemurafenib in melanoma with BRAF V600E mutation. N Engl J Med*, 364***,** 2507-2516.

Cheli, Y., Giuliano, S., Botton, T., Rocchi, S., Hofman, V., Hofman, P., Bahadoran, P., Bertolotto, C. and Ballotti, R. (2011) Mitf is the key molecular switch between mouse or human melanoma initiating cells and their differentiated progeny. Oncogene*, 30***,** 2307-2318.

Davies, H., Bignell, G.R., Cox, C., Stephens, P., Edkins, S., Clegg, S., Teague, J., Woffendin, H., Garnett, M.J., Bottomley, W. *et al.* (2002) Mutations of the BRAF gene in human cancer. Nature*, 417***,** 949-954.

de Wit, N.J., Rijntjes, J., Diepstra, J.H., van Kuppevelt, T.H., Weidle, U.H., Ruiter, D.J. and van Muijen, G.N. (2005) Analysis of differential gene expression in human melanocytic tumour lesions by custom made oligonucleotide arrays. Br J Cancer*, 92***,** 2249-2261.

Eichhoff, O.M., Weeraratna, A., Zipser, M.C., Denat, L., Widmer, D.S., Xu, M., Kriegl, L., Kirchner, T., Larue, L., Dummer, R. *et al.* (2011) Differential LEF1 and TCF4 expression is involved in melanoma cell phenotype switching. Pigment Cell Melanoma Res*, 24***,** 631-642.

Eichhoff, O.M., Zipser, M.C., Xu, M., Weeraratna, A.T., Mihic, D., Dummer, R. and Hoek, K.S. (2010) The immunohistochemistry of invasive and proliferative phenotype switching in melanoma: a case report. Melanoma Res*, 20***,** 349-355.

Fang, D., Nguyen, T.K., Leishear, K., Finko, R., Kulp, A.N., Hotz, S., Van Belle, P.A., Xu, X., Elder, D.E. and Herlyn, M. (2005) A tumorigenic subpopulation with stem cell properties in melanomas. Cancer Res*, 65***,** 9328-9337.

Flaherty, K.T., Puzanov, I., Kim, K.B., Ribas, A., McArthur, G.A., Sosman, J.A., O'Dwyer, P.J.L., R.J., Grippo, J.F., Nolop, K. and Chapman, P.B. (2010) Inhibition of mutated, activated BRAF in metastatic melanoma. N Engl J Med*, 363***,** 809-819.

Folberg, R., Arbieva, Z., Moses, J., Hayee, A., Sandal, T., Kadkol, S., Lin, A., Valyi-Nagy, K., Setty, S., Leach, L. *et al.* (2006) Tumor cell plasticity in uveal melanoma: microenvironment directed dampening of the invasive and metastatic genotype and phenotype accompanies the generation of vasculogenic mimicry patterns. Am J Pathol*, 169***,** 1376-1389.

Freedman, J.A., Tyler, D.S., Nevins, J.R. and Augustine, C.K. (2011) Use of gene expression and pathway signatures to characterize the complexity of human melanoma. Am J Pathol*, 178***,** 2513-2522.

Fukunaga-Kalabis, M., Roesch, A. and Herlyn, M. (2011) From cancer stem cells to tumor maintenance in melanoma. J Invest Dermatol*, 131***,** 1600-1604.

Geertsen, R.C., Hofbauer, G.F., Yue, F.Y., Manolio, S., Burg, G. and Dummer, R. (1998) Higher frequency of selective losses of HLA-A and -B allospecificities in metastasis than in primary melanoma lesions. J Invest Dermatol*, 111***,** 497-502.

Gey, G.O., Coffman, W.D. and Kubicek, M.T. (1952) Tissue culture studies of the proliferative capacity of cervical carcinoma and normal epithelium. Cancer Res*, 12***,** 264-265.

Hodi, F.S., O'Day, S.J., McDermott, D.F., Weber, R.W., Sosman, J.A., Haanen, J.B., Gonzalez, R., Robert, C., Schadendorf, D., Hassel, J.C. *et al.* (2010) Improved survival with ipilimumab in patients with metastatic melanoma. N Engl J Med*, 363***,** 711-723.

Hoek, K.S. (2007) DNA microarray analyses of melanoma gene expression: a decade in the mines. Pigment Cell Res*, 20***,** 466-484.

Hoek, K.S., Eichhoff, O.M., Schlegel, N.C., Döbbeling, U., Kobert, N., Schaerer, L., Hemmi, S. and Dummer, R. (2008a) In vivo switching of human melanoma cells between proliferative and invasive states. Cancer Res*, 68***,** 650-656.

Hoek, K.S. and Goding, C.R. (2010) Cancer stem cells versus phenotype-switching in melanoma. Pigment Cell Melanoma Res*, 23***,** 746-759.

Hoek, K.S., Schlegel, N.C., Brafford, P., Sucker, A., Ugurel, S., Kumar, R., Weber, B.L., Nathanson, K.L., Phillips, D.J., Herlyn, M. *et al.* (2006) Metastatic potential of melanomas defined by specific gene expression profiles with no BRAF signature. Pigment Cell Res*, 19***,** 290-302.

Hoek, K.S., Schlegel, N.C., Eichhoff, O.M., Widmer, D.S., Praetorius, C., Einarsson, S.O., Valgeirsdottir, S., Bergsteinsdottir, K., Schepsky, A., Dummer, R. *et al.* (2008b) Novel MITF targets identified using a two-step DNA microarray strategy. Pigment Cell Melanoma Res*, 21***,** 665-676.

Javelaud, D., Alexaki, V.I., Pierrat, M.J., Hoek, K.S., Dennler, S., Van Kempen, L., Bertolotto, C., Ballotti, R., Saule, S., Delmas, V. *et al.* (2011) GLI2 and M-MITF transcription factors control exclusive gene expression programs and inversely regulate invasion in human melanoma cells. Pigment Cell Melanoma Res*, 24***,** 932-943.

Jeffs, A.R., Glover, A.C., Slobbe, L.J., Wang, L., He, S., Hazlett, J.A., Awasthi, A., Woolley, A.G., Marshall, E.S., Joseph, W.R. *et al.* (2009) A gene expression signature of invasive potential in metastatic melanoma cells. PLoS One*, 4***,** e8461.

Kerr, M.K. and Churchill, G.A. (2001) Bootstrapping cluster analysis: assessing the reliability of conclusions from microarray experiments. Proc Natl Acad Sci USA*, 98***,** 8961-8965.

Klimek, V.M., Wolchok, J.D., Chapman, P.B., Houghton, A.N. and Hwu, W.J. (2000) Systemic chemotherapy. Clin Plast Surg*, 27***,** 451-461.

Losee, J.R. and Ebeling, A.H. (1914) The cultivation of human tissue in vitro. J Exp Med*, 19***,** 593-602.

Miller, A.J. and Mihm, M.C.J. (2006) Melanoma. N Engl J Med*, 355***,** 51-65.

Niu, G., Wright, K.L., Huang, M., Song, L., Haura, E., Turkson, J., Zhang, S., Wang, T., Sinibaldi, D., Coppola, D. *et al.* (2002) Constitutive Stat3 activity up-regulates VEGF expression and tumor angiogenesis. Oncogene*, 21***,** 2000-2008.

O'Connell, M.P., Fiori, J.L., Kershner, E.K., Frank, B.P., Indig, F.E., Taub, D.D., Hoek, K.S. and Weeraratna, A.T. (2009) Heparan sulfate proteoglycan modulation of

Wnt5A signal transduction in metastatic melanoma cells. J Biol Chem*, 284*, 28704-28712.

Orgaz, J.L., Ladhani, O., Hoek, K.S., Fernández-Barral, A., Mihic, D., Aguilera, O., Seftor, E.A., Bernad, A., Rodríguez-Peralto, J.L., Hendrix, M.J. *et al.* (2009) Loss of pigment epithelium-derived factor enables migration, invasion and metastatic spread of human melanoma. Oncogene*, 28*, 4147-4161.

Pinner, S., Jordan, P., Sharrock, K., Bazley, L., Collinson, L., Marais, R., Bonvin, E., Goding, C. and Sahai, E. (2009) Intravital imaging reveals transient changes in pigment production and Brn2 expression during metastatic melanoma dissemination. Cancer Res*, 69*, 7969-7977.

Pochec, E., Litynska, A., Amoresano, A. and Casbarra, A. (2003) Glycosylation profile of integrin alpha 3 beta 1 changes with melanoma progression. Biochim Biophys Acta*, 1643*, 113-123.

Postovit, L.M., Margaryan, N.V., Seftor, E.A., Kirschmann, D.A., Lipavsky, A., Wheaton, W.W., Abbott, D.E., Seftor, R.E. and Hendrix, M.J. (2008) Human embryonic stem cell microenvironment suppresses the tumorigenic phenotype of aggressive cancer cells. Proc Natl Acad Sci USA*, 105*, 4329-4334.

Quintana, E., Shackleton, M., Sabel, M.S., Fullen, D.R., Johnson, T.M. and Morrison, S.J. (2008) Efficient tumour formation by single human melanoma cells. Nature*, 456*, 593-598.

Riker, A.I., Enkemann, S.A., Fodstad, O., Liu, S., Ren, S., Morris, C., Xi, Y., Howell, P., Metge, B., Samant, R.S. *et al.* (2008) The gene expression profiles of primary and metastatic melanoma yields a transition point of tumor progression and metastasis. BMC Med Genomics*, 1*, 13.

Roesch, A., Fukunaga-Kalabis, M., Schmidt, E.C., Zabierowski, S.E., Brafford, P., Vultur, A., Basu, D., Gimotty, P., Vogt, T. and Herlyn, M. (2010) A temporarily distinct subpopulation of slow-cycling melanoma cells is required for continuous tumor growth. Cell*, 141*, 583-594.

Schartl, M., Wilde, B., Laisney, J.A., Taniguchi, Y., Takeda, S. and Meierjohann, S. (2010) A mutated EGFR is sufficient to induce malignant melanoma with genetic background-dependent histopathologies. J Invest Dermatol*, 130*, 249-258.

Schatton, T., Murphy, G.F., Frank, N.Y., Yamaura, K., Waaga-Gasser, A.M., Gasser, M., Zhan, Q., Jordan, S., Duncan, L.M., Weishaupt, C. *et al.* (2008) Identification of cells initiating human melanomas. Nature*, 451*, 345-349.

Seftor, E.A., Meltzer, P.S., Kirschmann, D.A., Margaryan, N.V., Seftor, R.E. and Hendrix, M.J. (2006) The epigenetic reprogramming of poorly aggressive melanoma cells by a metastatic microenvironment. J Cell Mol Med*, 10*, 174-196.

Shackleton, M. and Quintana, E. (2010) Progress in understanding melanoma propagation. Mol Oncol*, 4*, 451-457.

Ueno, Y., Sakurai, H., Tsunoda, S., Choo, M.K., Matsuo, M., Koizumi, K. and Saiki, I. (2008) Heregulin-induced activation of ErbB3 by EGFR tyrosine kinase activity promotes tumor growth and metastasis in melanoma cells. Int J Cancer*, 123*, 340-347.

Van Dross, R., Browning, P.J. and Pelling, J.C. (2006) Do truncated cyclins contribute to aberrant cyclin expression in cancer? Cell Cycle*, 5*, 472-477.

Wei, D., Le, X., Zheng, L., Wang, L., Frey, J.A., Gao, A.C., Peng, Z., Huang, S., Xiong, H.Q., Abbruzzese, J.L. *et al.* (2003) Stat3 activation regulates the expression of vascular endothelial growth factor and human pancreatic cancer angiogenesis and metastasis. Oncogene*, 22*, 319-329.

Xie, T.X., Wei, D., Liu, M., Gao, A., Ali-Osman, F., Sawaya, R. and Huang, S. (2004) Stat3 activation regulates the expression of matrix metalloproteinase-2 and tumor invasion and metastasis. Oncogene*, 23*, 3550-3560.

Zipser, M.C., Eichhoff, O.M., Widmer, D.S., Schlegel, N.C., Schoenewolf, N.L., Stuart, D., Liu, W., Gardner, H., Smith, P.D., Nuciforo, P. *et al.* (2011) A proliferative melanoma cell phenotype is responsive to RAF/MEK inhibition independent of BRAF mutation status. Pigment Cell Melanoma Res*, 24*, 326-333.

WORKING TITLE

5.2 Hypoxia contributes to melanoma heterogeneity by triggering phenotype switching.

AUTHORS
Daniel S Widmer, Keith S Hoek, Phil F. Cheng, Ossia M Eichhoff, Thomas Biedermann, Marieke Raijmaakers, Reinhard Dummer and Mitchell P. Levesque

AFFILIATION
Department of Dermatology, University Hospital of Zürich, Zürich, Switzerland

CORRESPONDENCE ADDRESS
Mitchell P. Levesque,
Department of Dermatology,
University Hospital of Zürich,
Gloriastrasse 31,
CH-8091 Zürich,
Switzerland
Phone: +41442554115
E-mail: mitchellpaul.levesque@usz.ch

5.2.1 Abstract

We have previously reported a model for melanoma progression in which oscillation between melanoma cell phenotypes characterized by invasion or proliferation is fundamental to tumor heterogeneity and disease progression (Hoek et al., 2006). In this study we examine the possible role of hypoxia as one of the microenvironmental influences driving metastatic progression by promoting a switch from a proliferative to an invasive phenotype.

To determine if melanoma tumors are heterogeneous for melanoma phenotypes, we set up multiple cell cultures from a single tumor, which resulted in melanoma cells of both phenotypes originating from the same lesion. Immunohistochemistry on primary human cutaneous melanoma biopsies showed intratumor heterogeneity for cells expressing melanocytic markers, and a loss of these markers correlated to hypoxic regions. To examine the role of hypoxia in melanoma progression, we performed microarray experiments on proliferative phenotype melanoma cells exposed to hypoxic conditions *in vitro* and found up-regulation of invasive-phenotype-specific genes combined with a down-regulation of proliferative-phenotype-specific genes. Furthermore, we show that the down-regulation of melanocytic markers is dependent on HIF1α, a known regulator of the hypoxic response. *In vitro* invasion assays showed that a hypoxic environment increases the invasiveness of proliferative melanoma cell cultures. Moreover, extended periods of hypoxia increased the invasive potential of proliferative phenotype cells in a dose-dependent fashion. Importantly, invasiveness was still increased when cells were returned to normoxia for 48 hours. In contrast, invasive phenotype melanoma cells showed no increase in invasive potential upon exposure to hypoxia. Thus, exposure of proliferative melanoma cells to hypoxic microenvironments is sufficient, in a HIF1α-dependent manner, to down-regulate melanocytic marker expression and increase their invasive potential.

5.2.2 Introduction

Malignant melanoma is a growing public health burden since it is one of the few cancers still escalating in incidence (Jemal et al., 2009). Despite advances in understanding the molecular nature of melanoma in recent decades, few treatment options are available for metastatic melanoma. Unfortunately these therapies only marginally increase overall patient survival (Bollag et al., 2010; Lui et al., 2007; Robert et al., 2011). One reason why melanoma is difficult to treat is its heterogeneity (Fidler, 1978). Many different classes of melanoma cells have been discovered, thus exacerbating the search for a general melanoma therapy (Cheli et al., 2011; Goodall et al., 2008; Goodall et al., 2004; Javelaud et al., 2011; Roesch et al., 2010). The source for this heterogeneity is unclear, but evidence suggests that it is driven by microenvironmental factors (Postovit et al., 2006).
In the process of studying melanoma heterogeneity we described different subtypes of melanoma cells *in vitro* (Hoek et al., 2006) that can be distinguished by gene expression analysis (Widmer et al., 2012). We found that these differences in gene expression correlated with alterations in *in vitro* cell morphology, proliferation rate, invasion, Tgfβ susceptibility and *in vivo* tumor growth kinetics (Hoek et al., 2006; Hoek et al., 2008). These experiments have identified a proliferative phenotype and an invasive melanoma cell phenotype. Previous work from our group showed that primary and metastatic lesions are commonly composed of a mixture of both phenotypes (Eichhoff et al., 2011; Eichhoff et al., 2010). The identified subtypes are independent of genetic differences and clinical stage of the corresponding tumor (Eichhoff et al., 2011). We subsequently hypothesized that melanoma cells, responding to changes in microenvironmental conditions, change their transcription programs to switch back-and-forth between proliferative and invasive states and thereby drive metastatic progression (Hoek et al., 2008a).

In this study we examine the possible role of hypoxia as one of the microenvironmental factors driving metastatic progression by promoting a switch from a proliferative to an invasive phenotype.
As other cancers, melanoma tumors include regions of hypoxia and anoxia caused by an imbalance in both oxygen supply and consumption. It has long been known that the perfusion of tumors is heterogeneous resulting in a wide range of pO_2 levels both within and between tumors (Chaplin et al., 1986). The distance that oxygen diffuses from blood vessels through normal tissues is between 100 to 150 μm. Tissues with larger distance from blood vessels become increasingly hypoxic (Brown, 1990). It is estimated that the proportion of solid tumors with hypoxic (or anoxic) areas is up to 50-60% (Vaupel and Mayer, 2007). The negative impact of tumor hypoxia has been studied extensively. Early studies have shown that hypoxia-induced gene amplification can lead to resistance to

treatment (Luk et al., 1990; Rice et al., 1987). Tumor hypoxia is known to reduce the sensitivity of solid tumors to radiation therapy and can negatively influence treatment outcome and patient survival in multiple cancer types (Hockel et al., 1996; Vergis et al., 2008).

Furthermore, it is known that hypoxia can cause a down-regulation of DNA repair genes, leading to a deregulation of DNA repair pathways (Mihaylova et al., 2003). Especially intermittent hypoxia, or cycles of hypoxia and reoxygenation, have been shown to lead to DNA damage caused by reactive oxygen species (ROS) (Bindra and Glazer, 2005). Moreover, it was observed that short periods of hypoxia followed by reoxygenation caused more lung micrometastases than chronic hypoxia, suggesting that transient hypoxia might increase the invasive potential of tumors (Cairns et al., 2001).

The intracellular oxygen sensing mechanism relies on a heterodimeric transcription factor complex called hypoxia inducible factor 1 (HIF1). Under normoxic conditions the HIF1α protein is hydroxylated and thus targeted for degradation by the proteasome. If oxygen levels are too low for hydroxylation, HIF1α is instead translocated into the nucleus where it complexes with aryl-hydrocarbon receptor nuclear translocator (ARNT), the constitutively expressed β-subunit of the HIF1 heterodimeric transcription factor (Ivan et al., 2001; Jaakkola et al., 2001). HIF1 binds to hypoxia response element (HRE) sequences in the promoters of hundreds of target genes such as the genes encoding vascular endothelial growth factor (*VEGF*), glucose transporter type 1 (*SLC2A1*) and carbonic anhydrase IX (*CA9*), and thereby activates their transcription (Semenza, 2007; Wenger et al., 2005). In solid cancers, including melanoma, HIF1 is reported to be involved in driving processes of migration, invasion and metastasis (Michaylira and Nakagawa, 2006).

In many cancer types the induction of an EMT-like process by exposure to an intralesional hypoxic microenvironment is currently under investigation. Hypoxia has been shown to induce the expression of EMT-critical transcription factors such as *SNAIL1*, *SNAIL2*, *TWIST1*, *ZEB1*, *ZEB2* and *TCF3*. In this way hypoxia is thought to influence, directly or indirectly, EMT processes including the down-regulation of epithelial markers such as E-cadherin (*CDH1*), desmoplakin (*DSP*), plakoglobin (*JUP*), and the up-regulation of mesenchymal factors like N-cadherin (*CDH2*), vimentin (*VIM*) and fibronectin (*FN1*) (Evans et al., 2007; Krishnamachary et al., 2003; Peinado and Cano, 2008). Furthermore, lysyl oxidase (*LOX*) and lysyl oxidase-like 2 (*LOXL2*) are known HIF1 targets with the potential to regulate *SNAIL* during hypoxia-induced metastasis (Peinado and Cano, 2008; Yang et al., 2008).

Another interesting HIF1α target gene is *ANGPTL4*. It is known to have a role in cancer biology, but the data is conflicting. There are studies showing a pro-tumorigenic role of this gene in breast cancer (Padua et al., 2008) and colorectal cancer (Kim et al., 2011), but there is also a study providing evidence of an inhibitory role in melanoma metastasis (Galaup et al., 2006).

Two recent studies of hypoxia in melanoma demonstrate a role of hypoxia in down-regulation of the master regulator of melanocyte differentiation, microphthalmia associated transcription factor (MITF). A study by Cheli and co-workers (Cheli et al., 2011) showed that hypoxic conditions lead to a decrease in MITF expression and that a deletion of MITF is sufficient to increase the metastatic potential of mouse and human melanoma cells *in vivo*. They identified BHLHE40 (BHLHB2, DEC1) as a mediator of the observed hypoxia/HIF1α dependent inhibitory effect on MITF. In another study also published in 2011, the authors (Feige et al., 2011) found the exact same factor to be responsible for hypoxia induced down-regulation of MITF.
Interestingly, this down-regulation of MITF in the melanoma cells is consistent with what the phenotype switching model proposes during a switch from proliferative phenotype to invasive phenotype melanoma cells.

In order to investigate intratumor phenotypical heterogeneity *in vivo*, we isolated and characterized cell cultures of both phenotypes out of the same melanoma metastasis, but from different regions of the tumor. Furthermore, by using invasion assays on human short term melanoma cultures we describe the effects of hypoxia on proliferative and invasive melanoma cell cultures. To find a set of genes with a possible role in hypoxia-triggered switching from a proliferative to an invasive melanoma phenotype we performed DNA microarrays and custom qRT-PCR arrays on hypoxia treated melanoma cells. The results suggest that hypoxia, through HIF1α, alters the gene expression pattern of proliferative melanoma cells, making them more invasive in *in vitro* assays. Furthermore, we investigate the role of *ANGPTL4* in hypoxia-induced melanoma phenotype switching.

5.2.3 Results

5.2.3.1 Melanoma tumors are heterogeneous for proliferative and invasive phenotype melanoma cells.

The phenotype switching model proposes that differences in the microenvironment within a tumor will produce melanoma cells in one of two phenotypic states: proliferative or invasive. To confirm this hypothesis, we excised three pieces of melanoma tissues out of one melanoma lymph node metastasis and started three independent cell cultures following standard protocols (Geertsen et al., 1998) (Figure 1A). The resulting cell cultures were assessed for phenotype-specific characteristics in morphology and network formation on Matrigel. Culture A and C were composed of big cells with a fibroblastic morphology, whereas cells from culture B were small round cells (Figure 1B). When grown on Matrigel, cultures A and C formed big clusters with network-like connections between cells, while the cells from culture B were spread on the Matrigel as single cells or small clusters of cells (Figure 1B). When compared to previously characterized proliferative and invasive cell cultures (Zipser et al., 2011)(Figure S1 and S2), cultures A and C showed a classical invasive phenotype, whereas cell culture B presented a proliferative phenotype (Figure 1B). Previous work in our laboratory demonstrated the differential expression of a specific set of genes between the two phenotypes (Eichhoff et al., 2011; Eichhoff et al., 2010; Hoek et al., 2008a; Hoek et al., 2006; Widmer et al., 2012). MITF was shown to be exclusively expressed by proliferative phenotype cells whereas WNT5A was shown to be a good marker gene for the invasive phenotype. A comparison of gene expression of these phenotype specific marker genes (i.e. MITF, WNT5A) (Figure 1C) and *in vitro* invasion assays (Figure 1D) largely corroborate the proliferative phenotype of culture B and the invasive phenotype of cultures A and C. Interestingly, although culture A had a typical invasive phenotype *in vitro* (Figure 1B) and expressed markers specific to invasive phenotype cells (Figure 1C), the invasive ability of culture A cells was not significantly higher than the invasive ability of the proliferative control cells *in vitro* (Figure 1D). Taken together, we would classify two of the three cell cultures as invasive (i.e. A and C) and one (i.e. B) as proliferative phenotype. These results confirm that intralesional phenotypic heterogeneity in the form of gene expression, *in vitro* morphology, and invasive ability does occur in melanoma.

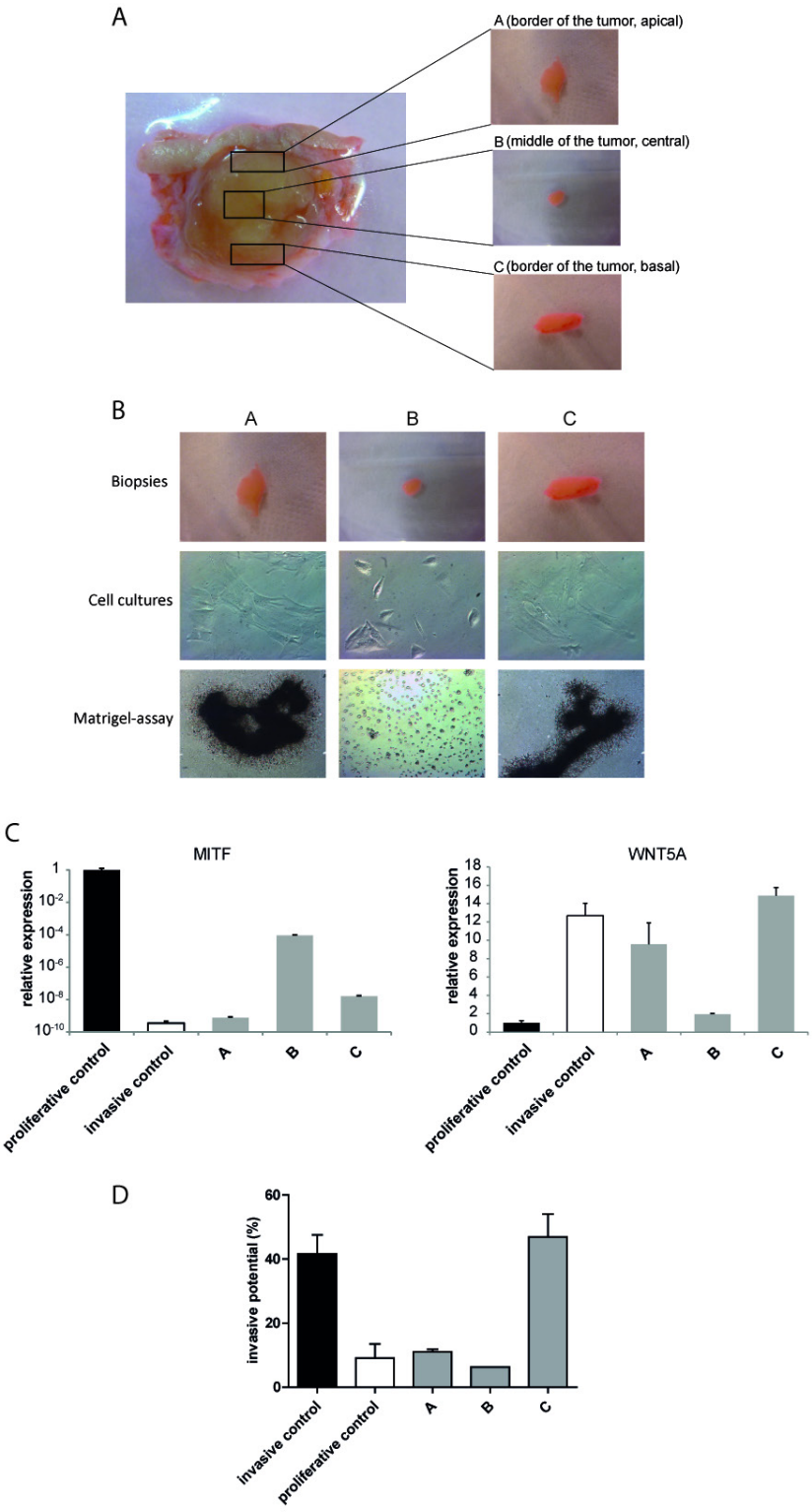

Figure 1: Cell cultures obtained from one melanoma metastasis have heterogeneous phenotypes. Three pieces of a melanoma lymph node metastasis were used to set up three independent melanoma cell cultures (i.e. A, B and C) following standard protocols (A). The cell cultures originating from the same lesion have different morphologies; cultures A and C show an invasive morphology, whereas culture B exhibits a morphology typical of the proliferative phenotype. When growing on a basement membrane-mimicking layer of Matrigel, cultures A and C form networks, similar to previously identified invasive phenotype cell cultures (Figure S1 and S2),

while culture B shows a growth pattern typical of proliferative phenotype melanoma cell cultures (B). qRT-PCR of marker-genes for the proliferative phenotype (*MITF*) and the invasive phenotype (*WNT5A*) show a phenotype specific expression in A, B and C (C). *In vitro* invasion assays show a low invasive potential for cultures A and B, similar to the proliferative control; whereas culture C exhibits a high invasive ability (D).

5.2.3.2 Regions negative for melanocytic makers correlate with hypoxic regions in melanoma.

To gain more insight into the nature of intratumor heterogeneity in patients, we stained Clark's level IV primary human cutaneous melanoma biopsies for key markers of melanocytic function, hypoxia response, proliferation, and vascularization. GLUT1 (*SLC2A1*) is a glucose transporter that has been shown to be upregulated in hypoxic tissue (Bashan et al., 1992; Loike et al., 1992). CD31 (*PECAM-1*) is expressed constitutively on the surface of adult and embryonic endothelial cells and therefore used widely as a marker for blood vessels (Pusztaszeri et al., 2006). MELANA is a protein involved in melanosome biogenesis and has been widely used to identify melanocytic lesions (Busam et al., 1998). Overview pictures of a representative melanoma tumor are shown in the top row (A, B, C) of Figure 2, with boxes on the right hand side of A, B and C indicating the regions of higher magnification shown in A', B' and C' and boxes on the left side highlighting the magnified region in A'', B'' and C'' (Figure 2). The immunohistochemical stainings show that the tumor is composed of tumor cell nodules (Figure 2, A'', B'' and C''), which are surrounded by stroma and endothelial cells (Figure 2, C'', arrowheads). We could observe an up-regulation of GLUT1 with increasing distance from blood vessels in multiple regions of the tumor (arrowheads). As a positive control we can see that also the basal keratinocytes have an elevated expression of GLUT1 (Figure 2, B''), consistent with their distance from the vessels. Panel A of Figure 2 shows that the majority, but not all of the cells in the tumor express MELANA. In the hypoxic areas, which are indicated by arrowheads in A', we found down-regulation of the melanocytic marker MELANA (Figure 2, A', arrowheads as compared to Figure 2, B') and MITF (data not shown). The brown staining is caused by pigment deposited by the tumor cells. Since proliferative phenotype cell cultures strongly express these melanocytic markers, whereas invasive phenotype cell cultures do not express them at all, their expression indicates a de-differentiation of the melanoma cells and point towards a gain of invasive phenotype characteristics (Eichhoff et al., 2011; Eichhoff et al., 2010; Hoek et al., 2008a; Hoek et al., 2006; Zipser et al., 2011). These data suggests that by exposure to a hypoxic microenvironment, melanoma cells down-regulate melanocytic marker genes.

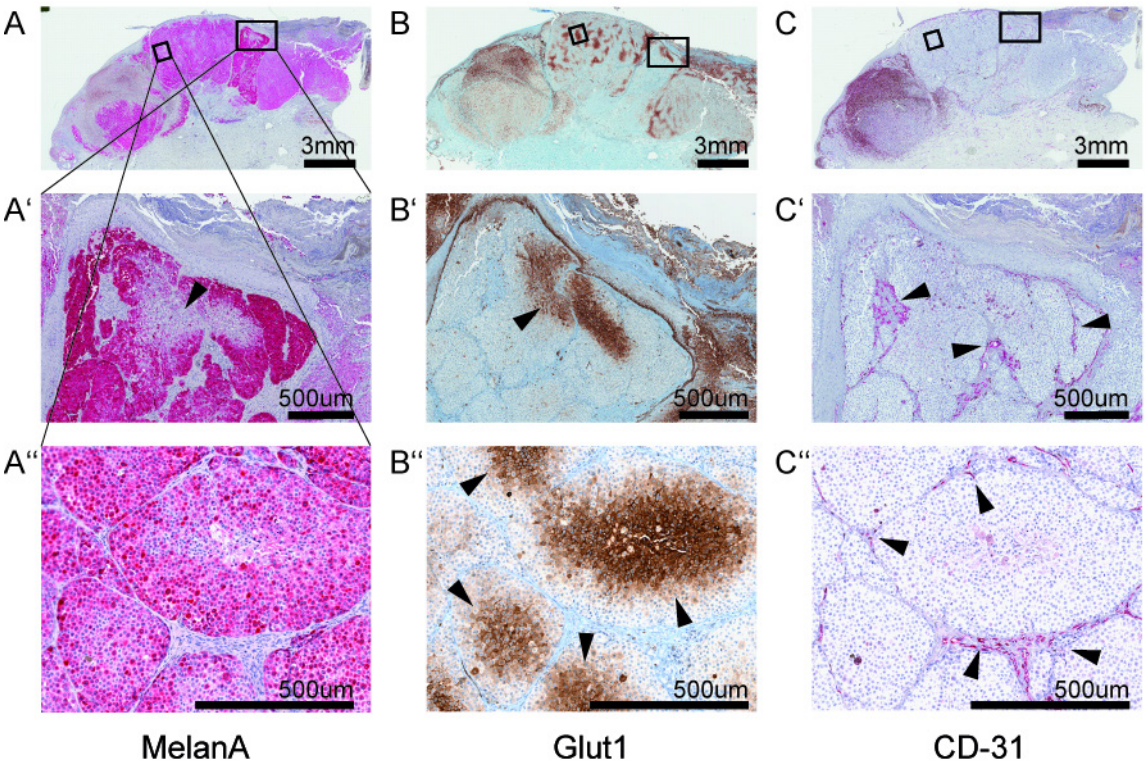

Figure 2: Immunohistochemistry of a primary cutaneous melanoma. Staining for MELANA (left column) shows regions with high expression and regions that have lost expression of this melanocytic marker (arrowhead). Glut1 (middle column) stains hypoxic areas (arrowheads) which are overlapping with MELANA negative regions. The tumor tissue becomes increasingly hypoxic with growing distance from blood vessels as seen with a CD-31 staining (right column, arrowheads).

5.2.3.3 Hypoxia-regulated EMT genes are differentially expressed between the two phenotypes

Intratumoral hypoxia has been shown to induce regulators of epithelial to mensenchymal transition (EMT) and metastasis in breast-, colon-, prostate- and non-small cell lung cancer (Hung et al., 2009; Jo et al., 2009; Luo et al., 2006; Peinado and Cano, 2008; Sipos and Galamb, 2012). An expression analysis of some of the genes known to be involved in this process shows a phenotype-specific expression pattern (Figure 3). The members of the *LOX* family are copper-dependent amine oxidases that catalyze the covalent cross-linking of the component side chains of collagen and elastin in the extracellular matrix. *LOX* has been shown to be involved in EMT, but also in hypoxia-induced tumor invasiveness and metastasis (Baranwal and Alahari, 2009; Elloul et al., 2010; Erler et al., 2006; Peinado et al., 2008). *LOX* is significantly upregulated (9-fold) in the invasive phenotype melanoma cells (Figure 3). *ZEB1* encodes transcription factor, which is also significantly upregulated by over 6-fold in the invasive phenotype cells and has a described role in EMT, tumor invasiveness, and metastasis (Jia et al., 2012; Postigo

and Dean, 1997; Spaderna et al., 2008; Xiong et al., 2012). MMP2 is a matrix metalloproteinase known to be involved in the breakdown of extracellular matrix components (ECM) as well as in tumor invasion and metastasis; *MMP2* mRNA levels are also enriched by 3-fold in invasive phenotype cells (Hojilla et al., 2003; Ray and Stetler-Stevenson, 1994; Stamenkovic, 2003). In development, as well as in the process of EMT and cancer progression, E-cadherin (CDH1) is repressed and leads to a loss of the ECM as well as of adherens and tight junctions (Peinado et al., 2007). However, mesenchymal cadherins, such as N-cadherin (CDH2), are upregulated during EMT (Oda et al., 1998; Peinado et al., 2004). This cadherin switching can also be observed in proliferative and invasive melanoma phenotypes, with an up-regulation of CDH1 in proliferative cells and an up-regulation of CDH2 in invasive cells (Figure 3). Other classical EMT genes, such as those encoding SNAIL and TWIST, do not appear to be differentially regulated between the phenotypes (data not shown). These findings suggest that an EMT-like process is involved in the switching of melanoma cells from proliferative to invasive phenotypes.

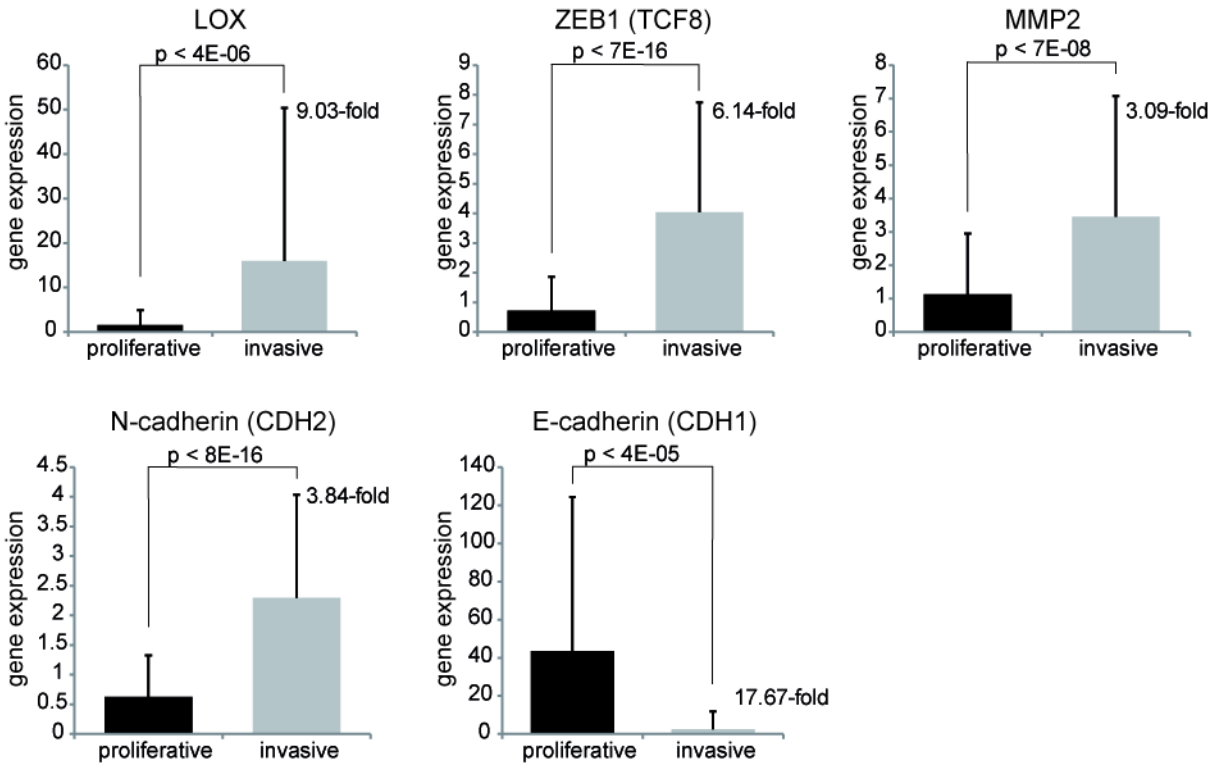

Figure 3: Markers for epithelial to mesenchymal transition (EMT) are significantly upregulated in the invasive phenotype melanoma cell cultures. *LOX*, *ZEB1*, *MMP2* and N-cadherin (*CDH1)* are significantly upregulated in invasive phenotype melanoma cells compared to proliferative phenotype melanoma cells. E-cadherin (*CDH1*) was significantly upregulated in the proliferative phenotype melanoma cells compared to invasive phenotype melanoma cells. The y-axis displays the normalized gene expression signal intensity resulting from DNA microarray experiments described in (Widmer et al., 2012). The p-value is the result of a t-test performed

between 104 proliferative and 100 invasive cell lines; the error bars represent the standard deviation.

5.2.3.4 Hypoxia downregulates melanocytic markers and upregulates EMT and angiogenesis markers in proliferative melanoma cells

To determine the effect of hypoxia treatment on melanoma cells, we exposed proliferative and invasive phenotype melanoma cell cultures to 1% oxygen for 72 h *in vitro* (protocol adapted from (Olbryt et al., 2006)) and then performed DNA microarray analyses. Because the invasive melanoma cell cultures showed only a minor change in gene expression when exposed to hypoxic conditions (data not shown), we further examined the effect of hypoxia on the proliferative melanoma cell cultures only (i.e. M010817). We identified 110 genes that are significantly differentially expressed in hypoxia-treated proliferative melanoma cells compared to normoxic (untreated) cells (Table 1). A Gene Set Enrichment Analysis (GSEA) on www.broadinstitute.org/gsea showed that of the 10 most overlapping gene sets, 7 were linked directly to hypoxia (Table S1) indicating that the change we observed was mainly caused by the effect of hypoxia on the cells.

Table 1: Genes that are differentially expressed between untreated and hypoxia treated proliferative melanoma cell cultures. "up" means that the probeset is upregulated in hypoxia-treated cells versus non-treated controls. The p-value is multiple testing corrected for false discovery rate (FDR) resulting from an ANOVA test. FC stands for "fold-change".

Probe Set ID	p-value (FDR)	FC		Gene Symbol	Gene Description
242517_at	0.043	36.10	up	KISS1R	KISS1 receptor
223333_s_at	0.042	20.68	up	ANGPTL4	angiopoietin-like 4
210095_s_at	0.019	16.55	up	IGFBP3	insulin-like growth factor binding protein 3
221009_s_at	0.047	10.99	up	ANGPTL4	angiopoietin-like 4
219888_at	0.047	10.49	up	SPAG4	sperm associated antigen 4
212143_s_at	0.035	9.06	up	IGFBP3	insulin-like growth factor binding protein 3
202499_s_at	0.018	9.01	up	SLC2A3	solute carrier family 2 member 3
243115_at	0.016	6.98	up	---	---
222088_s_at	0.020	5.65	up	SLC2A14	solute carrier family 2 member 14
202498_s_at	0.019	5.37	up	SLC2A3	solute carrier family 2 member 3
208180_s_at	0.030	5.14	up	HIST1H4H	histone cluster 1, H4h
210512_s_at	0.034	5.02	up	VEGFA	vascular endothelial growth factor A
236180_at	0.049	4.94	up	---	---
213397_x_at	0.044	4.86	up	RNASE4	ribonuclease, RNase A family, 4
224797_at	0.044	4.86	up	ARRDC3	arrestin domain containing 3
206924_at	0.025	4.78	up	IL11	interleukin 11
53991_at	0.049	4.76	up	DENND2A	DENN/MADD domain containing 2A
202022_at	0.038	4.69	up	ALDOC	aldolase C, fructose-bisphosphate
228051_at	0.020	4.67	up	KIAA1244	KIAA1244
232035_at	0.027	4.64	up	LOC100507025	hypothetical LOC100507025
204627_s_at	0.016	4.56	up	ITGB3	integrin, beta 3
221886_at	0.038	4.53	up	DENND2A	DENN/MADD domain containing 2A

205158_at	0.026	4.35	up	RNASE4	ribonuclease, RNase A family, 4
204401_at	0.038	3.99	up	KCNN4	potassium intermediate/small conductance calcium-activated channel, subfamily N, member 4
216236_s_at	0.016	3.97	up	SLC2A14	solute carrier family 2 member 14
208078_s_at	0.022	3.86	up	SIK1	salt-inducible kinase 1
1556410_a_at	0.023	3.85	down	KRTAP19-1	keratin associated protein 19-1
202497_x_at	0.012	3.82	up	SLC2A3	solute carrier family 2 member 3
226722_at	0.012	3.81	up	FAM20C	family with sequence similarity 20, member C
209566_at	0.040	3.81	up	INSIG2	insulin induced gene 2
211527_x_at	0.043	3.72	up	VEGFA	vascular endothelial growth factor A
209457_at	0.025	3.70	up	DUSP5	dual specificity phosphatase 5
1554049_s_at	0.025	3.43	down	DCAF8	DDB1 and CUL4 associated factor 8
218498_s_at	0.025	3.40	up	ERO1L	ERO1-like (S. cerevisiae)
225898_at	0.029	3.40	up	WDR54	WD repeat domain 54
225750_at	0.025	3.34	up	ERO1L	ERO1-like (S. cerevisiae)
221031_s_at	0.050	3.28	up	APOLD1	apolipoprotein L domain containing 1
225381_at	0.038	3.27	up	LOC399959	hypothetical LOC399959
242094_at	0.038	3.27	up	---	---
202887_s_at	0.020	3.24	up	DDIT4	DNA-damage-inducible transcript 4
212171_x_at	0.047	3.23	up	VEGFA	vascular endothelial growth factor A
202912_at	0.025	3.14	up	ADM	adrenomedullin
236219_at	0.025	3.11	down	TMEM20	transmembrane protein 20
226552_at	0.016	3.02	up	IER5L	immediate early response 5-like
1554036_at	0.022	2.91	down	ZBTB24	zinc finger and BTB domain containing 24
226348_at	0.016	2.90	up	---	---
242260_at	0.029	2.90	down	MATR3	Matrin 3
214297_at	0.016	2.88	up	CSPG4	chondroitin sulfate proteoglycan 4
202686_s_at	0.025	2.84	up	AXL	AXL receptor tyrosine kinase
205199_at	0.045	2.84	up	CA9	carbonic anhydrase IX
214701_s_at	0.044	2.81	up	FN1	fibronectin 1
200986_at	0.016	2.77	up	SERPING1	serpin peptidase inhibitor, clade G (C1 inhibitor), member 1
228366_at	0.015	2.77	down	---	---
214963_at	0.012	2.75	down	NUP160	nucleoporin 160kDa
226347_at	0.025	2.71	up	---	---
231856_at	0.036	2.71	up	KIAA1244	KIAA1244
215001_s_at	0.045	2.70	up	GLUL	glutamate-ammonia ligase
229377_at	0.033	2.69	up	GRTP1	growth hormone regulated TBC protein 1
222044_at	0.021	2.69	down	PCIF1	PDX1 C-terminal inhibiting factor 1
217761_at	0.016	2.68	down	ADI1	acireductone dioxygenase 1
210793_s_at	0.040	2.67	down	NUP98	nucleoporin 98kDa
211924_s_at	0.022	2.66	up	PLAUR	plasminogen activator, urokinase receptor
204224_s_at	0.033	2.65	down	GCH1	GTP cyclohydrolase 1
204584_at	0.025	2.63	up	L1CAM	L1 cell adhesion molecule
203238_s_at	0.016	2.62	up	NOTCH3	notch 3
244546_at	0.038	2.61	down	CYCS	cytochrome c, somatic
1556361_s_at	0.025	2.60	down	ANKRD13C	ankyrin repeat domain 13C
1557607_at	0.041	2.60	up	LOC284080	hypothetical LOC284080
229305_at	0.015	2.58	down	MLF1IP	MLF1 interacting protein
216512_s_at	0.025	2.56	down	DCT	dopachrome tautomerase
221497_x_at	0.038	2.52	up	EGLN1	egl nine homolog 1 (C. elegans)
201890_at	0.049	2.49	down	RRM2	ribonucleotide reductase M2
1555772_a_at	0.038	2.49	down	CDC25A	cell division cycle 25 homolog A (S. pombe)
230752_at	0.038	2.49	down	---	---
203339_at	0.031	2.48	down	SLC25A12	solute carrier family 25 (mitochondrial carrier, Aralar), member 12

1557608_a_at	0.036	2.47	up	LOC284080	hypothetical LOC284080
210845_s_at	0.016	2.46	up	PLAUR	plasminogen activator, urokinase receptor
222118_at	0.021	2.46	down	CENPN	centromere protein N
212706_at	0.035	2.40	up	RASA4	RAS p21 protein activator 4
1564970_at	0.019	2.40	down	SETDB2	SET domain, bifurcated 2
201042_at	0.044	2.40	up	TGM2	transglutaminase 2
231003_at	0.048	2.37	down	SLC35B3	solute carrier family 35, member B3
223492_s_at	0.035	2.37	up	LRRFIP1	leucine rich repeat (in FLII) interacting protein 1
218897_at	0.016	2.36	down	TMEM177	transmembrane protein 177
205337_at	0.033	2.36	down	DCT	dopachrome tautomerase
227263_at	0.048	2.35	up	C8orf58	chromosome 8 open reading frame 58
237172_at	0.025	2.34	down	---	---
218309_at	0.028	2.34	up	CAMK2N1	calcium/calmodulin-dependent protein kinase II inhibitor 1
205891_at	0.025	2.34	up	ADORA2B	adenosine A2b receptor
211965_at	0.038	2.33	up	ZFP36L1	zinc finger protein 36, C3H type-like 1
235707_at	0.043	2.31	down	LOC221710	hypothetical protein LOC221710
201489_at	0.016	2.30	down	PPIF	peptidylprolyl isomerase F
210513_s_at	0.025	2.30	up	VEGFA	vascular endothelial growth factor A
228559_at	0.022	2.30	down	CENPN	centromere protein N
241252_at	0.049	2.30	down	ESCO2	establishment of cohesion 1 homolog 2 (S. cerevisiae)
201792_at	0.043	2.28	up	AEBP1	AE binding protein 1
211258_s_at	0.025	2.27	up	TGFA	transforming growth factor, alpha
1568781_at	0.029	2.26	down	---	---
206741_at	0.046	2.25	up	C3orf32	chromosome 3 open reading frame 32
229250_at	0.025	2.24	down	TPCN2	two pore segment channel 2
214797_s_at	0.029	2.24	up	CDK18	cyclin-dependent kinase 18
227283_at	0.040	2.23	up	EFR3B	EFR3 homolog B (S. cerevisiae)
1559399_s_at	0.021	2.23	down	ZCCHC10	zinc finger, CCHC domain containing 10
227935_s_at	0.038	2.23	down	PCGF5	polycomb group ring finger 5
232667_at	0.043	2.23	down	---	---
214962_s_at	0.038	2.22	down	NUP160	nucleoporin 160kDa
218024_at	0.039	2.21	down	BRP44L	brain protein 44-like
212899_at	0.016	2.21	up	CDK19	cyclin-dependent kinase 19
223707_at	0.047	2.21	down	RPL27A	ribosomal protein L27a
204146_at	0.042	2.19	down	RAD51AP1	RAD51 associated protein 1
231892_at	0.042	2.18	down	C9orf100	chromosome 9 open reading frame 100
201170_s_at	0.020	2.18	up	BHLHE40	basic helix-loop-helix family, member e40
202094_at	0.021	2.16	down	BIRC5	baculoviral IAP repeat-containing 5
227526_at	0.025	2.16	up	CDON	Cdon homolog (mouse)
242138_at	0.043	2.15	down	DLX1	distal-less homeobox 1
202997_s_at	0.045	2.14	up	LOXL2	lysyl oxidase-like 2
222400_s_at	0.016	2.13	down	ADI1	acireductone dioxygenase 1
214866_at	0.040	2.13	up	PLAUR	plasminogen activator, urokinase receptor
214744_s_at	0.049	2.11	down	RPL23	ribosomal protein L23
213164_at	0.038	2.11	up	SLC5A3	solute carrier family 5 (sodium/myo-inositol cotransporter), member 3
204999_s_at	0.016	2.11	down	ATF5	activating transcription factor 5
221203_s_at	0.044	2.09	up	YEATS2	YEATS domain containing 2
226574_at	0.035	2.09	down	PSPC1	paraspeckle component 1
224571_at	0.016	2.09	up	IRF2BP2	interferon regulatory factor 2 binding protein 2
228959_at	0.049	2.08	up	PDK3	pyruvate dehydrogenase kinase, isozyme 3
205076_s_at	0.022	2.08	up	MTMR11	myotubularin related protein 11
214882_s_at	0.045	2.08	down	SRSF2	serine/arginine-rich splicing factor 2
201468_s_at	0.020	2.08	down	NQO1	NAD(P)H dehydrogenase, quinone 1
1560433_at	0.041	2.07	down	---	---

205055_at	0.044	2.06	down	ITGAE	integrin, alpha E
203166_at	0.032	2.05	up	CFDP1	craniofacial development protein 1
242538_at	0.022	2.04	down	TFDP1	Transcription factor Dp-1
205348_s_at	0.038	2.03	down	DYNC1I1	dynein, cytoplasmic 1, intermediate chain 1
1553994_at	0.041	2.02	up	NT5E	5'-nucleotidase, ecto (CD73)
214140_at	0.028	2.02	down	SLC25A16	solute carrier family 25 member 16
229426_at	0.015	2.02	down	COX5A	cytochrome c oxidase subunit Va
206913_at	0.033	2.01	down	BAAT	bile acid CoA: amino acid N-acyltransferase
210117_at	0.039	2.01	down	SPAG1	sperm associated antigen 1
229892_at	0.039	2.01	down	EP400NL	EP400 N-terminal like
217996_at	0.038	2.00	up	PHLDA1	pleckstrin homology-like domain, family A, member 1

To assess the degree of overlap between hypoxia-induced gene expression and phenotype-specific gene expression, we looked at the expression of genes that we identified by comparing 12 invasive and 6 proliferative primary short term melanoma cell cultures in microarray analysis (Table S2). We found 2645 genes showing a significantly differential expression between proliferative and invasive phenotypes (Table S2) and an at least 2-fold up- or down-regulation. These genes were tested for differential expression between hypoxia-treated proliferative melanoma phenotype cells and untreated controls. We found that 82 genes of this list are significantly altered in their expression levels upon hypoxia treatment (Table 2). When we tested 33000 genes (all the genes on the microarray), we found 110 genes which where regulated significantly by hypoxia. After we reduced the number of tested genes to 2545 (8% of 33000) we still got 82 (75% of 110) genes as a result. This suggests a close relationship between hypoxia and gene expression differences between phenotypes.

Table 2: Genes that are differentially expressed between proliferative and invasive melanoma cell cultures were analyzed for differential expression between hypoxia-treated proliferative and untreated control proliferative melanoma cell cultures. Phenotype specificity: "1" indicates genes upregulated upon hypoxia treatment and upregulated in the invasive phenotype melanoma cell cultures, "2" indicates genes down-regulated upon hypoxia treatment and down-regulated in the invasive phenotype melanoma cell cultures. "0" indicates genes without consistent change in gene expression. The p-value is multiple testing corrected (FDR) and results from an ANOVA test. FC stands for "fold-change".

Probe Set ID	p-value (FDR)	FC		Gene Symbol	Gene Description	Phenotype Specificity
200632_s_at	0.020	8.58	up	NDRG1	N-myc downstream regulated 1	1
200986_at	0.005	2.77	up	SERPING1	serpin peptidase inhibitor, clade G (C1 inhibitor), member 1	1
201042_at	0.012	2.40	up	TGM2	transglutaminase 2	1
201489_at	0.005	2.30	down	PPIF	peptidylprolyl isomerase F	2
201490_s_at	0.015	2.32	down	PPIF	peptidylprolyl isomerase F	2
202178_at	0.025	2.27	up	PRKCZ	protein kinase C, zeta	0
202619_s_at	0.024	3.17	up	PLOD2	procollagen-lysine, 2-oxoglutarate 5-dioxygenase 2	1
202627_s_at	0.025	2.45	up	SERPINE1	serpin peptidase inhibitor, clade E	1

					(nexin, plasminogen activator inhibitor type 1), member 1	
202686_s_at	0.007	2.84	up	AXL	AXL receptor tyrosine kinase	1
202733_at	0.022	3.49	up	P4HA2	prolyl 4-hydroxylase, alpha polypeptide II	1
202769_at	0.023	2.17	up	CCNG2	cyclin G2	1
202770_s_at	0.024	2.13	up	CCNG2	cyclin G2	1
202912_at	0.007	3.14	up	ADM	adrenomedullin	1
203238_s_at	0.005	2.62	up	NOTCH3	notch 3	1
203477_at	0.023	2.23	up	COL15A1	collagen, type XV, alpha 1	1
203851_at	0.031	2.63	up	IGFBP6	insulin-like growth factor binding protein 6	1
203910_at	0.045	2.29	up	ARHGAP29	Rho GTPase activating protein 29	1
203939_at	0.023	3.04	up	NT5E	5'-nucleotidase, ecto (CD73)	1
204298_s_at	0.049	2.23	up	LOX	lysyl oxidase	1
204347_at	0.039	2.97	up	AK4	adenylate kinase 4	1
204348_s_at	0.031	3.13	up	AK4	adenylate kinase 4	1
204584_at	0.007	2.63	up	L1CAM	L1 cell adhesion molecule	0
204595_s_at	0.031	9.04	up	STC1	stanniocalcin 1	1
204596_s_at	0.016	5.39	up	STC1	stanniocalcin 1	1
204597_x_at	0.033	12.71	up	STC1	stanniocalcin 1	1
205076_s_at	0.007	2.08	up	MTMR11	myotubularin related protein 11	1
205158_at	0.007	4.35	up	RNASE4	ribonuclease, RNase A family, 4	1
205337_at	0.009	2.36	down	DCT	dopachrome tautomerase	2
205338_s_at	0.014	2.25	down	DCT	dopachrome tautomerase	2
205348_s_at	0.010	2.03	down	DYNC1I1	dynein, cytoplasmic 1, intermediate chain 1	2
206432_at	0.044	2.12	down	HAS2	hyaluronan synthase 2	0
207543_s_at	0.028	3.17	up	P4HA1	prolyl 4-hydroxylase, alpha polypeptide I	1
209566_at	0.011	3.81	up	INSIG2	insulin induced gene 2	1
209611_s_at	0.042	2.01	up	SLC1A4	solute carrier family 1, member 4	0
210095_s_at	0.005	16.55	up	IGFBP3	insulin-like growth factor binding protein 3	1
210367_s_at	0.024	2.21	up	PTGES	prostaglandin E synthase	1
210495_x_at	0.049	2.32	up	FN1	fibronectin 1	1
210512_s_at	0.009	5.02	up	VEGFA	vascular endothelial growth factor A	1
211527_x_at	0.012	3.72	up	VEGFA	vascular endothelial growth factor A	1
211719_x_at	0.029	2.32	up	FN1	fibronectin 1	1
211959_at	0.027	6.84	up	IGFBP5	insulin-like growth factor binding protein 5	1
212143_s_at	0.009	9.06	up	IGFBP3	insulin-like growth factor binding protein 3	1
212281_s_at	0.035	2.04	down	TMEM97	transmembrane protein 97	2
213397_x_at	0.012	4.86	up	RNASE4	ribonuclease, RNase A family, 4	1
213603_s_at	0.040	2.11	up	RAC2	ras-related C3 botulinum toxin substrate 2 (rho family, small GTP binding protein Rac2)	1
214696_at	0.044	2.18	down	C17orf91	chromosome 17 open reading frame 91	0
214701_s_at	0.012	2.81	up	FN1	fibronectin 1	1
214702_at	0.016	4.52	up	FN1	fibronectin 1	1
214962_s_at	0.010	2.22	down	NUP160	nucleoporin 160kDa	2
214963_at	0.005	2.75	down	NUP160	nucleoporin 160kDa	2
216442_x_at	0.044	2.52	up	FN1	fibronectin 1	1
216512_s_at	0.007	2.56	down	DCT	dopachrome tautomerase	2
216513_at	0.024	2.37	down	DCT	dopachrome tautomerase	2
217996_at	0.010	2.00	up	PHLDA1	pleckstrin homology-like domain, family A, member 1	0
218718_at	0.047	2.18	up	PDGFC	platelet derived growth factor C	1
218849_s_at	0.038	2.53	up	PPP1R13L	protein phosphatase 1, regulatory (inhibitor) subunit 13 like	1
218897_at	0.005	2.36	down	TMEM177	transmembrane protein 177	2

219121_s_at	0.020	2.57	down	ESRP1	epithelial splicing regulatory protein 1	2
220425_x_at	0.022	2.74	down	ROPN1B	ropporin, rhophilin associated protein 1B	2
220865_s_at	0.032	2.09	down	PDSS1	prenyl (decaprenyl) diphosphate synthase, subunit 1	2
221024_s_at	0.045	2.29	up	SLC2A10	solute carrier family 2 (facilitated glucose transporter), member 10	1
221031_s_at	0.014	3.28	up	APOLD1	apolipoprotein L domain containing 1	0
221478_at	0.015	2.69	up	BNIP3L	BCL2/adenovirus E1B 19kDa interacting protein 3-like	1
221479_s_at	0.022	2.41	up	BNIP3L	BCL2/adenovirus E1B 19kDa interacting protein 3-like	1
221601_s_at	0.048	2.01	down	FAIM3	Fas apoptotic inhibitory molecule 3	2
221841_s_at	0.023	2.17	up	KLF4	Kruppel-like factor 4 (gut)	1
221870_at	0.040	2.10	up	EHD2	EH-domain containing 2	1
222044_at	0.007	2.69	down	PCIF1	PDX1 C-terminal inhibiting factor 1	2
45297_at	0.033	2.35	up	EHD2	EH-domain containing 2	1
223492_s_at	0.010	2.37	up	LRRFIP1	leucine rich repeat (in FLII) interacting protein 1	1
223707_at	0.013	2.21	down	RPL27A	ribosomal protein L27a	0
224191_x_at	0.028	2.53	down	ROPN1	ropporin, rhophilin associated protein 1	2
224602_at	0.036	2.31	up	C4orf3	chromosome 4 open reading frame 3	1
224797_at	0.012	4.86	up	ARRDC3	arrestin domain containing 3	1
225021_at	0.034	2.18	up	ZNF532	zinc finger protein 532	1
225342_at	0.037	4.06	up	AK4	adenylate kinase 4	1
225381_at	0.010	3.27	up	LOC399959	hypothetical LOC399959	1
225846_at	0.018	2.94	down	ESRP1	epithelial splicing regulatory protein 1	2
226348_at	0.005	2.90	up	---	---	0
226550_at	0.014	4.60	up	---	---	0
226574_at	0.010	2.09	down	PSPC1	paraspeckle component 1	2
226682_at	0.016	3.05	up	RORA	RAR-related orphan receptor A	1
227935_s_at	0.010	2.23	down	PCGF5	polycomb group ring finger 5	0
228069_at	0.024	2.02	down	FAM54A	family with sequence similarity 54, member A	2
228188_at	0.020	2.49	up	FOSL2	FOS-like antigen 2	1
228245_s_at	0.024	2.13	up	LOC100509231	ovostatin homolog 2-like	0
228843_at	0.024	2.94	up	ARL10	ADP-ribosylation factor-like 10	1
228955_at	0.014	2.12	down	---	---	0
228987_at	0.031	2.98	down	---	---	0
229250_at	0.007	2.24	down	TPCN2	two pore segment channel 2	2
230521_at	0.031	2.29	down	C9orf100	chromosome 9 open reading frame 100	2
230746_s_at	0.034	14.98	up	LOC100288985	Hypothetical protein LOC100288985	1
231003_at	0.014	2.37	down	SLC35B3	solute carrier family 35, member B3	0
231535_x_at	0.048	2.51	down	ROPN1	ropporin, rhophilin associated protein 1	2
235086_at	0.014	3.21	down	THBS1	thrombospondin 1	0
235117_at	0.014	2.50	down	CHAC2	ChaC, cation transport regulator homolog 2 (E. coli)	2
235707_at	0.012	2.31	down	LOC221710	hypothetical protein LOC221710	2
236480_at	0.024	2.84	up	---	---	0
240432_x_at	0.024	2.29	up	KLF7	Kruppel-like factor 7 (ubiquitous)	1
241252_at	0.014	2.30	down	ESCO2	establishment of cohesion 1 homolog 2 (S. cerevisiae)	2
242260_at	0.008	2.90	down	MATR3	Matrin 3	2
242450_at	0.043	2.16	down	RGMB	RGM domain family, member B	0
1553118_at	0.034	2.19	down	THEM4	thioesterase superfamily member 4	2
1553747_at	0.037	2.03	down	MGC16025	hypothetical LOC85009	2
1553994_at	0.011	2.02	up	NT5E	5'-nucleotidase, ecto (CD73)	1
1553995_a_at	0.024	2.17	up	NT5E	5'-nucleotidase, ecto (CD73)	1
1554036_at	0.007	2.91	down	ZBTB24	zinc finger and BTB domain containing 24	2

1554037_a_at	0.015	2.48	down	ZBTB24	zinc finger and BTB domain containing 24	2
1555225_at	0.031	2.30	down	C1orf43	chromosome 1 open reading frame 43	2
1556410_a_at	0.007	3.85	down	KRTAP19-1	keratin associated protein 19-1	2
1558105_a_at	0.015	3.19	up	---	---	0
1560208_at	0.019	2.02	up	---	---	0
1564970_at	0.005	2.40	down	SETDB2	SET domain, bifurcated 2	2

A closer comparison between these two lists showed that 69 of 82 genes were regulated in a phenotype specific manner, meaning that invasive phenotype-specific genes are up-regulated and proliferative phenotype-specific genes are down-regulated by hypoxia treatment (Table 2).

The expression levels of 8 genes involved in melanoma invasion, angiogenesis or melanocyte development were tested additionally by qRT-PCR on proliferative melanoma cell cultures (i.e. M010817) treated for 72 h with 1% O_2, to confirm the results of the microarray analyses. Interestingly, in contrast to the microarray results, *MITF* and *MELANA* were differentially regulated between hypoxia-treated proliferative phenotype melanoma cell cultures and the non-treated cells (Figure 4). *MITF*, *MELANA* and *IRF4,* which are all important in melanocyte and melanoma biology (Bharti et al., 2006; Hodgkinson et al., 1993; Hoek et al., 2008b; Jeffs et al., 2009), are significantly downregulated upon hypoxia treatment (Figure 4 top row). *PLAUR*, *SERPINE1* and *LOX* which play a role in melanoma invasion and metastasis (Erler and Giaccia, 2006; Vassalli et al., 1991) are significantly upregulated by a hypoxic microenvironment (Figure 4 middle row). *ANGPTL4* and *VEGFA,* which are involved in neovascularization and numerous other pathways important to tumor biology (Galaup et al., 2006; Lacal et al., 2005) were also highly and significantly upregulated in hypoxia-treated melanoma cells (Figure 4 lowest row).

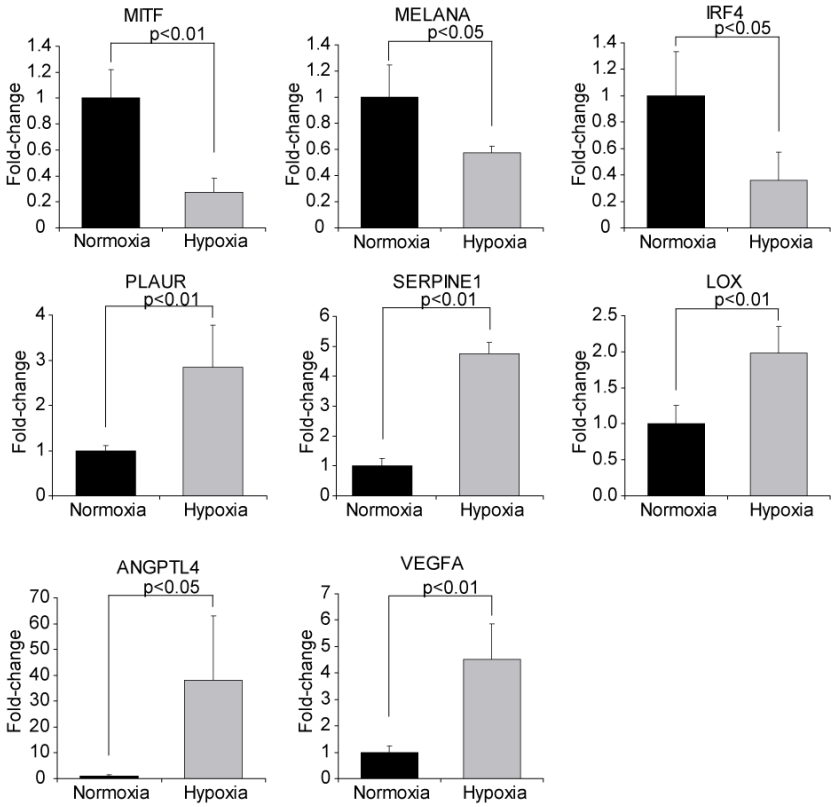

Figure 4: qRT-PCR of key-genes using RNA from hypoxia-treated proliferative melanoma cell cultures vs. untreated control cells. Markers for proliferative phenotype melanoma cells are downregulated upon hypoxia treatment (i.e. *MITF*, *MELANA*, *IRF4*). Factors known to be involved in melanoma invasion were strongly upregulated by hypoxia (*PLAUR*, *SERPINE1*, *LOX*). Genes important for angiogenesis were also strongly upregulated upon hypoxia treatment (*ANGPTL4* and *VEGFA*). The p-values are calculated from a t-test; the error bars represent the standard deviation.

5.2.3.5 Hypoxia changes in vitro invasive potential in proliferative melanoma cells in a dose-dependent manner

To further test if hypoxia drives proliferative cells to a more invasive state, we treated proliferative phenotype cells with 1% O2 for 48 h and tested their invasiveness *in vitro* by performing Boyden chamber experiments. The proliferative cell cultures treated with hypoxia showed a significant increase in invasion compared to the non-treated control cells (Figure 5A). The relative invasion increased by 2-fold for M080423, 2.3-fold for M000921 and even 4.2-fold for M010817. However, invasive phenotype cells (i.e. M080307) in identical treatment conditions did not show any change in invasiveness (p-value=0.399) (Figure 5A). Furthermore, we tested if the gain in invasion is still present when the cells were returned tonormoxia for 48 h after a hypoxia treatment period of 48 h. In Figure 5B (dark grey bar) we show that the effect remained significant after cells were returned to normoxia 48 h prior to invasion testing. When the cells were exposed to hypoxia for 96 h, the effect was intensified (Figure 5B, white bar).

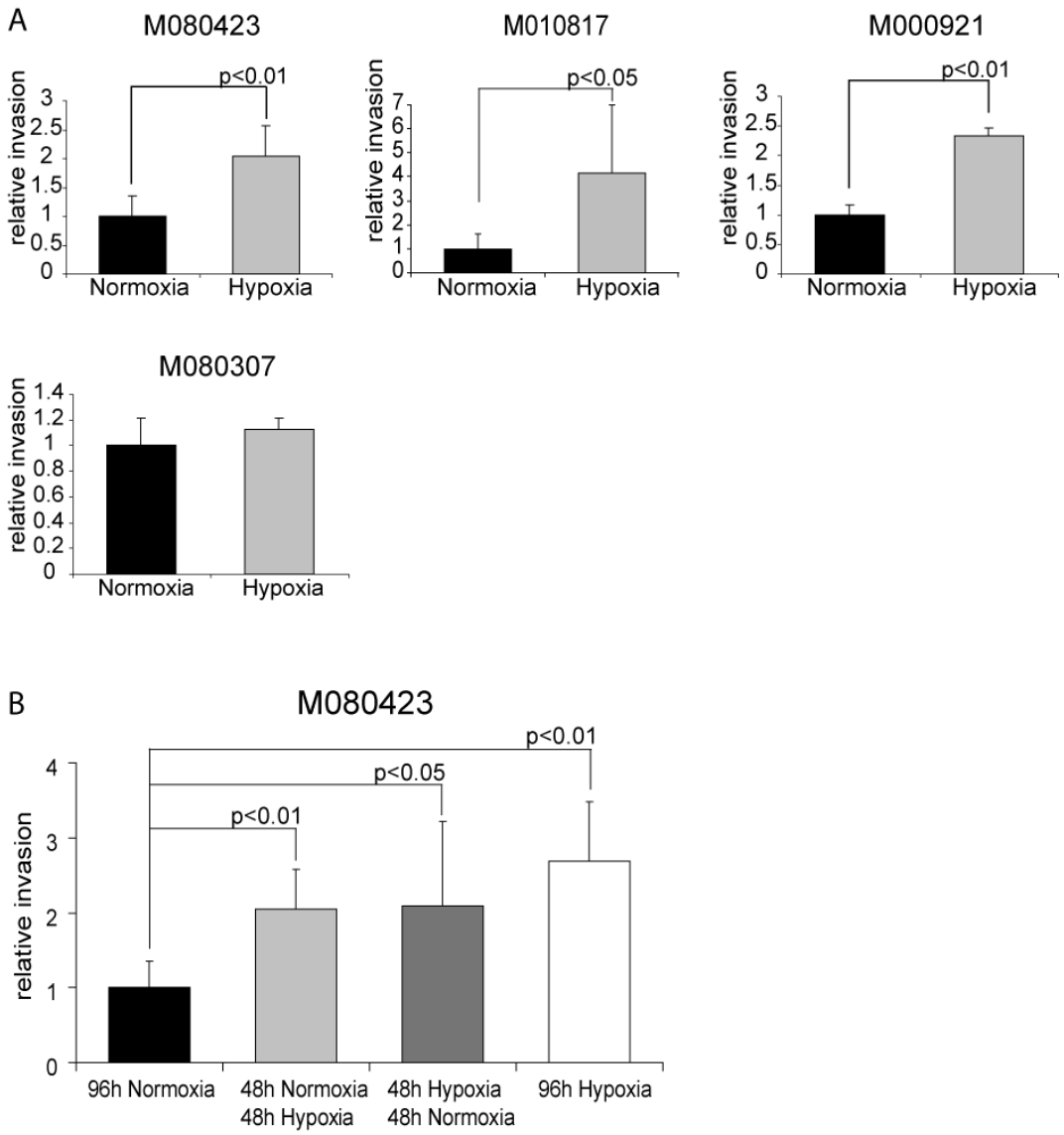

Figure 5: Hypoxia increases *in vitro* invasion in proliferative melanoma cells. Proliferative melanoma cell cultures (M080423, M010817 and M000921) show significantly increased *in vitro* invasiveness when treated with hypoxia for 72 hours. The Invasive phenotype cell culture (M080307) does not show an altered *in vitro* invasiveness (p-value=0.399) (A). Hypoxia treatment induces increased invasiveness in a dose dependent fashion (B). In this experiment a proliferative melanoma cell culture was pre-incubated in normoxia or hypoxia for 48 hours (light grey and dark gray bars, respectively) and subsequently analyzed in a Boyden chamber assay in hypoxia or normoxia for 48 hours. The effect of hypoxia treatment on invasiveness could still be observed when performed under normoxic conditions (dark grey bar). Increased incubation time in hypoxia resulted in increased invasiveness (white bar). The p-values are derived from a t-test; the error bars represent the standard deviation.

5.2.3.6 ANGPTL4 is not required for the hypoxia-induced increase in invasion and the down-regulation of melanocytic factors

Because *ANGPTL4* was one of the top upregulated genes in our microarrays upon hypoxia treatment (Table 1) and because of its ambiguous role in cancer biology we decided to further investigate the role of this gene in melanoma. As mentioned above, we first confirmed the up-regulation by hypoxia by qRT-PCR level (Figure 4). To investigate the role of *ANGPTL4* in the process of hypoxia-induced phenotype switching, we treated proliferative melanoma cell cultures with siRNA against *ANGPTL4* during exposure to hypoxia (1% O_2 for 48h) (Figure 6). The down-regulation of *ANGPTL4* (siANGPTL4) did not significantly change hypoxia-induced *in vitro* invasion in two proliferative cell cultures (p-value=0.94 for M010817, p-value=0.28 for M080423) compared to cells treated with control siRNA (sicontrol) (Figure 6A). Furthermore, the knockdown of *ANGPTL4* (si_RNA2/3_72h) during hypoxia treatment (1%O_2 for 72h) did not affect the expression of *MELANA* and *MITF* and the expression levels of these genes did not return to the levels seen under normoxic conditions (Normoxia) (Figure 6B). At the protein level we found that MELANA was downregulated upon hypoxia treatment (1% O_2 for 72h) (H_sico) in two proliferative melanoma cell cultures (M010817 and M000921) compared to normoxic controls (N_nosi). When *ANGPTL4* was knocked down by siRNA (H_siA), the protein level of MELANA was not returned to the levels found in normoxic controls (N_nosi), but were even further reduced (Figure 6C).

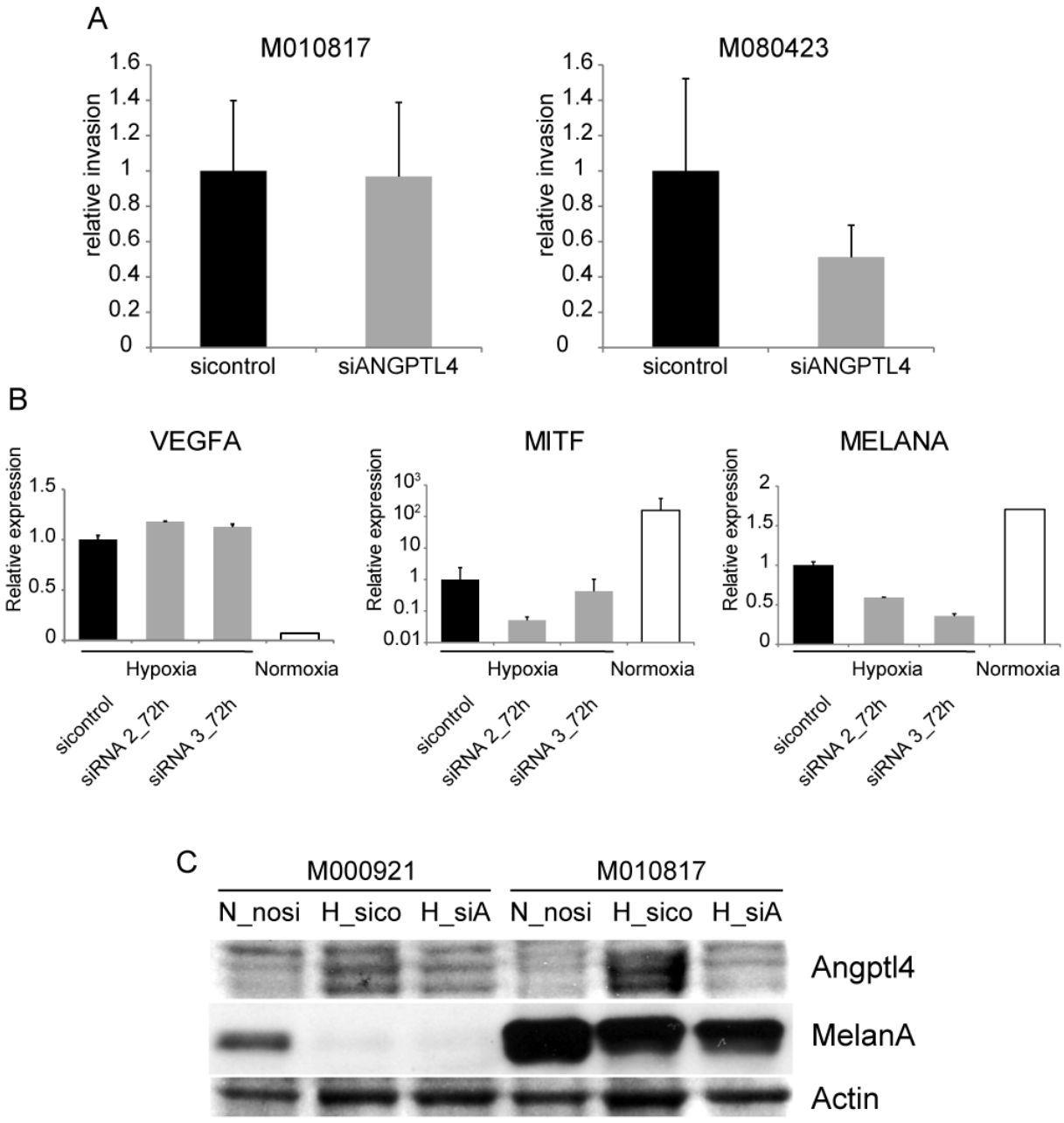

Figure 6: *ANGPTL4* is not required for a hypoxia-induced increase in invasion and down-regulation of melanocytic factors. Knock-down of *ANGPTL4* by siRNA in proliferative melanoma cell cultures under hypoxic culture conditions for 48 hours (siANGPTL4) does not significantly affect *in vitro* invasion compared to control siRNA-treated (sicontrol) cell cultures (p-value=0.94 for M010817, p-value=0.28 for M080423) (A). The change in gene expression of *VEGFA*, *MITF* and *MELANA* in M010817 caused by treatment with hypoxia for 72 hours (sicontrol) cannot be prevented by a knock-down of ANGPTL4 (siRNA2/3_72h)) (B). On the protein level this finding could be confirmed: Knocking down *ANGPTL4* (H_siA) could not inhibit down-regulation of MELANA compared to normoxic control (N_nosi) caused by a hyopoxic environment (H_sico) for 48 hours (C).

5.2.3.7 Down-regulation of MELANA during hypoxia is mediated by HIF1α

The inverse correlation of hypoxic areas with the expression of melanocytic markers like MELANA (Figure 2) raises the question, whether the decrease in the expression of this protein is mediated by HIF1α, a known regulator of the hypoxic response. To test this possibility, we treated proliferative phenotype melanoma cells (i.e. M000921) with chemicals to either suppress or activate signaling through HIF1α. To inhibit HIF1α transcriptional activity we treated the cells with Echinomycin during exposure to hypoxia (1%O_2 for 72h) (Kong et al., 2005). The induction of HIF1α as well as the down-regulation of MELANA could be inhibited under hypoxia (Figure 7A). The same results could be seen when we enhanced HIF1α degradation with the chemical compound YC-1 (Chun et al., 2001) (Figure 7B). $CoCl_2$ stabilizes HIF1α by inhibiting proline hydroxylases, leading to HIF1α expression also under normoxic conditions (Epstein et al., 2001). We observed accumulation of HIF1α also under normoxic conditions upon treatment with $CoCl_2$, leading to down-regulation of MELANA (Figure 7B). Since these compounds might have off-target effects and since their specificity is unclear, we also performed siRNA mediated knock-down of HIF1α using two different siRNAs against the HIF1α transcript (Figure 7C). The results confirm a HIF1α-dependent expression of MELANA, suggesting a role for HIF1α in the phenotype switch induced by tumor hypoxia.

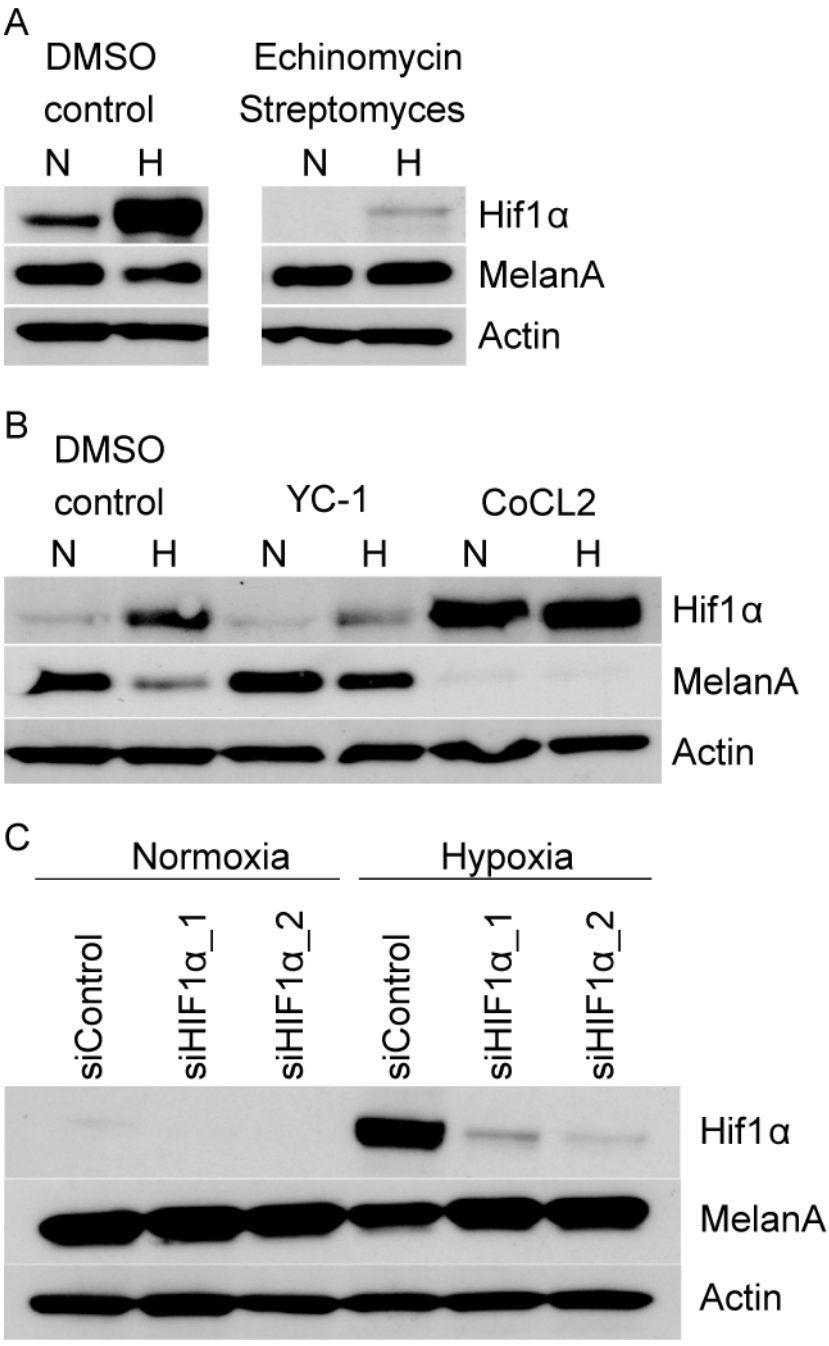

Figure 7: Down-regulation of MELANA upon hypoxia treatment is HIF1α dependent. Echinomycin enhances HIF1α degradation, leading to inhibition of MELANA down-regulation under hypoxic conditions (A). Treatment of proliferative melanoma cell cultures with YC-1 decreases HIF1α levels and also reduces MELANA down-regulation. $CoCl_2$ stabilizes HIF1α under normoxic conditions leading to a down-regulation of MELANA in normoxia (B). Under normoxia, no HIF1α could be detected (C). When proliferative cells (M000921) are treated with hypoxia, HIF1α is stabilized and MELANA is downregulated (siControl). When HIF1α is knocked down by siHIF1α (siHIF1a_1/2), MELANA expression is restored (C). N: normoxia, H: hypoxia.

5.2.3.8 Looking for the mediator

It is likely that there are intermediate factors acting downstream of HIF1α, which induce the suppression of MELANA gene expression. To find HIF1α targets that might repress MELANA, we performed siRNA knock-down of HIF1α followed by qRT-PCR analysis. We tested 90 genes that are part of the Melanoma Phenotype Specific Expression (MPSE) gene set, and which have been previously identified to be differentially expressed between a large number of proliferative and invasive phenotype melanoma cell lines (Widmer et al., 2012). We used the service from SA-Biosciences (Qiagen) to assemble a custom qRT-PCR array with these 90 genes. This array was used to find genes that are downregulated when treated with hypoxia, but rescued when *HIF1α* is knocked down. The results show 12 genes that are at least two-fold down-regulated upon hypoxia treatment (hypoxia sico) compared to normoxic controls (normoxia sico) (Figure 8A) and at least two-fold upregulated when *HIF1α* was knocked down under hypoxic conditions (hypoxia siHIF1α) compared to normal hypoxia (hypoxia sico). Of the 12 genes, 8 were upregulated in the proliferative phenotype cell cultures (Figure 8A, gene-names in green) and 4 were upregulated in invasive phenotype cell cultures (Figure 8A, gene-names in red). We were also interested in genes that were upregulated at least two-fold upon hypoxia treatment (hypoxia sico), but had an at least two-fold decreased expression when HIF1α is knocked down under hypoxic conditions (hypoxia siHIF1α) compared to normal hypoxia (hypoxia sico). Of the 12 genes fulfilling these criteria, 10 were upregulated in the invasive phenotype cells (Figure 8B, gene-names in red), whereas 2 genes were upregulated in the proliferative phenotype cell cultures (Figure 8B, gene-names in green) (Figure 8B). The results show that 18 out of the 24 genes regulated by HIF1α were differentially regulated between the proliferative and invasive melanoma cell lines in such a way that proliferative genes were downregulated and invasive genes are upregulated by HIF1α.

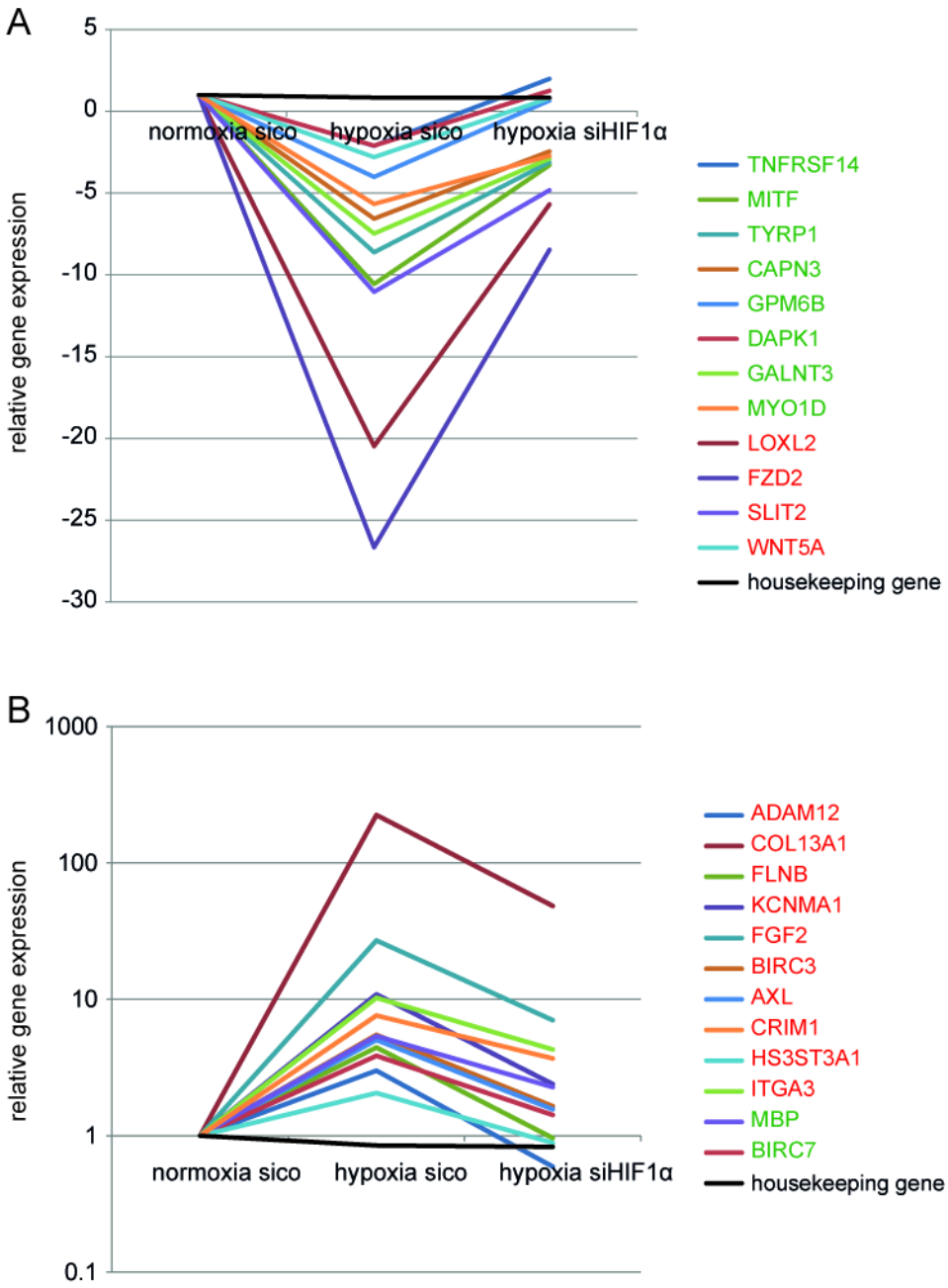

Figure 8: qRT-PCR using RNA from hypoxia- and/or siHIF1α-treated proliferative phenotype melanoma cell cultures. Genes which were at least 2-fold down-regulated when grown in a hypoxic environment (hypoxia sico) compared to untreated cells (normoxia sico) are shown. When *HIF1α* was knocked down (hypoxia siHIF1α), these genes were at least 2-fold upregulated compared to cells treated with control siRNA (hypoxia sico). Gene names in green highlight genes that were upregulated in the proliferative phenotype melanoma cell cultures (A). In (B) we show genes that were at least 2-fold upregulated between hypoxia treated cells (hypoxia sico) and control cells (normoxia sico), but when *HIF1α* was knocked down (hypoxia siHIF1α), these genes were at least 2-fold downregulated as compared to cells treated with control siRNA (hypoxia sico). Gene names in red indicate genes that were upregulated in the invasive phenotype melanoma cell cultures. This experiment was performed in duplicate with two different siRNAs against *HIF1α*. (Gene abbreviations are explained in supplemental material (Table S2)).

5.2.4 Discussion

The characterization of different subpopulations of melanoma cells in a tumor is of major clinical relevance, since all the subpopulations of melanoma cells need to be killed for successful therapeutic intervention. The exceptional transcriptional and phenotypic plasticity of melanoma cells has so far prevented the discovery of single prognostic factors or target molecules appropriate for general melanoma therapy. In our previous work we demonstrated that the invasive phenotype melanoma cell is less susceptible to MAPK inhibition and that proliferative phenotype melanoma cells temporarily switch their phenotype to one with more invasive features during drug treatment (Zipser et al., 2011). Furthermore, immunotherapy targeting melanocytic markers will not eradicate the invasive phenotype cells, since these markers are not expressed once the cells modulate their transcriptional networks.

In this study we show that melanoma tumors are heterogeneous for the proliferative and invasive phenotypes of melanoma cells, which we have previously demonstrated to be highly relevant to melanoma biology in both *in vitro* and xenograft models. By isolating distinct fractions of melanoma cells within a single lymph node metastasis, we established cell cultures with features from both phenotypes, thereby confirming intratumor heterogeneity within this lesion (Figure 1).

At the genetic level, melanoma turns out to be much more variable than previously thought. Recently published studies have shown inter- and intratumoral heterogeneity for driver mutations like *BRAF* or *KIT*, suggesting a limited scope for current therapies in personalized medicine that target specifically mutated serine or tyrosine kinases (Sakaizawa et al., 2012; Yancovitz et al., 2012). Not only is intrinsic genetic heterogeneity of importance as a basis for tumor progression, but acquired heterogeneity that is induced by microenvironmental factors may also lead to therapeutic resistance. To overcome intrinsic as well as acquired resistance, it is imperative to understand tumor heterogeneity at the genetic and transcriptional levels.

Immunohistochemical stainings of tumors show regions with high GLUT1expression, indicating hypoxic regions which anti-correlate with the melanocytic markers MITF and MELANA (Figure 2). We have previously shown that melanoma cells with high MITF and MELANA expression are only weakly invasive *in vitro*, whereas melanoma cells with no MITF and MELANA expression are highly invasive (Eichhoff et al., 2011; Hoek et al., 2006; Zipser et al., 2011). These results suggest that in a hypoxic microenvironment, melanocytic markers are downregulated, which is a sign of cell-dedifferentiation that is also evident in invasive phenotype cells. These data confirm the results of an earlier study in which proliferative markers (i.e. MELANA and MITF) were anti-correlated with invasive

markers (WNT5A) and hypoxia (GLUT1) in melanoma (Eichhoff et al., 2010). Conversely to what Eichhoff et al. reported, we also observed GLUT1 expression in many nested, nicely organized tumor regions. Even though the staining for CD31 suggests the presence of blood vessels around the tumor cell nests, it seems that either the nests are too large or the blood vessels are not fully functional so that the melanoma cells become hypoxic.
Eichhoff et al. also showed that in a distal metastasis, melanoma cells can have the shape and marker expression of normal epidermal melanocytes, underpinning the highly plastic behavior of melanoma cells during disease progression.

Epithelial to mesenchymal transition (EMT) and its reverse process, called mesenchymal to epithelial transition (MET) are basic developmental programs during embryogenesis that were first described in studies with chicken embryos (Pérez-Pomares and Muñoz-Chápuli, 2002; Trelstad et al., 1967). Since then, many of the factors involved in EMT have been demonstrated to have a role in cancer invasion and metastasis in multiple epithelial cancers (Janda et al., 2002; Kiemer et al., 2001; Xue et al., 2003). The mechanisms seen in epithelial cancers going through EMT can also be seen in melanoma even though this is not a classical epithelial cancer (Dissanayake et al., 2007; Koefinger et al., 2011; Poser et al., 2001; Wels et al., 2011). EMT genes are reported to play a role in the generation of stem-like cells (Mani et al., 2008), which have a fibroblast-like, mesenchymal appearance. In fact, recent data suggest that these two subsets of melanoma cells share many characteristics (Hoek and Goding, 2010). In an analysis of microarray data from melanoma cells with either proliferative or invasive characteristics, we observed that many EMT genes are differentially expressed between the proliferative and invasive phenotypes (Figure 3 and Table S2).
In microarray experiments of proliferative phenotype melanoma cells, which were treated with hypoxia compared to non-treated controls, 110 genes were differentially expressed (Table 1). Among these genes, many are known to play a role in hypoxia. A Gene Set Enrichment Analysis (GSEA) suggests that the observed changes in gene expression are a consequence of hypoxia treatment (Table S1), since the differentially expressed genes in our experiments are significantly enriched in other previously published hypoxia experiments. Furthermore many genes listed in Table 1 are known to be regulated by HIF1α (i.e. *CA9*, *VEGFA*, *IGFBP3*, *SPAG4*) (Benita et al., 2009; Ortiz-Barahona et al., 2010). Several genes have a role in melanoma invasion and metastasis (i.e. *PLAUR*, *AXL* and *FN1*) (Jeffs et al., 2009; Kääriäinen et al., 2006; Rofstad et al., 2002; Sensi et al., 2011) and are significantly upregulated by a hypoxic microenvironment (Table 1).
Surprisingly, *MITF*, one of the most important genes in the phenotype switching model did not change its expression significantly upon hypoxia treatment as determined by

microarray analysis (Table 1). For this reason, we checked the level of *MITF* expression using qRT-PCR together with other key genes that are diagnostic of the melanoma cells in either the proliferative or invasive states. The results could not confirm the data from the microarrays, since the qRT-PCR analysis of *MITF* expression showed clear, statistically significant differential regulation, as did two target genes of *MITF* (i.e. *MELANA*, *IRF4*). Although these genes were differentially expressed, the result was not significant because of a too high variance among the samples of one sample group. Generally, due to the strict statistical analysis including FDR multiple testing correction, the rate of type II errors (false negative results) is probably higher than of type I errors (false positives).
Furthermore, the results show a very high overlap of genes, which are differentially regulated between the phenotypes (Table S2) and between hypoxia-treated and untreated proliferative cells. As expected, we found a down-regulation of "proliferative genes" and an up-regulation of "invasive genes" upon treatment with hypoxia. This was true for 88% of the genes shown in Table 2. Thus, the observed change in gene expression suggests a directed change in phenotype-specific expression patterns.

We tested if hypoxia increases the *in vitro* invasive potential of proliferative melanoma cells by performing Boyden chamber invasion assays. The results showed a significant increase in invasion from 2- to more than 4-fold for all tested proliferative cell cultures (Figure 5A). An invasive cell line that we tested (i.e. M080307) did not show an increase in invasive potential (Figure 5A). This was expected, since also in the microarray experiments the difference between treated and untreated cells was marginal. We also showed that this increase in *in vitro* invasiveness is dose dependent (Figure 5B). It lasts at least 48 hours and increases with longer exposure time up to 96 hours (Figure 5B).

To find a gene that may potentiate the ability of proliferative cells to become more invasive in response to hypoxia exposure *in vitro*, we tested the role of angiopoietin-like 4 (*ANGPTL4*) in this process. *ANGPTL4* was previously identified as a regulator of lipid metabolism (Oike et al., 2005). It is known to be a target of peroxisome proliferators-activated receptors (PPARs) (Kersten et al., 2000), and to be upregulated after fasting and hypoxia (Belanger et al., 2002; Kersten et al., 2000). *ANGPTL4* was reported to prevent metastasis by inhibiting vascular leakiness and penetrability of tumor cells (Galaup et al., 2006; Ito et al., 2003). On the other hand, studies have shown pro-tumorigenic effects of *ANGPTL4* (Cazes et al., 2006; Galaup et al., 2006; Kim et al., 2011; Le Jan et al., 2003; Padua et al., 2008; Verine et al., 2010). Furthermore, it has been shown to be involved in wound healing (Goh et al., 2010) and to play a role in integrin signaling and intracellular O_2^- production to induce tumor cell apoptosis (Zhu et al., 2011).

Our results suggest that *ANGPTL4* is not necessary for the increase in invasion or the down-regulation of melanocytic markers in response to hypoxia treatment *in vitro* (Figure 6). It is likely that *ANGPTL4* does not act alone and that different experimental models with endothelial and other stromal involvement are necessary to uncover the role of *ANGPTL4* in hypoxia induced phenotype switching.

By stabilizing and inhibiting HIF1α as well as by knocking down *HIF1α*, we could show that the down-regulation of MELANA is HIF1α dependent (Figure 7). Possible mediators for this effect were identified by qRT-PCR analysis of 90 genes, which are differentially expressed between the two phenotypes (Widmer et al., 2012). Analysis of these data showed 12 genes to be down-regulated by hypoxia treatment, but not when *HIF1α* is knocked down (Figure 8). Of these, 8 genes are commonly down-regulated in the invasive melanoma cell cultures and therefore potentially involved in the switch from a proliferative to an invasive phenotype. Interestingly, *MITF* and its target tyrosinase-related protein 1 (*TYRP1*) are among this set (Figure 8). Also, *TNFRSF14*, *CAPN3*, *GPM6B* and *DAPK1*, which are potential targets of *MITF* that we have previously identified, are differentially expressed (Hoek et al., 2008b). This suggests a potent role of HIF1α-regulated *MITF* in the process of hypoxia induced phenotype switching. Furthermore, two of these genes are known to have a proapoptotic role: calpain 3 (*CAPN3*) (Moretti et al., 2009) and death associated protein kinase 1 (*DAPK1*) (Lin et al., 2007). Glycoprotein M6B (*GPM6B*) has been shown to be downregulated in highly invasive melanoma cells vs. poorly invasive lines (Seftor et al., 2002). *MYOD1* a gene coding for a motor protein and *GALNT3* which is involved in protein glycosylation do not have a known role in melanoma. Taken together the down-regulation of these genes can be interpreted as a *HIF1α*-induced dedifferentiation of the melanoma cells through loss in expression of key melanocytic marker and pro-apoptotic genes.
A set of 12 genes is also induced by hypoxia but not when *HIF1α* is knocked down (Figure 8). Ten of these genes are upregulated in the invasive phenotype melanoma cell cultures and are therefore of particular interest (Figure 8). One of the most interesting genes encodes fibroblast growth factor 2 (FGF2), a mitogenic and angiogenic factor that can act as an autocrine growth factor for melanoma cells (Becker et al., 1989; Halaban et al., 1988). *AXL*, a receptor tyrosine kinase, has been shown to be expressed only in MITF negative melanoma cells (Sensi et al., 2011) confirming our own results (Hoek et al., 2006; Widmer et al., 2012). Sensi et al. also showed that *AXL* increases the motility and invasion of melanoma cells. *HIF1α* seems to induce the expression of multiple genes, which encode proteins involved in interactions with the extracellular matrix, such as ADAM12, a disintegrin and metalloproteinase, COL13A1, a transmembrane collagen

chain, ITGA3, an integrin alpha subunit, and FLNB, a filamin known to bind to the actin cytoskeleton (Danen and Sonnenberg, 2003; Kveiborg et al., 2008; Lendeckel et al., 2005; Prockop and Kivirikko, 1995; Takafuta et al., 1998). The up-regulation of *BIRC3*, a gene encoding an apoptosis inhibitor, is consistent with the down-regulation of two pro-apoptotic genes (*CAPN3* and *DAPK1*). The potassium channel KCNMA1, which is also upregulated in the presence of hypoxia in a HIF1α-dependent manner, could be regulated by MITF over the microRNA miR-211 (Mazar et al., 2010). CRIM1, a transmembrane protein and HS3ST3A1, a heparin sulfate biosynthetic enzyme, do not have known roles in melanoma.
Further studies have to show if inhibition of one or more of these factors can inhibit the tumor promoting effect of HIF1α.

The influence of hypoxia on melanoma cells was also studied by Cheli et al. (Cheli et al., 2011) and Feige et al. (Feige et al., 2011). Cheli and coworkers exposed B16 melanoma cells to 1% oxygen for 24 hours and subsequently injected these cells subcutaneously into mice. They observed that the hypoxia-treated cells form significantly larger tumors than untreated control cells. After tail vein injection, hypoxia treated cells formed more lung tumors and visceral metastases. They concluded that hypoxia downregulates MITF by up-regulation of DEC1, which enhances the tumorigenic and metastatic potential of melanoma cells. Feige and coworkers chose a different approach to investigate the influence of hypoxia on melanoma cells. They used UACC-62, a human melanoma cell line that according to our studies is predicted to have a proliferative phenotype (Widmer et al., 2012). They injected this cell line subcutaneously into nude mice and waited until a measurable tumor had appeared. Then they treated the mice with dimethyloxalylglycine (DMOG), a prolyl-hydroxylase inhibitor and thereby HIF1α stabilizer. The DMOG treated mice exhibited smaller tumors and lived longer compared to PBS treated mice, which had to be killed because of tumor burden. The conclusion from these results was that induction of HIF1α leads to a down-regulation of MITF by up-regulation of DEC1 which suppresses tumorigenic and metastatic potential of melanoma cells.
Despite similar results from their respective *in vitro* experiments (i.e. that hypoxia modulates *MITF* expression through *HIF1α*), contradictory outcomes from *in vivo* tests led to opposite conclusions about the effect of hypoxia on melanoma progression.

In contrast to these two studies, we used human melanoma short term cultures which, as we previously showed, might more closely resemble melanoma biology than melanoma cell lines that had been passaged multiple times or even murine cells (Widmer et al., 2012). Furthermore, we use high-throughput gene expression analysis, allowing a broader

insight into the effect of hypoxia on melanoma cells. In our study we show the increase in invasion in human short term cell cultures *in vitro*, thereby, in principal supporting the data from Cheli et al. Also in our study, *DEC1* was upregulated in the microarray experiments but not significantly changed between proliferative and invasive phenotype cell lines, suggesting a role for DEC1 during the switch from proliferative to invasive phenotypes, but maybe not in the maintenance of the phenotypes once they are established. Further *in vivo* experiments with human short-term melanoma cultures are necessary to clarify the clinical relevance of these observations.

The data presented here suggest that hypoxia is a possible microenvironmental stimulus triggering a switch from a proliferative to an invasive melanoma cell phenotype. By downregulating melanocytic genes, HIF1α induces a dedifferentiation to a more invasive type of melanoma cell. Up-regulation of pro-angiogenic and pro-tumorigenic factors as well as of ECM modifying genes along with a down-regulation of pro-apoptotic genes may allow the invasive melanoma cells to contribute to melanoma progression.

5.2.5 Acknowledgements

We would like to thank Prof. Sabine Werner for her continuous support and for proof-reading the manuscript. Funding was provided by the Swiss National Science Foundation (PDFMP3_127249/1, DW), the Gottfried und Julia Bangerter Rhyner Stiftung (RD) and the Georg und Bertha Schwyzer-Winiker Stiftung (RD). We thank the Cancer Biology PhD Program of the University/ETH Zürich for support.

5.2.6 Supplementary data

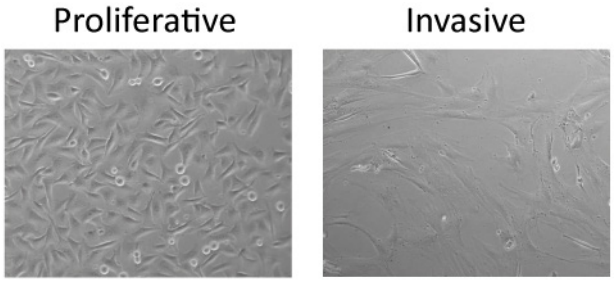

Figure S1: representative microscope pictures of a proliferative and an invasive melanoma cell culture serving as references for comparisons with freshly isolated cell cultures. Proliferative cell cultures are smaller, sometimes melanocytic looking while the invasive cell cultures are very big and flat more fibroblastic looking.

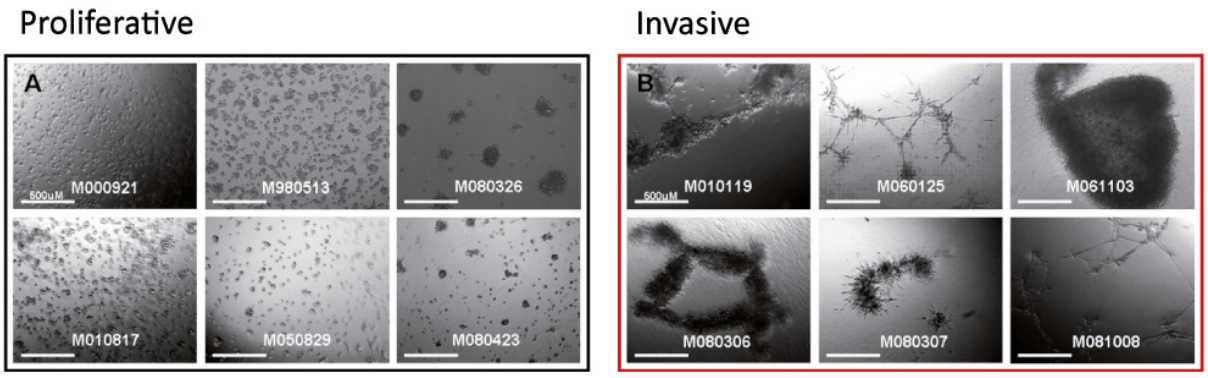

Figure S2: a selection of representative microscope pictures of proliferative and invasive melanoma cell cultures growing on a basement membrane mimicking layer of Matrigel. Proliferative cell cultures form small cell clusters or grow as single cells, whereas invasive cell cultures form networks or form big clumps of cells (Zipser et al., 2011).

Tabelle S1: Gene Set Enrichment Analysis on www.broadinstitute.org/gsea. In this analysis, genes which are differentially expressed between hypoxia treated proliferative melanoma cells and untreated controls (Table 1) were compared to a database 6769 published experiments. The program looked for overlaps and calculates the number of genes that overlap in both gene lists (Genes in Overlap (k)) and the p-value for this event (p-value). Of the 10 most overlapping experiments (Gene Set Name, Description), 7 were directly linked to hypoxia.

Gene Set Name	Genes in Gene Set (K)	Description	Genes in Overlap (k)	k/K	p-value
ELVIDGE_HYPOXIA_UP	174	Genes up-regulated in MCF7 cells (breast cancer) under hypoxia conditions.	16	0.092	0.00E+00
ELVIDGE_HYPOXIA_BY_DMOG_UP	132	Genes up-regulated in MCF7 cells (breast cancer) treated with hypoxia mimetic DMOG [PubChem=3080614].	16	0.1212	0.00E+00
ELVIDGE_HIF1A_AND_HIF2A_TARGETS_DN	105	Genes down-regulated in MCF7 cells (breast cancer) after knockdown of both HIF1A and HIF2A [Gene ID=3091, 2034] by RNAi.	13	0.1238	0.00E+00
ELVIDGE_HIF1A_TARGETS_DN	92	Genes down-regulated in MCF7 cells (breast cancer) after knockdown of HIF1A [Gene ID=3091] by RNAi.	12	0.1304	2.22E-16
KOBAYASHI_EGFR_SIGNALING_24HR_DN	252	Genes down-regulated in H1975 cells (non-small cell lung cancer, NSCLC) resistant to gefitinib [PubChem=123631] after treatment with EGFR inhibitor CL-387785 [PubChem=2776] for 24h.	15	0.0595	3.77E-15
WINTER_HYPOXIA_METAGENE	218	Genes regulated by hypoxia, based on literature searches.	14	0.0642	1.14E-14
MENSE_HYPOXIA_UP	99	Hypoxia response genes in both astrocytes and HeLa cell line.	10	0.101	8.98E-13
MANALO_HYPOXIA_UP	208	Genes up-regulated in response to both hypoxia and overexpression of an active form of HIF1A [Gene ID=3091].	12	0.0577	3.56E-12
BILD_HRAS_ONCOGENIC_SIGNATURE	260	Genes selected in supervised analyses to discriminate cells expressing activated HRAS [Gene ID=3265] oncogene from control cells expressing GFP.	12	0.0462	4.83E-11
SMID_BREAST_CANCER_BASAL_UP	676	Genes up-regulated in basal subtype of breast cancer samples.	17	0.0251	5.31E-11

Table S2: Top 100 of significantly differentially expressed genes between proliferative and invasive phenotype melanoma cell cultures. Sorted for fold change (FC). "up" means this gene is upregulated in invasive phenotype melanoma cell cultures compared to proliferatives.

Gene Symbol	FC		Gene Description
GREM1	353.31	up	gremlin 1
COL1A1	317.33	up	collagen, type I, alpha 1
GJA1	225.11	up	gap junction protein, alpha 1, 43kDa
TYRP1	203.21	down	tyrosinase-related protein 1
COL1A2	192.04	up	collagen, type I, alpha 2
COL3A1	142.26	up	collagen, type III, alpha 1
COL6A3	138.91	up	collagen, type VI, alpha 3
MLANA	134.29	down	melan-A
S100B	131.64	down	S100 calcium binding protein B
MFAP5	121.92	up	microfibrillar associated protein 5
SILV	119.23	down	silver homolog (mouse)
TNFRSF11B	118.11	up	tumor necrosis factor receptor superfamily, member 11b
STMN2	108.62	up	stathmin-like 2
LOC100509231	108.34	down	ovostatin homolog 2-like
CAPN3	100.48	down	calpain 3, (p94)
LOC100506621	93.31	up	hypothetical LOC100506621
EFEMP1	90.37	up	EGF-containing fibulin-like extracellular matrix protein 1
TMEM47	82.34	up	transmembrane protein 47
TRIM22	81.25	up	tripartite motif-containing 22
KIAA1199	74.05	up	KIAA1199
IGFBP3	73.87	up	insulin-like growth factor binding protein 3
LOX	73.06	up	lysyl oxidase
DCN	71.00	up	decorin
ATP8B1	70.99	up	ATPase, aminophospholipid transporter, class I, type 8B, member 1
KRTAP1-5	68.26	up	keratin associated protein 1-5
TAGLN	67.24	up	transgelin
LOXL1	63.58	up	lysyl oxidase-like 1
PSG5	63.20	up	pregnancy specific beta-1-glycoprotein 5
MAGEA6	61.79	down	melanoma antigen family A, 6
DSE	61.68	up	dermatan sulfate epimerase
CCDC80	61.34	up	coiled-coil domain containing 80
TRPM1	61.13	down	transient receptor potential cation channel, subfamily M, member 1
SERPINE1	59.64	up	serpin peptidase inhibitor, clade E (nexin, plasminogen activator inhibitor type 1), member 1
TMEM200A	56.22	up	transmembrane protein 200A
MAGEA3	53.62	down	melanoma antigen family A, 3
POSTN	52.61	up	periostin, osteoblast specific factor
PTX3	52.00	up	pentraxin 3, long
KRT34	51.29	up	keratin 34
PRAME	49.75	down	preferentially expressed antigen in melanoma
SLC45A2	49.57	down	solute carrier family 45, member 2
CPE	48.63	up	carboxypeptidase E
DCT	48.39	down	dopachrome tautomerase
COL5A2	48.23	up	collagen, type V, alpha 2
MAGEA12	48.04	down	melanoma antigen family A, 12
GPR143	47.39	down	G protein-coupled receptor 143
COL8A1	47.34	up	collagen, type VIII, alpha 1
EDIL3	47.15	up	EGF-like repeats and discoidin I-like domains 3

KRT19	45.89	up	keratin 19
COL5A1	45.66	up	collagen, type V, alpha 1
TGFBI	45.32	up	transforming growth factor, beta-induced, 68kDa
FBN1	45.17	up	fibrillin 1
TWIST2	44.68	up	twist homolog 2 (Drosophila)
TYR	43.24	down	tyrosinase (oculocutaneous albinism IA)
MBP	42.88	down	myelin basic protein
PHACTR1	42.66	down	phosphatase and actin regulator 1
LAYN	42.42	up	layilin
RAB38	41.29	down	RAB38, member RAS oncogene family
SCG5	40.27	up	secretogranin V (7B2 protein)
CDH11	40.18	up	cadherin 11, type 2, OB-cadherin (osteoblast)
VGLL3	39.86	up	vestigial like 3 (Drosophila)
MXRA5	39.60	up	matrix-remodelling associated 5
PDGFRA	39.41	up	platelet-derived growth factor receptor, alpha polypeptide
CYP1B1	39.27	up	cytochrome P450, family 1, subfamily B, polypeptide 1
THBS1	38.07	up	thrombospondin 1
STC2	38.02	up	stanniocalcin 2
ITGBL1	37.74	up	integrin, beta-like 1 (with EGF-like repeat domains)
THY1	37.03	up	Thy-1 cell surface antigen
UCHL1	36.84	up	ubiquitin carboxyl-terminal esterase L1 (ubiquitin thiolesterase)
HS3ST3B1	36.79	up	heparan sulfate (glucosamine) 3-O-sulfotransferase 3B1
FGF7	36.67	up	fibroblast growth factor 7
INHBA	36.09	up	inhibin, beta A
GPM6B	35.81	down	glycoprotein M6B
VCAN	35.60	up	versican
EDNRB	35.53	down	endothelin receptor type B
SSTR1	35.50	up	somatostatin receptor 1
OXTR	35.22	up	oxytocin receptor
LOC100507165	34.86	up	hypothetical LOC100507165
C10orf58	34.71	down	chromosome 10 open reading frame 58
ODZ2	34.40	up	odz, odd Oz/ten-m homolog 2 (Drosophila)
PLP1	34.28	down	proteolipid protein 1
LOC730755	34.25	up	keratin associated protein 2-4-like
FSTL1	34.25	up	follistatin-like 1
CA8	33.80	down	carbonic anhydrase VIII
EFEMP2	33.54	up	EGF-containing fibulin-like extracellular matrix protein 2
PRRX1	33.38	up	paired related homeobox 1
IL1R1	31.81	up	interleukin 1 receptor, type I
COL12A1	31.66	up	collagen, type XII, alpha 1
ALPK2	31.53	up	alpha-kinase 2
IGFBP6	31.46	up	insulin-like growth factor binding protein 6
BCL2A1	31.38	down	BCL2-related protein A1
CITED1	30.55	down	Cbp/p300-interacting transactivator, with Glu/Asp-rich carboxy-terminal domain, 1
RENBP	30.38	down	renin binding protein
C4orf49	30.28	up	chromosome 4 open reading frame 49
DSEL	29.72	up	dermatan sulfate epimerase-like
NEXN	29.42	up	nexilin (F actin binding protein)
LBH	29.04	up	limb bud and heart development homolog (mouse)
ABI3BP	28.54	up	ABI family, member 3 (NESH) binding protein
IGFBP5	28.23	up	insulin-like growth factor binding protein 5
PLAGL1	27.81	up	pleiomorphic adenoma gene-like 1
LOC100288911	27.45	up	hypothetical LOC100288911

5.2.7 References

Baranwal, S., and Alahari, S. K. (2009). Molecular mechanisms controlling E-cadherin expression in breast cancer. Biochem Biophys Res Commun *384*, 6-11.

Bashan, N., Burdett, E., Hundal, H. S., and Klip, A. (1992). Regulation of glucose transport and GLUT1 glucose transporter expression by O2 in muscle cells in culture. Am J Physiol *262*, C682-690.

Becker, D., Meier, C. B., and Herlyn, M. (1989). Proliferation of human malignant melanomas is inhibited by antisense oligodeoxynucleotides targeted against basic fibroblast growth factor. EMBO J *8*, 3685-3691.

Belanger, A. J., Lu, H., Date, T., Liu, L. X., Vincent, K. A., Akita, G. Y., Cheng, S. H., Gregory, R. J., and Jiang, C. (2002). Hypoxia up-regulates expression of peroxisome proliferator-activated receptor gamma angiopoietin-related gene (PGAR) in cardiomyocytes: role of hypoxia inducible factor 1alpha. J Mol Cell Cardiol *34*, 765-774.

Benita, Y., Kikuchi, H., Smith, A. D., Zhang, M. Q., Chung, D. C., and Xavier, R. J. (2009). An integrative genomics approach identifies Hypoxia Inducible Factor-1 (HIF-1)-target genes that form the core response to hypoxia. Nucleic Acids Res *37*, 4587-4602.

Bharti, K., Nguyen, M. T., Skuntz, S., Bertuzzi, S., and Arnheiter, H. (2006). The other pigment cell: specification and development of the pigmented epithelium of the vertebrate eye. Pigment Cell Res *19*, 380-394.

Bindra, R. S., and Glazer, P. M. (2005). Genetic instability and the tumor microenvironment: towards the concept of microenvironment-induced mutagenesis. Mutat Res *569*, 75-85.

Bollag, G., Hirth, P., Tsai, J., Zhang, J., Ibrahim, P. N., Cho, H., Spevak, W., Zhang, C., Zhang, Y., Habets, G.*, et al.* (2010). Clinical efficacy of a RAF inhibitor needs broad target blockade in BRAF-mutant melanoma. Nature *467*, 596-599.

Brown, J. M. (1990). Tumor hypoxia, drug resistance, and metastases. J Natl Cancer Inst *82*, 338-339.

Busam, K. J., Chen, Y. T., Old, L. J., Stockert, E., Iversen, K., Coplan, K. A., Rosai, J., Barnhill, R. L., and Jungbluth, A. A. (1998). Expression of melan-A (MART1) in benign melanocytic nevi and primary cutaneous malignant melanoma. Am J Surg Pathol *22*, 976-982.

Cairns, R. A., Kalliomaki, T., and Hill, R. P. (2001). Acute (cyclic) hypoxia enhances spontaneous metastasis of KHT murine tumors. Cancer research *61*, 8903-8908.

Cazes, A., Galaup, A., Chomel, C., Bignon, M., Brechot, N., Le Jan, S., Weber, H., Corvol, P., Muller, L., Germain, S., and Monnot, C. (2006). Extracellular matrix-bound angiopoietin-like 4 inhibits endothelial cell adhesion, migration, and sprouting and alters actin cytoskeleton. Circ Res *99*, 1207-1215.

Chaplin, D. J., Durand, R. E., and Olive, P. L. (1986). Acute hypoxia in tumors: implications for modifiers of radiation effects. Int J Radiat Oncol Biol Phys *12*, 1279-1282.

Cheli, Y., Giuliano, S., Guiliano, S., Botton, T., Rocchi, S., Hofman, V., Hofman, P., Bahadoran, P., Bertolotto, C., and Ballotti, R. (2011). Mitf is the key molecular switch between mouse or human melanoma initiating cells and their differentiated progeny. Oncogene *30*, 2307-2318.

Chun, Y. S., Yeo, E. J., Choi, E., Teng, C. M., Bae, J. M., Kim, M. S., and Park, J. W. (2001). Inhibitory effect of YC-1 on the hypoxic induction of erythropoietin and vascular endothelial growth factor in Hep3B cells. Biochem Pharmacol *61*, 947-954.

Danen, E. H., and Sonnenberg, A. (2003). Integrins in regulation of tissue development and function. J Pathol *201*, 632-641.

Dissanayake, S. K., Wade, M., Johnson, C. E., O'Connell, M. P., Leotlela, P. D., French, A. D., Shah, K. V., Hewitt, K. J., Rosenthal, D. T., Indig, F. E.*, et al.* (2007). The Wnt5A/protein kinase C pathway mediates motility in melanoma cells via the inhibition of metastasis suppressors and initiation of an epithelial to mesenchymal transition. J Biol Chem *282*, 17259-17271.

Eichhoff, O. M., Weeraratna, A., Zipser, M. C., Denat, L., Widmer, D. S., Xu, M., Kriegl, L., Kirchner, T., Larue, L., Dummer, R., and Hoek, K. S. (2011). Differential LEF1 and TCF4 expression is involved in melanoma cell phenotype switching. Pigment Cell Melanoma Res *24*, 631-642.
Eichhoff, O. M., Zipser, M. C., Xu, M., Weeraratna, A. T., Mihic, D., Dummer, R., and Hoek, K. S. (2010). The immunohistochemistry of invasive and proliferative phenotype switching in melanoma: a case report. Melanoma Res *20*, 349-355.
Elloul, S., Vaksman, O., Stavnes, H. T., Trope, C. G., Davidson, B., and Reich, R. (2010). Mesenchymal-to-epithelial transition determinants as characteristics of ovarian carcinoma effusions. Clin Exp Metastasis *27*, 161-172.
Epstein, A. C., Gleadle, J. M., McNeill, L. A., Hewitson, K. S., O'Rourke, J., Mole, D. R., Mukherji, M., Metzen, E., Wilson, M. I., Dhanda, A*., et al.* (2001). C. elegans EGL-9 and mammalian homologs define a family of dioxygenases that regulate HIF by prolyl hydroxylation. Cell *107*, 43-54.
Erler, J. T., Bennewith, K. L., Nicolau, M., Dornhofer, N., Kong, C., Le, Q. T., Chi, J. T., Jeffrey, S. S., and Giaccia, A. J. (2006). Lysyl oxidase is essential for hypoxia-induced metastasis. Nature *440*, 1222-1226.
Erler, J. T., and Giaccia, A. J. (2006). Lysyl oxidase mediates hypoxic control of metastasis. Cancer Res *66*, 10238-10241.
Evans, A. J., Russell, R. C., Roche, O., Burry, T. N., Fish, J. E., Chow, V. W., Kim, W. Y., Saravanan, A., Maynard, M. A., Gervais, M. L*., et al.* (2007). VHL promotes E2 box-dependent E-cadherin transcription by HIF-mediated regulation of SIP1 and snail. Mol Cell Biol *27*, 157-169.
Feige, E., Yokoyama, S., Levy, C., Khaled, M., Igras, V., Lin, R. J., Lee, S., Widlund, H. R., Granter, S. R., Kung, A. L., and Fisher, D. E. (2011). Hypoxia-induced transcriptional repression of the melanoma-associated oncogene MITF. Proc Natl Acad Sci U S A *108*, E924-933.
Fidler, I. J. (1978). Tumor heterogeneity and the biology of cancer invasion and metastasis. Cancer Res *38*, 2651-2660.
Galaup, A., Cazes, A., Le Jan, S., Philippe, J., Connault, E., Le Coz, E., Mekid, H., Mir, L. M., Opolon, P., Corvol, P*., et al.* (2006). Angiopoietin-like 4 prevents metastasis through inhibition of vascular permeability and tumor cell motility and invasiveness. Proc Natl Acad Sci U S A *103*, 18721-18726.
Geertsen, R. C., Hofbauer, G. F., Yue, F. Y., Manolio, S., Burg, G., and Dummer, R. (1998). Higher frequency of selective losses of HLA-A and -B allospecificities in metastasis than in primary melanoma lesions. J Invest Dermatol *111*, 497-502.
Goh, Y. Y., Pal, M., Chong, H. C., Zhu, P., Tan, M. J., Punugu, L., Tan, C. K., Huang, R. L., Sze, S. K., Tang, M. B*., et al.* (2010). Angiopoietin-like 4 interacts with matrix proteins to modulate wound healing. J Biol Chem *285*, 32999-33009.
Goodall, J., Carreira, S., Denat, L., Kobi, D., Davidson, I., Nuciforo, P., Sturm, R. A., Larue, L., and Goding, C. R. (2008). Brn-2 represses microphthalmia-associated transcription factor expression and marks a distinct subpopulation of microphthalmia-associated transcription factor-negative melanoma cells. Cancer Res *68*, 7788-7794.
Goodall, J., Martinozzi, S., Dexter, T. J., Champeval, D., Carreira, S., Larue, L., and Goding, C. R. (2004). Brn-2 expression controls melanoma proliferation and is directly regulated by beta-catenin. Mol Cell Biol *24*, 2915-2922.
Halaban, R., Kwon, B. S., Ghosh, S., Delli Bovi, P., and Baird, A. (1988). bFGF as an autocrine growth factor for human melanomas. Oncogene Res *3*, 177-186.
Hockel, M., Schlenger, K., Aral, B., Mitze, M., Schaffer, U., and Vaupel, P. (1996). Association between tumor hypoxia and malignant progression in advanced cancer of the uterine cervix. Cancer Res *56*, 4509-4515.
Hodgkinson, C. A., Moore, K. J., Nakayama, A., Steingrímsson, E., Copeland, N. G., Jenkins, N. A., and Arnheiter, H. (1993). Mutations at the mouse microphthalmia locus are associated with defects in a gene encoding a novel basic-helix-loop-helix-zipper protein. Cell *74*, 395-404.
Hoek, K. S., Eichhoff, O. M., Schlegel, N. C., Dobbeling, U., Kobert, N., Schaerer, L., Hemmi, S., and Dummer, R. (2008a). In vivo switching of human melanoma cells between proliferative and invasive states. Cancer Res *68*, 650-656.

Hoek, K. S., and Goding, C. R. (2010). Cancer stem cells versus phenotype-switching in melanoma. Pigment Cell Melanoma Res *23*, 746-759.
Hoek, K. S., Schlegel, N. C., Brafford, P., Sucker, A., Ugurel, S., Kumar, R., Weber, B. L., Nathanson, K. L., Phillips, D. J., Herlyn, M*., et al.* (2006). Metastatic potential of melanomas defined by specific gene expression profiles with no BRAF signature. Pigment Cell Res *19*, 290-302.
Hoek, K. S., Schlegel, N. C., Eichhoff, O. M., Widmer, D. S., Praetorius, C., Einarsson, S. O., Valgeirsdottir, S., Bergsteinsdottir, K., Schepsky, A., Dummer, R., and Steingrimsson, E. (2008b). Novel MITF targets identified using a two-step DNA microarray strategy. Pigment Cell Melanoma Res *21*, 665-676.
Hojilla, C. V., Mohammed, F. F., and Khokha, R. (2003). Matrix metalloproteinases and their tissue inhibitors direct cell fate during cancer development. Br J Cancer *89*, 1817-1821.
Hung, J. J., Yang, M. H., Hsu, H. S., Hsu, W. H., Liu, J. S., and Wu, K. J. (2009). Prognostic significance of hypoxia-inducible factor-1alpha, TWIST1 and Snail expression in resectable non-small cell lung cancer. Thorax *64*, 1082-1089.
Ito, Y., Oike, Y., Yasunaga, K., Hamada, K., Miyata, K., Matsumoto, S., Sugano, S., Tanihara, H., Masuho, Y., and Suda, T. (2003). Inhibition of angiogenesis and vascular leakiness by angiopoietin-related protein 4. Cancer Res *63*, 6651-6657.
Ivan, M., Kondo, K., Yang, H., Kim, W., Valiando, J., Ohh, M., Salic, A., Asara, J. M., Lane, W. S., and Kaelin, W. G., Jr. (2001). HIFalpha targeted for VHL-mediated destruction by proline hydroxylation: implications for O2 sensing. Science *292*, 464-468.
Jaakkola, P., Mole, D. R., Tian, Y. M., Wilson, M. I., Gielbert, J., Gaskell, S. J., Kriegsheim, A., Hebestreit, H. F., Mukherji, M., Schofield, C. J*., et al.* (2001). Targeting of HIF-alpha to the von Hippel-Lindau ubiquitylation complex by O2-regulated prolyl hydroxylation. Science *292*, 468-472.
Janda, E., Lehmann, K., Killisch, I., Jechlinger, M., Herzig, M., Downward, J., Beug, H., and Grünert, S. (2002). Ras and TGF[beta] cooperatively regulate epithelial cell plasticity and metastasis: dissection of Ras signaling pathways. J Cell Biol *156*, 299-313.
Javelaud, D., Alexaki, V. I., Pierrat, M. J., Hoek, K. S., Dennler, S., Van Kempen, L., Bertolotto, C., Ballotti, R., Saule, S., Delmas, V., and Mauviel, A. (2011). GLI2 and M-MITF transcription factors control exclusive gene expression programs and inversely regulate invasion in human melanoma cells. Pigment Cell Melanoma Res *24*, 932-943.
Jeffs, A. R., Glover, A. C., Slobbe, L. J., Wang, L., He, S., Hazlett, J. A., Awasthi, A., Woolley, A. G., Marshall, E. S., Joseph, W. R*., et al.* (2009). A gene expression signature of invasive potential in metastatic melanoma cells. PLoS One *4*, e8461.
Jemal, A., Siegel, R., Ward, E., Hao, Y., Xu, J., and Thun, M. J. (2009). Cancer statistics, 2009. CA Cancer J Clin *59*, 225-249.
Jia, B., Liu, H., Kong, Q., and Li, B. (2012). Overexpression of ZEB1 associated with metastasis and invasion in patients with gastric carcinoma. Mol Cell Biochem.
Jo, M., Lester, R. D., Montel, V., Eastman, B., Takimoto, S., and Gonias, S. L. (2009). Reversibility of epithelial-mesenchymal transition (EMT) induced in breast cancer cells by activation of urokinase receptor-dependent cell signaling. J Biol Chem *284*, 22825-22833.
Kersten, S., Mandard, S., Tan, N. S., Escher, P., Metzger, D., Chambon, P., Gonzalez, F. J., Desvergne, B., and Wahli, W. (2000). Characterization of the fasting-induced adipose factor FIAF, a novel peroxisome proliferator-activated receptor target gene. J Biol Chem *275*, 28488-28493.
Kiemer, A. K., Takeuchi, K., and Quinlan, M. P. (2001). Identification of genes involved in epithelial-mesenchymal transition and tumor progression. Oncogene *20*, 6679-6688.
Kim, S. H., Park, Y. Y., Kim, S. W., Lee, J. S., Wang, D., and DuBois, R. N. (2011). ANGPTL4 induction by prostaglandin E2 under hypoxic conditions promotes colorectal cancer progression. Cancer Res *71*, 7010-7020.
Koefinger, P., Wels, C., Joshi, S., Damm, S., Steinbauer, E., Beham-Schmid, C., Frank, S., Bergler, H., and Schaider, H. (2011). The cadherin switch in melanoma instigated by HGF is mediated through epithelial-mesenchymal transition regulators. Pigment Cell Melanoma Res *24*, 382-385.

Kong, D., Park, E. J., Stephen, A. G., Calvani, M., Cardellina, J. H., Monks, A., Fisher, R. J., Shoemaker, R. H., and Melillo, G. (2005). Echinomycin, a small-molecule inhibitor of hypoxia-inducible factor-1 DNA-binding activity. Cancer Res *65*, 9047-9055.
Krishnamachary, B., Berg-Dixon, S., Kelly, B., Agani, F., Feldser, D., Ferreira, G., Iyer, N., LaRusch, J., Pak, B., Taghavi, P., and Semenza, G. L. (2003). Regulation of colon carcinoma cell invasion by hypoxia-inducible factor 1. Cancer Res *63*, 1138-1143.
Kveiborg, M., Albrechtsen, R., Couchman, J. R., and Wewer, U. M. (2008). Cellular roles of ADAM12 in health and disease. Int J Biochem Cell Biol *40*, 1685-1702.
Kääriäinen, E., Nummela, P., Soikkeli, J., Yin, M., Lukk, M., Jahkola, T., Virolainen, S., Ora, A., Ukkonen, E., Saksela, O., and Hölttä, E. (2006). Switch to an invasive growth phase in melanoma is associated with tenascin-C, fibronectin, and procollagen-I forming specific channel structures for invasion. J Pathol *210*, 181-191.
Lacal, P. M., Ruffini, F., Pagani, E., and D'Atri, S. (2005). An autocrine loop directed by the vascular endothelial growth factor promotes invasiveness of human melanoma cells. Int J Oncol *27*, 1625-1632.
Le Jan, S., Amy, C., Cazes, A., Monnot, C., Lamande, N., Favier, J., Philippe, J., Sibony, M., Gasc, J. M., Corvol, P., and Germain, S. (2003). Angiopoietin-like 4 is a proangiogenic factor produced during ischemia and in conventional renal cell carcinoma. Am J Pathol *162*, 1521-1528.
Lendeckel, U., Kohl, J., Arndt, M., Carl-McGrath, S., Donat, H., and Röcken, C. (2005). Increased expression of ADAM family members in human breast cancer and breast cancer cell lines. J Cancer Res Clin Oncol *131*, 41-48.
Lin, Y., Stevens, C., and Hupp, T. (2007). Identification of a dominant negative functional domain on DAPK-1 that degrades DAPK-1 protein and stimulates TNFR-1-mediated apoptosis. J Biol Chem *282*, 16792-16802.
Loike, J. D., Cao, L., Brett, J., Ogawa, S., Silverstein, S. C., and Stern, D. (1992). Hypoxia induces glucose transporter expression in endothelial cells. Am J Physiol *263*, C326-333.
Lui, P., Cashin, R., Machado, M., Hemels, M., Corey-Lisle, P. K., and Einarson, T. R. (2007). Treatments for metastatic melanoma: synthesis of evidence from randomized trials. Cancer Treat Rev *33*, 665-680.
Luk, C. K., Veinot-Drebot, L., Tjan, E., and Tannock, I. F. (1990). Effect of transient hypoxia on sensitivity to doxorubicin in human and murine cell lines. J Natl Cancer Inst *82*, 684-692.
Luo, Y., He, D. L., Ning, L., Shen, S. L., Li, L., and Li, X. (2006). Hypoxia-inducible factor-1alpha induces the epithelial-mesenchymal transition of human prostatecancer cells. Chin Med J (Engl) *119*, 713-718.
Mani, S. A., Guo, W., Liao, M. J., Eaton, E. N., Ayyanan, A., Zhou, A. Y., Brooks, M., Reinhard, F., Zhang, C. C., Shipitsin, M.*, et al.* (2008). The epithelial-mesenchymal transition generates cells with properties of stem cells. Cell *133*, 704-715.
Mazar, J., DeYoung, K., Khaitan, D., Meister, E., Almodovar, A., Goydos, J., Ray, A., and Perera, R. J. (2010). The regulation of miRNA-211 expression and its role in melanoma cell invasiveness. PLoS One *5*, e13779.
Michaylira, C. Z., and Nakagawa, H. (2006). Hypoxic microenvironment as a cradle for melanoma development and progression. Cancer Biol Ther *5*, 476-479.
Mihaylova, V. T., Bindra, R. S., Yuan, J., Campisi, D., Narayanan, L., Jensen, R., Giordano, F., Johnson, R. S., Rockwell, S., and Glazer, P. M. (2003). Decreased expression of the DNA mismatch repair gene Mlh1 under hypoxic stress in mammalian cells. Mol Cell Biol *23*, 3265-3273.
Moretti, D., Del Bello, B., Cosci, E., Biagioli, M., Miracco, C., and Maellaro, E. (2009). Novel variants of muscle calpain 3 identified in human melanoma cells: cisplatin-induced changes in vitro and differential expression in melanocytic lesions. Carcinogenesis *30*, 960-967.
Oda, H., Tsukita, S., and Takeichi, M. (1998). Dynamic behavior of the cadherin-based cell-cell adhesion system during Drosophila gastrulation. Dev Biol *203*, 435-450.
Oike, Y., Akao, M., Kubota, Y., and Suda, T. (2005). Angiopoietin-like proteins: potential new targets for metabolic syndrome therapy. Trends Mol Med *11*, 473-479.

Olbryt, M., Jarzab, M., Jazowiecka-Rakus, J., Simek, K., Szala, S., and Sochanik, A. (2006). Gene expression profile of B 16(F10) murine melanoma cells exposed to hypoxic conditions in vitro. Gene Expr *13*, 191-203.
Ortiz-Barahona, A., Villar, D., Pescador, N., Amigo, J., and del Peso, L. (2010). Genome-wide identification of hypoxia-inducible factor binding sites and target genes by a probabilistic model integrating transcription-profiling data and in silico binding site prediction. Nucleic Acids Res *38*, 2332-2345.
Padua, D., Zhang, X. H., Wang, Q., Nadal, C., Gerald, W. L., Gomis, R. R., and Massague, J. (2008). TGFbeta primes breast tumors for lung metastasis seeding through angiopoietin-like 4. Cell *133*, 66-77.
Peinado, H., and Cano, A. (2008). A hypoxic twist in metastasis. Nat Cell Biol *10*, 253-254.
Peinado, H., Moreno-Bueno, G., Hardisson, D., Pérez-Gómez, E., Santos, V., Mendiola, M., de Diego, J. I., Nistal, M., Quintanilla, M., Portillo, F., and Cano, A. (2008). Lysyl oxidase-like 2 as a new poor prognosis marker of squamous cell carcinomas. Cancer Res *68*, 4541-4550.
Peinado, H., Olmeda, D., and Cano, A. (2007). Snail, Zeb and bHLH factors in tumour progression: an alliance against the epithelial phenotype? Nat Rev Cancer *7*, 415-428.
Peinado, H., Portillo, F., and Cano, A. (2004). Transcriptional regulation of cadherins during development and carcinogenesis. Int J Dev Biol *48*, 365-375.
Poser, I., Domínguez, D., de Herreros, A. G., Varnai, A., Buettner, R., and Bosserhoff, A. K. (2001). Loss of E-cadherin expression in melanoma cells involves up-regulation of the transcriptional repressor Snail. J Biol Chem *276*, 24661-24666.
Postigo, A. A., and Dean, D. C. (1997). ZEB, a vertebrate homolog of Drosophila Zfh-1, is a negative regulator of muscle differentiation. EMBO J *16*, 3935-3943.
Postovit, L. M., Seftor, E. A., Seftor, R. E., and Hendrix, M. J. (2006). Influence of the microenvironment on melanoma cell fate determination and phenotype. Cancer Res *66*, 7833-7836.
Prockop, D. J., and Kivirikko, K. I. (1995). Collagens: molecular biology, diseases, and potentials for therapy. Annu Rev Biochem *64*, 403-434.
Pusztaszeri, M. P., Seelentag, W., and Bosman, F. T. (2006). Immunohistochemical expression of endothelial markers CD31, CD34, von Willebrand factor, and Fli-1 in normal human tissues. J Histochem Cytochem *54*, 385-395.
Pérez-Pomares, J. M., and Muñoz-Chápuli, R. (2002). Epithelial-mesenchymal transitions: a mesodermal cell strategy for evolutive innovation in Metazoans. Anat Rec *268*, 343-351.
Ray, J. M., and Stetler-Stevenson, W. G. (1994). The role of matrix metalloproteases and their inhibitors in tumour invasion, metastasis and angiogenesis. Eur Respir J *7*, 2062-2072.
Rice, G. C., Ling, V., and Schimke, R. T. (1987). Frequencies of independent and simultaneous selection of Chinese hamster cells for methotrexate and doxorubicin (adriamycin) resistance. Proc Natl Acad Sci U S A *84*, 9261-9264.
Robert, C., Thomas, L., Bondarenko, I., O'Day, S., M, D. J., Garbe, C., Lebbe, C., Baurain, J. F., Testori, A., Grob, J. J*., et al.* (2011). Ipilimumab plus dacarbazine for previously untreated metastatic melanoma. N Engl J Med *364*, 2517-2526.
Roesch, A., Fukunaga-Kalabis, M., Schmidt, E. C., Zabierowski, S. E., Brafford, P. A., Vultur, A., Basu, D., Gimotty, P., Vogt, T., and Herlyn, M. (2010). A temporarily distinct subpopulation of slow-cycling melanoma cells is required for continuous tumor growth. Cell *141*, 583-594.
Rofstad, E. K., Rasmussen, H., Galappathi, K., Mathiesen, B., Nilsen, K., and Graff, B. A. (2002). Hypoxia promotes lymph node metastasis in human melanoma xenografts by up-regulating the urokinase-type plasminogen activator receptor. Cancer Res *62*, 1847-1853.
Sakaizawa, K., Goto, Y., Kiniwa, Y., Uchiyama, A., Harada, K., Shimada, S., Saida, T., Ferrone, S., Takata, M., Uhara, H., and Okuyama, R. (2012). Mutation analysis of BRAF and KIT in circulating melanoma cells at the single cell level. Br J Cancer *106*, 939-946.

Seftor, E. A., Meltzer, P. S., Kirschmann, D. A., Pe'er, J., Maniotis, A. J., Trent, J. M., Folberg, R., and Hendrix, M. J. (2002). Molecular determinants of human uveal melanoma invasion and metastasis. Clin Exp Metastasis *19*, 233-246.
Semenza, G. L. (2007). Oxygen-dependent regulation of mitochondrial respiration by hypoxia-inducible factor 1. Biochem J *405*, 1-9.
Sensi, M., Catani, M., Castellano, G., Nicolini, G., Alciato, F., Tragni, G., De Santis, G., Bersani, I., Avanzi, G., Tomassetti, A.*, et al.* (2011). Human cutaneous melanomas lacking MITF and melanocyte differentiation antigens express a functional Axl receptor kinase. J Invest Dermatol *131*, 2448-2457.
Sipos, F., and Galamb, O. (2012). Epithelial-to-mesenchymal and mesenchymal-to-epithelial transitions in the colon. World J Gastroenterol *18*, 601-608.
Spaderna, S., Schmalhofer, O., Wahlbuhl, M., Dimmler, A., Bauer, K., Sultan, A., Hlubek, F., Jung, A., Strand, D., Eger, A.*, et al.* (2008). The transcriptional repressor ZEB1 promotes metastasis and loss of cell polarity in cancer. Cancer Res *68*, 537-544.
Stamenkovic, I. (2003). Extracellular matrix remodelling: the role of matrix metalloproteinases. J Pathol *200*, 448-464.
Takafuta, T., Wu, G., Murphy, G. F., and Shapiro, S. S. (1998). Human beta-filamin is a new protein that interacts with the cytoplasmic tail of glycoprotein Ibalpha. J Biol Chem *273*, 17531-17538.
Trelstad, R. L., Hay, E. D., and Revel, J. D. (1967). Cell contact during early morphogenesis in the chick embryo. Dev Biol *16*, 78-106.
Vassalli, J. D., Sappino, A. P., and Belin, D. (1991). The plasminogen activator/plasmin system. J Clin Invest *88*, 1067-1072.
Vaupel, P., and Mayer, A. (2007). Hypoxia in cancer: significance and impact on clinical outcome. Cancer Metastasis Rev *26*, 225-239.
Vergis, R., Corbishley, C. M., Norman, A. R., Bartlett, J., Jhavar, S., Borre, M., Heeboll, S., Horwich, A., Huddart, R., Khoo, V.*, et al.* (2008). Intrinsic markers of tumour hypoxia and angiogenesis in localised prostate cancer and outcome of radical treatment: a retrospective analysis of two randomised radiotherapy trials and one surgical cohort study. Lancet Oncol *9*, 342-351.
Verine, J., Lehmann-Che, J., Soliman, H., Feugeas, J. P., Vidal, J. S., Mongiat-Artus, P., Belhadj, S., Philippe, J., Lesage, M., Wittmer, E.*, et al.* (2010). Determination of angptl4 mRNA as a diagnostic marker of primary and metastatic clear cell renal-cell carcinoma. PLoS One *5*, e10421.
Wels, C., Joshi, S., Koefinger, P., Bergler, H., and Schaider, H. (2011). Transcriptional activation of ZEB1 by Slug leads to cooperative regulation of the epithelial-mesenchymal transition-like phenotype in melanoma. J Invest Dermatol *131*, 1877-1885.
Wenger, R. H., Stiehl, D. P., and Camenisch, G. (2005). Integration of oxygen signaling at the consensus HRE. Sci STKE *2005*, re12.
Widmer, D. S., Cheng, P. F., Eichhoff, O. M., Belloni, B. C., Zipser, M. C., Schlegel, N. C., Javelaud, D., Mauviel, A., Dummer, R., and Hoek, K. S. (2012). Systematic classification of melanoma cells by phenotype-specific gene expression mapping. Pigment Cell Melanoma Res.
Xiong, H., Hong, J., Du, W., Lin, Y. W., Ren, L. L., Wang, Y. C., Su, W. Y., Wang, J. L., Cui, Y., Wang, Z. H., and Fang, J. Y. (2012). Roles of STAT3 and ZEB1 proteins in E-cadherin down-regulation and human colorectal cancer epithelial-mesenchymal transition. J Biol Chem *287*, 5819-5832.
Xue, C., Plieth, D., Venkov, C., Xu, C., and Neilson, E. G. (2003). The gatekeeper effect of epithelial-mesenchymal transition regulates the frequency of breast cancer metastasis. Cancer Res *63*, 3386-3394.
Yancovitz, M., Litterman, A., Yoon, J., Ng, E., Shapiro, R. L., Berman, R. S., Pavlick, A. C., Darvishian, F., Christos, P., Mazumdar, M.*, et al.* (2012). Intra- and inter-tumor heterogeneity of BRAF(V600E))mutations in primary and metastatic melanoma. PLoS One *7*, e29336.
Yang, M. H., Wu, M. Z., Chiou, S. H., Chen, P. M., Chang, S. Y., Liu, C. J., Teng, S. C., and Wu, K. J. (2008). Direct regulation of TWIST by HIF-1alpha promotes metastasis. Nat Cell Biol *10*, 295-305.

Zhu, P., Tan, M. J., Huang, R. L., Tan, C. K., Chong, H. C., Pal, M., Lam, C. R., Boukamp, P., Pan, J. Y., Tan, S. H*., et al.* (2011). Angiopoietin-like 4 protein elevates the prosurvival intracellular O2(-):H2O2 ratio and confers anoikis resistance to tumors. Cancer Cell *19*, 401-415.
Zipser, M. C., Eichhoff, O. M., Widmer, D. S., Schlegel, N. C., Schoenewolf, N. L., Stuart, D., Liu, W., Gardner, H., Smith, P. D., Nuciforo, P*., et al.* (2011). A proliferative melanoma cell phenotype is responsive to RAF/MEK inhibition independent of BRAF mutation status. Pigment Cell Melanoma Res *24*, 326-333.

5.3 Engineering melanoma progression in a humanized environment *in vivo*

This work is a combination of melanoma research and work initiated during my Master's thesis in the lab of Ernst Reichmann of the Children's Hospital in Zürich where we developed a human dermo-epidermal skin substitute, grafted onto the back of immunocompromised rats. The fully orthotopic, humanized *in vivo* model for melanoma described in this study has a number of advantages compared to earlier developed melanoma models and can contribute to study melanoma progression in a humanized, clinically relevant context.

I contributed to this study by providing the immunohistochemical stainings shown in this paper (in figure 2 and figure 5) and by participating in experiment planning and discussions.

This study was published in the *Journal of Investigative Dermatology*

Engineering Melanoma Progression in a Humanized Environment *In Vivo*

Gregor Kiowski[1,4], Thomas Biedermann[2,4], Daniel S. Widmer[3], Gianluca Civenni[1], Charlotte Burger[1], Reinhard Dummer[3], Lukas Sommer[1] and Ernst Reichmann[2]

To overcome the lack of effective therapeutics for aggressive melanoma, new research models closely resembling the human disease are required. Here we report the development of a fully orthotopic, humanized *in vivo* model for melanoma, faithfully recapitulating human disease initiation and progression. To this end, human melanoma cells were seeded into engineered human dermo–epidermal skin substitutes. Transplantation onto the back of immunocompromised rats consistently resulted in the development of melanoma, displaying the hallmarks of their parental tumors. Importantly, all initial steps of disease progression were recapitulated, including the incorporation of the tumor cells into their physiological microenvironment, transition of radial to vertical growth, and establishment of highly vascularized, aggressive tumors with dermal involvement. Because all cellular components can be individually accessed using this approach, it allows manipulation of the tumor cells, as well as of the keratinocyte and stromal cell populations. Therefore, in one defined model system, tumor cell-autonomous and non-autonomous pathways regulating human disease progression can be investigated in a humanized, clinically relevant context.

Journal of Investigative Dermatology advance online publication, 1 September 2011; doi:10.1038/jid.2011.275

INTRODUCTION

Cutaneous melanoma arising from transformation of melanocytes is the most aggressive form of skin cancer (Gray-Schopfer *et al.*, 2007). Once systemic malignant disease has been established, the long-term survival of patients is poor, as despite immense research efforts only few evidence-based effective therapeutics have emerged (Dummer *et al.*, 2008; Kuphal and Bosserhoff, 2009). This poor translation of basic research to the clinics has led to the understanding that new research models are needed. In particular, the development of fully humanized orthotopic systems has been deemed crucial, because such systems would allow the investigation of central processes of human melanoma formation in their original tissue context (Khavari, 2006; Dirks, 2010; Weinberg *et al.*, 2010). This remains technically challenging, however, because of the staggered nature of human melanoma progression. First, neoplastic cells emerge from their original microenvironment at the dermo–epidermal junction. Subsequently, the cells establish radial growth by proliferation within the confines of the epidermis, leaving the underlying basement membrane intact. Accumulating invasive traits, the cells then switch to a vertical growth pattern by pushing through the basement membrane into the dermal compartment (Guerry *et al.*, 1993). Following extensive dermal growth, hypoxic areas are established within the tumor, which not only triggers neovascularization but also enhances tumor cell aggressiveness and survival (Pouysségur *et al.*, 2006; Lee and Herlyn, 2007).

Thus, to model the inherent complexity of human melanoma, a system is required that allows the exact recapitulation of all these steps *in vivo*. Whereas orthotopic *in vitro* model systems have emerged using organotypic skin reconstructs (Hsu *et al.*, 1998; Bechetoille *et al.*, 2000; Eves *et al.*, 2000; Meier *et al.*, 2000; Berking *et al.*, 2001; Haass *et al.*, 2005), fully orthotopic, humanized *in vivo* models are still missing. Neither subcutaneous injection into immunocompromised mice (Quintana *et al.*, 2008, 2010; Schatton *et al.*, 2008) nor more recent advances, including intradermal injections into human foreskin grafts (Juhasz *et al.*, 1993; Boiko *et al.*, 2010) or skin reconstructs using human devitalized dermal substrate (Chudnovsky *et al.*, 2005), provide the structural context equivalent to the site of human tumor formation. On one hand, subcutaneous or intradermal injections, even into a human skin graft (Juhasz *et al.*, 1993; Boiko *et al.*, 2010), cannot recapitulate the important early steps of invasion from the epidermal compartment through the basement membrane into the dermis. On the other hand, the use of a devitalized dermal substrate (Chudnovsky *et al.*, 2005) creates an unfavorable chimeric environment, as the

[1]*Cell and Developmental Biology, Institute of Anatomy, University of Zurich, Zurich, Switzerland;* [2]*Tissue Biology Research Unit, Department of Surgery, University Children's Hospital Zurich, Zurich, Switzerland and* [3]*Department of Dermatology, University Hospital Zurich, Zurich, Switzerland*

[4]*These authors contributed equally to this work.*

Correspondence: Lukas Sommer, Cell and Developmental Biology, Institute of Anatomy, University of Zurich, Winterthurerstrasse 190, CH-8057 Zurich, Switzerland. E-mail: lukas.sommer@anatom.uzh.ch or Ernst Reichmann, Tissue Biology Research Unit, Department of Surgery, University Children's Hospital Zurich, August Forel-Strasse 7, Ch-8008 Zurich, Switzerland. E-mail: Ernst.Reichmann@kispi.uzh.ch

Received 8 March 2011; revised 24 June 2011; accepted 4 July 2011

© 2011 The Society for Investigative Dermatology

graft gets populated with recipient fibroblasts rather than with human stromal cells (Medalie *et al.*, 1996; Bhowmick *et al.*, 2004; Khavari, 2006; Gaggioli *et al.*, 2007; Ridky *et al.*, 2010).

The system described here surpasses the existing models in combining the structural and microenvironmental prerequisites of a humanized orthotopic model. Furthermore, it retains the possibility to experimentally influence every cell type in the system independently. This is achieved using recently developed human dermo–epidermal skin substitutes that are grafted onto the back of immunocompromised rats (Pontiggia *et al.*, 2009; Biedermann *et al.*, 2010). On the basis of this approach, our model features the initial incorporation of melanoma cells into their physiological microenvironment, as well as crucial steps of human disease progression, such as the invasion of tumor cells through the basement membrane, their interactions with human stroma, tumor neovascularization, and tumor cell dissemination.

RESULTS

Melanoma development in engineered human skin substitutes

Aiming at the orthotopic positioning of human melanoma cells into an epidermal stratum basale of human origin, we took advantage of human dermo–epidermal skin substitutes (Pontiggia *et al.*, 2009; Biedermann *et al.*, 2010; Figure 1). These substitutes were engineered from freshly isolated human keratinocytes (KCs) that were plated onto high-density type-I collagen hydrogels containing primary human dermal fibroblasts. In such composites, melanocytes have been shown to incorporate into their orthotopic location *in vitro* (Haass *et al.*, 2005). To assess their incorporation *in vivo*, we transplanted dermo–epidermal skin substitutes into full-thickness wounds on the back of immunocompromised rats (Pontiggia *et al.*, 2009; Biedermann *et al.*, 2010; Figure 2a), potentially allowing to create tumors with extensions closely representing those of patients' tumors. Using polypropylene rings to shelter the grafts from the surrounding rat skin prevented wound healing through recipient-derived cells and resulted in the maturation of the skin substitutes to a state macroscopically resembling human skin (Figure 2b). The epidermal compartment revealed normal stratification (Figure 2c) and a laminin-10 (Lam10)-positive basement membrane tightly anchoring the cytokeratin-10 (K10)-expressing epidermis to the dermal compartment (Figure 2d). Staining of the skin grafts for the rat-specific endothelial marker CD31 (rCD31) revealed a fully vascularized dermal compartment, indicating good acceptance of the graft (Figure 2e). The integrity of the humanized dermal compartment (Figure 2e, white dotted line), marked by the human fibroblast-specific antibody CD90 (Thy1) (hCD90), was maintained for at least 12 weeks, the latest time point analyzed. Moreover, Ki67-positive proliferating cells in the stratum basale, in conjunction with the expression of the wound-specific cytokeratin 16 (K16), indicated sustained homeostasis of the epidermal tissue (Figure 2f). Importantly, the addition of human melanocytes resulted in their recruitment to the stratum basale (Figure 2g) where they fully differentiated into dendritic pigment-producing melanocytes (Figure 2h).

Given the functional integration of melanocytes into their physiological surroundings, we sought to determine the behavior of human melanoma cells in this experimental setup (for detailed information about all samples used, see Supplementary Table S1 online). To this end, we replaced the melanocyte fraction with human melanoma cells expressing green fluorescent protein (GFP). Six weeks after transplantation, multiple large tumors pushing through an otherwise well-developed epidermis were observed (Figure 2i). Macroscopically, these tumors showed partial pigmentation (Figure 2i, black arrowhead) and a prominent vasculature that readily ruptured upon touching, leading to excessive bleeding (Figure 2i, white arrowhead). Macroscopic GFP expression confirmed that the tumors originated from the seeded melanoma cells (Figure 2j). Histological analyses further revealed large, densely growing, non-necrotic GFP-positive tumors, expressing the two commonly used melanoma markers MelanA and S100 (Figure 2k–n).

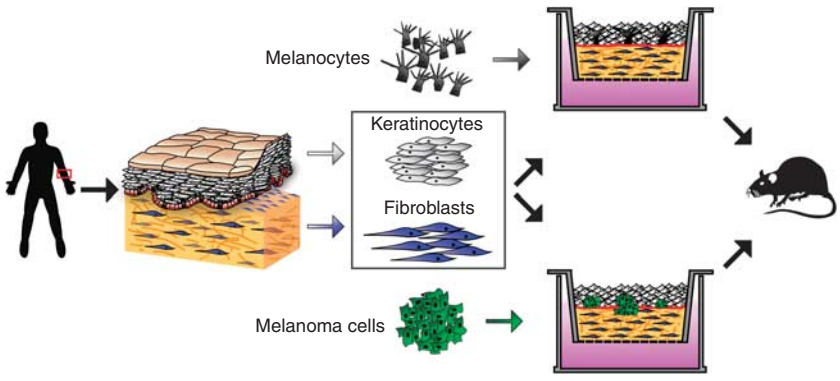

Figure 1. Experimental approach. Scheme illustrating the experimental approach using human organotypic skin substitutes as the basis for a humanized *in vivo* melanoma model. The two main components, keratinocytes (KCs) and dermal fibroblasts, are enzymatically isolated from human neonatal foreskin samples. A two-step approach, during which the isolated KCs are seeded onto high-density type-I collagen hydrogels containing human dermal fibroblasts, allows the engineering of a human dermo–epidermal skin equivalent suitable for transplantation. Addition of human melanocytes or melanoma cells results in their orthotopic incorporation into the skin composites.

Engineering human melanoma progression *in vivo*

To analyze the steps of melanoma progression, we added human GFP-expressing primary melanoma cells in the physiological ratio of melanocytes to KCs into the skin substitutes. Following tumor development over 42 days *in vivo*, the typical stages of melanoma progression were revealed (Figure 3a–c). At the day of transplantation, the tumor cells were already uniformly integrated into the thin epidermis (Figure 3a). Importantly, the *in vitro*-generated skin substitute did not reveal any melanoma cells in the dermal compartment (Figure 3a). This was crucial to our model, as inclusion of tumor cells into the dermis would have compromised the experimental setup, in which dermal tumor growth needs to be established as a part of disease progression. At 28 days after transplantation, the graft was fully integrated and epidermal maturation became evident by the appearance of distinct KC layers (Figure 3b, middle panel). At this time point, the tumor cells had integrated into their natural surrounding in the basal layer of the epidermis, where the presence of melanomas *in situ* already marked the onset of radial, lentiginous tumor growth (Figure 3b, right panel). After 42 days, tumor cell nests had become vascularized (Figure 3c, arrowheads) and progressed to invasive tumors disintegrating the epidermis and penetrating the dermis (Figure 3c, middle and right panel). Histopathologically, the resulting reconstituted tumors showed strong resemblance to the original patient tumor from which the cells had been derived (Figure 3d and e). Although the reconstituted tumor was smaller at the time point analyzed, both lesions showed a similar nodular growth pattern featuring lentiginous nests, a similar overall cell morphology, epithelial spread of single cells (Figure 3d and e, insets 1), and dermal invasion (Figure 3d and e, insets 2). Strikingly, both parental and reconstituted tumors substantially interfered with the epidermal integrity (Figure 3d and e), which presumably correlated with ulceration, a clinically significant prognostic feature (Gershenwald *et al.*, 2010). These data demonstrate that reconstitution of a primary melanoma in a humanized environment not only recapitulates the onset of human disease *in vivo* but also gives rise to tumors histologically resembling their original human counterparts.

However, although primary melanoma biopsies are rarely accessible, a plethora of metastasis samples and cell lines are available for research. Therefore, we explored the potential of cells derived from human metastasis samples to assume

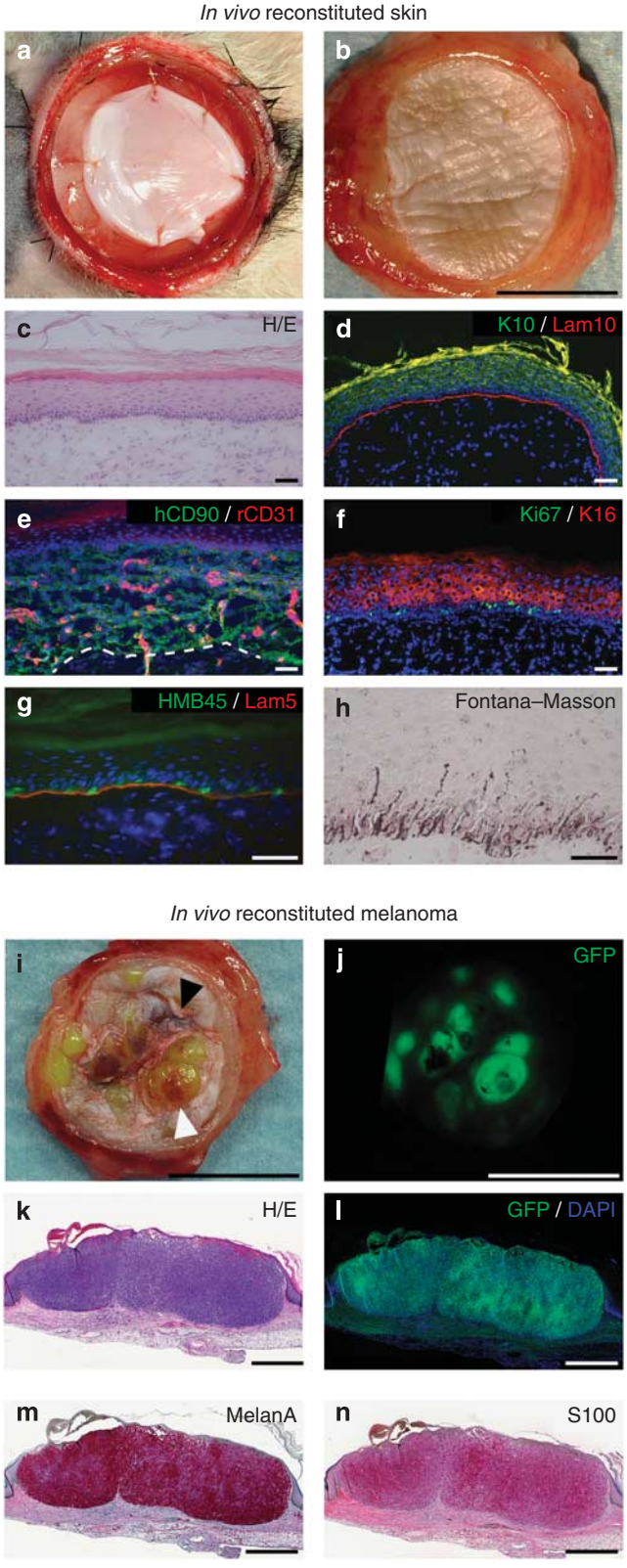

Figure 2. Transplantation of human skin substitutes containing either melanocytes or melanoma cells. Transplantation of a human dermo-epidermal skin substitute (**a**) drives its maturation within 3 weeks (**b**). Bar = 1 cm. Analysis of the resulting skin by (**c**) hematoxylin and eosin (H/E), (**d**) laminin-10 (Lam10) and cytokeratin-10 (K10), (**e**) hCD90 and rat-specific endothelial marker CD31 (rCD31), and (**f**) Ki67 and K16 stainings reveal typical skin histology and sustained homeostasis. Bars = 50 µm. (**g**) Addition of human melanocytes (HMB45) results in their orthotopic incorporation into the stratum basale contacting the underlying basement membrane (Lam5) *in vivo*. (**h**) This leads to fully differentiated dendritic, pigment-producing melanocytes (Fontana–Masson). Bars = 20 µm. (**i** and **j**) Replacing the melanocytes with green fluorescent protein (GFP)-expressing human melanoma cells (ID4286) results in ulcerated, bleeding (white arrowhead), partially pigmented (black arrowhead), GFP-expressing tumors. Bars = 1 cm. (**k**–**n**) Analysis reveals a dense lesion uniformly expressing GFP, MelanA, and S100. Bars = 1 mm.

primary tumor characteristics if exposed to the appropriate microenvironment. Intriguingly, metastasis-derived melanoma cells recapitulated the key events of early disease progression, indicating a remarkable context-dependent plasticity (Lipkin, 2008; Roesch *et al.*, 2010). Strikingly, cells derived from an axillary skin metastasis, not only adopted a progression pattern similar to transplanted primary melanoma cells but were also found to recapitulate many histopathological characteristics of the primary patient tumor, from which the metastasis had originated (Figure 4a and b and Supplementary Figure S1 online). Tumor growth started at the dermo–epidermal junction, giving rise to tumors mirroring the original tumor cell morphology, nodular growth pattern, ulceration, as well as dermal and epidermal invasion (Figure 4a and b, insets 1). Furthermore, 50% of all reconstituted tumors (6/12) derived from this axillary skin metastasis sample gave rise to satellite metastases in the skin, similar to those found in the corresponding primary tumor (Figure 4a and b, insets 2 and Supplementary Figure S1 online, inset 2). Intriguingly, these features were recapitulated irrespective of whether the cells had been maintained as xenografts in mice (Figure 4b) or as sphere cultures *in vitro* (Supplementary Figure S1 online). Moreover, analysis of the most commonly used clinical melanoma markers S100, MelanA, HMB45, as well as the clinically relevant prognostic factor Ki67 (Balch *et al.*, 2009), further confirmed the close resemblance between reconstituted tumors and their patient-matched counterparts (Supplementary Figure S2 online). This showed that even melanoma cells isolated from metastases harbor the potential to recapitulate original primary tumor growth if placed in the appropriate tissue context.

Subcutaneous xenotransplantation into immunocompromised mice represents the most widely used method for the analysis of human melanoma formation (Khavari, 2006; Becker *et al.*, 2010). Therefore, we compared the histology of the reconstituted tumor (Figure 4b) with a matched subcutaneous xenograft (Figure 4c), revealing an advantageous effect of the humanized environment on tumor growth. Whereas the humanized model system (Figure 4b) allowed the generation of large, non-necrotic lesions closely resembling human melanoma histopathology (Figure 4a), subcutaneous inoculation resulted in highly necrotic tumors that lacked any epidermal involvement (Figure 4c and Supplementary Figure S3 online). Despite the abundant vascularization (Supplementary Figure S3d online), higher magnification revealed only a small rim of healthy (Figure 4c, inset 1), proliferating (Supplementary Figure S3e online) cells on the periphery of the tumor-facing necrotic areas inside the tumor (inset 2). This suggests that additional influences from the

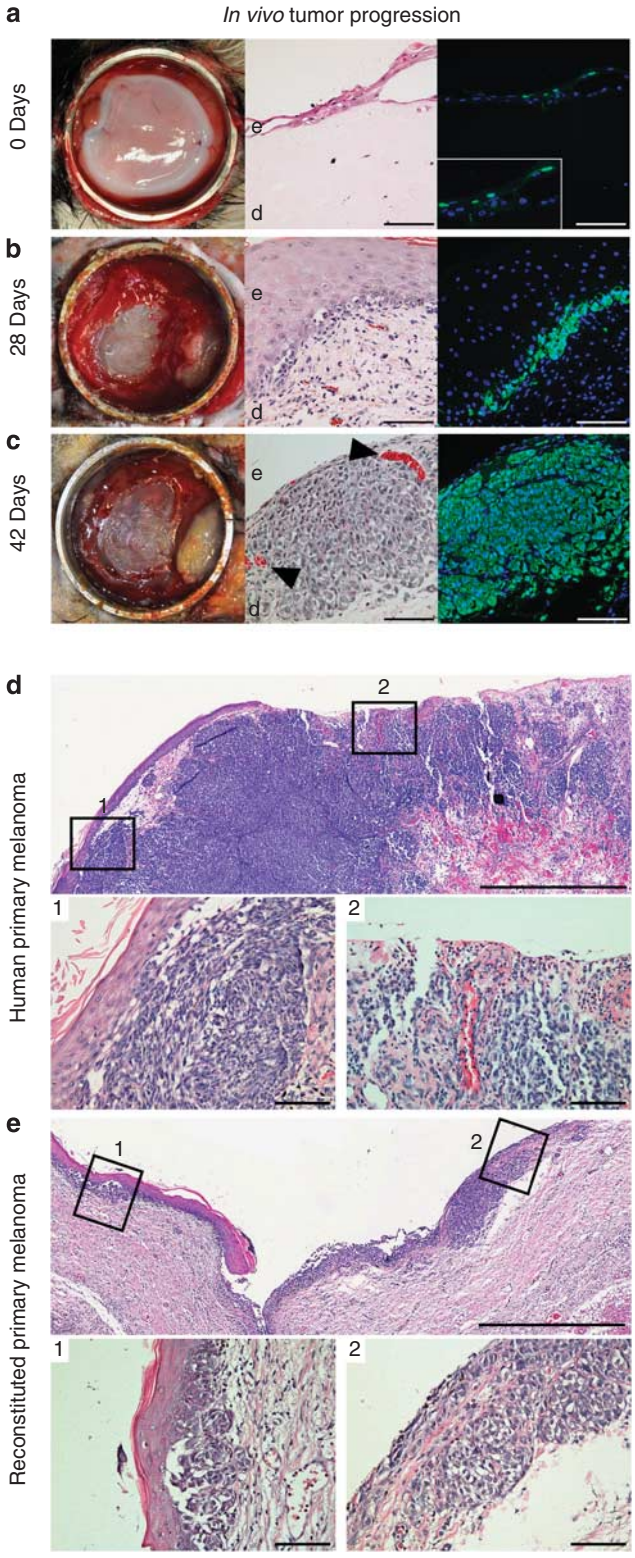

Figure 3. Human melanoma induction and progression in engineered skin substitutes *in vivo*. (**a**–**c**) Growth kinetics of green fluorescent protein (GFP)-expressing human primary melanoma cells (ID12741) upon transplantation. The left panels show the macroscopic maturation of the transplants, whereas the middle and left panels show a magnified view of consecutive hematoxylin and eosin (H/E)- and GFP-stained transversal sections (e, epidermis; d, dermis). Bars = 100 µm. (**d** and **e**) Histological comparison of the reconstituted tumor (ID12741) and the corresponding primary patient tumor (ID12741). Apart from the differences in size, both lesions show a similar nodular growth pattern featuring lentiginous nests and epithelial spread of single cells (insets 1), dermal invasion and ulceration (insets 2), vascularization, and a similar overall cell morphology. Overview bars = 1 mm, inset bars = 100 µm.

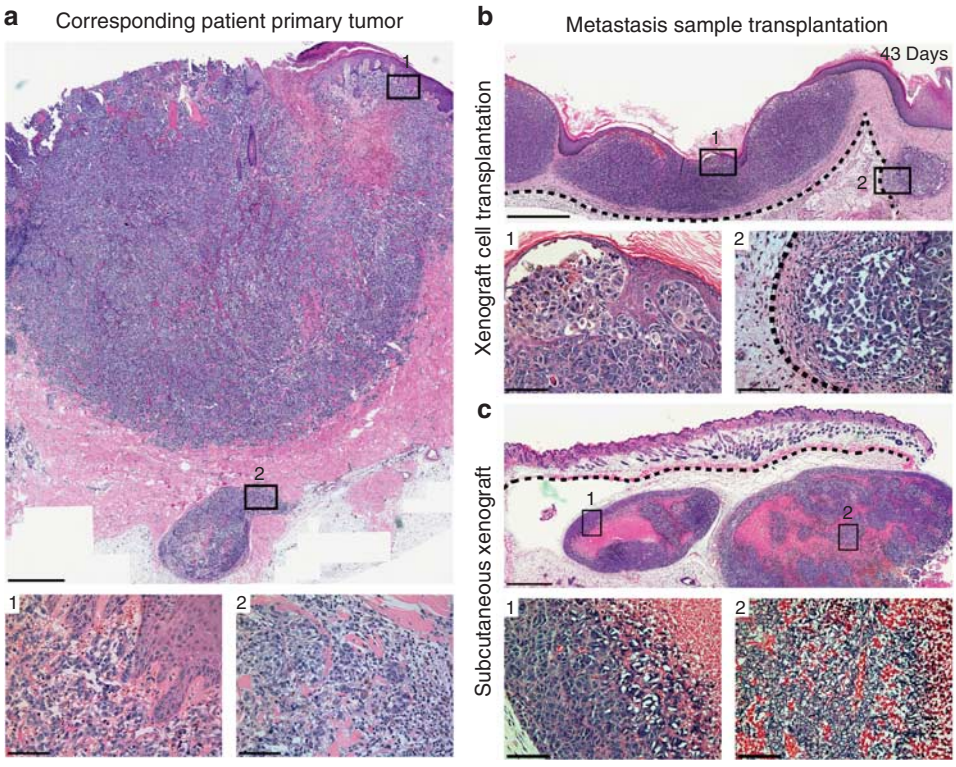

Figure 4. Reconstitution of a primary melanoma from an axillary skin metastasis sample. (**a**) Patient-matched primary tumor (ID11928) that gave rise to the metastasis used for reconstitution. (**b**) Tumor reconstituted from cells originally isolated from the corresponding axillary skin metastasis (ID4286). The resulting tumors show identical growth characteristics as the original primary tumor (insets). Note the barrier presented by the distinct human–rat tissue border (dotted lines) restricting tumor growth to the humanized dermal compartment. (**c**) Matched subcutaneous xenograft (ID4286) in a Swiss nude mouse. Subcutaneous inoculation results in highly necrotic (inset 1), encapsulated tumors growing in the subdermal fat tissue without epithelial involvement (inset 2). Dotted line, border between murine skin and subdermal fat tissue. Overview bars = 1 mm, inset bars = 100 μm.

microenvironment are required to sustain tumor growth and progression independent of the vasculature. In addition, none of the reconstituted tumors ($N = 19$ tumors derived from three different patient samples), including their occasionally arising dermal metastases, ever invaded the underlying rat tissue (Figure 4b and Supplementary Figure S1 online, dotted lines). Taken together, this indicates a favorable effect of the engineered human stroma on human melanoma cell growth and progression (Bhowmick *et al.*, 2004; Ridky *et al.*, 2010), highlighting the paramount importance of a fully humanized environment in studying melanoma progression.

Vascularization and hypoxia in reconstituted melanoma

A crucial step during tumor progression and a promising target for drug development is neoangiogenesis. A key parameter guiding this process is hypoxia resulting from the imbalance of oxygen supply and consumption in a growing tumor mass. (Pouysségur *et al.*, 2006; Bedogni and Powell, 2009). To validate the potential use of reconstituted melanoma in studying neoangiogenesis, we immunohistochemically assessed vascularization and hypoxia in reconstituted skin and tumors. The dermal compartment of skin substitutes transplanted without melanoma cells displayed hypoxia and vascularization similar to the dermis of normal skin (Figure 5a and b, arrowheads). In contrast, in reconstituted melanoma samples, we observed a correlation between pronounced hypoxia and tumor vessel ingrowth (Figure 5c–e). GFP tracking of melanoma cells revealed that tumor vessels were predominantly host derived (data not shown), in agreement with the previous reports (Civenni *et al.*, 2011). Both, in an early-stage patient sample and the reconstituted tumor after 25 days, blood vessel ingrowth was found along highly hypoxic regions (Figure 5c and d, arrowheads). This onset of hypoxia-guided blood vessel ingrowth most likely set the basis for the subsequent rapid progression to the highly vascularized, non-necrotic lesions observed after 42 days *in vivo* (Figure 5e and f).

Reconstituting the switch from radial to vertical growth in melanoma

As malignant disease remains the central challenge in melanoma therapy, we further investigated the potential of the system to faithfully recapitulate the early phases of human tumor progression. The first step toward malignant disease is the switch from radial to vertical tumor growth. Radial growth is restricted to the epidermal compartment, whereas vertical growth extends through the basement membrane into the dermis. Thus, we analyzed the functional integrity of the basement membrane in reconstituted tumors at different progression stages (Figure 6a). Starting with an intact, fully

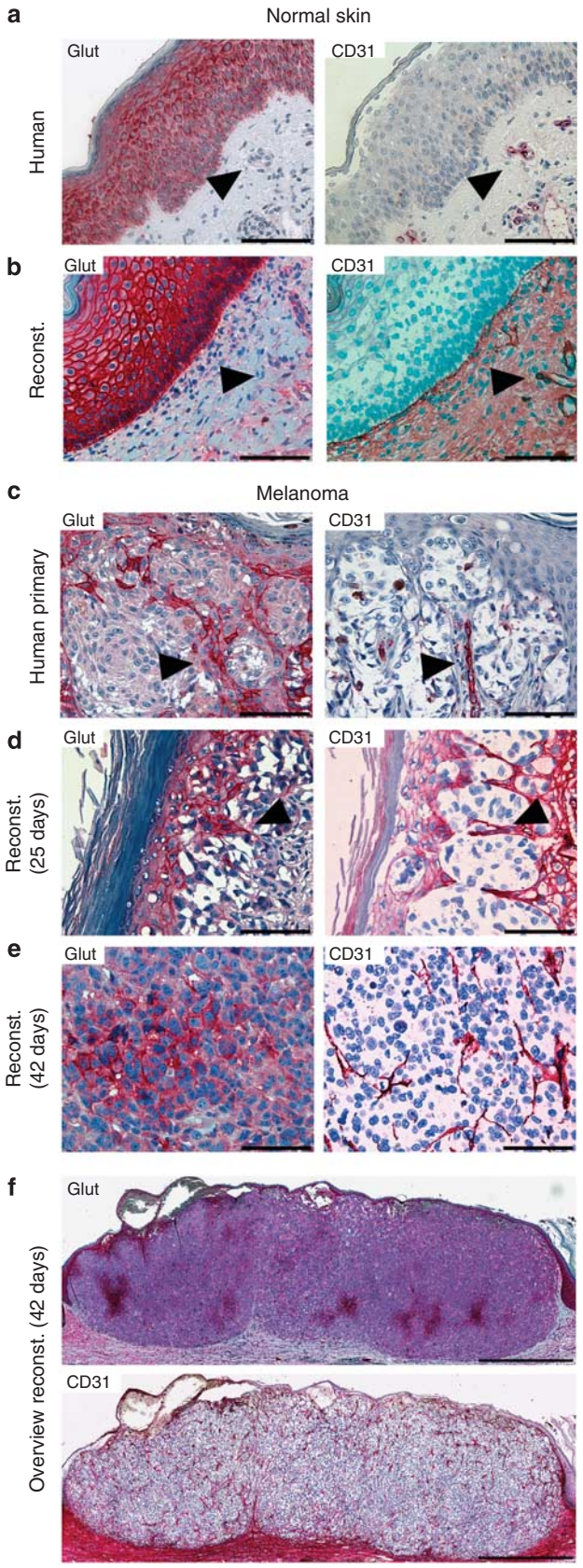

functional basement membrane, initial radial growth progressively reduced the underlying basement membrane until complete loss ensued.

A key event driving this malignant progression is thought to be a process reminiscent of epithelial-to-mesenchymal transition that is associated with the acquisition of an invasive, mesenchymal phenotype in epithelial tumor cells (Thiery, 2002). Although not an epithelial tumor, human melanoma express E-cadherin (Hsu *et al.*, 2000), the loss of which has been functionally implicated in epithelial-to-mesenchymal transition and tumor cell dissemination in some tumor types (Thiery, 2002). This makes E-cadherin an interesting candidate to investigate potential epithelial-to-mesenchymal transition-like processes underlying melanoma cell dissemination. Therefore, we compared the expression pattern of E-cadherin on histological samples of primary patient ($N=4$) and reconstituted melanoma ($N=9$ tumors derived from three different patient samples; Figure 6b–g). During the early stages of tumor development (radial growth phase), neither of the primary human tumors analyzed nor any of the reconstituted tumors showed an overt downregulation of E-cadherin, which was strongly expressed in epidermal lesions extending from the epidermis (Figure 6b and e). Strikingly, E-cadherin expression was even retained in bigger lesions showing distinct vertical growth phase characteristics (Figure 6c and f). In contrast, both in the reconstituted tumors and in the patient samples, substantial downregulation of E-cadherin was only observed in dermal tumor cell infiltrates that had lost all contacts with the epidermis (Figure 6d and g). In addition, in 12 out of 13 samples analyzed ($N=4$ patient samples and nine reconstituted tumors), E-cadherin-negative cells were observed, which appeared to move away from the parental tumor (Figure 6b–g, arrowheads). Taken together, our data show that even complex events such as dermal invasion, the induction of neoangiogenesis, and early tumor cell dissemination were faithfully recapitulated using our humanized melanoma reconstitution approach.

DISCUSSION

Here we describe a fully humanized *in vivo* system faithfully recapitulating all initial steps of human melanoma progression. In the same system, radial growth including pagetoid spread, vertical growth, marker expression, angiogenesis, ulceration, and hypoxia were validated in direct comparison with patient-matched tumor samples. Interestingly, all these

Figure 5. Vascularization and hypoxia in the reconstituted tumors. (**a** and **b**) Immunohistochemical analysis of vascularization (CD31) and the hypoxia-associated glucose transporter-1 (Glut) (arrowheads) in adjacent histological sections of human skin and reconstituted (Reconst.) dermal epidermal skin substitute. (**c** and **d**) Comparison of an early-stage patient sample (ID 16754) and a reconstituted tumor (ID 4286) after 25 days indicates blood vessel ingrowth along a highly hypoxic region (arrowheads). (**e**) After 42 days *in vivo*, the reconst. tumors (ID 4286) are highly vascularized and contain only a few small hypoxic regions. Bars = 100 µm. (**f**) Overview over hypoxia and the intricate capillary network observed in the reconst. tumor after 42 days *in vivo*. Bars = 1 mm.

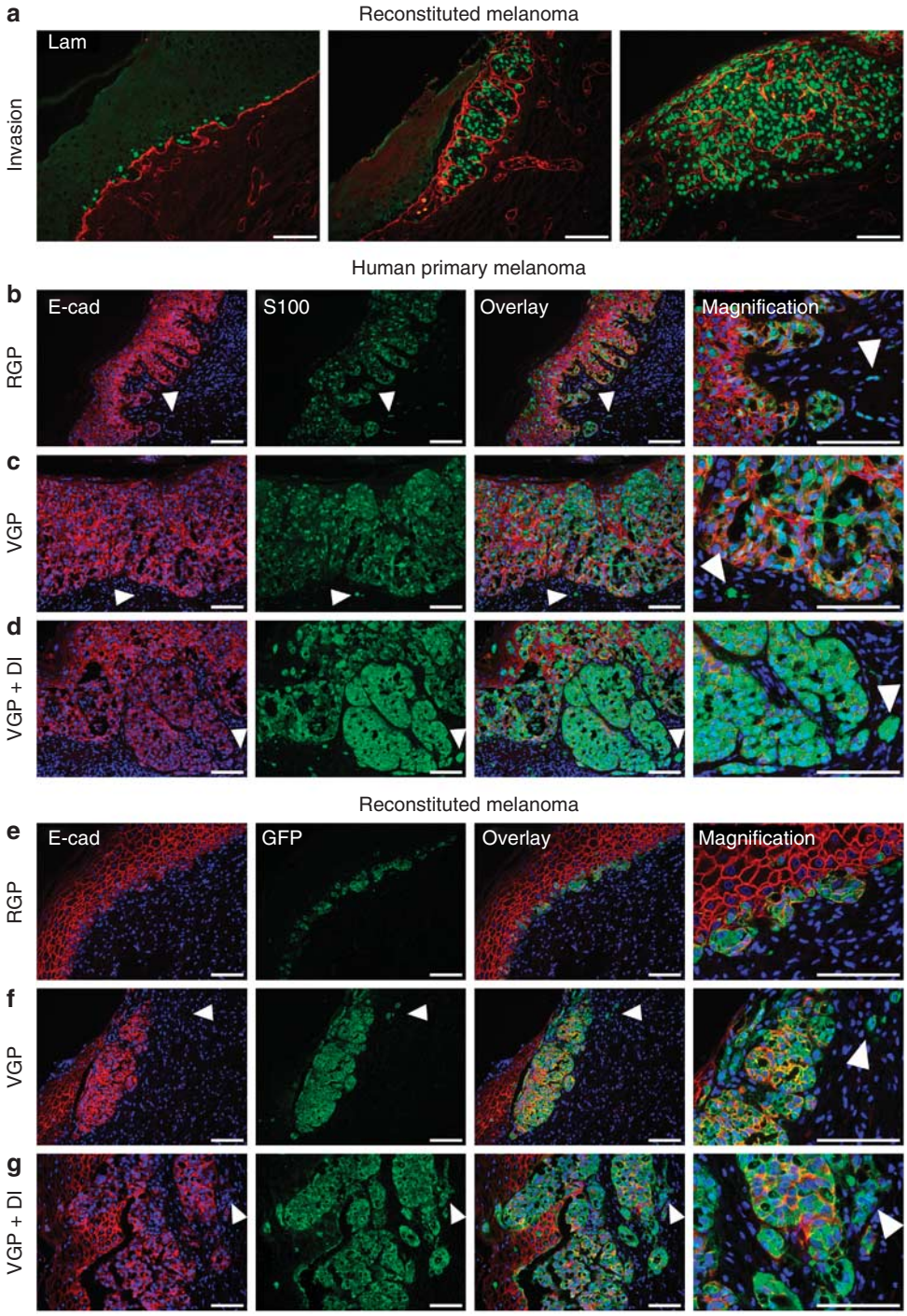

Figure 6. Reconstituting the switch from radial to vertical growth in melanoma. (**a**) Staining for the basement membrane marker Laminin-5 (Lam5) reveals successive degradation of the basement membrane in a reconstituted melanoma (ID12741). The final loss of the basement membrane marks the onset of vertical tumor growth. Bars = 100 μm. (**b**–**g**) Comparison of E-cadherin (E-cad) expression in progressing stages of human primary (**b**–**d**) and reconstituted melanoma (**e**–**g**). (**b**) Radially growing human primary tumor (ID12826). (**c**, **d**) Vertically growing human primary tumor (ID16754) with and without dermal infiltrates (DIs). (**e**–**g**) Corresponding stages of a reconstituted tumor using human primary melanoma cells (ID12741). Arrowheads indicate cells negative for E-cadherin without contact with their parental tumors. To visualize the tumor borders, the patient samples were counterstained with S100 and the reconstituted tumors with green fluorescent protein (GFP). RGP, radial growth phase; VGP, vertical growth phase. Bars = 100 μm.

traits were reestablished upon tumor reconstitution with samples derived from both primary melanomas and the more abundant metastases biopsies. This demonstrates the potential of cancer cells to adapt to the local environment, making our system amenable to a wide range of human melanoma samples. This concurs with recently described

dynamic processes mediating tumor initiation and maintenance (Mani *et al.*, 2008; Roesch *et al.*, 2010). Along this line, it will be interesting to assess how environmental cues override the intrinsic differences between primary and metastatic tumor cells.

A crucial point to consider for every model system is its efficiency and reproducibility. Achieving an overall reconstitution efficiency of about 90% (17 tumors out of 19 transplantations using three individual patient samples), the method described here provides a reliable and repeatable experimental setup. Importantly, irrespective of the cells' origin or previous expansion *in vivo* or *in vitro*, the different samples did not exhibit any discernible differences with respect to the key events of disease progression. This makes our model a valuable tool for preclinical drug testing in an experimental setup reminiscent of the patient's situation. For *in vitro* tumor cell expansion, we have purposely used melanoma sphere cultures rather than adherent cell cultures. This is because such cultures contain higher numbers of tumor-initiating cells than adherent cell cultures and are able to establish a cellular heterogeneity closely resembling that of patients' tumors (Fang *et al.*, 2005; Civenni *et al.*, 2011; Thurber *et al.*, 2011). Because melanoma spheres can readily be generated both from fresh tumor biopsy samples and cell lines passaged as adherent cultures, this method is applicable to a large variety of samples.

Most patients die of metastatic disease and not of primary tumor growth (Nguyen and Massagué, 2007). Therefore, we also assessed systemic metastatic spread upon transplantation by checking all animals for metastatic lesions in the inguinal and axillary lymph nodes, lung, intestine, and liver. Unfortunately, no macroscopic visceral metastases were found in the range of this study. Considering that metastatic disease is a rare event, which in humans can take decades to evolve (Nguyen and Massagué, 2007), we did not expect to find distant metastases already after 42 days *in vivo*. However, whether single tumor cells are already present in the internal organs at the time point analyzed could not concludingly be determined and is subject to further investigations.

In contrast to previously described model systems (Juhasz *et al.*, 1993; Chudnovsky *et al.*, 2005; Boiko *et al.*, 2010), we use organotypic skin substitutes as the basis for an orthotopic *in vivo* model. This approach offers the advantage to reconstruct skin grafts from distinct cellular components, allowing the engineering of a fully humanized organotypic environment. Moreover, all cell types used for melanoma reconstruction can be manipulated, including the melanoma cells, the KCs, and the dermal fibroblasts. To our knowledge, for the first time, this will allow *in vivo* studies addressing the influence of a human microenvironment on tumor progression in a defined experimental setup. The significance of such studies becomes apparent by our observation that the humanized dermal compartment clearly exerted a favorable effect on tumor growth as compared with the neighboring rat tissue. Given the known influence of stromal fibroblast on tumor growth and progression (Bhowmick *et al.*, 2004; Gaggioli *et al.*, 2007; Ridky *et al.*, 2010), the use of a fully humanized dermal compartment containing human fibroblasts is therefore favorable over a chimeric dermal compartment that results from the repopulation of devitalized human dermal substrate with recipient animal fibroblasts (Medalie *et al.*, 1996; Chudnovsky *et al.*, 2005; Khavari, 2006).

The influence of the microenvironment has to be considered especially when studying tumorigenesis in subcutaneous xenografts (Quintana *et al.*, 2008, 2010; Schatton *et al.*, 2008). Subcutaneous injections are placed into the subdermal compartment, which according to our findings represents an unphysiological environment for tumor growth and is associated with extensive necrosis in the transplanted tumor tissue. Thus, recent controversial findings regarding the nature of melanoma-initiating cells (Quintana *et al.*, 2008, 2010; Schatton *et al.*, 2008; Refaeli *et al.*, 2009; Boiko *et al.*, 2010; Roesch *et al.*, 2010) may indeed partly be attributed to the use of subcutaneous xenografts in some of these studies (Dirks, 2010). Moreover, apart from creating an unphysiological environment, subcutaneous xenografts do not recapitulate the invasive behavior of melanoma (Khavari, 2006), and thus should not be considered an orthotopic model system. As a result, it has been suggested that studies performed with human samples should be validated in a humanized *in vivo* environment (Weinberg *et al.*, 2010). A recent report has used intradermal injections into human foreskin grafts (Boiko *et al.*, 2010). However, similar to subcutaneous injections, intradermal inoculation cannot entirely reproduce the early stages of tumor progression. This is because the initial influence of the microenvironment and the crucial switch from radial to vertical growth are sidestepped upon dermal seeding of melanoma cells. Thus, even if applied to the context of a human skin graft, intradermal injections also do not represent a fully orthotopic model system.

Although our model closely mimics human disease progression, the use of immunocompromised recipient animals for transplantation creates the inherent problem of an incomplete immune system. As the immune system is considered to have an important impact on growth and progression of tumors, including human melanoma (Kim *et al.*, 2006; McAllister and Weinberg, 2010; Schatton *et al.*, 2010; Civenni *et al.*, 2011), this aspect falls short in every model system using human cells. Indeed, only few host macrophages and natural killer cells were found close to or within the reconstituted human tumors in our model system (data not shown). Despite this limitation, we feel that the use of human patient samples remains crucial for the development of therapeutics targeting human cancer cells. This is particularly relevant given the significantly different architecture of human and rodent skin, with human melanocytes mainly residing in the interfollicular epidermis and rodent melanocytes being mostly confined to hair follicles (Khavari, 2006). Therefore, although crucial for the identification of molecular processes involved in tumorigenesis, genetic mouse melanoma models only approximate the human disease (Becker *et al.*, 2010), thus impeding their direct translation to the clinic.

In contrast, the model system described here allows the faithful recapitulation of the central steps of human

melanoma growth and progression in a physiological, humanized environment *in vivo*. This in turn will help to translate basic research into a clinically more relevant context by providing the opportunity to devise and test therapeutics in a model system closely resembling the human disease.

MATERIALS AND METHODS

Construction of the human organotypic skin cultures

This study was conducted according to the Declaration of Helsinki Principles. Human foreskin samples were obtained from patients after obtaining permission from the Ethics Commission of the Canton Zurich and after informed consent given by parents or patients. Organotypic cultures were prepared as previously established (Costea *et al.*, 2003; Pontiggia *et al.*, 2009; Biedermann *et al.*, 2010). Corresponding to the physiological ratio of melanocytes to KCs ($\sim$1:5), 5×10^4 melanocytes or melanoma cells were seeded onto each dermal equivalent. Culturing for 1 week with regular medium changes gave rise to the dermo–epidermal skin substitutes used for transplantation. Detailed procedures are described in the Supplementary information online.

Transplantation of the human organotypic skin substitutes

The study protocol was approved by the Local Committee for Experimental Animal Research (permission number 135/2010). The surgical procedure was performed as described previously (Pontiggia *et al.*, 2009; Schneider *et al.*, 2009; Biedermann *et al.*, 2010). Detailed procedures are described in the Supplementary information online.

Tumor cell isolation and xenograft inoculation

All patients enrolled in the study were treated at the Dermatology Department of the University Hospital of Zurich. The biobank project including the establishment of cell cultures was approved by the local IRB (EK647 and EK800; Ethics Committee of Canton Zurich) and all patients gave written informed consent. The patient samples used for transplantation were derived from one primary tumor and two metastases (see Supplementary Table S1 online). Detailed procedures are described in the Supplementary information online.

Cell culture and staining procedures

Detailed procedures are described in the Supplementary information online.

CONFLICT OF INTEREST

The authors state no conflict of interest.

ACKNOWLEDGMENTS

We thank Benedetta Belloni and Nikita Kobert for assistance, and the Cancer Biology PhD Program of the University of Zurich for support. This work was financially supported by the Swiss National Science Foundation, the Swiss Cancer League, the Promedica Stiftung Chur, the EU-FP6 project EuroSTEC (soft tissue engineering for congenital birth defects in children, contract: LSHB-CT-2006-037409), the Bangerter-Rymer Stiftung (RD), and the University of Zurich. We are grateful to the Fondation Gaydoul and the sponsors of ''DonaTissue'' (Thérèse Meier, Robert Zingg, the Vontobel Foundation, and the Werner Spross Foundation) for their generous financial support and interest in our work.

SUPPLEMENTARY MATERIAL

Supplementary material is linked to the online version of the paper at http://www.nature.com/jid

REFERENCES

Balch CM, Gershenwald JE, Soong S-J *et al.* (2009) Final version of 2009 AJCC melanoma staging and classification. *J Clin Oncol* 27:6199–206

Bechetoille N, Haftek M, Staquet MJ *et al.* (2000) Penetration of human metastatic melanoma cells through an authentic dermal-epidermal junction is associated with dissolution of native collagen types IV and VII. *Melanoma Res* 10:427–34

Becker JC, Houben R, Schrama D *et al.* (2010) Mouse models for melanoma: a personal perspective. *Exp Dermatol* 19:157–64

Bedogni B, Powell MB (2009) Hypoxia, melanocytes and melanoma—survival and tumor development in the permissive microenvironment of the skin. *Pigment Cell Melanoma Res* 22:166–74

Berking C, Takemoto R, Satyamoorthy K *et al.* (2001) Basic fibroblast growth factor and ultraviolet B transform melanocytes in human skin. *Am J Pathol* 158:943–53

Bhowmick NA, Neilson EG, Moses HL (2004) Stromal fibroblasts in cancer initiation and progression. *Nature* 432:332–7

Biedermann T, Pontiggia L, Böttcher-Haberzeth S *et al.* (2010) Human eccrine sweat gland cells can reconstitute a stratified epidermis. *J Invest Dermatol* 130:1996–2009

Boiko AD, Razorenova OV, van de Rijn M *et al.* (2010) Human melanoma-initiating cells express neural crest nerve growth factor receptor CD271. *Nature* 466:133–7

Chudnovsky Y, Adams AE, Robbins PB *et al.* (2005) Use of human tissue to assess the oncogenic activity of melanoma-associated mutations. *Nat Genet* 37:745–9

Civenni G, Walter A, Kobert N *et al.* (2011) Human CD271-positive melanoma stem cells associated with metastasis establish tumor heterogeneity and long-term growth. *Cancer Res* 71:3098–109

Costea DE, Loro LL, Dimba EAO *et al.* (2003) Crucial effects of fibroblasts and keratinocyte growth factor on morphogenesis of reconstituted human oral epithelium. *J Invest Dermatol* 121:1479–86

Dirks P (2010) Cancer stem cells: invitation to a second round. *Nature* 466:40–1

Dummer R, Hauschild A, Jost L *et al.* (2008) Cutaneous malignant melanoma: ESMO clinical recommendations for diagnosis, treatment and follow-up. *Ann Oncol* 19(Suppl 2):ii86–8

Eves P, Layton C, Hedley S *et al.* (2000) Characterization of an *in vitro* model of human melanoma invasion based on reconstructed human skin. *Br J Dermatol* 142:210–22

Fang D, Nguyen TK, Leishear K *et al.* (2005) A tumorigenic subpopulation with stem cell properties in melanomas. *Cancer Res* 65:9328–37

Gaggioli C, Hooper S, Hidalgo-Carcedo C *et al.* (2007) Fibroblast-led collective invasion of carcinoma cells with differing roles for RhoGTPases in leading and following cells. *Nat Cell Biol* 9:1392–400

Gershenwald JE, Soong S-J, Balch CM, Committee AJCoCAMS (2010) 2010 TNM staging system for cutaneous melanoma … and beyond. *Ann Surg Oncol* 17:1475–7

Gray-Schopfer V, Wellbrock C, Marais R (2007) Melanoma biology and new targeted therapy. *Nature* 445:851–7

Guerry D, Synnestvedt M, Elder DE *et al.* (1993) Lessons from tumor progression: the invasive radial growth phase of melanoma is common, incapable of metastasis, and indolent. *J Invest Dermatol* 100:342S–5S

Haass NK, Smalley KSM, Li L *et al.* (2005) Adhesion, migration and communication in melanocytes and melanoma. *Pigment Cell Res* 18:150–9

Hsu MY, Meier FE, Nesbit M *et al.* (2000) E-cadherin expression in melanoma cells restores keratinocyte-mediated growth control and down-regulates expression of invasion-related adhesion receptors. *Am J Pathol* 156:1515–25

Hsu MY, Shih DT, Meier FE *et al.* (1998) Adenoviral gene transfer of beta3 integrin subunit induces conversion from radial to vertical growth phase in primary human melanoma. *Am J Pathol* 153:1435–42

Juhasz I, Albelda SM, Elder DE *et al.* (1993) Growth and invasion of human melanomas in human skin grafted to immunodeficient mice. *Am J Pathol* 143:528–37

Khavari PA (2006) Modelling cancer in human skin tissue. *Nat Rev Cancer* 6:270–80

Kim R, Emi M, Tanabe K *et al.* (2006) Tumor-driven evolution of immunosuppressive networks during malignant progression. *Cancer Res* 66:5527–36

Kuphal S, Bosserhoff A (2009) Recent progress in understanding the pathology of malignant melanoma. *J Pathol* 219:400–9

Lee JT, Herlyn M (2007) Microenvironmental influences in melanoma progression. *J Cell Biochem* 101:862–72

Lipkin G (2008) Plasticity of the cancer cell: implications for epigenetic control of melanoma and other malignancies. *J Invest Dermatol* 128:2152–5

Mani SA, Guo W, Liao M-J *et al.* (2008) The epithelial-mesenchymal transition generates cells with properties of stem cells. *Cell* 133:704–15

McAllister SS, Weinberg RA (2010) Tumor-host interactions: a far-reaching relationship. *J Clin Oncol* 28:4022–8

Medalie DA, Eming SA, Tompkins RG *et al.* (1996) Evaluation of human skin reconstituted from composite grafts of cultured keratinocytes and human acellular dermis transplanted to athymic mice. *J Invest Dermatol* 107:121–7

Meier F, Nesbit M, Hsu MY *et al.* (2000) Human melanoma progression in skin reconstructs: biological significance of bFGF. *Am J Pathol* 156:193–200

Nguyen DX, Massagué J (2007) Genetic determinants of cancer metastasis. *Nat Rev Genet* 8:341–52

Pontiggia L, Biedermann T, Meuli M *et al.* (2009) Markers to evaluate the quality and self-renewing potential of engineered human skin substitutes *in vitro* and after transplantation. *J Invest Dermatol* 129:480–90

Pouysségur J, Dayan F, Mazure NM (2006) Hypoxia signalling in cancer and approaches to enforce tumour regression. *Nature* 441:437–43

Quintana E, Shackleton M, Foster HR *et al.* (2010) Phenotypic heterogeneity among tumorigenic melanoma cells from patients that is reversible and not hierarchically organized. *Cancer Cell* 18:510–23

Quintana E, Shackleton M, Sabel MS *et al.* (2008) Efficient tumour formation by single human melanoma cells. *Nature* 456:593–8

Refaeli Y, Bhoumik A, Roop DR *et al.* (2009) Melanoma-initiating cells: a compass needed. *EMBO Rep* 10:965–72

Ridky TW, Chow JM, Wong DJ *et al.* (2010) Invasive three-dimensional organotypic neoplasia from multiple normal human epithelia. *Nat Med* 16:1450–5

Roesch A, Fukunaga-Kalabis M, Schmidt EC *et al.* (2010) A temporarily distinct subpopulation of slow-cycling melanoma cells is required for continuous tumor growth. *Cell* 141:583–94

Schatton T, Murphy GF, Frank NY *et al.* (2008) Identification of cells initiating human melanomas. *Nature* 451:345–9

Schatton T, Schütte U, Frank NY *et al.* (2010) Modulation of T-cell activation by malignant melanoma initiating cells. *Cancer Res* 70:697–708

Schneider J, Biedermann T, Widmer D *et al.* (2009) Matriderm versus integra: a comparative experimental study. *Burns* 35:51–7

Thiery JP (2002) Epithelial-mesenchymal transitions in tumour progression. *Nat Rev Cancer* 2:442–54

Thurber AE, Douglas G, Sturm EC *et al.* (2011) Inverse expression states of the BRN2 and MITF transcription factors in melanoma spheres and tumour xenografts regulate the NOTCH pathway. *Oncogene* 30:3036–48

Weinberg R, Fisher DE, Rich J (2010) Dynamic and transient cancer stem cells nurture melanoma. *Nat Med* 16:758

5.4 Differential LEF1 and TCF4 expression is involved in melanoma cell phenotype switching

WNT signaling is known to play an important role in neotransformation and malignant progression in various cancer types. In melanoma it was shown that WNT signaling could have a role in disease progression. This study investigated the role of WNT signaling in melanoma phenotype switching. We could show that differential activity of the β-catenin co-factors LEF1/TCF4 regulates phenotype switching by canonical and non-canonical WNT-pathways.

I contributed to this study by performing experiments for the characterization of the cell cultures and confirmation of the cell culture phenotypes, and by participating in experiment planning and discussions.

This study was published in *Pigment Cell & Melanoma Research*

Differential LEF1 and TCF4 expression is involved in melanoma cell phenotype switching

Ossia M. Eichhoff[1], Ashani Weeraratna[2], Marie C. Zipser[1], Laurence Denat[3], Daniel S. Widmer[1], Mai Xu[2], Lydia Kriegl[4], Thomas Kirchner[4], Lionel Larue[3], Reinhard Dummer[1] and Keith S. Hoek[1]

1 Department of Dermatology, University Hospital of Zürich, Zürich, Switzerland **2** Laboratory of Molecular Biology and Immunology, Molecular and Cellular Oncogenesis Program, The Wistar Institute, Philadelphia, PA, USA **3** Institut Curie, Developmental Genetics of Melanocytes UMR3347 CNRS, U1021 INSERM, 91405 Orsay, France **4** Department of Pathology, Ludwig Maximilians University, Munich, Germany

CORRESPONDENCE K. S. Hoek, e-mail: keith.hoek@usz.ch

KEYWORDS melanoma/LEF1/TCF4/MITF/WNT5A

PUBLICATION DATA Received 20 January 2011, revised and accepted for publication 18 May 2011, published online 20 May 2011

doi: 10.1111/j.1755-148X.2011.00871.x

Summary

Recent observations suggest that melanoma cells drive disease progression by switching back and forth between phenotypic states of proliferation and invasion. Phenotype switching has been linked to changes in Wnt signalling, and we therefore looked for cell phenotype-specific differences in the levels and activity of β-catenin and its LEF/TCF co-factors. We found that while cytosolic β-catenin distribution is phenotype-specific (membrane-associated in proliferative cells and cytosolic in invasive cells), its nuclear distribution and activity is not. Instead, the expression patterns of two β-catenin co-factors, LEF1 and TCF4, are both phenotype-specific and inversely correlated. LEF1 is preferentially expressed by differentiated/proliferative phenotype cells and TCF4 by dedifferentiated/invasive phenotype cells. Knock-down experiments confirmed that these co-factors are important for the phenotype-specific expression of M-MITF, WNT5A and other genes and that LEF1 suppresses TCF4 expression independently of β-catenin. Our data show that melanoma cell phenotype switching behaviour is regulated by differential LEF1/TCF4 activity.

Introduction

Dysregulation or mutation of the Wnt pathway is implicated in both neotransformation and malignant progression of various cancer types (Klarmann et al., 2008; Mikesch et al., 2007; Robinson et al., 2008; Segditsas and Tomlinson, 2006; Takigawa and Brown, 2008). Aberrant Wnt pathway activation has been identified in about a third of melanomas, and immunohistochemical evidence of nuclear β-catenin is associated with an improved prognosis, suggesting that changes in Wnt signalling have a role in melanoma progression (Chien et al., 2009; Larue and Delmas, 2006; Rimm et al., 1999). While cytoplasmic β-catenin turn-over is regulated by a destruction complex of factors including glycogen synthase kinase 3β (GSK3β) (Adams et al., 1998; Clevers, 2006; Klaus and Birchmeier, 2008; Nelson and Nusse, 2004), active Wnt signalling blocks GSK3β's capacity to drive β-catenin turnover and facilitates its transfer to the nucleus where it interacts with LEF/TCF

Significance

The phenotype switching model for melanoma progression hypothesizes that microenvironmental signalling received by melanoma cells regulates cycles of back and forth switching between states of proliferation and invasion to drive metastatic spread. M-MITF expression is a critical factor in determining melanoma cell phenotype, and while Wnt signalling is implicated in its regulation, the details remain unclear. We describe here how canonical Wnt signalling drives melanocytic gene expression in proliferative phenotype melanoma cells via LEF1 and how the suppression of LEF1 via non-canonical Wnt signalling facilitates down-regulation of these genes and the proliferative to invasive phenotype switch.

© 2011 John Wiley & Sons A/S

family transcription factors to regulate the expression of target genes (Novak and Dedhar, 1999). LEF/TCF family members (LEF1, TCF1, TCF3 and TCF4) share a high binding affinity for the Wnt responsive element (WRE) sequence within target gene promoters. However, LEF/TCF factors lack the ability to induce transcription on their own and require β-catenin interaction to achieve this (Arce et al., 2006).

In melanocytic cells, Wnt signalling via the LEF1/β-catenin complex is known to activate transcription of a melanocyte-specific form of the gene encoding microphthalmia-associated transcription factor (M-MITF) (Larue and Delmas, 2006; Larue et al., 2003; Takeda et al., 2000; Vance and Goding, 2004). M-MITF is the master regulator for melanocyte development and homeostasis and is critically important to melanoma biology (Levy et al., 2006; Steingrimsson et al., 2004). M-MITF functions by binding target gene promoter DNA at E- and M-Box sequence motifs and activates target genes including those that encode melanocyte-specific factors such as melan-A, Dct and Tyr as well as cell cycle control components such as p21, p16 and Cdk2 (Carreira et al., 2005; Hoek et al., 2008b; Loercher et al., 2005). Importantly, many melanoma lines have been shown to down-regulate the expression of M-MITF (Alexaki et al., 2010; Bittner et al., 2000; Carreira et al., 2006; Hoek et al., 2006; Jeffs et al., 2009), and this correlates with immunohistochemical analyses of human primary and metastatic melanoma that show frequent heterogeneity in their staining patterns for M-MITF and other melanocytic markers (Busam et al., 2001; Carreira et al., 2006). While some tumour areas are positive, others are composed of marker-negative cells. Marker-negative cells likely correspond to melanoma lines and cultures, which down-regulate the expression of melanocytic markers and instead up-regulate many TGFβ targets including the Wnt pathway antagonist *WNT5A* (Bittner et al., 2000; Eichhoff et al., 2010; Hoek et al., 2006; Katoh, 2009). In addition to differences in gene expression, melanocytic marker-positive and marker-negative melanoma cells have distinct phenotypic characteristics. For example, marker-positive cells are morphologically differentiated, strongly proliferative and yet weakly invasive. Conversely, marker-negative cells are morphologically dedifferentiated, weakly proliferative and yet strongly invasive. Critically, we have shown in xenograft experiments that either of these phenotypes will spontaneously give rise to the other in vivo (Hoek et al., 2008a). We have therefore speculated that in vitro, where spontaneous phenotype change is not observed because intra-tumoural microenvironmental changes are absent, their differences are maintained by epigenetic mechanisms. Because melanoma cell phenotype is not dependent on primary melanoma subtype, disease stage or metastatic location, a new hypothesis for disease progression has been proposed. The phenotype switching model for melanoma progression holds that melanoma cells, in response to microenvironmentally regulated changes in signalling, switch back and forth between states of proliferation and invasion and in this way are driven to metastatic spread (Carreira et al., 2006; Hoek et al., 2008a; Hoek and Goding, 2010; Hoek et al., 2006).

In invasive phenotype melanoma cells, we hypothesized that down-regulation of M-MITF (and other melanocytic markers) may be driven by the interruption (via WNT5A activity) of Wnt signal-mediated stabilization of β-catenin (Hoek et al., 2006). Here, we investigated β-catenin expression and localization in proliferative and invasive phenotype melanoma cells and examined the expression and activity of LEF/TCF transcription co-factors in an effort to understand the role of Wnt signalling in melanoma cell phenotype regulation. We describe here that while β-catenin levels and activity do not change across phenotypes, those of LEF1 and TCF4 are inversely correlated and each underlies multiple phenotype-specific differences in melanoma gene expression and behaviour. This shows that the β-catenin interacting factors LEF1 and TCF4 are critically involved in melanoma cell phenotype switching.

Results

Proliferative and invasive melanoma cell phenotypes

Samples were characterized as either proliferative or invasive phenotype according to their expression signatures as previously described (Hoek et al., 2006; Zipser et al., 2011). Phenotype-specific expression of the key proteins M-MITF and WNT5A was confirmed by Western blotting (Figure 1A). Light microscope examination revealed phenotype-specific morphologies where proliferative phenotype cells are small, round and often express dendritic processes, while invasive phenotype cells are larger, flattened and often fibroblastic in shape (Figure 1B, Figure S1). In vitro analyses of proliferation and invasion characteristics confirmed the phenotype assignments made by gene expression analysis (Figure 1C,D).

Phenotype-specific characteristics of β-catenin

Based on immunohistochemical analyses of paraffin-embedded tumour samples, we had previously reported that β-catenin expression levels were substantially higher in proliferative phenotype melanoma cells than in the invasive phenotype (Hoek et al., 2006). However, Western blot experiments showed that proliferative phenotype cells have less β-catenin in the cytosol than invasive phenotype cells and that this is accompanied by the presence of serine 33/37 phosphorylation and unphosphorylated (active) GSK3β (Figure 2A, Figure S3A). The higher levels of β-catenin protein present in the cytosol of invasive phenotype cells prompted us to determine whether this had an

© 2011 John Wiley & Sons A/S

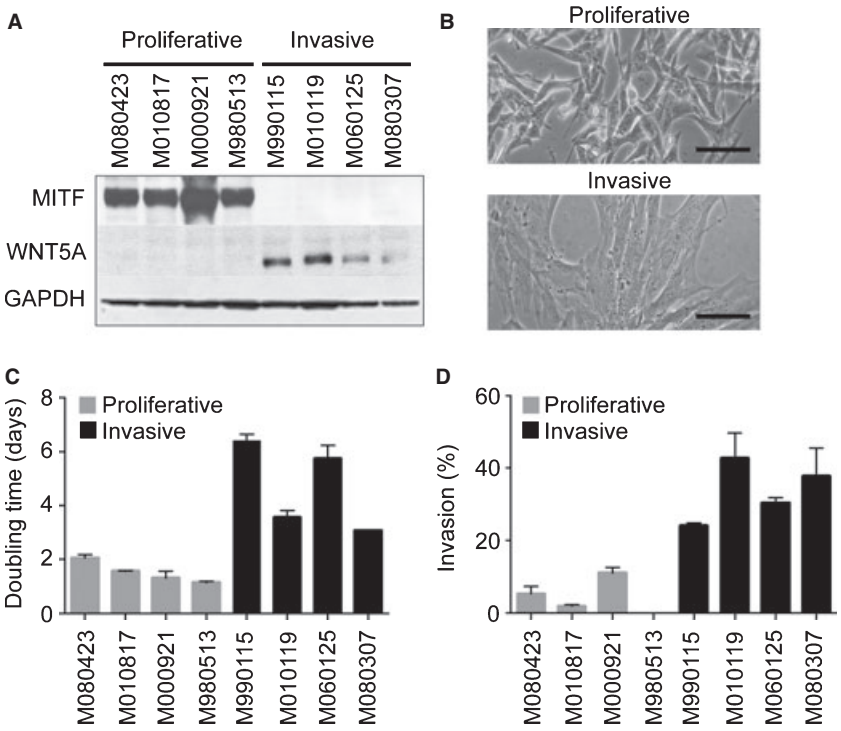

Figure 1. Proliferative and invasive melanoma cell phenotypes. Four examples each of melanoma cultures expressing proliferative or invasive phenotype gene signatures were selected for the study. (A) Expression of two factors with known phenotype specificity (M-MITF, WNT5A) by Western blot confirmed phenotype assignments. (B) Light microscope observations of cells in culture showed distinctive and phenotype-specific morphologies. Proliferative phenotype cells are smaller, rounded and often express dendritic processes, while invasive phenotype cells are larger, flattened and morphologically similar to fibroblasts. More examples of these morphologies can be found in Figure S1. The black bars represent 100 microns. (C) In vitro cell proliferation experiments show that proliferative phenotype cells have a significantly shorter doubling time than invasive phenotype cells ($P < 0.001$). (D) In vitro invasion experiments show that invasive phenotype cells are significantly more efficient at passing through a basement-membrane matrix-coated filter than proliferative phenotype cells ($P < 0.002$).

effect on β-catenin nuclear localization and activity. We found that while β-catenin levels varied relative to the histone 2B control, there was no significant difference for β-catenin between nuclear extracts of proliferative and invasive phenotype cells (Figure 2A). We also measured β-catenin nuclear activity using a β-catenin/TCF transcription assay (TOPflash/FOPflash) and again found no significant differences in β-catenin-dependent transcriptional activity between cell phenotypes (Figure 2B). We then used immunofluorescence to investigate β-catenin's cellular distribution. This showed that in proliferative phenotype cells, most β-catenin was associated with the cell membrane, while in invasive phenotype cells, it was diffusely localized to the cytosol (Figure 2C,D). These data indicated that differences in nuclear β-catenin expression and activity do not underlie observed phenotype-specific gene expression differences.

LEF1 and TCF4 are proliferative and invasive phenotype-specific, respectively

As differential regulation of β-catenin levels did not appear to be important for phenotype specificity, we examined the expression patterns of the LEF/TCF family. RT-PCR analysis showed that among this family of transcription factors, only the *LEF1* and *TCF4* genes have significant phenotype-specific expression, $P < 0.002$ and $P < 0.0005$, respectively (Figure 3A). Interestingly, a Pearson's correlation analysis shows that the expression of *LEF1* and *TCF4* is inversely correlated ($R = -0.53$, $P < 0.04$). *TCF3* gene expression is not phenotype-specific ($P < 0.4$, data not shown), and *TCF1* gene expression was not detectable (data not shown). These results are consistent with previously published DNA microarray data (Hoek et al., 2006) from 86 samples identified with proliferative or invasive phenotype expression signatures (Figure S2). The phenotype-specific expression of LEF1 and TCF4 protein was confirmed by Western blotting (Figure 3B). Immunostaining sections of paraffin-embedded human primary melanoma tissues with anti-bodies targeting LEF1 and TCF4 revealed examples where M-MITF and LEF1 were inversely correlated in their expression with TCF4 (Figure 3C). However, we also saw many examples where the expression of LEF1 and TCF4 was not inversely correlated, which we have previously observed with other phenotype-specific markers (Eichhoff et al., 2010).

© 2011 John Wiley & Sons A/S

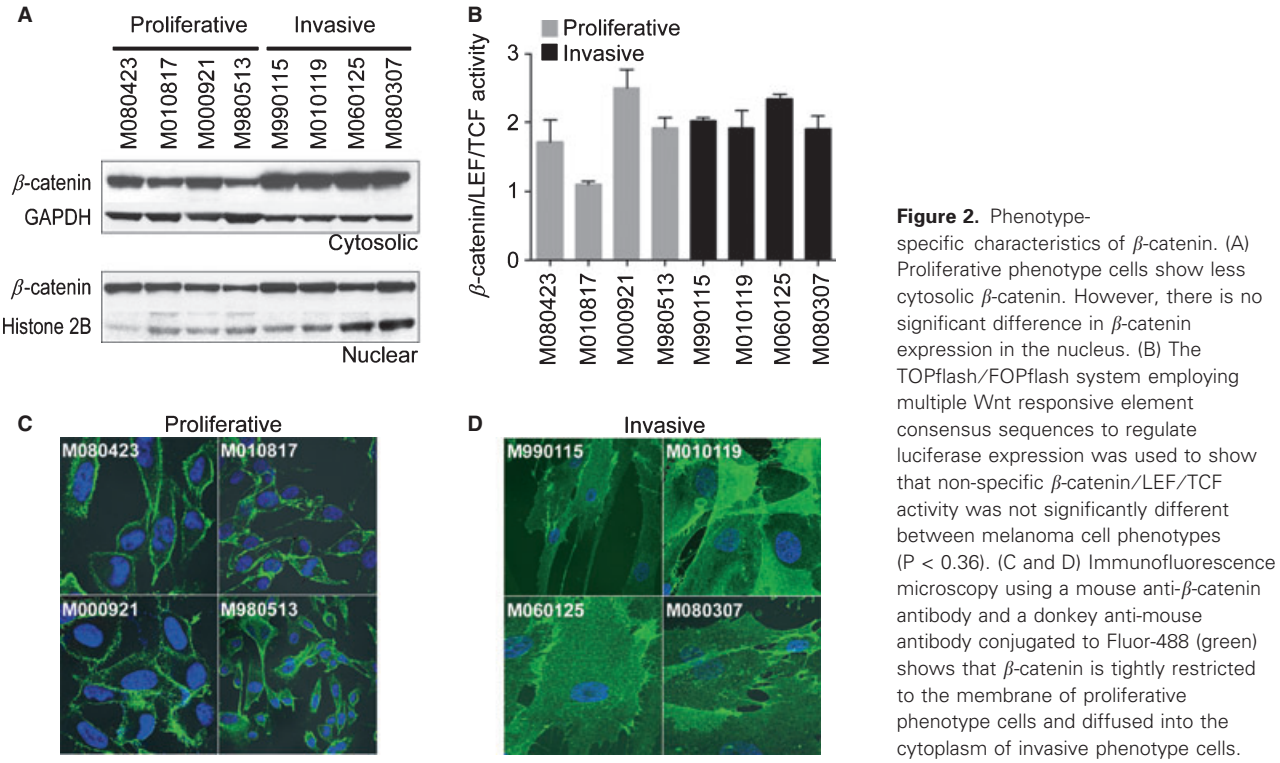

Figure 2. Phenotype-specific characteristics of β-catenin. (A) Proliferative phenotype cells show less cytosolic β-catenin. However, there is no significant difference in β-catenin expression in the nucleus. (B) The TOPflash/FOPflash system employing multiple Wnt responsive element consensus sequences to regulate luciferase expression was used to show that non-specific β-catenin/LEF/TCF activity was not significantly different between melanoma cell phenotypes ($P < 0.36$). (C and D) Immunofluorescence microscopy using a mouse anti-β-catenin antibody and a donkey anti-mouse antibody conjugated to Fluor-488 (green) shows that β-catenin is tightly restricted to the membrane of proliferative phenotype cells and diffused into the cytoplasm of invasive phenotype cells.

LEF1 regulates phenotype-specific gene expression

Because invasive phenotype melanoma cells down-regulate both *LEF1* and melanocytic marker genes, we studied the effects of silencing *LEF1* in proliferative melanoma cells. We confirmed that knock-down of LEF1 reduced the expression of melanocytic genes such as *MITF* and *MLANA* (encodes melan-A/MART1) and also confirmed this effect at the protein level (Figure 4A,B). Although knock-down of β-catenin had the same effect on these target genes, the effect on M-MITF appeared to be weak at the protein level (Figure 4A,C). Interestingly, we found that silencing LEF1 consistently up-regulated the expression of *TCF4* and *WNT5A* genes and protein (Figures 4A,B and S8). However, this effect was not replicated by silencing β-catenin, demonstrating that LEF1 blocks *TCF4* and *WNT5A* expression in a β-catenin-independent manner (Figure 4A,B). In functional assays, we found that knock-down of LEF1 significantly reduces cell proliferation and increases invasiveness (Figure 4D). Although knock-down of β-catenin reduced proliferation to the same extent, its impact on cell invasiveness was mild (Figure 4D). This suggests that while LEF1/β-catenin is important for proliferative processes, LEF1 is independently involved in suppressing the invasive phenotype. Importantly, TOPflash/FOPflash reporter assays in proliferative phenotype cells showed that while knock-down of β-catenin significantly down-regulated reporter expression, knock-down of the LEF1 co-factor did not. We speculate that LEF1 knock-down allows TCF4 to be up-regulated and take its place, as the assay does not discriminate between LEF/TCF co-factors (Figure 4D). Furthermore, we include experiments performed on FO1 melanoma cells transfected with a luciferase construct carrying an M-MITF promoter and constructs expressing LEF1 or TCF4. These experiments show that LEF1 activates MITF expression, while TCF4 does not (Figure 5A).

Silencing of TCF4 in invasive phenotype melanoma cells

Phenotype-specific expression of TCF4 in invasive phenotype cells suggests that the TCF4/β-catenin complex may have a role in driving the invasive gene signature. We found that knock-down of TCF4 expression in invasive phenotype cells resulted in some down-regulation of WNT5A at both the mRNA and protein levels (Figure 5B,C). However, silencing of β-catenin had little effect on the expression of either WNT5A or TCF4 (Figure 5B,C). Furthermore, functional assays show that knock-down of TCF4 significantly decreases invasiveness (Figure 5D). While silencing of β-catenin also decreased invasiveness, the effect was weak and not significant (Figure 5D). Intact β-catenin/TCF4 signalling in invasive phenotype cells is demonstrated by luciferase reporter assays that show significant reduction in luciferase activity to background levels by silencing either TCF4 or β-catenin.

Exogenous WNT5A suppresses the proliferative phenotype

WNT5A is reported to be a key gene in the aggressive/invasive melanoma cell phenotype (Hoek et al.,

© 2011 John Wiley & Sons A/S

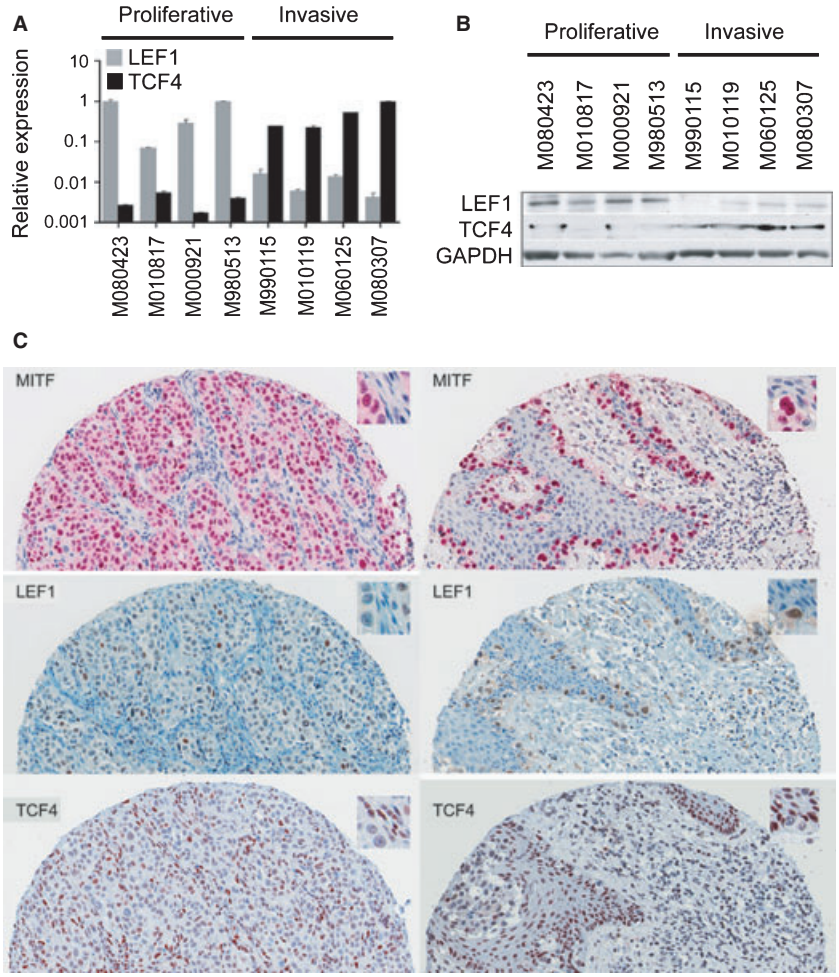

Figure 3. β-catenin co-factors LEF1 and TCF4 are proliferative and invasive-specific, respectively. (A) Real-time PCR analyses show that transcription co-factor LEF1 is preferentially expressed in proliferative phenotype melanoma cells ($P < 0.002$), while transcription co-factor TCF4 is preferentially expressed in invasive phenotype melanoma cells ($P < 0.001$). (B) Western blot analysis confirms the phenotype-specific inverse correlation of LEF1 and TCF4 expression in melanoma cells. (C) Immunohistochemical analyses show examples of M-MITF/LEF1 expression inversely correlating with TCF4 in human primary melanoma biopsies.

2006; Weeraratna et al., 2002). Furthermore, because TCF4 is important for *WNT5A* expression, we were interested in examining the effects of WNT5A on cell phenotype-specific characteristics. We first depleted WNT5A from an invasive phenotype cell by siRNA-mediated knock-down. Consistent with previous studies (Dissanayake et al., 2007), we confirmed that protein kinase C (PKC) phosphorylation is decreased by WNT5A knock-down and this was accompanied by a decrease in invasiveness (Figure 6A,B). However, we detected no effect on either proliferation or the expression of LEF1 (data not shown). Interestingly, WNT5A knock-down in invasive phenotype cells did not significantly impact β-catenin/LEF/TCF activity, although TCF4 expression was somewhat decreased (Figure S3C,D). It has also been reported that WNT5A antagonizes melanocytic gene expression in B16 mouse melanoma and it has been shown that the treatment of WNT5A-low cell lines with recombinant WNT5A protein decreases *MLANA* expression (Chien et al., 2009; Dissanayake et al., 2008). Accordingly, we found that the treatment of proliferative phenotype cells with recombinant WNT5A protein down-regulated both LEF1 and melanocytic marker protein expression (Figure 6C). To test that LEF1 down-regulation is responsible for the loss of melanocytic marker expression, we transfected proliferative phenotype cells with a LEF1-expressing construct prior to WNT5A treatment, which rescued melanocytic marker expression from WNT5A-induced down-regulation (Figure 6D). Furthermore, we examined the effects of WNT5A on β-catenin cellular localization and stability. Western blot analyses showed that upon treatment of proliferative phenotype cells with recombinant WNT5A, β-catenin serine 33/37 phosphorylation was decreased while serine 9 phosphorylation of the GSK3β pool was increased (Figure S4B). We therefore over-expressed WNT5A in proliferative phenotype cells. Immunofluorescence microscopy shows that exogenous WNT5A expression in proliferative phenotype cells delocalizes β-catenin from the membrane to the cytosol (Figure 6E). Furthermore, untransfected proliferative phenotype cells show that β-catenin co-localizes with short actin bundles at the cell membrane, while in invasive phenotype cells, actin is instead concentrated in long actinic fibres. Upon WNT5A transfection of proliferative phenotype cells, we observed the formation of actinic stress

© 2011 John Wiley & Sons A/S

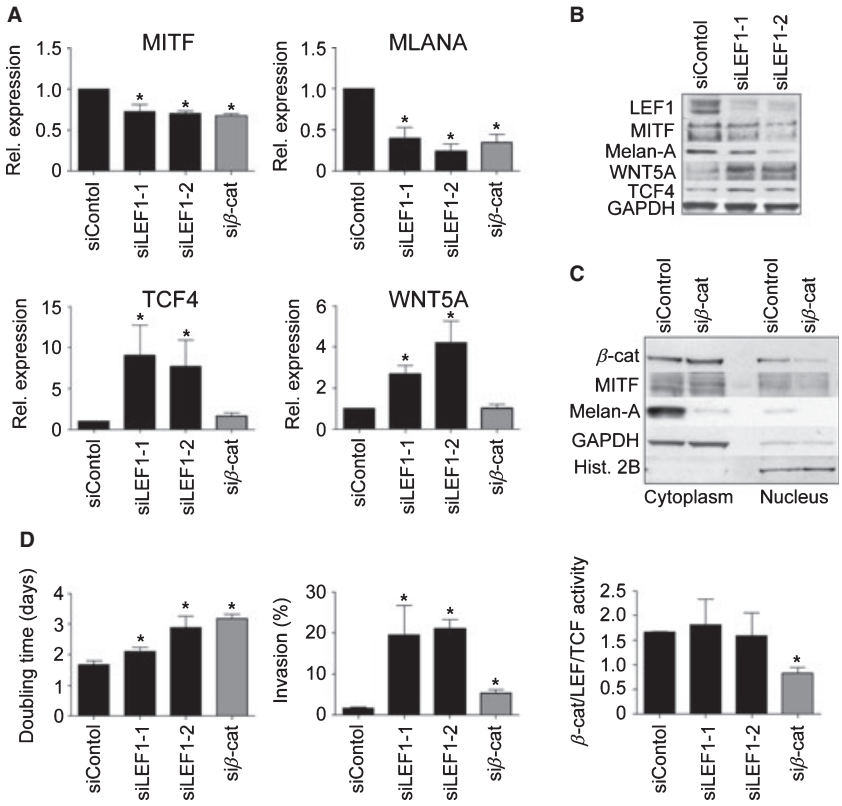

Figure 4. LEF1 regulates proliferative phenotype-specific gene expression. (A) siRNA-mediated silencing of LEF1 in M000921 down-regulates *MITF* and *MLANA* (Melan-A) expression and up-regulates *TCF4* and *WNT5A* expression. siRNA-mediated silencing of β-catenin down-regulated *MITF* and *MLANA*, but had no significant effect on *TCF4* or *WNT5A*. All real-time PCR data represent averages of three independent experiments with standard deviation (error bars). See also Figure S8 for additional examples. (B and C) Western blotting confirmed the results of LEF1 and β-catenin silencing at the protein level. (D) Silencing either LEF1 or β-catenin reduces the proliferation rate ($P < 0.04$) and increases invasiveness ($P < 0.04$). While silencing β-catenin nullifies Wnt responsive element-mediated luciferase expression ($P < 0.02$), silencing LEF1 does not. *$P < 0.05$.

fibres, as is characteristic of invasive phenotype cells (Figure 6E).

Discussion

While canonical Wnt signalling is important for melanocytic gene expression, survival and proliferation, it is rare that genetic mutations in melanoma involve members of Wnt pathway (Bennett, 2008; Larue et al., 2003; Reifenberger et al., 2002). In melanocyte development, β-catenin activation via the canonical Wnt pathway is thought to influence neural crest stem cell fate by up-regulating the expression of specific melanocytic markers (Dorsky et al., 1998). For example, in the melanocyte nucleus, β-catenin cooperates with LEF1 at the *MITF-M* promoter to express melanocyte-specific MITF (Yasumoto et al., 2002). In melanoma, which we hypothesize is driven by cells switching between phenotypes of proliferation and invasion, M-MITF is thought to be an essential regulator because knock-down of its gene reduces proliferation and increases invasiveness (Carreira et al., 2005, 2006; Hoek et al., 2008a). Likewise, the expression of WNT5A is reported to be another important regulator of phenotype as its over-expression decreases melanocytic marker expression and increases invasiveness (Dissanayake et al., 2008, 2007). Therefore, Wnt signal regulation of the balance of power between phenotype-critical factors such as M-MITF and WNT5A may be key to melanoma cell phenotype.

It is generally agreed that the tumourigenic effects of β-catenin on melanoma are largely mediated via its effects on the *MITF* gene (Widlund et al., 2002). Because proliferative, and not invasive, phenotype melanoma cells express canonical Wnt target genes, we had hypothesized that β-catenin levels were highest in the proliferative phenotype (Hoek et al., 2006). However, we now report that nuclear β-catenin levels and activity are not significantly different between the phenotypes (Figure 2). Because proliferative, and not invasive, phenotype cells have such a distinct canonical Wnt signalling gene signature, we reasoned that β-catenin must yet play a critical role by interacting with LEF/TCF transcription co-factors, which are regulated in a phenotype-specific fashion. Accordingly, we found that LEF1 and TCF4 expression patterns were strongly correlated with melanoma cell phenotype and that LEF1 was preferentially expressed by proliferative phenotype cells and TCF4 by invasive phenotype cells. The specific expression of LEF1 in proliferative phenotype cells agrees with previous reports which show that LEF1/β-catenin underlies melanocytic gene expression, characteristic of both melanocytes and proliferative phenotype melanoma cells (Schepsky et al., 2006). Knock-down experiments targeting LEF1 and β-catenin in proliferative phenotype cells confirmed their importance for the expression of

© 2011 John Wiley & Sons A/S

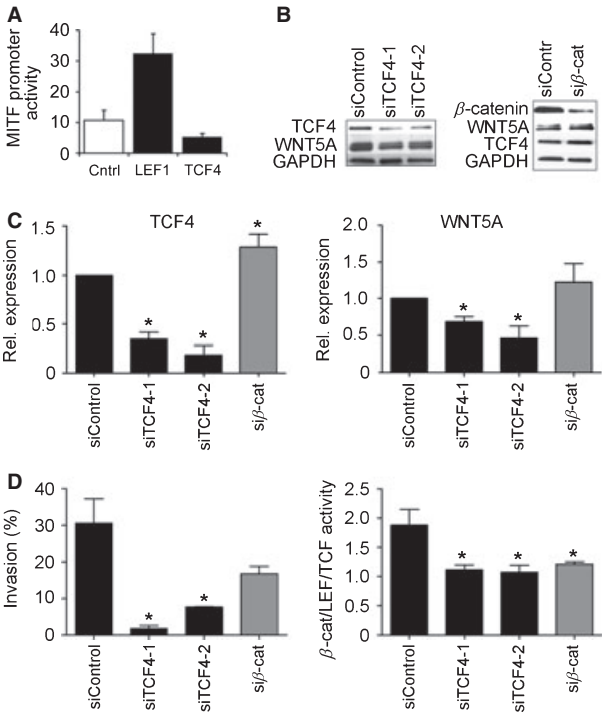

Figure 5. Silencing of TCF4 in invasive phenotype melanoma. (A) FO1 melanoma cells expressing a luciferase construct with a *M-MITF* promoter exogenously treated with LEF1 shows activation of luciferase activity, while treatment with TCF4 does not. (B and C) Silencing of TCF4 in invasive phenotype cells also downregulated the expression of WNT5A on RNA and protein levels. Silencing of β-catenin had no effect on WNT5A or TCF4 expression levels. (D) Silencing of TCF4 as well as β-catenin showed significantly lower activities of the TOPflash/FOPflash reporter assay ($P < 0.04$). Invasion assays showed significant decrease in invasiveness upon silencing TCF4 ($P < 0.03$) and milder effects for the silencing of β-catenin ($P < 0.09$). *$P < 0.05$.

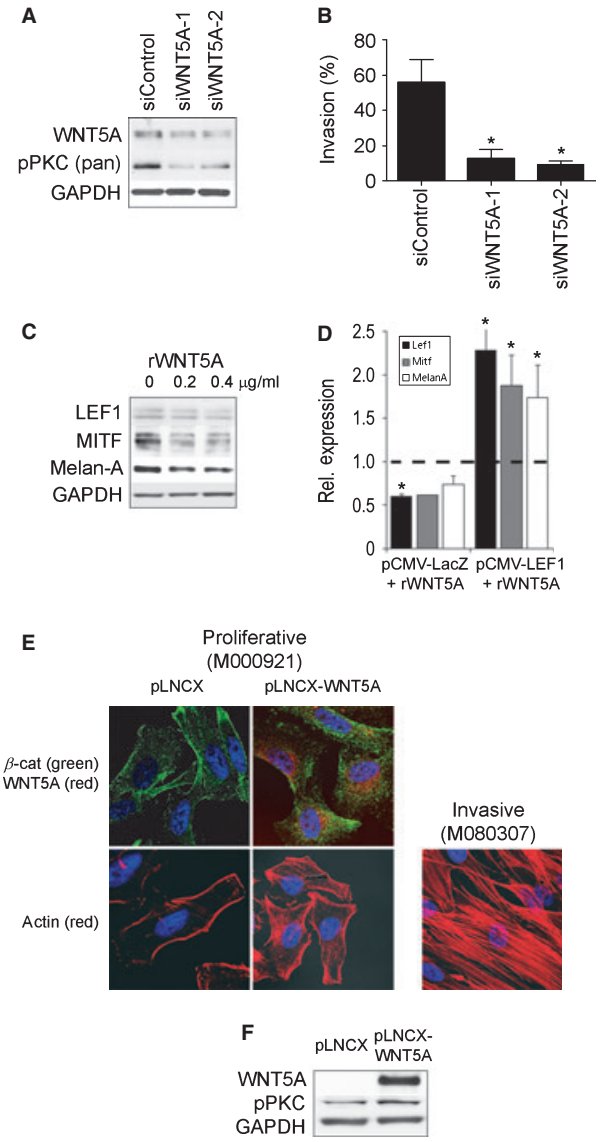

Figure 6. WNT5A suppresses the proliferative phenotype. (A and B) Silencing WNT5A in invasive phenotype melanoma cells reduces the phosphorylation of protein kinase C (PKC) and significantly reduces in vitro invasiveness ($P < 0.05$). (C) Treating proliferative phenotype melanoma cells with recombinant WNT5A down-regulates the expression of *LEF1*, *MITF* and *MLANA*. (D) Transfection of proliferative phenotype cells with either a LacZ-expressing or LEF1-expressing vector showed that WNT5A down-regulation of melanocytic markers is LEF1-dependent. (E) Proliferative phenotype melanoma cells transformed with a WNT5A-expression construct shows that WNT5A released β-catenin from the membrane into the cytosol and promoted the formation of intracellular actin fibres. (F) Western blot and densitometry show that induced expression of WNT5A in proliferative phenotype cells increases phospho-PKC levels. *$P < 0.05$.

melanocytic markers and cell proliferation. This also confirmed that in proliferative phenotype melanoma cells, melanocytic gene expression is driven by canonical Wnt signalling via β-catenin interaction with LEF1 at the *MITF-M* promoter as the effects of LEF1 knock-down correlate with those described for silencing *MITF* (Carreira et al., 2006; Hoek et al., 2008a). However, we show here for the first time that LEF1 knock-down significantly increases invasiveness in melanoma cells, demonstrating that LEF1 has a critical role in phenotype determination beyond the regulation of melanocytic gene expression.

LEF/TCF transcription factors are referred to as non-classical transcription factors because they require β-catenin interaction to activate their target genes (Brantjes et al., 2002). However, LEF/TCF transcription factors are also involved in gene repression (Arce et al., 2009). For example, in a mouse melanoma model, it is known that LEF1/β-catenin suppresses $p16^{INK4a}$ expression (Delmas et al., 2007). We have shown that in proliferative phenotype melanoma cells, while LEF1 drives melanocytic Wnt target genes in a β-catenin-dependent fashion, it also represses, independently of β-catenin, the expression of genes including *TCF4* and

© 2011 John Wiley & Sons A/S

WNT5A. Conversely, in invasive melanoma cells, LEF1 expression is strongly down-regulated. Instead, TCF4 expression plays an important role in regulating cell invasiveness and Wnt reporter gene expression. Interestingly, TCF4 activation of *WNT5A* expression is independent of β-catenin. *WNT5A* expression is also reported to be activated by TGFβ signalling, and Smad-responsive elements (SRE) have been found at the *WNT5A* promoter (Katoh, 2009). Vascular endothelial growth factor (*VEGF*), another target of TGFβ signalling, has been shown in human pulmonary artery smooth muscle cells to be activated by the specific binding of a TCF4/Smad complex to SREs in the *VEGF* promoter (Clifford et al., 2008). As microarray data analyses of melanoma cell cultures have shown *VEGF* up-regulation in invasive phenotype cells (Hoek et al., 2006), it would be interesting to investigate whether Smads are similarly involved in WNT5A regulation by TCF4. This could explain the differential and phenotype-specific expression of Wnt and TGFβ target genes.

WNT5A is a signalling ligand of the non-canonical Wnt pathway and has been reported to increase during melanoma progression and correlate with a worsened patient prognosis (Da Forno et al., 2008). However, our own examination of *WNT5A* expression has shown that clinical stage does not determine whether or not cultured cells will express it, but rather that *WNT5A* expression is dictated by the cultured cells' phenotype (invasive or proliferative). That *WNT5A* expression is not disease stage-specific is further supported by the examination of published DNA microarray data acquired from melanoma tissues samples (Smith et al., 2005). We also find that in vivo *WNT5A* expression is variable within both primary lesions and late-stage metastases and inversely correlates with melanocytic marker expression (Eichhoff et al., 2010). Weeraratna and colleagues have described WNT5A as a major contributor to melanoma cell invasiveness, showing that WNT5A signals via PKC phosphorylation to antagonize melanocytic marker expression, inhibit E-cadherin expression, activate cytoskeletal reorganization and drive a process similar to epithelial–mesenchymal transition (EMT) (Dissanayake et al., 2007; Weeraratna et al., 2002). We had also noted that the increased expression of WNT5A (along with a host of other genes) correlates with in vitro invasiveness (Hoek et al., 2006). Here, we confirm that knock-down of WNT5A expression in invasive phenotype cells reduces their invasiveness. Furthermore, we confirm that WNT5A antagonizes melanocytic marker expression but show here that it does so by inhibiting LEF1 expression (Figure 6C,D).

Interestingly, we found that β-catenin was strongly associated with the membrane in proliferative phenotype cells and cytosolic in invasive phenotype cells (Figure 2C,D). Additionally, we note that short actin bundles co-localize with β-catenin at the proliferative phenotype membrane, but in invasive cells, actin is organized into long filaments (stress fibres) throughout the cytosol. Actin filament reorganization observed in proliferative phenotype melanoma cells induced to over-express WNT5A is presumed to be involved in cell motility and recapitulates the filament patterns seen in invasive phenotype cells. In agreement with other reports where WNT5A treatment stimulated actin filament reorganization (O'connell et al., 2009; Weeraratna et al., 2002), we confirm that WNT5A drives stress fibre formation but show here that this is a phenotype-specific phenomenon (Figure S4C).

The finding that expression of WNT5A in proliferative phenotype melanoma causes β-catenin to dissociate from the membrane into the cytosol, as is seen in invasive phenotype cells, correlates with immunohistochemical findings which show that β-catenin dissociation from the cell membrane is associated with increased tumour invasiveness (Demunter et al., 2002). Furthermore, a cytosolic localization of β-catenin associated with E-cadherin loss correlates with a worsened patient prognosis (Bachmann et al., 2005). Moreover, the group of Anja Bosserhoff has reported that cytosolic localization of β-catenin is induced by E-cadherin loss (Kuphal et al., 2004), and WNT5A has been shown to down-regulate E-cadherin via PKC activation (Dissanayake et al., 2007). For β-catenin stabilization, where phosphorylation of Ser9 on GSK3β blocks β-catenin breakdown, it has been shown in cutaneous squamous and basal cell carcinomas as well as in endometrial cancer that Ser9 phosphorylation of GSK3β is driven by PKC signalling (Haughian et al., 2009; Ma et al., 2007). In line with these and other studies (Hur and Zhou, 2010), our data support the idea that stabilization of β-catenin is achieved via WNT5A/PKC-driven inhibition of GSK3β-mediated phosphorylation (Figure 6, Figure S4). Therefore, we postulate that β-catenin localization is regulated by WNT5A signalling and this may be crucial for effecting melanoma cell motility and invasion.

In the present study, we demonstrate that Wnt signalling differences between the two phenotypes are influenced by a switch in LEF/TCF factors and that these factors are involved in specifying phenotype-specific gene expression. We conclude that the proliferative phenotype is specifically driven by canonical Wnt signalling via an interaction between LEF1 and β-catenin. Furthermore, we show that LEF1 represses the expression of invasive phenotype-specific genes including TCF4 and WNT5A independently of its interaction with β-catenin (Figure 4). LEF1 may do this directly by binding to WRE sequences that are present in both the upstream and transcribed regions of these genes (data not shown). When expressed, both TCF4 and WNT5A have critical roles in maintaining the dedifferentiated and invasive characteristics of invasive phenotype cells. With LEF1-mediated repression of WNT5A lifted, canonical Wnt signalling is subsequently antago-

© 2011 John Wiley & Sons A/S

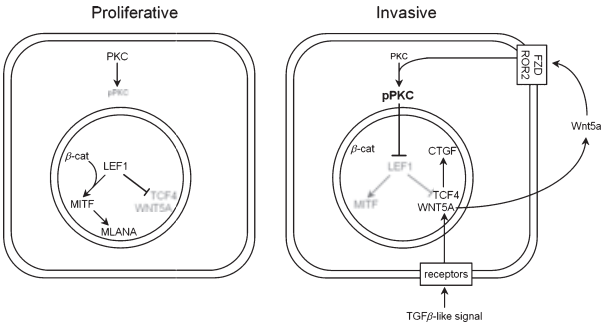

Figure 7. Phenotype switching model for melanoma progression. Proliferative phenotype melanoma cells express melanocytic factors such as *MITF* and *MLANA*. Their expression is driven by Wnt signalling via the LEF1/β-catenin complex, while LEF1 represses invasive phenotype-specific gene expression in a β-catenin-independent manner. Changes in microenvironmental conditions (e.g. hypoxia) activate a TGFβ-like signal to up-regulate critical genes including *WNT5A*. WNT5A acts in an autocrine manner by binding to frizzled or ROR2 receptor kinases and repressing melanocytic gene expression and cell proliferation via activated protein kinase C-mediated suppression of *LEF1* expression. Down-regulated LEF1 levels relieve suppression of genes such as *TCF4* and *WNT5A* to further drive the expression of invasive phenotype-specific genes (e.g. *CTGF*) and increase cell invasiveness.

nized to trigger dedifferentiation and increase invasive behaviour.

The switch of cellular phenotypes in melanoma is likely to be regulated by microenvironmental influences such as inflammation and hypoxia. Either of these conditions can drive TGFβ activation of WNT5A in proliferative phenotype cells and the surrounding stroma (Hoek et al., 2006). Such an influx of WNT5A would work to suppress LEF1 expression (which activates TCF4 expression), change β-catenin subcellular localization patterns and precipitate the switching of proliferative phenotype cells to the invasive state (Figure 7, Figure S5).

Methods

Melanoma cell culture and treatment

Melanoma cell cultures were established from surplus material from cutaneous metastases removed by surgery after having obtained written, informed consent approved by the local IRB (EK647 and EK800). Clinical diagnosis was confirmed by a board-certified dermatopathologist (RD). Melanoma cells were released from tissue material and cultured as previously described (Geertsen et al., 1998). Cell cultures were maintained in RPMI (Invitrogen, Carlsbad, CA, USA) supplemented with 10% heat-inactivated foetal calf serum, 5 mM glutamine and 1 mM sodium pyruvate and grown at 37°C and 5% CO_2. Treatments with recombinant WNT5A protein were carried out in serum-free media.

RNA extraction, cDNA synthesis and RT-PCR

Total RNA was extracted from melanoma cell cultures using Trizol according to manufacturer's instructions (Invitrogen). One microgram of total RNA was used for cDNA synthesis using Promega's Reverse Transcription System according to the supplied protocol (Promega, Madison, WI, USA). Gene expression was quantified using the Light Cycler DNA Master SYBR Green kit (Roche, Basel, Switzerland) on 1 μg of template cDNA with Roche's Light Cycler 4.0 instrument. Primers used were 5′-AAACGGCTACCACATCCA AG-3′ and 5′-CCTCCAATGGATCCTCGTTA-3′ (18s RNA), 5′-AG-GGCTCCTACGAGA GTGCT-3′ and 5′GACACCCCATGGCACTTG-3′ (WNT5A). All other gene-specific primers were purchased from Qiagen (Venlo, the Netherlands). Messenger RNA levels were compared against standard curves and normalized to 18s RNA. Gene expression changes after siRNA treatment were also normalized against levels in cells transfected with control siRNA.

Western blot analyses

Cells were washed twice with cold PBS and lysed at 4°C in RIPA protein lysis buffer as previously reported (Dissanayake et al., 2007). To obtain cytosolic and nuclear protein fractions, cells were lysed in protein lysis buffer A [10 mM HEPES (pH 7.9), 10 mM KCl, 1.5 mM $MgCl_2$, 0.625% NP-40, protease and phosphatase inhibitors]. After incubation at 4°C for 10 min, nuclei were pelleted by centrifugation at 5000 *g* for 5 min and the supernatant was kept as the cytoplasmic fraction (which was further centrifuged another three times to remove remaining particulates). Pelleted nuclei were washed three times in protein lysis buffer A, resuspended in protein lysis buffer B [20 mM HEPES (pH 7.9), 1.5 mM $MgCl_2$, 420 mM NaCl, 25% glycerol, protease and phosphatase inhibitors] and rotated for 1 h at 4°C. After centrifugation at 16 000 *g* for 20 min at 4°C, the supernatant was used as the nuclear fraction. Proteins were separated by SDS-PAGE on 4–12% Tris–glycine gels (Invitrogen) under reducing conditions and transferred onto nitrocellulose membrane (Invitrogen). Membranes were probed with primary antibodies diluted as follows: anti-MITF 1:500 (Abcam, Cambridge, UK), anti-LEF1 1:500 (Cell Signalling, Danvers, MA, USA), anti-MelanA 1:1000 (Abcam), anti-WNT5A 1:500 (R&D, Abingdon, UK), anti-β-catenin 1:1000 (BD Bioscience, Franklin Lakes, NJ, USA), anti-β-catenin phosphoserine 33/37 1:500 (R&D), anti-GSK3β 1:1000 (Cell Signalling), anti-GSK3β phosphoserine 9 1:500 (Cell Signalling), anti phospho-PKC (pan) 1:1000 (Cell Signalling), anti-TCF4 1:2000 (abgent, San Diego, CA, USA), anti-GAPDH 1:1000 (Abcam) and anti-histone 2B 1:500 (Cell Signalling). Horseradish peroxidase-conjugated secondary antibodies rabbit anti-goat (Santa Cruz Biotechnology, Santa Cruz, CA, USA), goat anti-rabbit (Bio-Rad, Hercules, CA, USA) or rabbit anti-mouse (Abcam) were incubated with the membrane, and bound antibodies were detected using a chemiluminescence kit (GE Healthcare, Buckinghamshire, UK). Densitometry analyses were also conducted for each blot (Figure S6).

Immunofluorescence

Cells were seeded to a density of 2×10^5 (proliferative phenotype) or 7.5×10^4 (invasive phenotype) cells per well into one-well chamber slides and incubated at 37°C and 5% CO_2 overnight. Where proliferative cells were to be transfected with expression constructs, 2×10^5 cells were transfected and incubated for 48 h before staining. Cells were washed in PBS and fixed in 4% paraformaldehyde for 30 min at room temperature. After two additional washes, unspecific binding was blocked with sterile-filtered blocking buffer (0.2% Triton X-100, 0.2% BSA, 1% goat serum, 0.2% casein, 0.2% gelatin and 0.02% sodium azide) for 1 h at room temperature. For WNT5A staining, unspecific binding of streptavidin was additionally blocked using an avidin–biotin blocking kit (Dako, Glostrup, Denmark) prior to the blocking buffer. Antibodies were diluted in blocking buffer (1:250 for anti-β-catenin or 1:10 for

© 2011 John Wiley & Sons A/S

biotin-conjugated anti-WNT5A), and cells were incubated overnight at 4°C. Secondary antibodies anti-mouse-Alexa Fluor-488 or streptavidin-Alexa Fluor-568 (Invitrogen) were diluted 1:2000 in blocking buffer and incubated with the cells for 1 h at room temperature. F-actin staining was carried out using a rhodamine-tagged phalloidin stain (Invitrogen) diluted 1:40 in blocking buffer and incubated with the cells for 15 min. Cells were washed three times for 5 min in PBS and mounted into Prolong Gold antifade reagent (Invitrogen). Images were taken using a Leica Sp50 confocal microscope.

siRNA and plasmid transfection

Silencing RNA (siRNA) transfection of melanoma cells was carried out using INTERFERRin transfection solution according to the manufacturer's protocol (Polyplus-transfection, Illkirch, France). Cells were transfected with 20 nM of siRNA (Qiagen) for 72 h before RNA, or protein was extracted. As control siRNA, the All-Star negative siRNA sequence (Qiagen) was used, and gene-specific siRNAs targeting siLEF1 (SI00114933, SI00114940), siTCF4 (SI00048965, SI03101805), validated siβ-catenin (SI02662478) and siWNT5A (SI03072776, SI03095421) were obtained from Qiagen. The transfection of melanoma cells with pLNCX control (Clontech, Mountain View, CA, USA), pLNCX-WNT5A, pCMV3.1_lacZ control (Invitrogen) and pCMV6-XL4-LEF1 (OriGene Technologies Inc, Rockville, MD, USA) expression vectors and TOPflash/FOPflash luciferase reporter assays were achieved using jetPEI solution according to the manufacturer's protocol (Polyplus-transfection).

Proliferation assay

Cells were seeded in 24-well microplates in a density of 2×10^4 cells, and cell growth was determined with a standard colorimetric assay measuring 3-(4,5-dimethylthiazol-2-yl)-2,5 diphenyltetrazolium bromide (MTT) (Sigma-Aldrich, St Louis, MO, USA) reactivity after 48 and 96 h to calculate cell culture doubling times. Doubling times were calculated using a standard method (Davis, 2001). This assay was compared against standard BrdU (Millipore, Billerica, MA, USA) and Neubauer chamber cell-counting approaches (Figure S7).

Invasion assay

Cells were seeded on 8-μm transwell microporous filters (BD Bioscience) uncoated or coated with Matrigel (BD Biosciences). Prior to seeding, melanoma cells were cultured for 48 h in RPMI medium containing 3% FCS, and 5×10^5 (proliferative phenotype) or 3.5×10^5 (invasive phenotype) cells were diluted in 500 μl RPMI with no FCS and seeded onto the transwell inserts. RPMI containing 10% FCS was added to the bottom chamber as a chemoattractant. After 20 h of incubation at 37°C and 5% CO_2, any cells remaining on the upper side of the filter were removed with cotton swab. The membrane was then stained using Diff-Quick H&E staining solutions (ThermoFisher Scientific, Waltham, MA, USA), and the cells were counted under a light microscope using eight face fields per membrane. Invasion was calculated as the ratio of the number of cells migrating through a matrigel-coated membrane to the number of cells migrating through uncoated membrane.

Luciferase reporter assays

Melanoma cell cultures were seeded into 24-well plates in a density of 2×10^4 cells prior to transfection. TOPflash/FOPflash constructs (Herzig et al., 2007; Korinek et al., 1997) were co-transfected together with Renilla luciferase plasmid pRL-SV40 (Promega) to normalize for transfection efficiency. After 48 h, cells were lysed in passive lysis buffer (Promega), and luciferase activity was measured by luciferase reporter assay (Promega) using a Wallac Victor^2 1420 Multilable counter (Perkin Elmer, Waltham, MA, USA). For the *MITF* promoter-specific assays, FO1 cells (kindly provided by Dr R Baserga) were cultured in RPMI-1640 medium containing 10% FCS and 5 mM L-glutamine. Cells were transiently transfected in 6-well plates using 6 μl of FuGene (Roche) and 2 μg of total plasmid DNA. Cells were cotransfected with the PGK::β-galactosidase construct as a control and the Mitf::luciferase construct as previously described (Goodall et al., 2004). The expression vectors for LEF1 (#710) and TCF4 (#714) were used as previously reported (Hecht and Stemmler, 2003). The amount of DNA was normalized against pBluescript. Luciferase and β-galactosidase activity was measured 48 h after transfection, and luciferase activity was normalized against β-galactosidase activity.

Immunohistochemistry

Immunohistochemical staining was performed on 5-μm sections of paraffin-embedded melanoma tissues. For MITF staining, an anti-MITF primary (clone 5 + D5, 1:50; Abcam, Cambridge, UK) was used as described previously (Eichhoff et al., 2010). For LEF1 staining, an anti-LEF1 monoclonal rabbit antibody (1:150; Cell Signaling Technology, Boston, MA, USA) was used with staining being performed using a Ventana Benchmark XT autostainer and the XT ultraView DAB kit, using CC1 as pretreatment for 30 min (Ventana Medical Systems, Tucson, AZ, USA). For TCF staining, an anti-TCF4 monoclonal mouse antibody (1:50; Zytomed Systems, Berlin, Germany) was used as previously described (Kriegl et al., 2010).

Statistical analysis

For all quantitative sample comparison, Student's two-sample heteroscedastic t-test was used.

Acknowledgements

TOPflash/FOPflash constructs were kindly provided by Prof G Christophori (University of Basel, Switzerland). We thank Mirka Schmid for her expert technical assistance. We also thank Fred Indig and Sarah Subaran (Research Resources Branch of the National Institute on Aging, Baltimore, MD) for their expert assistance with the confocal imaging experiments. Funding was provided by the Swiss National Science Foundation (Project number 320030-119989, KSH and RD), the Julia Bangerter Rhyner Stiftung (RD) and the Intramural Program of the National Institute on Aging (AW).

References

Adams, C.L., Chen, Y.T., Smith, S.J., and Nelson, W.J. (1998). Mechanisms of epithelial cell-cell adhesion and cell compaction revealed by high-resolution tracking of E-cadherin-green fluorescent protein. J. Cell Biol. *142*, 1105–1119.

Alexaki, V.I., Javelaud, D., Van Kempen, L.C. et al. (2010). GLI2-mediated melanoma invasion and metastasis. J. Natl Cancer Inst. *102*, 1148–1159.

Arce, L., Yokoyama, N.N., and Waterman, M.L. (2006). Diversity of LEF/TCF action in development and disease. Oncogene *25*, 7492–7504.

Arce, L., Pate, K.T., and Waterman, M.L. (2009). Groucho binds two conserved regions of LEF-1 for HDAC-dependent repression. BMC Cancer *9*, 159.

Bachmann, I.M., Straume, O., Puntervoll, H.E., Kalvenes, M.B., and Akslen, L.A. (2005). Importance of P-cadherin, beta-catenin, and Wnt5a/frizzled for progression of melanocytic tumors and prognosis in cutaneous melanoma. Clin. Cancer Res. *11*, 8606–8614.

Bennett, D.C. (2008). How to make a melanoma: what do we know of the primary clonal events? Pigment Cell Melanoma Res. *21*, 27–38.

© 2011 John Wiley & Sons A/S

Bittner, M., Meltzer, P., Chen, Y. et al. (2000). Molecular classification of cutaneous malignant melanoma by gene expression profiling. Nature *406*, 536–540.

Brantjes, H., Barker, N., Van Es, J., and Clevers, H. (2002). TCF: lady Justice casting the final verdict on the outcome of Wnt signalling. Biol. Chem. *383*, 255–261.

Busam, K.J., Iversen, K., Coplan, K.C., and Jungbluth, A.A. (2001). Analysis of microphthalmia transcription factor expression in normal tissues and tumors, and comparison of its expression with S-100 protein, gp100, and tyrosinase in desmoplastic malignant melanoma. Am. J. Surg. Pathol. *25*, 197–204.

Carreira, S., Goodall, J., Aksan, I., La Rocca, S.A., Galibert, M.D., Denat, L., Larue, L., and Goding, C.R. (2005). Mitf cooperates with Rb1 and activates p21Cip1 expression to regulate cell cycle progression. Nature *433*, 764–769.

Carreira, S., Goodall, J., Denat, L., Rodriguez, M., Nuciforo, P., Hoek, K.S., Testori, A., Larue, L., and Goding, C.R. (2006). Mitf regulation of Dia1 controls melanoma proliferation and invasiveness. Genes Dev. *20*, 3426–3439.

Chien, A.J., Moore, E.C., Lonsdorf, A.S., Kulikauskas, R.M., Rothberg, B.G., Berger, A.J., Major, M.B., Hwang, S.T., Rimm, D.L., and Moon, R.T. (2009). Activated Wnt/beta-catenin signaling in melanoma is associated with decreased proliferation in patient tumors and a murine melanoma model. Proc. Natl. Acad. Sci. USA *106*, 1193–1198.

Clevers, H. (2006). Wnt/beta-catenin signaling in development and disease. Cell *127*, 469–480.

Clifford, R.L., Deacon, K., and Knox, A.J. (2008). Novel regulation of vascular endothelial growth factor-A (VEGF-A) by transforming growth factor (beta)1: requirement for Smads, (beta)-CATENIN, AND GSK3(beta). J. Biol. Chem. *283*, 35337–35353.

Da Forno, P.D., Pringle, J.H., Hutchinson, P., Osborn, J., Huang, Q., Potter, L., Hancox, R.A., Fletcher, A., and Saldanha, G.S. (2008). WNT5A expression increases during melanoma progression and correlates with outcome. Clin. Cancer Res. *14*, 5825–5832.

Davis, J.M. (2001). Basic Cell Culture: A Practical Approach. (Oxford: Oxford University Press).

Delmas, V., Beermann, F., Martinozzi, S. et al. (2007). Beta-catenin induces immortalization of melanocytes by suppressing p16INK4a expression and cooperates with N-Ras in melanoma development. Genes Dev. *21*, 2923–2935.

Demunter, A., Libbrecht, L., Degreef, H., De Wolf-Peeters, C., and Van Den Oord, J.J. (2002). Loss of membranous expression of beta-catenin is associated with tumor progression in cutaneous melanoma and rarely caused by exon 3 mutations. Mod. Pathol. *15*, 454–461.

Dissanayake, S.K., Wade, M., Johnson, C.E. et al. (2007). The Wnt5A/protein kinase C pathway mediates motility in melanoma cells via the inhibition of metastasis suppressors and initiation of an epithelial to mesenchymal transition. J. Biol. Chem. *282*, 17259–17271.

Dissanayake, S.K., Olkhanud, P.B., O'connell, M.P. et al. (2008). Wnt5A regulates expression of tumor-associated antigens in melanoma via changes in signal transducers and activators of transcription 3 phosphorylation. Cancer Res. *68*, 10205–10214.

Dorsky, R.I., Moon, R.T., and Raible, D.W. (1998). Control of neural crest cell fate by the Wnt signalling pathway. Nature *396*, 370–373.

Eichhoff, O.M., Zipser, M.C., Xu, M., Weeraratna, A.T., Mihic, D., Dummer, R., and Hoek, K.S. (2010). The immunohistochemistry of invasive and proliferative phenotype switching in melanoma: a case report. Melanoma Res. *20*, 349–355.

Geertsen, R.C., Hofbauer, G.F., Yue, F.Y., Manolio, S., Burg, G., and Dummer, R. (1998). Higher frequency of selective losses of HLA-A and -B allospecificities in metastasis than in primary melanoma lesions. J. Invest. Dermatol. *111*, 497–502.

Goodall, J., Martinozzi, S., Dexter, T.J., Champeval, D., Carreira, S., Larue, L., and Goding, C.R. (2004). Brn-2 expression controls melanoma proliferation and is directly regulated by beta-catenin. Mol. Cell. Biol. *24*, 2915–2922.

Haughian, J.M., Reno, E.M., Thorne, A.M., and Bradford, A.P. (2009). Protein kinase C alpha-dependent signaling mediates endometrial cancer cell growth and tumorigenesis. Int. J. Cancer *125*, 2556–2564.

Hecht, A., and Stemmler, M.P. (2003). Identification of a promoter-specific transcriptional activation domain at the C terminus of the Wnt effector protein T-cell factor 4. J. Biol. Chem. *278*, 3776–3785.

Herzig, M., Savarese, F., Novatchkova, M., Semb, H., and Christofori, G. (2007). Tumor progression induced by the loss of E-cadherin independent of beta-catenin/Tcf-mediated Wnt signaling. Oncogene *26*, 2290–2298.

Hoek, K.S., and Goding, C.R. (2010). Cancer stem cells versus phenotype-switching in melanoma. Pigment Cell Melanoma Res. *23*, 746–759.

Hoek, K.S., Schlegel, N.C., Brafford, P. et al. (2006). Metastatic potential of melanomas defined by specific gene expression profiles with no BRAF signature. Pigment Cell Res. *19*, 290–302.

Hoek, K.S., Eichhoff, O.M., Schlegel, N.C., Dobbeling, U., Kobert, N., Schaerer, L., Hemmi, S., and Dummer, R. (2008a). In vivo switching of human melanoma cells between proliferative and invasive states. Cancer Res. *68*, 650–656.

Hoek, K.S., Schlegel, N.C., Eichhoff, O.M. et al. (2008b). Novel MITF targets identified using a two-step DNA microarray strategy. Pigment Cell Melanoma Res. *21*, 665–676.

Hur, E.M., and Zhou, F.Q. (2010). SK3 signalling in neural development. Nat. Rev. Neurosci. *11*, 539–551.

Jeffs, A.R., Glover, A.C., Slobbe, L.J. et al. (2009). A gene expression signature of invasive potential in metastatic melanoma cells. PLoS ONE *4*, e8461.

Katoh, M. (2009). Transcriptional mechanisms of WNT5A based on NF-kappaB, Hedgehog, TGFbeta, and Notch signaling cascades. Int. J. Mol. Med. *23*, 763–769.

Klarmann, G.J., Decker, A., and Farrar, W.L. (2008). Epigenetic gene silencing in the Wnt pathway in breast cancer. Epigenetics *3*, 59–63.

Klaus, A., and Birchmeier, W. (2008). Wnt signalling and its impact on development and cancer. Nat. Rev. Cancer *8*, 387–398.

Korinek, V., Barker, N., Morin, P.J., Van Wichen, D., De Weger, R., Kinzler, K.W., Vogelstein, B., and Clevers, H. (1997). Constitutive transcriptional activation by a beta-catenin-Tcf complex in APC-/- colon carcinoma. Science *275*, 1784–1787.

Kriegl, L., Horst, D., Reiche, J.A., Engel, J., Kirchner, T., and Jung, A. (2010). LEF-1 and TCF4 expression correlate inversely with survival in colorectal cancer. J. Transl. Med. *8*, 123.

Kuphal, S., Poser, I., Jobin, C., Hellerbrand, C., and Bosserhoff, A.K. (2004). Loss of E-cadherin leads to upregulation of NFkappaB activity in malignant melanoma. Oncogene *23*, 8509–8519.

Larue, L., and Delmas, V. (2006). The WNT/Beta-catenin pathway in melanoma. Front. Biosci. *11*, 733–742.

Larue, L., Kumasaka, M., and Goding, C.R. (2003). Beta-catenin in the melanocyte lineage. Pigment Cell Res. *16*, 312–317.

Levy, C., Khaled, M., and Fisher, D.E. (2006). MITF: master regulator of melanocyte development and melanoma oncogene. Trends Mol. Med. *12*, 406–414.

Loercher, A.E., Tank, E.M., Delston, R.B., and Harbour, J.W. (2005). MITF links differentiation with cell cycle arrest in melanocytes by transcriptional activation of INK4A. J. Cell Biol. *168*, 35–40.

© 2011 John Wiley & Sons A/S

Ma, C., Wang, J., Gao, Y., Gao, T.W., Chen, G., Bower, K.A., Odetallah, M., Ding, M., Ke, Z., and Luo, J. (2007). The role of glycogen synthase kinase 3beta in the transformation of epidermal cells. Cancer Res. *67*, 7756–7764.

Mikesch, J.H., Steffen, B., Berdel, W.E., Serve, H., and Muller-Tidow, C. (2007). The emerging role of Wnt signaling in the pathogenesis of acute myeloid leukemia. Leukemia *21*, 1638–1647.

Nelson, W.J., and Nusse, R. (2004). Convergence of Wnt, beta-catenin, and cadherin pathways. Science *303*, 1483–1487.

Novak, A., and Dedhar, S. (1999). Signaling through beta-catenin and Lef/Tcf. Cell. Mol. Life Sci. *56*, 523–537.

O'connell, M.P., Fiori, J.L., Baugher, K.M. et al. (2009). Wnt5A activates the calpain-mediated cleavage of filamin A. J. Invest. Dermatol. *129*, 1782–1789.

Reifenberger, J., Knobbe, C.B., Wolter, M., Blaschke, B., Schulte, K.W., Pietsch, T., Ruzicka, T., and Reifenberger, G. (2002). Molecular genetic analysis of malignant melanomas for aberrations of the WNT signaling pathway genes CTNNB1, APC, ICAT and BTRC. Int. J. Cancer *100*, 549–556.

Rimm, D.L., Caca, K., Hu, G., Harrison, F.B., and Fearon, E.R. (1999). Frequent nuclear/cytoplasmic localization of beta-catenin without exon 3 mutations in malignant melanoma. Am. J. Pathol. *154*, 325–329.

Robinson, D.R., Zylstra, C.R., and Williams, B.O. (2008). Wnt signaling and prostate cancer. Curr. Drug Targets *9*, 571–580.

Schepsky, A., Bruser, K., Gunnarsson, G.J., Goodall, J., Hallsson, J.H., Goding, C.R., Steingrimsson, E., and Hecht, A. (2006). The microphthalmia-associated transcription factor Mitf interacts with beta-catenin to determine target gene expression. Mol. Cell. Biol. *26*, 8914–8927.

Segditsas, S., and Tomlinson, I. (2006). Colorectal cancer and genetic alterations in the Wnt pathway. Oncogene *25*, 7531–7537.

Shin, S.Y., Yoon, S.C., Kim, Y.H., Kim, Y.S., and Lee, Y.H. (2002). Phosphorylation of glycogen synthase kinase-3beta at serine-9 by phospholipase Cgamma1 through protein kinase C in rat 3Y1 fibroblasts. Exp. Mol. Med. *34*, 444–450.

Smith, A.P., Hoek, K., and Becker, D. (2005). Whole-genome expression profiling of the melanoma progression pathway reveals marked molecular differences between nevi/melanoma in situ and advanced-stage melanomas. Cancer Biol. Ther. *4*, 1018–1029.

Steingrimsson, E., Copeland, N.G., and Jenkins, N.A. (2004). Melanocytes and the microphthalmia transcription factor network. Annu. Rev. Genet. *38*, 365–411.

Takeda, K., Yasumoto, K., Takada, R., Takada, S., Watanabe, K., Udono, T., Saito, H., Takahashi, K., and Shibahara, S. (2000). Induction of melanocyte-specific microphthalmia-associated transcription factor by Wnt-3a. J. Biol. Chem. *275*, 14013–14016.

Takigawa, Y., and Brown, A.M. (2008). Wnt signaling in liver cancer. Curr. Drug Targets *9*, 1013–1024.

Vance, K.W., and Goding, C.R. (2004). The transcription network regulating melanocyte development and melanoma. Pigment Cell Res. *17*, 318–325.

Weeraratna, A.T., Jiang, Y., Hostetter, G., Rosenblatt, K., Duray, P., Bittner, M., and Trent, J.M. (2002). Wnt5a signaling directly affects cell motility and invasion of metastatic melanoma. Cancer Cell *1*, 279–288.

Widlund, H.R., Horstmann, M.A., Price, E.R., Cui, J., Lessnick, S.L., Wu, M., He, X., and Fisher, D.E. (2002). {beta}-Catenin-induced melanoma growth requires the downstream target Microphthalmia-associated transcription factor. J. Cell Biol. *158*, 1079–1087.

Yasumoto, K., Takeda, K., Saito, H., Watanabe, K., Takahashi, K., and Shibahara, S. (2002). Microphthalmia-associated transcription factor interacts with LEF-1, a mediator of Wnt signaling. EMBO J. *21*, 2703–2714.

Zipser, M.C., Eichhoff, O.M., Widmer, D.S. et al. (2011). A proliferative melanoma cell phenotype is responsive to RAF/MEK inhibition independent of BRAF mutation status. Pigment Cell Melanoma Res. *24*, 326–333.

Supporting information

Additional Supporting Information may be found in the online version of this article:

Figure S1. In vitro phenotype-specific melanoma cell morphology.

Figure S2. Phenotype-specific expression patterns for LEF/TCF factors in melanoma.

Figure S3. Knock-down controls.

Figure S4. WNT5A regulates cytoskeletal organization and β-catenin cellular distribution.

Figure S5. Phenotype-specific localization of β-catenin.

Figure S6. Densitometry analyses.

Figure S7. Control experiments.

Figure S8. Lef-1 suppression of TCF4 and WNT5A expression.

Please note: Wiley-Blackwell are not responsible for the content or functionality of any supporting materials supplied by the authors. Any queries (other than missing material) should be directed to the corresponding author for the article.

Finally, it should be understood that TCF4 as cited in this work refers to the product of the gene located at chromosome 10q25.3 which now has the formal designation of TCF7L2 and should not be confused with an unrelated bHLH factor also called TCF4.

© 2011 John Wiley & Sons A/S

5.5 A proliferative melanoma cell phenotype is responsive to RAF/MEK inhibition independent of BRAF mutation status

Because of the high number of melanoma tumors harboring an activating mutation in the MAPK pathway, therapies that target tyrosine kinases in the MAPK pathway have become increasingly popular in recent years. Unfortunately, the initially good response to these drugs is followed by a relapse in almost all patients. This study tested the response of proliferative and invasive cell cultures to two unspecific tyrosine kinase inhibitors. Surprisingly, the response was not only dependent on the mutation status of the cells but also on the phenotype, suggesting an adaptation of the treatment in a way that all subpopulations of melanoma cells are targeted.

I contributed to this study by performing experiments for the characterization of the cell cultures and confirming the cell culture phenotypes. Also, I contributed to phenotype prediction of the cell cultures based on gene expression data and by participating in experiment planning and discussions.

This study was published in *Pigment Cell & Melanoma Research*

A proliferative melanoma cell phenotype is responsive to RAF/MEK inhibition independent of BRAF mutation status

Marie C. Zipser[1,*], Ossia M. Eichhoff[1,*], Daniel S. Widmer[1], Natalie C. Schlegel[2], Nicola L. Schoenewolf[1], Darrin Stuart[3], Weihua Liu[4], Humphrey Gardner[4], Paul D. Smith[5], Paolo Nuciforo[6], Reinhard Dummer[1] and Keith S. Hoek[1]

1 Department of Dermatology, University Hospital of Zurich, Zurich, Switzerland **2** Department of Biomedicine, University of Basel, Basel, Switzerland **3** Oncology Disease Area, Novartis Institutes for BioMedical Research, Emeryville, CA, USA **4** Novartis Institutes for BioMedical Research, Cambridge, MA, USA **5** Cancer and Infection Research Area, AstraZeneca, Alderley Park, Macclesfield, UK **6** Oncology Translational Laboratories, Molecular Pathology, Novartis Pharma, Basel, Switzerland

CORRESPONDENCE Keith Hoek, e-mail: keith.hoek@usz.ch
*These authors contributed equally.

KEYWORDS melanoma/phenotype switching/MAPK inhibition

PUBLICATION DATA Received 6 August 2010, revised and accepted for publication 17 December 2010, published online 22 December 2010

doi: 10.1111/j.1755-148X.2010.00823.x

Summary

Oncogenic mutations within the MAPK pathway are frequent in melanoma, and targeting of MAPK signaling has yielded spectacular responses in a significant number of patients that last for several months before relapsing. We investigated the effects of two different inhibitors of MAPK signaling in proliferative and invasive melanoma cell cultures with various mutations in the MAPK pathway. Proliferative melanoma cells were more susceptible to pathway inhibition than invasive phenotype cells, irrespective of BRAF mutation status, while invasive phenotype cell response was dependent on BRAF mutation status. Critically, MAPK pathway inhibition of proliferative phenotype cells resulted in acquisition of invasive phenotype characteristics. These results show that melanoma cell phenotype is an important factor in MAPK pathway inhibition response. This suggests that while current therapeutic strategies target proliferative melanoma cells, future approaches should also account for the invasive phenotype population.

Introduction

Melanoma is a heterogeneous malignancy whose cells may present with any of a range of distinct molecular profiles. For example, the mitogen-activated protein kinase (MAPK) pathway is frequently activated in melanoma by RAS/RAF gene mutations (Curtin et al., 2005; Thomas et al., 2007; Davies et al., 2002; Smalley and Flaherty, 2009). This pathway responds to receptor tyrosine kinases including receptors for epidermal and vascular endothelial growth factors (Fecher et al., 2008) and regulates melanoma cell proliferation, survival, and migration. Activating mutations in MAPK pathway kinases account for increases in melanoma cell proliferation and resistance to apoptosis (Russo et al., 2009), and this renders melanoma a viable target for MAPK

Significance

Recent trials with MAPK inhibitors have shown promising results in many patients with metastatic melanoma; however, nearly all responding patients experience disease relapse. We describe here how melanoma cells respond to MAPK inhibition in a phenotype-specific manner, suggesting that slow-cycling invasive phenotype cells provide a treatment-resistant pool from which disease relapse may be derived. The implication is that while MAPK inhibition may successfully treat proliferating cells, another cell population needs to be addressed at the same time.

© 2011 John Wiley & Sons A/S

pathway-specific drugs. Critically, a significant number of patients have been shown to respond, sometimes profoundly, to such treatment. However, nearly all responding patients relapse within 1 yr. The development of resistance can be explained in part by the occurrence of new mutations as reported for MEK (Dhomen and Marais, 2009; Eggermont et al., 2009; Smalley and Flaherty, 2009; Davies et al., 2002; Emery et al., 2009; Flaherty et al., 2010).

We recently proposed a phenotype switching model of melanoma progression. This model identifies two opposing types of melanoma cell, characterized by gene expression profiling and other in vitro analyses (Hoek et al., 2006), which are distinguished by one being proliferative and the other invasive in phenotype (Hoek et al., 2008). The model hypothesizes that melanoma cells switch between proliferative and invasive states and so drive repeated tumorigenic and disseminating phases of disease progression. We investigated the effects of treating melanoma cells with MAPK pathway inhibitors in the context of both the phenotype switching model and BRAF mutational status.

Results

Genotype inconsistencies between tissue and culture

We investigated gene mutations in melanoma material derived from 14 patients using both short-term cultures derived from primary lesions and metastases of melanoma as well as (in ten cases) corresponding paraffin-embedded tumor material. All mutations detected were restricted to MAPK pathway components including EGFR, H-RAS, N-RAS, K-RAS and BRAF. Interestingly, while six cell culture/biopsy pairs (60%) showed faithful reproduction of their gene mutation profiles, four culture/biopsy pairs (40%) did not (Table 1).

Gene expression signatures of melanoma proliferation, invasion, and Matrigel surface organization

By examining the expression of 105 specific genes (Table S1), we assessed the gene expression profile of melanoma cell cultures to predict phenotype according to methods our group established (Hoek et al., 2006) and identified six cultures, which correlated with the proliferative signature and eight, which correlated with the invasive signature (Figure 1). As we previously identified (Hoek et al., 2006), phenotype-specific expression signatures show no significant relationship with the mutation status of the genes we tested (Table 1). At the same time, we confirm that melanoma cells do show signature-specific characteristics (phenotypes) of proliferation, invasion as well as MITF and fibronectin expression (Figures 2A,B,C). However, for the first time we show that cultured melanoma cells display phenotype-specific organizational characteristics when seeded on a basement membrane-like matrix. Specifically, proliferative phenotype cells formed small and isolated clusters, while invasive phenotype cells formed connected networks or aggregates (Figure 3).

Phenotype-specific responses to MAPK pathway inhibition

In proliferative phenotype melanoma cells, MAPK pathway inhibition reduced proliferation by as much as 80% independently of BRAF mutation status. In contrast, invasive phenotype cells were significantly more resistant (Figure 4A,B). Furthermore, invasive phenotype cell susceptibility to RAF265 (and to a lesser degree AZD6244, data not shown) varied between BRAF mutant and wild-type cells, with BRAF mutants being more susceptible (Figure 4C). In contrast, we found that proliferative and invasive phenotype cells were equally susceptible to treatment with the receptor tyrosine kinase inhibitor TKI258 (Figure 4D).

Proliferative to invasive phenotype switching induced by MAPK inhibition

We found that treatment of proliferative phenotype cells with MAPK inhibitors induced, in addition to growth rate reduction, MITF down-regulation. Furthermore, MAPK inhibitor-treated proliferative phenotype cells (regardless of BRAF mutant status) adopted an invasive phenotype organization when seeded on basement membrane matrix (Figure 5A). Interestingly, when the inhibitor was removed from growth medium the cells soon reverted back to their proliferative phenotype behavior (Figure 5A). Additionally, MITF activity is critical for determining melanoma cell phenotype (Carreira et al., 2006) and Western blot experiments show that MITF-target melan-A expression was down-regulated by MAPK inhibitor treatment in a dose-dependent manner but this returned to normal levels after cells were removed from inhibitor (Figure 5B). However, while there was a trend toward increased in vitro invasiveness, in some samples this was not significant (data not shown).

Discussion

The observation that cell culture genotype is not always the same as that of the tissue suggests intralesional heterogeneity. This mirrors a study, which found that within-nevi melanocytes are heterogeneous for the BRAF mutation (Lin et al., 2009). The implication is that the mutations are not always founder events but may also be driven by host-specific conditions and, as was recently published, therapy (Emery et al., 2009).

In previous publications, our laboratory introduced the hypothesis that melanoma progression is driven by cells switching between phenotypes of proliferation and invasion (Hoek et al., 2006, 2008). The earlier study found no correlation between BRAF and NRAS mutation status and the gene signatures, which were associated with

© 2011 John Wiley & Sons A/S

Table 1. Cell culture origin and characterization

								Cell culture			Paraffin material		
Patient	Sex	Age	Primary type	Culture	Culture origin	TNM stage at culture	Phenotype	BRAF	NRAS	Other	BRAF status	NRAS status	Others
1	F	29	SSM	M980513	Lymph node metastasis iliacal	T2aN3M1c	Proliferative	V600E	wt	HRAS (Q61K)	V600E	wt	–
2	F	37	n.a.	M010817	Skin metastasis left upper arm	TxN1bM1c	Proliferative	wt	Q61R	–	wt	Q61R	–
3	M	39	NM	M050829	Skin metastasis retroauricular right	T3aN3M0	Proliferative	wt	Q61L	–	wt	Q61L	–
4	F	52	Amelanotic	M000921	Epigastric metastasis	TxNxM1c	Proliferative	V600E	wt	–	V600E	wt	–
5	F	65	NM	M080423	Lymph node metastasis hepatoduodenal	T3bN1aM1a	Proliferative	wt	G12D	–	wt	G12D	–
6	M	57	NM	M080326	Primary plantar	T4bN2aM0	Proliferative	V600E	wt	–	V600E	wt	–
7	M	51	SSM	M080306	Primary capillitium	T2N1bM0	Invasive	wt	wt	–	wt	wt	HRAS (Q61K)
8	M	72	NM	M061103	Skin metastasis capillitium	T4N1bM0	Invasive	wt	wt	HRAS (Q61K)	wt	wt	EGFR (G719S) KRAS (G12S) HRAS (Q61K)
9	F	51	n.a.	M060125	Skin metastasis scapula	TxNxM1c	Invasive	V600E	wt	HRAS (Q61K)	n.a.	n.a.	n.a.
10	M	73	NM	M010119	Skin metastasis shoulder	T2bN3M0	Invasive	L597S	wt	–	L597S	wt	–
11	M	78	LMM	M081008	Primary face	T1aN0M0	Invasive	wt	wt	–	n.a.	n.a.	n.a.
12	M	55	SSM	M080307	Soft tissue metastasis axilla	T4N2M1c	Invasive	wt	wt	HRAS (Q61K)	V600K	wt	–
13	n.a.	n.a.	n.a.	MaMel45a	n.a.	n.a.	Invasive	V600E	wt	n.a.	n.a.	n.a.	n.a.
14	n.a.	n.a.	n.a.	MaMel06	n.a.	n.a.	Invasive	V600E	wt	n.a.	n.a.	n.a.	n.a.

F, female; M, male; SSM, superficial spreading melanoma; NM, nodular melanoma; LMM, lentigo maligna melanoma; n.a., not applicable.

© 2011 John Wiley & Sons A/S

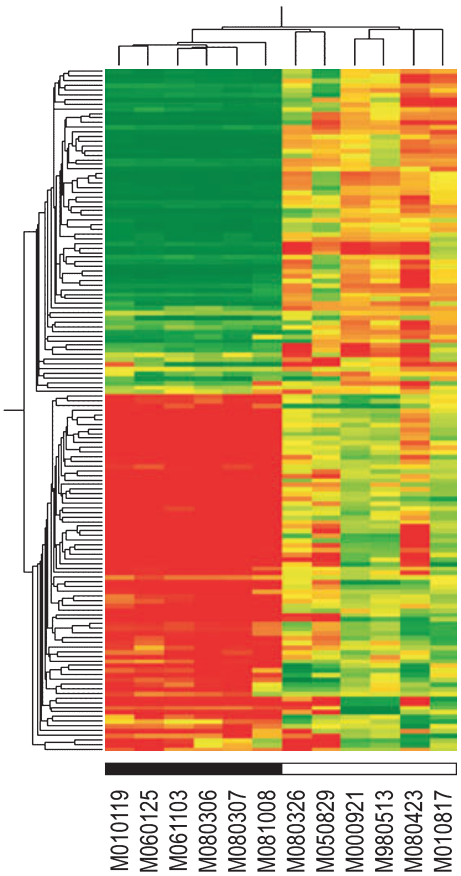

Figure 1. DNA microarray analysis to predict phenotype. Normalized signal intensity data for 105 genes (Supplementary Table 1), previously identified as showing phenotype-specific gene expression patterns (Hoek et al., 2006), were used to cluster samples into predicted proliferative (black bar) and invasive (white bar) phenotype groups.

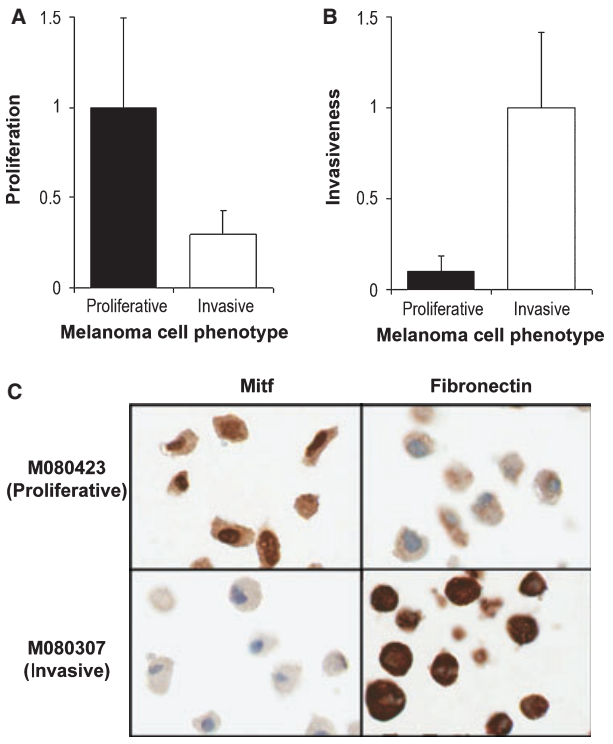

Figure 2. In vitro appearance and functional behaviors of proliferative and invasive phenotype melanoma cell cultures. (A) Proliferative phenotype cells proliferate significantly faster ($P < 0.001$) than invasive phenotype cells. The values are the mean of six different proliferative phenotype cultures relative to the mean of eight different invasive phenotype cultures. The error bars represent the standard deviation of the data. (B) Invasion was significantly lower in proliferative phenotype cells than in invasive phenotype cells ($P < 0.002$). The values are the mean of six different proliferative phenotype cultures relative to the mean of eight different invasive phenotype cultures. The error bars represent the standard deviation of the data. (C) Representational immunostaining of cultured proliferative and invasive phenotype cells for MITF and fibronectin showing phenotype-specific expression patterns for these factors.

phenotype, and we confirm this lack of correlation here. Interestingly, in addition to confirming the association between gene expression and characteristics of proliferation and invasion, we uncovered a correlation between gene expression and the capacity to form cellular networks on a basement membrane-like matrix. This network formation by invasive phenotype cells is reminiscent of the behavior previously described for invasive melanoma cell lines (e.g. C8161) and interpreted by others as vascular mimicry behavior (Hendrix et al., 2002, 2003). In previous experiments, we injected phenotypes subcutaneously into the flanks of nude mice and made two critical observations: first, while proliferative phenotype cells initiate tumorigenesis relatively quickly, it takes weeks for invasive phenotype cells to do the same; and second, no matter which phenotype was used, the end-state tumors contained cells of both phenotype, indicating that switching had occurred (Hoek et al., 2008). Together our combined findings continue to support two distinct states, which melanoma cells may switch between to drive metastatic progression of the disease.

While BRAF/NRAS mutation status was phenotype independent, we were still interested in the response of these phenotypes to MAPK pathway inhibitors. The identification of distinct phenotypic differences among melanoma cells (Hoek et al., 2006) and the discovery of their capacity to switch between these phenotypes, as monitored by observing immunohistochemical staining pattern changes of MITF, which is tightly specific for the proliferative phenotype (Hoek et al., 2008; Eichhoff et al., 2010), suggested to us a possible explanation for relapse from initially successful MAPK pathway inhibition therapy.

That proliferative phenotype cells are significantly more susceptible to MAPK pathway inhibition is a striking finding which, in the light of the phenotype switching model, suggests that while proliferative phenotype cells within metastases are suitably susceptible to

© 2011 John Wiley & Sons A/S

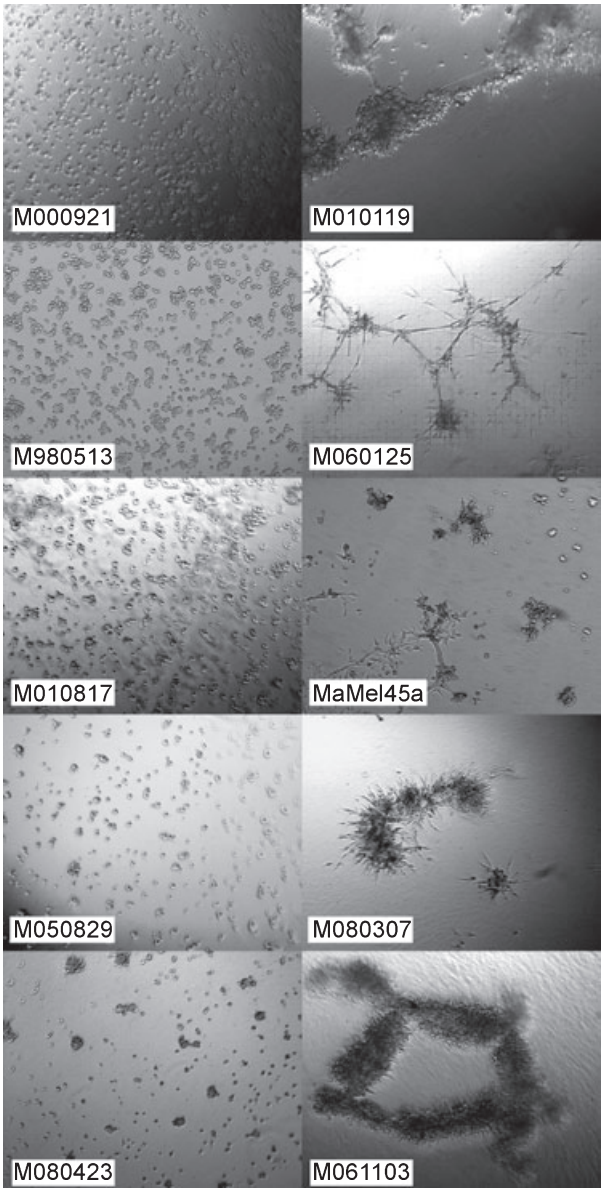

Figure 3. Phenotype-specific Matrigel surface organization. Despite identical growth conditions, melanoma cells display phenotype-specific organizational characteristics when seeded on a basement membrane-like matrix. Specifically, proliferative phenotype cells (e.g. M980513) adopted an organization of small and isolated clusters, while invasive phenotype cells (e.g. M081008) formed connected networks.

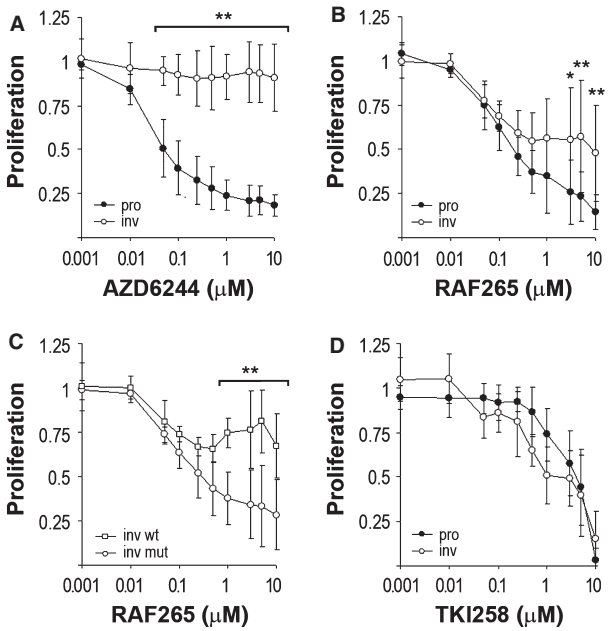

Figure 4. Kinase inhibitor treatment of proliferative and invasive phenotype cells. (A and B) Invasive phenotype cells (8 different patient samples) were less responsive to either AZD6244 or RAF265 than proliferative phenotype cells (six different patient samples). (C) Within the invasive phenotype, BRAF-mutated cells (four different patient samples) were more susceptible to treatment with RAF265 compared to BRAF wild type cells (four different patient samples). (D) Proliferative (six different patient samples) and invasive (five different patient samples) phenotype cells did not show any differences in proliferation response to treatment with TKI258. Error bars represent standard deviation. One asterisk (*) denotes $P < 0.05$, while two asterisks (**) denote $P < 0.01$.

inhibitor treatments (and probably reflect observed tumor mass reductions), invasive phenotype cells largely survive treatment to permit later relapse and continued disease progression. Supporting this, we note a recent study conducted by other researchers who used PLX4032 (specific for mutant BRAF) against a range of cell lines for which they had also obtained gene expression profiling data (Tap et al., 2010). Like us, they found that samples with a melanocytic gene signature were significantly more susceptible to inhibition, although they did not make the connection this has with melanoma cell phenotype switching. Interestingly, we found that inhibitor response in invasive phenotype samples was dependent upon whether BRAF was wild type or mutated. It has been shown that such a response difference is because of the higher affinity of RAF265 for mutant BRAF (Mordant et al., 2010), and this is also supported by the PLX4032 study (Tap et al., 2010). However, the BRAF mutation status dependency of invasive phenotype cell response contrasts with the absence of a similar dependency in proliferative phenotype samples. Why this may be so is not yet clear.

While no previous study investigating MAPK pathway inhibitors has acknowledged a melanoma cell phenotype switching context, there have been some interesting results. Haass et al. (2008) assessed tumor cell proliferation with AZD6244 in nine melanoma cell lines (five BRAF wild type and four $BRAF^{V600E}$), finding that AZD6244 was more effective against $BRAF^{V600E}$ melanoma lines. Hoeflich et al. (2009) investigated seventeen melanoma cell lines and their response to treatment with GDC-0879, a specific RAF inhibitor,

© 2011 John Wiley & Sons A/S

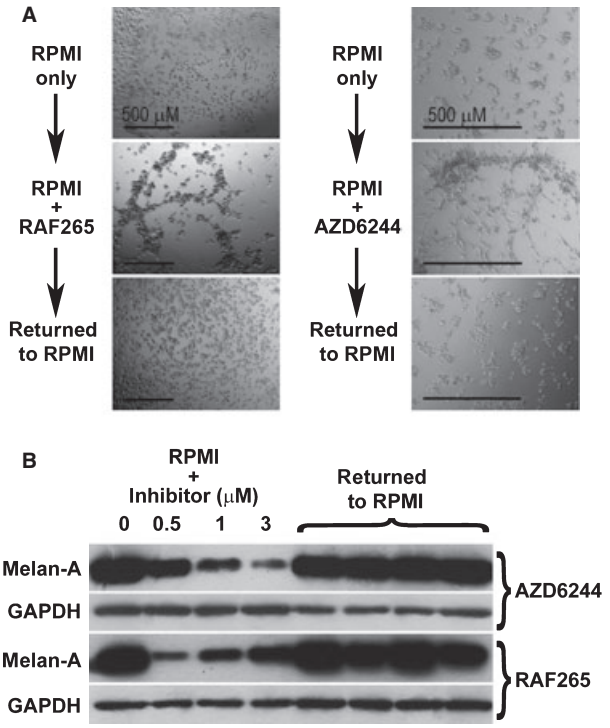

Figure 5. Phenotype switching under MAPK inhibition. (A) After 2 weeks of treatment in RPMI complete medium with RAF265 or AZD6244, cells acquired invasive phenotype organizational characteristics on basement membrane-like matrix when compared to RPMI controls. Original (proliferative phenotype) patterning was restored after 2 weeks in RPMI without RAF265. (B) Melan-A expression was significantly down-regulated by treating proliferative phenotype cells with AZD6244 or RAF265. Original melan-A expression levels were returned after 2 weeks in RPMI without RAF265.

reporting that $BRAF^{V600E}$ mutation predicts higher sensitivity of melanoma cell lines to the RAF inhibitor. Sondergaard et al. (2010), using the specific RAF inhibitor PLX4032, described that while BRAF wild types were resistant to treatment there was differential sensitivity to the drug within the $BRAF^{V600E}$ subset of melanoma lines they used. These studies all showed variation in inhibitor response, even within BRAF mutant subsets. We speculate that the differentiation of the cultures these groups used into proliferative and invasive phenotypes may resolve at least some of the observed variation.

In contrast to the MAPK inhibitor treatments, TKI258 treatment was equally effective against the phenotypes. However, this may be explained by its capacity to target a wider variety of different receptors including those for fibroblast, vascular endothelial and platelet-derived growth factors. However, having a broader target molecule population for a drug is often correlated with increased drug-related side effects and while at least one clinical safety trial has been completed in melanoma patients, the results had not yet been made public at the time this manuscript was submitted (ClinicalTrials.gov Identifier NCT00303251).

The observation that proliferative cells responded to MAPK inhibition by down-regulating MITF activity and reducing proliferation agrees with other studies showing that suppression of both MITF and BRAF inhibits proliferation (Kido et al., 2009). However, we also found that MAPK inhibition of proliferative cells induced invasive phenotype-like organization when the cells were plated onto a basement membrane-like matrix. Additional gene expression analyses showed that treated proliferative phenotype cells expressed a gene signature, which strongly resembled that of invasive phenotype cells (data not shown). This leads us to speculate that switching from a proliferative phenotype to an invasive one may be facilitated by a reduction in MAPK signaling.

The differential susceptibility of melanoma cell phenotypes to MAPK inhibition and the apparent relationship between MAPK signaling and phenotype switching has potential relevance to clinical therapy. Interpretation of our findings in the context of the phenotype switching model for melanoma progression agrees that MAPK inhibitor-based treatments would initially drive disease stabilization and regression. However, we also suggest that invasive phenotype cells could be much less affected (and perhaps even increased in number). Surviving invasive phenotype cells, providing a pool from which cells carrying resistance mutations could arise, would be free to later switch back to the proliferative phenotype and precipitate relapse of disease, contributing to the limited response duration, which has been observed in several clinical trials.

Methods

Cell culture and media

Surplus material from cutaneous melanoma and melanoma metastases removed by surgery were obtained after written informed consent approved by the local IRB (EK647 and EK800). Clinical diagnosis was confirmed by histology and immunohistochemistry. Melanoma cells were released from tissue sections and grown as previously described (Geertsen et al., 1998). Patient origin was confirmed through genotyping of patient-derived paraffin-embedded tissues and peripheral blood mononuclear cells using 11 different gene loci (AmpFlSTR SGM Plus PCR Amplification Kit; Applied Biosystems, Foster City, CA, USA).

Genotyping

DNA was extracted from each cell culture and paraffin punch using a QIAamp DNA Mini kit (Qiagen, Valencia, CA, USA). OncoCarta™ Panel v1.0 workflow was used to investigate 238 known mutations in 19 oncogenes using a PCR and primer extension method followed by mass spectrometry readout (Sequenom, San Diego, CA, USA). The oncogenes were ABL1, AKT1, AKT2, BRAF, CDK, EGFR, ERBB2, FGFR1, FGFR3, FLT3, HRAS, JAK2, KIT, KRAS, MET, NRAS, PDGFRA, PIK3CA, and RET, the full list of mutations investigated is available for download from the Sequenom website (http://www.sequenom.com/OncoCarta).

© 2011 John Wiley & Sons A/S

Gene expression profiling

Melanoma cell culture RNA extraction and gene expression profiling, including normalization and analyses, were performed as previously described (Hoek et al., 2006). Phenotype-specific profile identification was performed by hierarchically clustering sample data using 105 genes previously established to show melanoma phenotype-specific expression patterns (Hoek et al., 2006). Cultures with profiles not clearly assignable to either proliferative or invasive signatures (i.e. their profiles were intermediate-type) were not selected.

In vitro invasion and proliferation assays

For invasion analyses, cells were seeded on 8-μm pore PET filters with a uniform layer of BD Matrigel™ basement membrane matrix (BD Biosciences, Heidelberg, Germany). RPMI containing 10% FCS was used as chemoattractant. After 22 h of incubation, the membrane was stained using a standard H&E protocol, and cells were counted under a light microscope. Invasion values were calculated by dividing the number of cells migrating through matrix-coated inserts by the number of cells migrating through uncoated inserts. For the proliferation assay, melanoma cells were seeded to a density of 2×10^4 cells in each well of a twenty-four-well plate. After 96 h, proliferation was estimated using a colorimetric (MTT) assay. To assess proliferation during treatment with MAPK pathway targeting inhibitors, cells were seeded in order to achieve confluency after 96 h (up to 4×10^4 cells) in triplicate. After 24 h, cells were treated with RPMI complete containing AZD6244 (Astra Zeneca, Mereside, UK), RAF265 (Novartis, Basel, Switzerland) or multitargeted receptor tyrosine kinase inhibitor TKI258 (Novartis) at various concentrations (1 nM–10 μM). Proliferation was measured using MTT assay after a further 72 h.

Matrigel surface organization

Empty 48-well plates were coated with Matrigel™ and seeded with 4×10^4 melanoma cells in 400 μl of RPMI complete medium. Cell morphology and organization were assessed using phase contrast microscopy after incubation for 24 h.

Western blotting

Cells were washed twice with cold phosphate-buffered saline (PBS) and lysed at 4°C in lysis buffer containing 20 mM Tris–HCl (pH 7.5), 1% Triton X-100 (Sigma-Aldrich, St Louis, MO, USA), 137 mM NaCl, 10% glycerol and protease inhibitors (Roche, Basel, Switzerland). Proteins were separated by SDS–PAGE under reducing conditions and then transferred onto nitrocellulose membranes (Invitrogen, Basel, Switzerland). Membranes were probed with a mouse anti-melan-A monoclonal antibody (Abcam, Cambridge, UK) followed by horseradish peroxidase-conjugated rabbit anti-mouse secondary antibody (Bio-Rad, Reinach, Switzerland). Bound antibodies were detected by chemiluminescence (ECL; GE Healthcare, Buckinghamshire, UK).

Statistical analyses

For all quantitative sample comparisons, PRISM (GraphPad Software, La Jolla, CA) was used to perform two-way ANOVA.

Acknowledgements

Funding was provided by the Swiss National Science Foundation (Project number 320030-119989, KH and RD) and the Gottfried und Julia Bangerter Rhyner Stiftung (RD). Melanoma lines MaMel45a and MaMel06 were kindly provided by Prof. Dr Dirk Schadendorf (Essen, Germany). RAF265 and TKI258 were provided by Novartis (Basel, Switzerland), and AZD6244/ARRY-142886 was provided by Astra-Zeneca (Macclesfield, UK).

References

Carreira, S., Goodall, J., Denat, L., Rodriguez, M., Nuciforo, P., Hoek, K.S., Testori, A., Larue, L., and Goding, C.R. (2006). Mitf regulation of Dia1 controls melanoma proliferation and invasiveness. Genes Dev. *20*, 3426–3439.

Curtin, J.A., Fridlyand, J., Kageshita, T. et al. (2005). Distinct sets of genetic alterations in melanoma. N. Engl. J. Med. *353*, 2135–2147.

Davies, H., Bignell, G.R., Cox, C. et al. (2002). Mutations of the BRAF gene in human cancer. Nature *417*, 949–954.

Dhomen, N., and Marais, R. (2009). BRAF signaling and targeted therapies in melanoma. Hematol. Oncol. Clin. North Am. *23*, 529–545.

Eggermont, A.M., Testori, A., Marsden, J., Hersey, P., Quirt, I., Petrella, T., Gogas, H., MacKie, R.M., and Hauschild, A. (2009). Utility of adjuvant systemic therapy in melanoma. Ann. Oncol., *20*(Suppl 6), vi30–vi34.

Eichhoff, O.M., Zipser, M.C., Xu, M., Weeraratna, A.T., Mihic, D., Dummer, R., and Hoek, K.S. (2010). The immunohistochemistry of invasive and proliferative phenotype switching in melanoma: a case report. Melanoma Res. *20*, 349–355.

Emery, C.M., Vijayendran, K.G., Zipser, M.C. et al. (2009). MEK1 mutations confer resistance to MEK and B-RAF inhibition. Proc. Natl. Acad. Sci. U S A *106*, 20411–20416.

Fecher, L.A., Amaravadi, R.K., and Flaherty, K.T. (2008). The MAPK pathway in melanoma. Curr. Opin. Oncol. *20*, 183–189.

Flaherty, K.T., Puzanov, I., Kim, K.B. et al. (2010). Inhibition of mutated, activated BRAF in metastatic melanoma. N. Engl. J. Med. *363*, 809–819.

Geertsen, R.C., Hofbauer, G.F., Yue, F.Y., Manolio, S., Burg, G., and Dummer, R. (1998). Higher frequency of selective losses of HLA-A and -B allospecificities in metastasis than in primary melanoma lesions. J. Invest. Dermatol. *111*, 497–502.

Haass, N.K., Sproesser, K., Nguyen, T.K., Contractor, R., Medina, C.A., Nathanson, K.L., Herlyn, M., and Smalley, K.S. (2008). The mitogen-activated protein/extracellular signal-regulated kinase kinase inhibitor AZD6244 (ARRY-142886) induces growth arrest in melanoma cells and tumor regression when combined with docetaxel. Clin. Cancer Res. *14*, 230–239.

Hendrix, M.J., Seftor, R.E., Seftor, E.A., Gruman, L.M., Lee, L.M., Nickoloff, B.J., Miele, L., Sheriff, D.D., and Schatteman, G.C. (2002). Transendothelial function of human metastatic melanoma cells: role of the microenvironment in cell-fate determination. Cancer Res. *62*, 665–668.

Hendrix, M.J., Seftor, E.A., Hess, A.R., and Seftor, R.E. (2003). Vasculogenic mimicry and tumour-cell plasticity: lessons from melanoma. Nat. Rev. Cancer *3*, 411–421.

Hoeflich, K.P., Herter, S., Tien, J. et al. (2009). Antitumor efficacy of the novel RAF inhibitor GDC-0879 is predicted by BRAFV600E mutational status and sustained extracellular signal-regulated kinase/mitogen-activated protein kinase pathway suppression. Cancer Res. *69*, 3042–3051.

Hoek, K.S., Schlegel, N.C., Brafford, P. et al. (2006). Metastatic potential of melanomas defined by specific gene expression profiles with no BRAF signature. Pigment Cell Res. *19*, 290–302.

Hoek, K.S., Eichhoff, O.M., Schlegel, N.C., Dobbeling, U., Kobert, N., Schaerer, L., Hemmi, S., and Dummer, R. (2008). In vivo switching of human melanoma cells between proliferative and invasive states. Cancer Res. *68*, 650–656.

Kido, K., Sumimoto, H., Asada, S., Okada, S.M., Yaguchi, T., Kawamura, N., Miyagishi, M., Saida, T., and Kawakami, Y.

© 2011 John Wiley & Sons A/S

(2009). Simultaneous suppression of MITF and BRAF V600E enhanced inhibition of melanoma cell proliferation. Cancer Sci. *100*, 1863–1869.

Lin, J., Takata, M., Murata, H., Goto, Y., Kido, K., Ferrone, S., and Saida, T. (2009). Polyclonality of BRAF mutations in acquired melanocytic nevi. J. Natl Cancer Inst. *101*, 1423–1427.

Mordant, P., Loriot, Y., Leteur, C., Calderaro, J., Bourhis, J., Wislez, M., Soria, J.C., and Deutsch, E. (2010). Dependence on phosphoinositide 3-kinase and RAS-RAF pathways drive the activity of RAF265, a novel RAF/VEGFR2 inhibitor, and RAD001 (Everolimus) in combination. Mol. Cancer Ther. *9*, 358–368.

Russo, A.E., Torrisi, E., Bevelacqua, Y., Perrotta, R., Libra, M., McCubrey, J.A., Spandidos, D.A., Stivala, F., and Malaponte, G. (2009). Melanoma: Molecular pathogenesis and emerging target therapies (Review). Int. J. Oncol. *34*, 1481–1489.

Smalley, K.S., and Flaherty, K.T. (2009). Integrating BRAF/MEK inhibitors into combination therapy for melanoma. Br. J. Cancer *100*, 431–435.

Sondergaard, J.N., Nazarian, R., Wang, Q. et al. (2010). Differential sensitivity of melanoma cell lines with BRAFV600E mutation to the specific Raf inhibitor PLX4032. J. Transl. Med. *8*, 39.

Tap, W.D., Gong, K.W., Dering, J. et al. (2010). Pharmacodynamic characterization of the efficacy signals due to selective BRAF inhibition with PLX4032 in malignant melanoma. Neoplasia *12*, 637–649.

Thomas, R.K., Baker, A.C., Debiasi, R.M. et al. (2007). High-throughput oncogene mutation profiling in human cancer. Nat. Genet. *39*, 347–351.

Supporting information

Additional Supporting Information may be found in the online version of this article:

Table S1. A specific group of 105 genes for which expression is significantly associated with melanoma cell phenotype.

Please note: Wiley-Blackwell are not responsible for the content or functionality of any supporting materials supplied by the authors. Any queries (other than missing material) should be directed to the corresponding author for the article.

© 2011 John Wiley & Sons A/S

5.6 Novel MITF targets identified using a two-step DNA microarray strategy

The microphthalmia-associated transcription factor (MITF) is the master regulator of melanocytic development and pigment production, cell cycle regulation, migration and survival. Also in melanoma, this gene is involved in numerous pathways and has been the center of many studies. The aim of this project was to identify new target genes of MITF by using a new strategy involving two DNA microarray based approaches. This work resulted in the confirmation of many known MITF targets and the identification of a high number of novel targets. Since this study was published, a number of these novel targets have been confirmed by other groups.

I contributed to this study by performing data analysis of the microarray experiments and conducting correlation analysis of gene expression data. Also, I identified upstream MITF recognition sequences (Figure 4). Furthermore I participated in discussions and contributed to writing the final paper.

This study was published in *Pigment Cell & Melanoma Research*

Novel MITF targets identified using a two-step DNA microarray strategy

Keith S. Hoek[1], Natalie C. Schlegel[1], Ossia M. Eichhoff[1], Daniel S. Widmer[1], Christian Praetorius[2], Steingrimur O. Einarsson[2,3], Sigridur Valgeirsdottir[3], Kristin Bergsteinsdottir[2], Alexander Schepsky[2,4], Reinhard Dummer[1] and Eirikur Steingrimsson[2]

1 Department of Dermatology, University Hospital of Zürich, Zürich, Switzerland **2** Department of Biochemistry and Molecular Biology, Faculty of Medicine, University of Iceland, Reykjavik, Iceland **3** NimbleGen Systems of Iceland LLc, Reykjavik, Iceland **4** Signalling and Development Lab, Marie Curie Research Institute, Oxted, Surrey, UK

CORRESPONDENCE Keith S. Hoek, e-mail: keith.hoek@usz.ch

KEYWORDS microphthalmia-associated transcription factor/microarray/melanoma/melanocyte/transcription/correlation

PUBLICATION DATA Received 20 June 2008, revised and accepted for publication 18 August 2008

doi: 10.1111/j.1755-148X.2008.00505.x

Summary

Malignant melanoma is a chemotherapy-resistant cancer with high mortality. Recent advances in our understanding of the disease at the molecular level have indicated that it shares many characteristics with developmental precursors to melanocytes, the mature pigment-producing cells of the skin and hair follicles. The development of melanocytes absolutely depends on the action of the microphthalmia-associated transcription factor (MITF). MITF has been shown to regulate a broad variety of genes, whose functions range from pigment production to cell-cycle regulation, migration and survival. However, the existing list of targets is not sufficient to explain the role of MITF in melanocyte development and melanoma progression. DNA microarray analysis of gene expression offers a straightforward approach to identify new target genes, but standard analytical procedures are susceptible to the generation of false positives and require additional experimental steps for validation. Here, we introduce a new strategy where two DNA microarray-based approaches for identifying transcription factor targets are combined in a cross-validation protocol designed to help control false-positive generation. We use this two-step approach to successfully re-identify thirteen previously recorded targets of MITF-mediated upregulation, as well as 71 novel targets. Many of these new targets have known relevance to pigmentation and melanoma biology, and further emphasize the critical role of MITF in these processes.

Introduction

Malignant melanoma is an aggressive form of cancer with a high mortality rate. Although early stage disease is easily treatable, advanced stages of the disease are highly resistant to treatment and patients rarely survive longer than 10 months. The microphthalmia-associated transcription factor (MITF) is a member of the basic helix-loop-helix leucine-zipper transcription factor family and has been shown to be a critical regulator of

Significance

While the microphthalmia-associated transcription factor (MITF) is recognized as a master regulator for both melanocyte development and melanoma progression the number of known target genes is relatively small. This high throughput study of gene expression in melanoma cell lines serves to identify with high probability novel candidates for MITF-mediated activation in a melanocytic context.

© 2008 The Authors, Journal Compilation © 2008 Blackwell Munksgaard

melanocyte development and survival (Steingrimsson et al., 2004). Various isoforms of MITF are also important for the development and homeostasis of other cell types including retinal pigment epithelia, osteoclasts and mast cells (Kawaguchi and Noda, 2000; Nechushtan et al., 1997; Planque et al., 2004). In melanoma, MITF is reported to be a critical factor in regulating proliferation (Carreira et al., 2006; Hoek et al., 2008), and amplification of the *MITF* gene is associated with poor patient survival (Garraway et al., 2005; Ugurel et al., 2007). Table 1 shows that MITF is reported to regulate the expression of a broad variety of genes, many of them involved in pigmentation. Despite this variety of known targets MITF must regulate multiple other genes to account for all aspects of MITF function during melanocyte development and melanoma progression. Thus, in order to further characterize the role of MITF in melanocyte and melanoma development, it is important to identify additional MITF target genes.

Endogenous expression of *MITF* is driven by signals which likely also activate other genes. Experiments where a constitutively active expression vector is used to drive *MITF* expression short-circuit this background of normally co-regulated factors. This changes the

Table 1. Verification of reported Mitf target genes

Symbol	Title	References	Cell type	Fold[a]	Co[b]
ACP5	Acid phosphatase 5, tartrate resistant	Luchin et al., (2000)	Osteoclast	209	7
BCL2	B-cell CLL/lymphoma 2	McGill et al., (2002)	Melanoma	<2	7
BEST1	Bestrophin 1	Esumi et al., (2007)	RPE	<2	7
BIRC7	Baculoviral IAP repeat-containing 7	Dynek et al., (2008)	Melanoma	214	7
CDK2	Cyclin-dependent kinase 2	Du et al., (2004)	Melanocyte	3	7
CLCN7	Chloride channel 7	Meadows et al., (2007)	Osteoclast	4	7
DCT	Dopachrome tautomerase	Yasumoto et al., (2002)	Melanocyte	218	7
EDNRB	Endothelin receptor type B	Sato-Jin et al., (2007)	Melanocyte	15	7
GPNMB	Glycoprotein (transmembrane) nmb	Loftus et al., (2008)	Melanoblast	251	7
GPR143	G protein-coupled receptor 143 (Oa1)	Vetrini et al., (2004)	Melanocyte	19	6
MC1R	Melanocortin 1 receptor	Aoki and Moro, (2002)	Melanocyte	16	4
MLANA	Melan-A	Du et al., (2003)	Melanocyte	173	7
OSTM1	Osteopetrosis-associated transmembrane protein 1	Meadows et al., (2007)	Osteoclast	5	7
RAB27A	RAB27A, member RAS oncogene family	Chiaverini et al., (2008)	Melanocyte	13	7
SILV	Silver homolog (mouse)	Du et al., 2003)	Melanocyte	217	7
SLC45A2	Solute carrier family 45, member 2	Du and Fisher, (2002)	Melanocyte	222	7
TBX2	T-box 2	Carreira et al., (2000)	Melanocyte	4	5
TRPM1	Transient receptor potential cation channel, M1	Miller et al., (2004)	Melanocyte	137	6
TYR	Tyrosinase	Hou et al., (2000)	Melanocyte	267	7
TYRP1	Tyrosinase-related protein 1	Fang et al., (2002)	Melanocyte	<2	7
CADM1	Cell adhesion molecule 1	Ito et al., (2003)	Mast cell	<2	1
CDKN1A	Cyclin-dependent kinase inhibitor 1A (p21)	Carreira et al., (2005)	Melanocyte	<2	0
CDKN2A	Cyclin-dependent kinase inhibitor 2A (p16)	Loercher et al., (2005)	Melanocyte	<2	1
Cma1	Chymase 1, mast cell	Morii et al., (1997)	Mast cell	7	0
CTSK	Cathepsin K	Motyckova et al., (2001)	Osteoclast	<2	1
DIAPH1	Diaphanous homolog 1	Carreira et al., (2006)	Melanoma	<2	1
GZMB	Granzyme B	Ito et al., (1998)	Mast cell	10	0
HIF1A	Hypoxia-inducible factor 1, alpha subunit	Busca et al., (2005)	Melanoma	2	0
ITGA4	Integrin, alpha 4	Kim et al., (1998)	Melanocyte	3	0
KIT	v-kit Hardy-Zuckerman 4 feline sarcoma viral oncogene	Tsujimura et al., 1996)	Mast cell	<2	2
Mcpt2	Mast cell protease 2	Ge et al., (2001)	Mast cell	<2	0
Mcpt4	Mast cell protease 4	Jippo et al., (1999)	Mast cell	<2	0
Mcpt9	Mast cell protease 9	Ge et al., (2001)	Mast cell	<2	0
MET	Met proto-oncogene	McGill et al., (2006)	Melanocyte	<2	3
NDST2	N-deacetylase/N-sulfotransferase 2	Morii et al., (2001)	Melanocyte	<2	0
NGFR	Nerve growth factor receptor (p75)	Jippo et al., (1997)	Mast cell	3	0
OSCAR	Osteoclast associated, immunoglobulin-like receptor	So et al., (2003)	Osteoclast	4	0
PRKCB1	Protein kinase C, beta 1	Park et al., (2006)	Melanocyte	2	1
SERPINE1	Serpin peptidase inhibitor E1 (PAI-1)	Murakami et al., (2006)	Mast cell	6	0
SLC11A1	Solute carrier family 11, member 1	Gelineau-van Waes et al., (2008)	RPE	4	1
TPH1	Tryptophan hydroxylase 1	Ito et al., (1998)	Mast cell	<2	0
Tpsb2	Tryptase beta 2	Morii et al., (1996)	Mast cell	<2	1

[a]Fold change up on transformation of SK-MEL-28 with a *Mitf*-expressing vector ($P < 0.05$).
[b]Number of data sets in which correlation exceeds 0.5 with 207233_s_at (*MITF*).
RPE, retinal pigment epithelium.

© 2008 The Authors, Journal Compilation © 2008 Blackwell Munksgaard

context in which MITF operates and, in the absence of co-regulated activators and suppressors, potentially activates biologically irrelevant target genes. Alternatively, identification of novel MITF targets via correlation of mRNA expression patterns is complicated by factors which are co-regulated with MITF. This potential confusion of causality and correlation also risks generating false positives. However, each of these approaches serve to complement the other. Exogenous upregulation of *MITF* is unlikely to activate endogenously co-regulated factors, and analysis of endogenous expression patterns serves to filter out biologically irrelevant transcription activated by exogenous *MITF* expression. We show here how such a two-step strategy may detect additional targets for MITF-driven transcription.

Results

Endogenous MAPK signalling does not affect Mitf protein levels

If a transcription factor's function is primarily regulated by post-transcriptional or post-translational mechanisms then variations in the expression of its mRNA across a range of samples will not correlate with that of its targets. For MITF there are several reports which together detail a range of post-translational modifications which in melanocytes modify its regulatory activity, including ubiquitination, sumoylation, phosphorylation, and cleavage by caspases (Hemesath et al., 1998; Larribere et al., 2005; Murakami and Arnheiter, 2005; Wu et al., 2000; Xu et al., 2000). This complex layering of multiple post-translational regulation mechanisms would seem to preclude the usefulness of correlating *MITF* mRNA with that of potential targets. However, recent gene expression data in melanoma cell lines shows significant correlation of *MITF* mRNA with the expression of many of its known targets (Hoek et al., 2006). This suggests that, for at least some genes and certain contexts, variations in post-translational modification of MITF have a lesser influence over their activation.

Because of the interest in post-translational regulation of MITF activity, particularly in the context of the $BRAF^{V600E}$ mutation, it was important that we look for a correlation between MAPK signalling events and MITF protein levels. We therefore stained melanoma cell extracts to compare endogenous levels of phospho-ERK 1/2, phospho-JNK and phospho-p38 against MITF and found no correlation between them (Fig. 1). These results concur with similar data obtained previously by Kono et al. and we agree with their assessment that if MAPK signalling in melanoma has regulatory control over MITF it is not at the level of MITF turnover (Kono et al., 2006). However, it is important to consider that we are examining homeostatic conditions and there may yet be signals to which MITF-turnover rates (and therefore MITF function) are

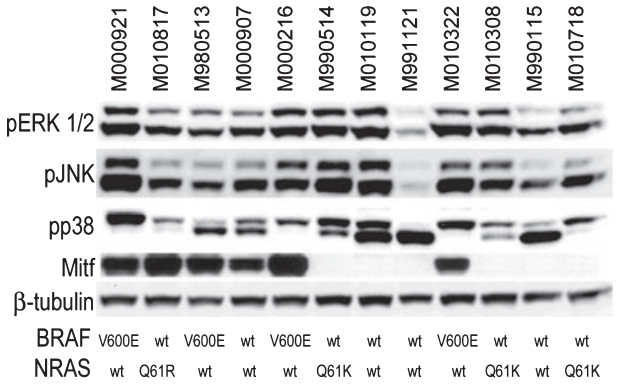

Figure 1. MAPK/JNK signalling and *MITF* expression. Cell extracts from a library of melanoma cultures were subject to western blotting against phosphorylated Erk1/Erk2, phosphorylated JNK, phosphorylated p38, and β-tubulin. MITF levels, as well as BRAF and NRAS mutation status were reported previously (Hoek et al., 2006). These data show that neither MAPK/JNK activation nor BRAF/NRAS mutation status correlate with Mitf expression in melanoma.

sensitive. Nevertheless, it is clear that in unstimulated cultured melanoma cells apparent MAPK signalling status is not related to MITF protein level, and this supports the notion that in unstimulated cultures expression of *MITF* mRNA may correlate with target gene expression.

Gene expression in Mitf-transfected SK-MEL-28 cells

To identify candidate MITF target genes, we generated a stable line of the melanoma cell line SK-MEL-28 (subclone SK-MEL-28-MITF-7) which expresses a FLAG-tagged Mitf protein. Normally, the SK-MEL-28 cells express very low levels of MITF and carry the $BRAF^{V600E}$ mutation. The SK-MEL-28-MITF-7 cells proliferated slower than the parental cell line. We cultured these cells as well as the original SK-MEL-28 cells in triplicates and then isolated RNA for microarray analysis from each culture separately. By comparing the genes expressed in *Mitf*-transfected cells with the genes expressed by the untransformed cells, we obtained a list of 10348 probes (equivalent to 6936 genes) upregulated at least twofold in the presence of *Mitf* (Fig. 2, Table S1). As a positive control, four of four separate probes for *MITF* showed upregulation (18- to 24-fold) of *MITF* expression in *Mitf*-transfected cells. Among the upregulated genes were 27 of 42 genes reported to be upregulated by MITF. This represents a significant ($P < 0.005$) overlap with the known target list. However, some of the genes upregulated by *Mitf*-transfection of SK-MEL-28 are likely to be because of secondary effects and to determine which are true targets, we performed a strictly controlled correlation analysis on data obtained from multiple other studies and compared the results with those generated from *Mitf*-transfection of SK-MEL-28.

© 2008 The Authors, Journal Compilation © 2008 Blackwell Munksgaard

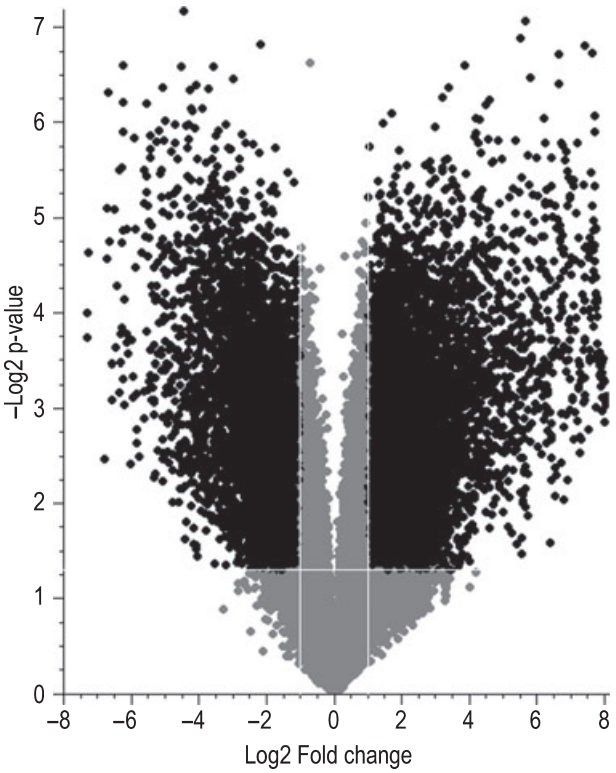

Figure 2. Exogenous Mitf drives gene expression change. A volcano plot showing the ratio of averaged untransformed and *Mitf*-transformed data reveals 9890 genes (black dots) which have significant and >2-fold change on *Mitf*-transformation of SK-MEL-28. Grey dots represent genes which did not meet these minimum criteria.

Correlation of melanocytic gene expression with MITF expression

To find genes whose expression patterns show strong and reproducible correlation with *MITF* expression it was important to consider data from independent sources. As we are primarily interested in MITF's function in a melanocytic context we restricted ourselves to selecting sources which examined gene expression in melanoma and melanocytes. Furthermore, to simplify comparison between sources, we considered only those which used the same array platform. Accordingly, we obtained from GEO data sets generated by seven different groups all using Affymetrix HG-U133 series platforms to examine in vitro gene expression in melanoma or melanocyte cultures. We assessed correlation by performing a Pearson correlation analysis on each probe set in comparison to *MITF* across all samples of each data set. If the calculated Pearson correlation coefficient (r) for a probe set exceeded 0.5 in all seven data sets then it was considered to be strongly correlated with *MITF*. We detected 154 different probe sets (110 genes; Table S2) which shared a correlation coefficient of at least 0.5 with 207233_s_at (*MITF*) in all seven data sets (Fig. 3). To determine whether or not these genes are true targets of MITF we compared this list with the list of genes identified as being upregulated by *Mitf*-transfection of SK-MEL-28.

Correlation and upregulation

To use these two different datasets to extract true MITF target genes, we compared the 110 genes which correlated with *MITF* expression in the different melanoma datasets, with the 6936 genes significantly upregulated in the transfected SK-MEL-28 cells. Of these lists, 84 genes showed both high correlation with *MITF* expression and significant upregulation of expression when SK-MEL-28 is transformed with an *Mitf*-expressing vector. Among these genes are thirteen known targets of MITF in melanocytes (Table 1). The finding that, among 84 genes, thirteen of 42 reported targets of MITF were detected has a significance (hypergeometric distribution) of $P < 10^{-18}$. Therefore it is highly likely that MITF has a direct regulatory relationship with the remaining 71 genes identified (Table 2).

Because our principal correlation criteria was very restrictive ($P < 10^{-13}$) we also performed a less strict analysis ($P < 0.004$). This determined that seven reported targets were probable false negatives in our principal study. Furthermore, we identified an additional 58 genes as being probable novel targets for MITF regulation (Table S3).

Upstream MITF recognition sequences

We looked for MITF recognition sequences in the upstream regions of strongly correlated novel candidates whose expression was increased by at least 50-fold upon Mitf transfection (*MBP, TNFRSF14, IRF4, RBM35A, PLA1A, APOLD1* and *KCNN2*). We searched both human and mouse sequences and found several instances of E- and M-boxes in the upstream regions of most of these genes (Fig. 4).

Discussion

The *MITF* gene has been termed a master regulator of melanocyte development as it can program cells towards the melanocyte lineage. For example, when fibroblasts are transfected with the *MITF* gene, they transform into dendritic cells expressing melanocyte marker genes (Tachibana, 1997). However, although a number of MITF target genes are known, most of them are involved in melanocyte differentiation and we know very little about the genes involved in the melanocyte developmental program. Similarly, as MITF is important for the development of melanomas it is of paramount interest to identify the target genes which turn normal melanocytes into malignant cells. Here we have used a dual approach to identify potential MITF target genes in melanocytes and melanoma cells, first by identifying genes upregulated by Mitf-transfection of SK-MEL-28 melanoma and then by comparing those to genes which

© 2008 The Authors, Journal Compilation © 2008 Blackwell Munksgaard

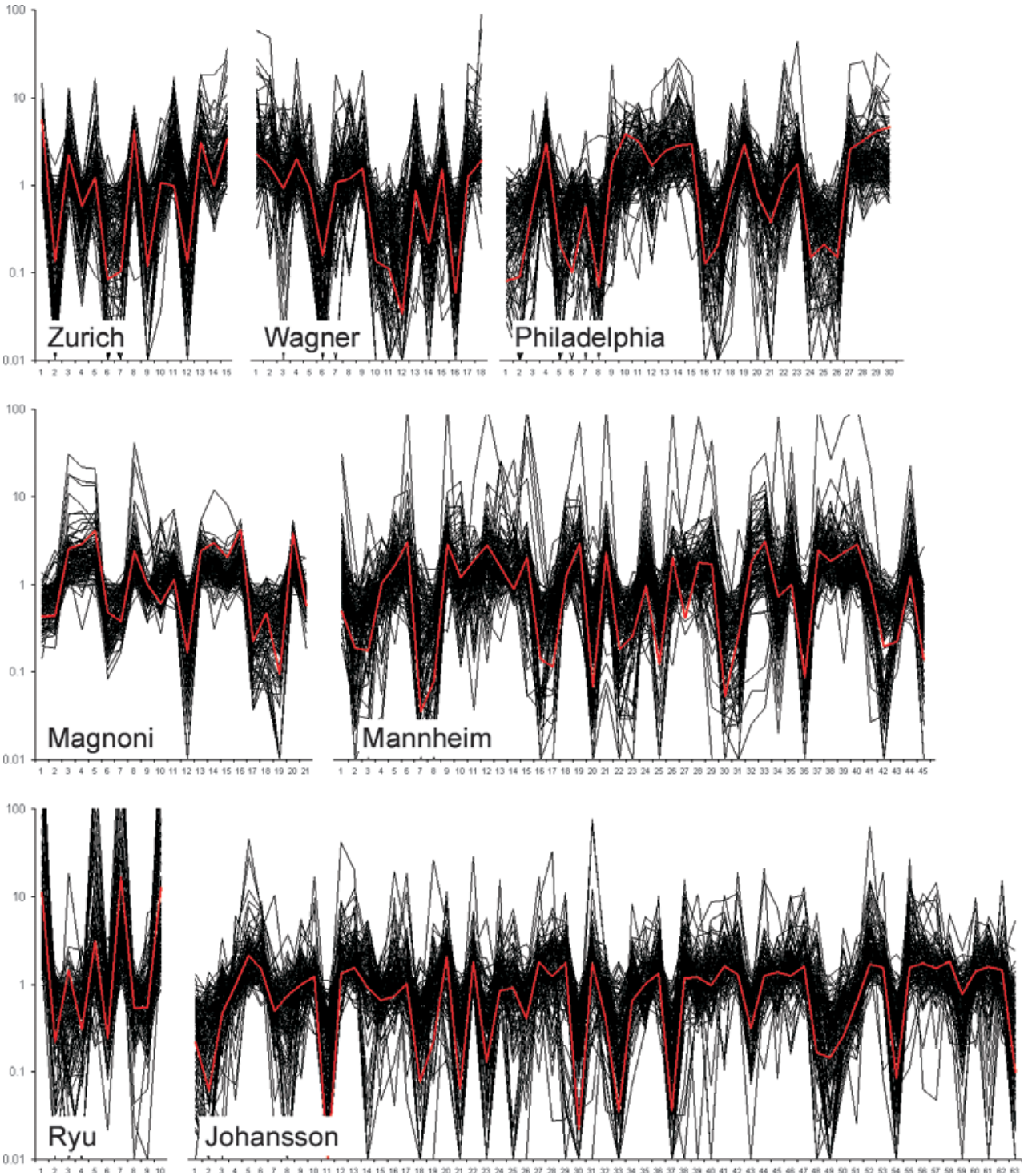

Figure 3. Correlation of gene expression with MITF. Normalized signal intensity values for 84 genes which both correlate with *MITF* expression and are upregulated by *Mitf*-transfection, are plotted against samples from the seven data sets used in the correlation analyses. *MITF* expression (207233_s_at) is plotted in red.

correlate with *MITF* expression in seven different data sets. Of the genes identified, ten (*TYR, DCT, SILV, MLANA, EDNRB, GPNMB, BIRC7, CDK2, SLC45A2* and *RAB27A*) have been previously reported as being activated by MITF in melanocytes or melanomas. All of those genes were found to be both closely correlated with endogenous MITF expression and upregulated upon transfection of SK-MEL-28 cells with an

© 2008 The Authors, Journal Compilation © 2008 Blackwell Munksgaard

Table 2. Novel targets for Mitf-mediated upregulation

Symbol	Title	r[a]	Fold[b]
MBP	Myelin basic protein	0.82	264
TNFRSF14	Tumor necrosis factor receptor superfamily 14	0.89	259
IRF4	Interferon regulatory factor 4	0.78	170
RBM35A	RNA-binding motif protein 35A	0.88	166
PLA1A	Phospholipase A1 member A	0.71	166
APOLD1	Apolipoprotein L domain containing 1	0.71	116
KCNN2	Potassium calcium-activated channel N2	0.55	52
INPP4B	Inositol polyphosphate-4-phosphatase, type II	0.72	45
CAPN3	Calpain 3	0.91	45
LGALS3	Lectin, galactoside-binding, soluble, 3	0.77	31
GREB1	GREB1 protein	0.76	19
FRMD4B	FERM domain containing 4B	0.74	16
SLC1A4	Solute carrier family 1, member 4	0.65	15
TBC1D16	TBC1 domain family, member 16	0.84	14
GMPR	Guanosine monophosphate reductase	0.67	13
ASAH1	N-acylsphingosine amidohydrolase 1	0.83	11
MICAL1	Microtubule-associated monoxygenase calponin/LIM containing 1	0.63	11
TMC6	Transmembrane channel-like 6	0.73	10
ITPKB	Inositol 1,4,5-trisphosphate 3-kinase B	0.8	9
SLC7A8	Solute carrier family 7, member 8	0.72	9
CA14	Carbonic anhydrase XIV	0.67	8
TMCC2	Transmembrane and coiled-coil domain family 2	0.78	7
GPR137B	G protein-coupled receptor 137B	0.82	7
RIPK5	Receptor interacting protein kinase 5	0.68	7
TDRD7	Tudor domain containing 7	0.78	7
PHACTR1	Phosphatase and actin regulator 1	0.83	7
RRAGD	Ras-related GTP binding D	0.84	7
AMDHD2	Amidohydrolase domain containing 2	0.68	7
SOX13	SRY (sex determining region Y)-box 13	0.66	6
KIAA1026	Kazrin	0.78	6
SORT1	Sortilin 1	0.79	6
LYST	Lysosomal trafficking regulator	0.68	6
STXBP1	Syntaxin binding protein 1	0.7	6
USP48	Ubiquitin specific peptidase 48	0.55	5
ZFYVE16	Zinc finger, FYVE domain containing 16	0.84	5
STX7	Syntaxin 7	0.78	5
HPS4	Hermansky-Pudlak syndrome 4	0.76	5
CDK5R1	Cyclin-dependent kinase 5, regulatory subunit 1 (p35)	0.7	5
PSEN2	Presenilin 2	0.69	5
RHOQ	Ras homolog gene family, member Q	0.73	5
PIR	Pirin	0.86	4
APOE	Apolipoprotein E	0.74	4
VAT1	Vesicle amine transport protein 1	0.75	4
GM2A	GM2 ganglioside activator	0.58	4
ST3GAL6	ST3 beta-galactoside alpha-2,3-sialyltransferase 6	0.81	4
IVNS1ABP	Influenza virus NS1A binding protein	0.72	4
GYG2	Glycogenin 2	0.77	4
GNPTAB	N-acetylglucosamine-1-phosphate transferase α and β	0.8	4
C14orf109	Chromosome 14 open reading frame 109	0.75	4
HPGD	Hydroxyprostaglandin dehydrogenase 15-(NAD)	0.74	3
ATP6V1C1	ATPase, H+ transporting, lysosomal 42kDa, V1 subunit C1	0.65	3
SEMA6A	Semaphorin	0.79	3
CHKA	Choline kinase alpha	0.78	3
ACSL1	Acyl-CoA synthetase long-chain family member 1	0.64	3
SGK3	Serum/glucocorticoid regulated kinase family, member 3	0.58	3
KIAA1598	KIAA1598	0.7	3
QDPR	Quinoid dihydropteridine reductase	0.75	3
IL6R	Interleukin 6 receptor	0.65	3
FAM53B	Family with sequence similarity 53, member B	0.74	3
GPM6B	Glycoprotein M6B	0.8	3

© 2008 The Authors, Journal Compilation © 2008 Blackwell Munksgaard

Table 2. Continued

Symbol	Title	r^a	Fold[b]
SCARB1	Scavenger receptor class B, member 1	0.67	3
MDH1	Malate dehydrogenase 1, NAD (soluble)	0.68	3
UBL3	Ubiquitin-like 3	0.73	3
ACO2	Aconitase 2, mitochondrial	0.61	2
ATP1A1	ATPase, Na+/K+ transporting, alpha 1 polypeptide	0.77	2
ATP6V1B2	ATPase, H+ transporting, lysosomal, V1 subunit B2	0.62	2
PPM1H	Protein phosphatase 1H (PP2C domain containing)	0.73	2
TFAP2A	Transcription factor AP-2 alpha	0.79	2
GAPDHS	Glyceraldehyde-3-phosphate dehydrogenase, spermatogenic	0.63	2
SLC19A2	Solute carrier family 19 (thiamine transporter), member 2	0.77	2
DAPK1	Death-associated protein kinase 1	0.67	2

[a]r = median correlation with 207233_s_at (*MITF*) from seven different data sets.
[b]Fold change up on transformation of SK-MEL-28 with a *Mitf*-expressing vector.

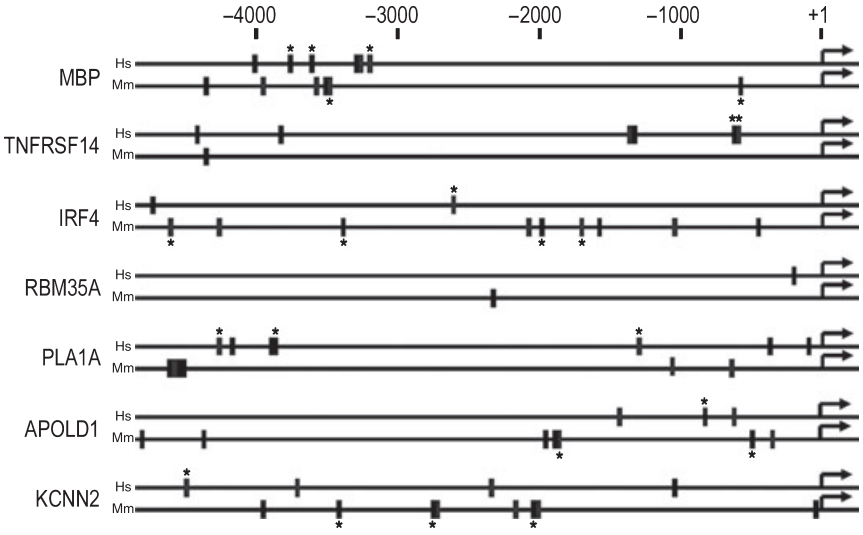

Figure 4. Upstream/promoter regions of novel MITF target genes. For both human (Hs) and mouse (Mm), upstream sequences of novel target genes with greater than 50-fold upregulation on *Mitf*-transfection of SK-MEL-28 were extracted from the UCSC Genome Browser database. These were interrogated for the presence of E-box (CAYRTG) and M-box (E-box flanked by a 5′ T or a 3′ A) sequences. M-boxes are highlighted with an asterisk.

Mitf-expressing vector (Table 1). We also identified three genes (*ACP5, OSTM1* and *CLD7*) which have previously been identified as being upregulated by Mitf in osteoclasts (Table 1).

Concomitantly, there were 29 genes previously reported to be regulated by MITF which did not meet the selection criteria (Table 2). For some of these genes it was found that the primary selection criteria was overly strict and they were omitted as false negatives. Both *TRPM1* and *GPR143* showed significant upregulation (137- and 19-fold, respectively) and failed to meet correlation criteria in only one of seven data sets. *TBX2* and *MC1R* also showed significant upregulation (3.5- and 16-fold, respectively) but missed correlation in two and three data sets, respectively. *TYRP1*, *BCL2* and *BEST1* passed the correlation criteria in all data sets but did not show significant changes in expression upon *Mitf*-transfection of SK-MEL-28 cells. Interestingly, others have shown that MITF transfection of the mouse melanoma line B16 fails to activate known targets, suggesting that MITF requires co-factors for its activity which are absent in B16 (Gaggioli et al., 2003; de la Serna et al., 2006). On the other hand, it is thought that upregulation of *TYRP1* and *BCL2* requires signalling through the KIT receptor (Grichnik et al., 1998; McGill et al., 2002), which may be inactive in SK-MEL-28 and would explain their failure to be upregulated. Intriguingly, a close *BCL2* relative, *BCL2A1* correlated with *MITF* in six of seven data sets and was upregulated 245-fold on *Mitf*-transfection (qualifying it as a probable false-negative). Like *BCL2*, this gene is involved in anti-apoptotic processes and has previously been described as expressed in melanoma (Kenny et al., 1997; Piva et al., 2006). That *BCL2A1* activation may not require KIT signalling suggests an independent mechanism for MITF to control apoptosis during melanoma progression. This is further supported by our confirmation that *BIRC7*, another anti-apoptotic factor reported to be regulated by MITF, is also upregulated 214-fold upon *Mitf*-transfection and

© 2008 The Authors, Journal Compilation © 2008 Blackwell Munksgaard

tightly correlates with *MITF* expression in all data sets (Table 1). For the remaining genes which were previously reported to be activated by MITF there are several possible explanations for why they were not identified here. First, we used an entirely melanocytic context for our study whereas some of the genes have only been shown to be regulated by MITF in other cell types (e.g. *CTSK*, cathepsin K, is reported only in osteoclasts (Motyckova et al., 2001)). Second, we were not able to identify genes whose activation by MITF is regulated by post-translational modifications of the transcription factor. Finally, it may also be that MITF does *not* regulate some of these genes and that the original attributions were mistaken.

We identify 71 genes as novel MITF-activated targets in melanoma and melanocytes (Table 2). Of these, three (*LYST, PSEN2* and *HPS4*) are known to be associated with pigmentation-specific processes (Gutierrez-Gil et al., 2007; Hutton and Spritz, 2008; Wang et al., 2006). Six others (*IL6R*, *IRF4, LGALS3, CAPN3, SORT1* and *RRAGD*) have previously been shown to be expressed in melanoma (Chang and Schimmer, 2007; Prieto et al., 2006; Schwabe et al., 1994; Sundram et al., 2003; Truzzi et al., 2008; Weeraratna et al., 2004; de Wit et al., 2005). Finally, three (*CA14, APOE* and *SCARB1*) have been identified in another pigment cell type, the retinal pigment epithelial cells (Duncan et al., 2002; Ishida et al., 2004; Ochrietor et al., 2005), thereby underpinning the accuracy of our approach. This left 59 genes not previously associated with melanoma or melanocytic functions. Some of these (*SLC1A4, SLC7A8, SLC19A2, ATP1A1, ATP6V1B2, ATP6V1C1, APOE, KCNN2, LYST, SCARB1* and *VAT*) are, like *SLC45A2* and *ACP5*, important for transport processes which suggests that MITF is involved in regulating cation flux as well as amino acid and lipid metabolism. Other genes (*ITPKB, SGK3, RHOQ, PPM1H, SEMA6A* and *TNFRSF14*) suggest, as do *RAB27A, IL6R, PSEN2, EDNRB* and *CAPN3*, that Mitf has important roles in regulating signal transduction.

The 264-fold upregulation of *MBP*, which encodes myelin basic protein (a major structural component of myelinating tissue), and the presence of M-boxes upstream of its transcription start site prompted us to investigate whether other myelinating cell-specific genes have a measurably significant relationship with MITF. Accordingly, the major myelin component *PLP1* was upregulated 254-fold by *Mitf*-transfection of SK-MEL-28 and correlated with *MITF* in six of seven data sets. *SOX10*, a myelination critical transcription factor (Stolt et al., 2002), also correlated with *MITF* in six of seven data sets and was upregulated 128-fold by *Mitf*-transfection. Similarly, the myelin-specific connexin *GJB1* showed correlation in five of seven data sets and was upregulated 202-fold on *Mitf*-transfection. Finally, both *FABP7* and *ERBB3* correlated in four of seven data sets and were also significantly upregulated (48- and 23-fold, respectively) on *Mitf*-transfection. Upregulation of *SOX10* by *Mitf*-transfection is an interesting finding as SOX10 has long been held to be a regulator of *MITF* (Lee et al., 2000), indicating the possibility that these transcription factors regulate each other's expression. It may be that the myelinating cell genes mentioned here are detected because they are directly regulated by SOX10 (Stolt et al., 2002), while its gene is being regulated by MITF, rather than being directly regulated by MITF itself. This, nevertheless, suggests that MITF may have a role alongside SOX10 in regulating the processes of myelination.

DNA microarray analysis of gene expression is a powerful method for the parallel assessment of thousands of transcriptional variations which drive biology. The principal agent of transcriptional change is the transcription factor, the protein which binds DNA to regulate the production of RNA. The potential for using microarrays to learn which transcription factors target which genes is now coming into realization. Particularly impressive is the application of chromatin immunoprecipitation and microarray analysis to identify regions of DNA which are bound by transcription factors (Buck and Lieb, 2004). However, the finding that a transcription factor may bind a piece of DNA does not necessarily identify the relevant context of that interaction. Similarly, showing that an experimentally induced transcription factor may upregulate a potential target gene is no guarantee that the relationship exists in the biology being studied. On the other hand, by looking at natural variation in a transcription factor's expression and comparing it to expression variation in potential target genes, it may be possible to verify a regulatory relationship identified under experimental conditions. Our strategy of combining two different microarray data analysis methods, a two-step approach intended to account for both irrelevance and non-causality, works very well and is a strategy with general application to the study of other transcription factors. This may have implications in other forms of cancer where transcription factors play important roles.

Microphthalmia-associated transcription factor-regulated gene products are among the most important targets for anti-melanoma therapies employing adaptive immune responses mediated by cytotoxic T-cells or antibodies. Many trials aim to activate cytotoxic T-cell responses against MITF-regulated antigens by vaccination with peptides or dendritic cell vaccines (Dummer and Nestle, 2000). For example, *GPM6B* and *SEMA6A* are membrane proteins whose expression is typically restricted to neuronal tissues. Their identification here as MITF-regulated factors may make them suitable targets for immunotherapeutic strategies. In conclusion, our study shows that our novel approach can identify new target genes of transcription factors and may therefore have implications for further cancer treatment.

© 2008 The Authors, Journal Compilation © 2008 Blackwell Munksgaard

Materials and methods

Western blotting

A library of melanomas which had been previously assessed for MITF expression and BRAF/NRAS mutation status (Hoek et al., 2006) was used to determine MAPK phosphorylation status. Cells were lysed in lysis buffer containing 20 mM Tris–HCl (pH 7.5), 1% Triton X-100 (Sigma-Aldrich, St Louis, MO, USA), 137 mM NaCl, 10% glycerol, protease inhibitors (Complete Mini +EDTA; Roche, Basel, Switzerland) and phosphatase inhibitors (Sigma Phosphatase inhibitor cocktails 1 & 2). Proteins were separated by SDS–PAGE under reducing conditions and transferred onto nitrocellulose membranes (Invitrogen, Carlsbad, CA, USA). Membranes were probed with a specific primary antibody to p-Erk1/2 (ab4819; Abcam, Cambridge, UK), p-p38 (ab4822; Abcam, Cambridge, UK) or p-JNK (9251; Cell Signaling, Danvers, MA, USA) followed by a horseradish peroxidase-conjugated goat anti-rabbit (Bio-Rad, Reinach, Switzerland) secondary antibody. Bound antibodies were detected by chemiluminescence (ECL; GE Healthcare, Buckinghamshire, UK).

Cell culturing and exogenous Mitf expression

SK-MEL-28 cell lines cells were maintained in Dulbecco minimal essential medium (DMEM; Invitrogen), supplemented with 10% fetal bovine serum, 100 U of penicillin/ml and 100 μg of streptomycin/ml and cultured in a humidified incubator at 37°C with 5% CO_2. For generating the SK-MEL-28 cell lines over-expressing *Mitf*, a neomycin-selectable vector expressing Flag epitope-tagged *Mitf* (+)(Carreira et al., 2006) was linearized by EcoRI digestion, gel purified and transfected into SK-MEL-28 cells with Exgen 500 (Fermentas, Glen Burnie, MD, USA). Individual clones were isolated following neomycin selection (Invitrogen). Positive clones were detected by Western blotting with an anti-Flag antibody (M2; Sigma-Aldrich) (data not shown) and used for further analysis. For the gene expression analysis the subclone SK-MEL-28-MITF-7 was grown to confluency and then incubated in serum-free medium for 4 h. Each experiment (SK-MEL-28 cells and the SK-MEL-28 cells stably transfected with *Mitf*) was performed in biological triplicate to ensure statistically relevant results. RNA was extracted from the cells using Trizol reagent (Invitrogen) and further purified using the RNeasy Mini Kit (Qiagen, Valencia, CA, USA) according to the manufacturer's recommendations. Isolated RNA was analysed for quality using a Bioanalyser (Agilent Technologies, Palo Alto, CA, USA). cDNA was prepared using Superscript III reverse transcriptase (Invitrogen) according to the manufacturer's instructions. The cDNA samples were labelled and hybridized according to Roche NimbleGen (Madison, WI, USA) standard procedures at the Roche NimbleGen Service Laboratory in Reykjavik, Iceland. The microarrays used in this experiment were NimbleGen Expression 12 × 135K microarrays. This microarray design (2007-09-12_HG18_opt_expr) comprises 12 subarrays (~8.9 mm × 6.5 mm), each containing 1 35 000 features (13 × 13 μm) on a standard 25 × 76 mm glass slide. The NimbleGen array design is based on the HG18 build from UCSC and interrogates 45034 unique transcripts. Unique sample tracking controls were added to each sample prior to loading onto 12-plex arrays to ensure the integrity of the hybridization experiment and to confirm sample identity on each array. After hybridisation the microarrays were scanned using an Axon GenePix 4000B scanner (Molecular Devices, Union City, CA, USA) at 5 μm resolution.

Fold-change analysis

All data analysis was performed using GeneSpring GX 7.3 (Agilent Technologies). Probe set data values below 0.01 were set to 0.01 and each measurement was divided by the 50th percentile of all measurements in that sample, then each probe measurement was divided by the median of its measurements across all samples. To determine gene expression patterns differentiating between sample classes, a statistical analysis (ANOVA) was used to identify probes with class-specific expression patterns. The statistical analysis used the Welch two-sample *t*-test, a P-value cut-off of 0.05 was used and the Benjamini and Hochberg false discovery rate (Benjamini et al., 2001) was employed for multiple testing correction. A two-fold change filter was then applied to identify genes undergoing changed expression on transformation with a *Mitf*-expressing vector.

Correlation analysis

We were interested in identifying the genes with expression patterns that significantly correlated with that of *MITF*. The correlation study we performed was based on the Pearson product-moment correlation coefficient and assumed both a normal distribution of data and a strictly linear relationship between *MITF* gene transcription and MITF function (i.e. target gene transcription). The risk in using this approach is that non-normal data distributions tend to degrade its efficiency and we cannot account for non-linear (e.g. multi-factorial) associations.

Ignoring multiple-testing issues, a probe set with a Pearson co-efficient (r) of 0.5 with *MITF* is considered significant ($P < 0.05$) only if it is derived using a minimum of 16 samples. However, because we analyzed correlation among 22 272 probe sets we recognized that this was a multiple-testing problem, and subsequently the minimum number of samples for an r of 0.5 to be significant becomes 81. Even with a data set of sufficient size it is desirable to consider data from multiple sources (when available) to avoid single study bias, which is an inherent risk in high-throughput analysis (Hoek, 2007). Nevertheless, even with smaller sample sizes a sufficient number of data sets will ensure that $r = 0.5$ is significant.

Therefore, our correlation analysis employed seven different sets of DNA microarray data extracted from various databases. The criteria for data set selection was that each had to comprise at least ten different samples and use a common platform. These included melanoma cell line data from GSE8332 (Wagner data set, 18 samples), GSE7127 (Johansson data set, 63 samples), GSE4843 (Mannheim data set, 45 samples), GSE4841 (Philadelphia data set, 30 samples), and GSE4840 (Zurich data set, 15 samples) (Hoek et al., 2006; Johansson et al., 2007; Wagner et al., 2007) extracted from the NCBI Gene Expression Omnibus (http://www.ncbi.nlm.nih.gov/projects/geo/), melanoma cell line data published by Ryu and co-workers (Ryu data set, 10 samples) (Ryu et al., 2007) extracted from the Public Library of Science (http://www.plosone.org), and untreated melanocyte culture data published by Magnoni and co-workers (Magnoni data set, 21 samples) (Magnoni et al., 2007). All data sets derive from experiments using HG-U133 series microarrays (Affymetrix, Santa Clara, CA, USA). Each data set was normalized as previously described and analyzed separately using GeneSpring GS 7.3 (Agilent Technologies) and identical protocols. To identify gene expression patterns which correlated with that of *MITF*, the expression patterns of 22272 probe sets were individually compared with the *MITF* probe set 207233_s_at by performing a Pearson correlation and selecting probe sets with correlation coefficients >0.5. Probe sets which failed to pass this filter in all seven data sets were discarded and for each remaining probe set the median correlation coefficient was calculated. Furthermore, for each probe set a critical t value was calculated from the correlation coefficient based on sample size and used for a t-distribution analysis to determine its P-value in each data set, which were then multiplied across the data sets and adjusted by multiple testing correction to generate a final P-value.

© 2008 The Authors, Journal Compilation © 2008 Blackwell Munksgaard

Our principal approach, requiring that a gene meet or exceed $r = 0.5$ in all seven data sets, ensures high significance ($P < 3 \times 10^{-13}$), provides increased confidence in interpreting identified genes as novel targets of MITF-regulation and (by identifying known targets) helps demonstrate the power of our two-step approach. However, we acknowledge that this will generate a large number of false negatives, necessitating a loosening of the correlation criteria. Statistically, if we consider only the four smallest data sets alone (Ryu, Zurich, Wagner, Magnoni) finding a gene with $r = 0.5$ in each is not significant ($P = 0.132$). However, as we are considering seven different data sets and a subgrouping of the four smallest represents only one permutation of 35 possible four-set combinations then the finding is significant ($P < 0.004$). Therefore, we considered genes which met or exceeded $r = 0.5$ in four to six (of seven) data sets as potential false negatives.

Target identification

The genes identified by assessing gene expression change resulting from transformation of SK-MEL-28 cells with an *Mitf*-expressing vector were combined with results of the correlation study. Genes which correlated with *MITF* expression but showed no significant change in expression on *Mitf*-induction were considered to be co-regulated genes (i.e. responding to the same transcriptional signals as *MITF*, but not governed by MITF). Genes which strongly correlated with *MITF* expression and showed significant change in expression on *Mitf*-induction were considered to be candidate targets for regulation by MITF.

Acknowledgements

This work was supported by grants from Krebsliga-Oncosuisse 01927-08-2006 (K.H.), Swiss National Foundation 320000-119989 (R.D. and K.H.), Julia Bangerter Rhyner Stiftung (R.D.) and research grants from the Science and Technology Council of Iceland, the University of Iceland Research Fund and from the Eimskip Fund of the University of Iceland (E.S., A.S. and C.P.). We thank Leila Virkki for proof-reading the manuscript and the Functional Genomics Center Zürich (Zürich, Switzerland) for additional computing resources.

References

Aoki, H., and Moro, O. (2002). Involvement of microphthalmia-associated transcription factor (MITF) in expression of human melanocortin-1 receptor (MC1R). Life Sci. *71*, 2171–2179.

Benjamini, Y., Drai, D., Elmer, G., Kafkafi, N., and Golani, I. (2001). Controlling the false discovery rate in behavior genetics research. Behav. Brain Res. *125*, 279–284.

Buck, M.J., and Lieb, J.D. (2004). ChIP-chip: considerations for the design, analysis, and application of genome-wide chromatin immunoprecipitation experiments. Genomics *83*, 349–360.

Busca, R., Berra, E., Gaggioli, C. et al. (2005). Hypoxia-inducible factor 1{alpha} is a new target of microphthalmia-associated transcription factor (MITF) in melanoma cells. J. Cell Biol. *170*, 49–59.

Carreira, S., Liu, B., and Goding, C.R. (2000). The gene encoding the T-box factor Tbx2 is a target for the microphthalmia-associated transcription factor in melanocytes. J. Biol. Chem. *275*, 21920–21927.

Carreira, S., Goodall, J., Aksan, I., La Rocca, S.A., Galibert, M.D., Denat, L., Larue, L., and Goding, C.R. (2005). Mitf cooperates with Rb1 and activates p21Cip1 expression to regulate cell cycle progression. Nature *433*, 764–769.

Carreira, S., Goodall, J., Denat, L., Rodriguez, M., Nuciforo, P., Hoek, K.S., Testori, A., Larue, L., and Goding, C.R. (2006). Mitf regulation of Dia1 controls melanoma proliferation and invasiveness. Genes Dev. *20*, 3426–3439.

Chang, H., and Schimmer, A.D. (2007). Livin/melanoma inhibitor of apoptosis protein as a potential therapeutic target for the treatment of malignancy. Mol. Cancer Ther. *6*, 24–30.

Chiaverini, C., Beuret, L., Flori, E., Busca, R., Abbe, P., Bille, K., Bahadoran, P., Ortonne, J.P., Bertolotto, C., and Ballotti, R. (2008). Microphthalmia associated transcription factor (MITF regulates rab27A gene expression and controls melanosomes transport. J. Biol. Chem. *283*, 12635–12642.

Du, J., and Fisher, D.E. (2002). Identification of Aim-1 as the underwhite mouse mutant and its transcriptional regulation by MITF. J. Biol. Chem. *277*, 402–406.

Du, J., Miller, A.J., Widlund, H.R., Horstmann, M.A., Ramaswamy, S., and Fisher, D.E. (2003). MLANA/MART1 and SILV/P-MEL17/GP100 are transcriptionally regulated by MITF in melanocytes and melanoma. Am. J. Pathol. *163*, 333–343.

Du, J., Widlund, H.R., Horstmann, M.A., Ramaswamy, S., Ross, K., Huber, W.E., Nishimura, E.K., Golub, T.R., and Fisher, D.E. (2004). Critical role of CDK2 for melanoma growth linked to its melanocyte-specific transcriptional regulation by MITF. Cancer Cell *6*, 565–576.

Dummer, R., and Nestle, F.O. (2000). Melanoma vaccines in development: looking to the future. BioDrugs *13*, 227–231.

Duncan, K.G., Bailey, K.R., Kane, J.P., and Schwartz, D.M. (2002). Human retinal pigment epithelial cells express scavenger receptors BI and BII. Biochem. Biophys. Res. Commun. *292*, 1017–1022.

Dynek, J.N., Chan, S.M., Liu, J., Zha, J., Fairbrother, W.J., and Vucic, D. (2008). Microphthalmia-associated transcription factor is a critical transcriptional regulator of melanoma inhibitor of apoptosis in melanomas. Cancer Res. *68*, 3124–3132.

Esumi, N., Kachi, S., Campochiaro, P.A., and Zack, D.J. (2007). VMD2 promoter requires two proximal E-box sites for its activity in vivo and is regulated by the MITF-TFE family. J. Biol. Chem. *282*, 1838–1850.

Fang, D., Tsuji, Y., and Setaluri, V. (2002). Selective down-regulation of tyrosinase family gene TYRP1 by inhibition of the activity of melanocyte transcription factor, MITF. Nucleic Acids Res. *30*, 3096–3106.

Gaggioli, C., Busca, R., Abbe, P., Ortonne, J.P., and Ballotti, R. (2003). Microphthalmia-associated transcription factor (MITF) is required but is not sufficient to induce the expression of melanogenic genes. Pigment Cell Res. *16*, 374–382.

Garraway, L.A., Widlund, H.R., Rubin, M.A. et al. (2005). Integrative genomic analyses identify MITF as a lineage survival oncogene amplified in malignant melanoma. Nature *436*, 117–122.

Ge, Y., Jippo, T., Lee, Y.M., Adachi, S., and Kitamura, Y. (2001). Independent influence of strain difference and mi transcription factor on the expression of mouse mast cell chymases. Am. J. Pathol. *158*, 281–292.

Gelineau-van Waes, J., Smith, L., van Waes, M., Wilberding, J., Eudy, J.D., Bauer, L.K., and Maddox, J. (2008). Altered expression of the iron transporter Nramp1 (Slc11a1) during fetal development of the retinal pigment epithelium in microphthalmia-associated transcription factor Mitf(mi) and Mitf(vitiligo) mouse mutants. Exp. Eye Res. *86*, 419–433.

Grichnik, J.M., Burch, J.A., Burchette, J., and Shea, C.R. (1998). The SCF/KIT pathway plays a critical role in the control of normal human melanocyte homeostasis. J. Invest. Dermatol. *111*, 233–238.

Gutierrez-Gil, B., Wiener, P., and Williams, J.L. (2007). Genetic effects on coat colour in cattle: dilution of eumelanin and phaeomelanin pigments in an F2-Backcross Charolais × Holstein population. BMC Genet. *8*, 56.

 © 2008 The Authors, Journal Compilation © 2008 Blackwell Munksgaard

Hemesath, T.J., Price, E.R., Takemoto, C., Badalian, T., and Fisher, D.E. (1998). MAP kinase links the transcription factor Microphthalmia to c-Kit signalling in melanocytes. Nature *391*, 298–301.

Hoek, K.S. (2007). DNA microarray analyses of melanoma gene expression: a decade in the mines. Pigment Cell Res. *20*, 466–484.

Hoek, K.S., Schlegel, N.C., Brafford, P. et al. (2006). Metastatic potential of melanomas defined by specific gene expression profiles with no BRAF signature. Pigment Cell Res. *19*, 290–302.

Hoek, K.S., Eichhoff, O.M., Schlegel, N.C., Doebbeling, U., Schaerer, L., Hemmi, S., and Dummer, R. (2008). In vivo switching of human melanoma cells between proliferative and invasive states. Cancer Res. *68*, 650–656.

Hou, L., Panthier, J.J., and Arnheiter, H. (2000). Signaling and transcriptional regulation in the neural crest-derived melanocyte lineage: interactions between KIT and MITF. Development *127*, 5379–5389.

Hutton, S.M., and Spritz, R.A. (2008). A comprehensive genetic study of autosomal recessive ocular albinism in caucasian patients. Invest. Ophthalmol. Vis. Sci. *49*, 868–872.

Ishida, B.Y., Bailey, K.R., Duncan, K.G., Chalkley, R.J., Burlingame, A.L., Kane, J.P., and Schwartz, D.M. (2004). Regulated expression of apolipoprotein E by human retinal pigment epithelial cells. J. Lipid Res. *45*, 263–271.

Ito, A., Morii, E., Maeyama, K., Jippo, T., Kim, D.K., Lee, Y.M., Ogihara, H., Hashimoto, K., Kitamura, Y., and Nojima, H. (1998). Systematic method to obtain novel genes that are regulated by mi transcription factor: impaired expression of granzyme B and tryptophan hydroxylase in mi/mi cultured mast cells. Blood *91*, 3210–3221.

Ito, A., Jippo, T., Wakayama, T., Morii, E., Koma, Y., Onda, H., Nojima, H., Iseki, S., and Kitamura, Y. (2003). SgIGSF: a new mast-cell adhesion molecule used for attachment to fibroblasts and transcriptionally regulated by MITF. Blood *101*, 2601–2608.

Jippo, T., Morii, E., Tsujino, K., Tsujimura, T., Lee, Y.M., Kim, D.K., Matsuda, H., Kim, H.M., and Kitamura, Y. (1997). Involvement of transcription factor encoded by the mouse mi locus (MITF) in expression of p75 receptor of nerve growth factor in cultured mast cells of mice. Blood *90*, 2601–2608.

Jippo, T., Lee, Y.M., Katsu, Y., Tsujino, K., Morii, E., Kim, D.K., Kim, H.M., and Kitamura, Y. (1999). Deficient transcription of mouse mast cell protease 4 gene in mutant mice of mi/mi genotype. Blood *93*, 1942–1950.

Johansson, P., Pavey, S., and Hayward, N. (2007). Confirmation of a BRAF mutation-associated gene expression signature in melanoma. Pigment Cell Res. *20*, 216–221.

Kawaguchi, N., and Noda, M. (2000). Mitf is expressed in osteoclast progenitors in vitro. Exp. Cell Res. *260*, 284–291.

Kenny, J.J., Knobloch, T.J., Augustus, M., Carter, K.C., Rosen, C.A., and Lang, J.C. (1997). GRS, a novel member of the Bcl-2 gene family, is highly expressed in multiple cancer cell lines and in normal leukocytes. Oncogene *14*, 997–1001.

Kim, D.K., Morii, E., Ogihara, H., Hashimoto, K., Oritani, K., Lee, Y.M., Jippo, T., Adachi, S., Kanakura, Y., and Kitamura, Y. (1998). Impaired expression of integrin alpha-4 subunit in cultured mast cells derived from mutant mice of mi/mi genotype. Blood *92*, 1973–1980.

Kono, M., Dunn, I.S., Durda, P.J., Butera, D., Rose, L.B., Haggerty, T.J., Benson, E.M., and Kurnick, J.T. (2006). Role of the mitogen-activated protein kinase signaling pathway in the regulation of human melanocytic antigen expression. Mol Cancer Res *4*, 779–792.

Larribere, L., Hilmi, C., Khaled, M., Gaggioli, C., Bille, K., Auberger, P., Ortonne, J.P., Ballotti, R., and Bertolotto, C. (2005). The cleavage of microphthalmia-associated transcription factor, MITF, by caspases plays an essential role in melanocyte and melanoma cell apoptosis. Genes Dev. *19*, 1980–1985.

Lee, M., Goodall, J., Verastegui, C., Ballotti, R., and Goding, C.R. (2000). Direct regulation of the Microphthalmia promoter by Sox10 links Waardenburg-Shah syndrome (WS4)-associated hypopigmentation and deafness to WS2. J. Biol. Chem. *275*, 37978–37983.

Loercher, A.E., Tank, E.M., Delston, R.B., and Harbour, J.W. (2005). MITF links differentiation with cell cycle arrest in melanocytes by transcriptional activation of INK4A. J. Cell Biol. *168*, 35–40.

Loftus, S.K., Antonellis, A., Matera, I. et al. (2008). Gpnmb is a melanoblast-expressed, MITF-dependent gene. Pigment Cell Melanoma Res. In press.

Luchin, A., Purdom, G., Murphy, K., Clark, M.Y., Angel, N., Cassady, A.I., Hume, D.A., and Ostrowski, M.C. (2000). The microphthalmia transcription factor regulates expression of the tartrate-resistant acid phosphatase gene during terminal differentiation of osteoclasts. J. Bone Miner. Res. *15*, 451–460.

Magnoni, C., Tenedini, E., Ferrari, F. et al. (2007). Transcriptional profiles in melanocytes from clinically unaffected skin distinguish the neoplastic growth pattern in patients with melanoma. Br. J. Dermatol. *156*, 62–71.

McGill, G.G., Horstmann, M., Widlund, H.R. et al. (2002). Bcl2 regulation by the melanocyte master regulator Mitf modulates lineage survival and melanoma cell viability. Cell *109*, 707–718.

McGill, G.G., Haq, R., Nishimura, E.K., and Fisher, D.E. (2006). c-Met expression is regulated by Mitf in the melanocyte lineage. J. Biol. Chem. *281*, 10365–10373.

Meadows, N.A., Sharma, S.M., Faulkner, G.J., Ostrowski, M.C., Hume, D.A., and Cassady, A.I. (2007). The expression of Clcn7 and Ostm1 in osteoclasts is coregulated by microphthalmia transcription factor. J. Biol. Chem. *282*, 1891–1904.

Miller, A.J., Du, J., Rowan, S., Hershey, C.L., Widlund, H.R., and Fisher, D.E. (2004). Transcriptional regulation of the melanoma prognostic marker melastatin (TRPM1) by MITF in melanocytes and melanoma. Cancer Res. *64*, 509–516.

Morii, E., Tsujimura, T., Jippo, T., Hashimoto, K., Takebayashi, K., Tsujino, K., Nomura, S., Yamamoto, M., and Kitamura, Y. (1996). Regulation of mouse mast cell protease 6 gene expression by transcription factor encoded by the mi locus. Blood *88*, 2488–2494.

Morii, E., Jippo, T., Tsujimura, T., Hashimoto, K., Kim, D.K., Lee, Y.M., Ogihara, H., Tsujino, K., Kim, H.M., and Kitamura, Y. (1997). Abnormal expression of mouse mast cell protease 5 gene in cultured mast cells derived from mutant mi/mi mice. Blood *90*, 3057–3066.

Morii, E., Ogihara, H., Oboki, K., Sawa, C., Sakuma, T., Nomura, S., Esko, J.D., Handa, H., and Kitamura, Y. (2001). Inhibitory effect of the mi transcription factor encoded by the mutant mi allele on GA binding protein-mediated transcript expression in mouse mast cells. Blood *97*, 3032–3039.

Motyckova, G., Weilbaecher, K.N., Horstmann, M., Rieman, D.J., Fisher, D.Z., and Fisher, D.E. (2001). Linking osteopetrosis and pycnodysostosis: regulation of cathepsin K expression by the microphthalmia transcription factor family. Proc. Natl. Acad. Sci. U.S.A. *98*, 5798–5803.

Murakami, H., and Arnheiter, H. (2005). Sumoylation modulates transcriptional activity of MITF in a promoter-specific manner. Pigment Cell Res. *18*, 265–277.

Murakami, M., Ikeda, T., Saito, T., Ogawa, K., Nishino, Y., Nakaya, K., and Funaba, M. (2006). Transcriptional regulation of plasminogen activator inhibitor-1 by transforming growth factor-beta, activin A and microphthalmia-associated transcription factor. Cell Signal *18*, 256–265.

© 2008 The Authors, Journal Compilation © 2008 Blackwell Munksgaard

Nechushtan, H., Zhang, Z., and Razin, E. (1997). Microphthalmia (mi) in murine mast cells: regulation of its stimuli-mediated expression on the translational level. Blood *89*, 2999–3008.

Ochrietor, J.D., Clamp, M.F., Moroz, T.P., Grubb, J.H., Shah, G.N., Waheed, A., Sly, W.S., and Linser, P.J. (2005). Carbonic anhydrase XIV identified as the membrane CA in mouse retina: strong expression in Muller cells and the RPE. Exp. Eye Res. *81*, 492–500.

Park, H.Y., Wu, C., Yonemoto, L., Murphy-Smith, M., Wu, H., Stachur, C.M., and Gilchrest, B.A. (2006). MITF mediates cAMP-induced protein kinase C-beta expression in human melanocytes. Biochem. J. *395*, 571–578.

Piva, R., Pellegrino, E., Mattioli, M. et al. (2006). Functional validation of the anaplastic lymphoma kinase signature identifies CEBPB and BCL2A1 as critical target genes. J. Clin. Invest. *116*, 3171–3182.

Planque, N., Raposo, G., Leconte, L., Anezo, O., Martin, P., and Saule, S. (2004). Microphthalmia transcription factor induces both retinal pigmented epithelium and neural crest melanocytes from neuroretina cells. J. Biol. Chem. *279*, 41911–41917.

Prieto, V.G., Mourad-Zeidan, A.A., Melnikova, V. et al. (2006). Galectin-3 expression is associated with tumor progression and pattern of sun exposure in melanoma. Clin. Cancer Res. *12*, 6709–6715.

Ryu, B., Kim, D.S., Deluca, A.M., and Alani, R.M. (2007). Comprehensive expression profiling of tumor cell lines identifies molecular signatures of melanoma progression. PLoS ONE *2*, e594.

Sato-Jin, K., Nishimura, E.K., Akasaka, E. et al. (2007). Epistatic connections between microphthalmia-associated transcription factor and endothelin signaling in Waardenburg syndrome and other pigmentary disorders. FASEB J. *22*, 1155–1168.

Schwabe, M., Zhao, J., and Kung, H.F. (1994). Differential expression and ligand-induced modulation of the human interleukin-6 receptor on interleukin-6-responsive cells. J. Biol. Chem. *269*, 7201–7209.

de la Serna, I.L., Ohkawa, Y., Higashi, C., Dutta, C., Osias, J., Kommajosyula, N., Tachibana, T., and Imbalzano, A.N. (2006). The microphthalmia-associated transcription factor requires SWI/SNF enzymes to activate melanocyte-specific genes. J. Biol. Chem. *281*, 20233–20241.

So, H., Rho, J., Jeong, D., Park, R., Fisher, D.E., Ostrowski, M.C., Choi, Y., and Kim, N. (2003). Microphthalmia transcription factor and PU.1 synergistically induce the leukocyte receptor osteoclast-associated receptor gene expression. J. Biol. Chem. *278*, 24209–24216.

Steingrimsson, E., Copeland, N.G., and Jenkins, N.A. (2004). Melanocytes and the Microphthalmia Transcription Factor Network. Annu. Rev. Genet. *38*, 365–411.

Stolt, C.C., Rehberg, S., Ader, M., Lommes, P., Riethmacher, D., Schachner, M., Bartsch, U., and Wegner, M. (2002). Terminal differentiation of myelin-forming oligodendrocytes depends on the transcription factor Sox10. Genes Dev. *16*, 165–170.

Sundram, U., Harvell, J.D., Rouse, R.V., and Natkunam, Y. (2003). Expression of the B-cell proliferation marker MUM1 by melanocytic lesions and comparison with S100, gp100 (HMB45), and MelanA. Mod. Pathol. *16*, 802–810.

Tachibana, M. (1997). Evidence to suggest that expression of MITF induces melanocyte differentiation and haploinsufficiency of MITF causes Waardenburg syndrome type 2A. Pigment Cell Res. *10*, 25–33.

Truzzi, F., Marconi, A., Lotti, R., Dallaglio, K., French, L.E., Hempstead, B.L., and Pincelli, C. (2008). Neurotrophins and Their Receptors Stimulate Melanoma Cell Proliferation and Migration. J. Invest. Dermatol. *128*, 2031–2040.

Tsujimura, T., Morii, E., Nozaki, M., Hashimoto, K., Moriyama, Y., Takebayashi, K., Kondo, T., Kanakura, Y., and Kitamura, Y. (1996). Involvement of transcription factor encoded by the mi locus in the expression of c-kit receptor tyrosine kinase in cultured mast cells of mice. Blood *88*, 1225–1233.

Ugurel, S., Houben, R., Schrama, D., Voigt, H., Zapatka, M., Schadendorf, D., Brocker, E.B., and Becker, J.C. (2007). Microphthalmia-associated transcription factor gene amplification in metastatic melanoma is a prognostic marker for patient survival, but not a predictive marker for chemosensitivity and chemotherapy response. Clin. Cancer Res. *13*, 6344–6350.

Vetrini, F., Auricchio, A., Du, J., Angeletti, B., Fisher, D.E., Ballabio, A., and Marigo, V. (2004). The microphthalmia transcription factor (Mitf) controls expression of the ocular albinism type 1 gene: link between melanin synthesis and melanosome biogenesis. Mol. Cell. Biol. *24*, 6550–6559.

Wagner, K.W., Punnoose, E.A., Januario, T. et al. (2007). Death-receptor O-glycosylation controls tumor-cell sensitivity to the proapoptotic ligand Apo2L/TRAIL. Nat. Med. *13*, 1070–1077.

Wang, R., Tang, P., Wang, P., Boissy, R.E., and Zheng, H. (2006). Regulation of tyrosinase trafficking and processing by presenilins: partial loss of function by familial Alzheimer's disease mutation. Proc. Natl. Acad. Sci. U.S.A. *103*, 353–358.

Weeraratna, A.T., Becker, D., Carr, K.M. et al. (2004). Generation and analysis of melanoma SAGE libraries: SAGE advice on the melanoma transcriptome. Oncogene *23*, 2264–2274.

de Wit, N.J., Rijntjes, J., Diepstra, J.H., van Kuppevelt, T.H., Weidle, U.H., Ruiter, D.J., and van Muijen, G.N. (2005). Analysis of differential gene expression in human melanocytic tumour lesions by custom made oligonucleotide arrays. Br. J. Cancer *92*, 2249–2261.

Wu, M., Hemesath, T.J., Takemoto, C.M., Horstmann, M.A., Wells, A.G., Price, E.R., Fisher, D.Z., and Fisher, D.E. (2000). c-Kit triggers dual phosphorylations, which couple activation and degradation of the essential melanocyte factor Mi. Genes Dev. *14*, 301–312.

Xu, W., Gong, L., Haddad, M.M., Bischof, O., Campisi, J., Yeh, E.T., and Medrano, E.E. (2000). Regulation of microphthalmia-associated transcription factor MITF protein levels by association with the ubiquitin-conjugating enzyme hUBC9. Exp. Cell Res. *255*, 135–143.

Yasumoto, K., Takeda, K., Saito, H., Watanabe, K., Takahashi, K., and Shibahara, S. (2002). Microphthalmia-associated transcription factor interacts with LEF-1, a mediator of Wnt signaling. EMBO J. *21*, 2703–2714.

Supporting information

Additional Supporting Information may be found in the online version of this article:

Table S1 Genes undergoing significant upregulation on transfection of SK-MEL-28 with an Mitf-expressing vector.

Table S2 One hundred and ten genes with significant and strong correlation with *MITF* expression.

Table S3 Probable false negatives (correlation in four to six of seven data sets plus significant upregulation on Mitf-transfection of SK-MEL-28).

Please note: Wiley-Blackwell are not responsible for the content or functionality of any supporting materials supplied by the authors. Any queries (other than missing material) should be directed to the corresponding author for the article.

© 2008 The Authors, Journal Compilation © 2008 Blackwell Munksgaard

6. Discussion

Rene Laennec, who invented the stethoscope in 1819, described melanoma as a disease in 1806, and used the name melanoma for the first time in a publication in 1812 (Laennec, 1812). But as far back as the fifth century B.C., the famous Greek physician Hippocrates referred to a “black cancer” and “fatal black tumors”. In former times, moles and other birthmarks were associated with religion and magic rather than with medical conditions (Bennett and Hall, 1994). As late as the 17th century, a publication stated that the color of a mole and its position on the body could be used to predict the character of a person (Saunders, 1671) and even revealed murderers and liars. Melanomas have also been found on mummies of the pre-Colombian Incas in Peru (Urteaga and Pack, 1966). Despite a long history of recognizing melanoma, to date there is no cure. Until recently the median survival time for a patient with metastatic melanoma was 8-9 months with a 3-year overall survival rate of less than 15% (Balch et al., 2009). In the past few years new treatments have been developed that increase overall survival; (Bollag et al., 2010; Robert et al., 2011) unfortunately, resistance still develops in almost all cases. Understanding intra- and inter-tumoral heterogeneity is critical to being able to target all described genetic and epigenetic subsets of melanoma cells to completely cure this disease. Melanoma cells have been found to be highly plastic on multiple levels, able to change phenotype, dedifferentiate into stem-cell like states and even contribute to neovascularisation of a tumor (Hendrix et al., 2003; Hendrix et al., 2007; Mihic-Probst et al., 2012). Although a plethora of mutations has been reported for melanoma, so far no mutation seems to be required for either melanoma initiation or progression (Flaherty and Fisher, 2011).

The main aim of my thesis was to find a trigger for melanoma phenotype switching between proliferative and invasive states. Hypoxia was considered to be a good candidate for a microenvironmental factor capable of inducing an EMT-like process in proliferative melanoma cells to establish an invasive phenotype. Our results demonstrated that hypoxia can alter multiple characteristics of proliferative melanoma cells so that they more closely resemble the invasive phenotype. Microarray experiments revealed a change in gene expression of multiple

important factors possibly involved in a switch. We showed that *in vitro* invasion increased in a dose-dependent fashion, indicating that the gene expression changes are followed by functional adaptations of the cells, allowing them to digest ECM and possibly leave their surroundings.
The phenotype switching model proposes that the microenvironment of the tumor cells causes the melanoma cells to switch between two phenotypes of proliferation and invasion and thereby drive tumor progression. The data presented in this study and by others (Cheli et al., 2012; Feige et al., 2011) suggest that tumor hypoxia serves as a possible trigger for the switch from a differentiated, pigment-producing melanoma cell to a dedifferentiated, stem cell-like melanoma cell. Interestingly, hypoxia did not seem to have an impact on already invasive melanoma cells, suggesting a state-specific potential to respond to hypoxic microenvironments. Moreover, in our microarray experiments, the transcriptional effects of hypoxia on invasive cells were marginal, and *in vitro* invasion was not altered upon hypoxia treatment.

We believe that by conducting high-throughput gene expression analysis we can gain important insight into melanoma progression. Online databases contain data from thousands of microarray experiments. Such a large collection of samples allows simultaneous meta-analyses of many datasets to look for patterns across experiments and platforms. Although each of these studies were done to test a specific hypothesis, the fact that microarrays allow a global view of gene expression provides a great opportunity to apply different questions and analytic tools to better understand melanoma biology. Thus, another aim of this thesis was to use microarray data to expand our knowledge on melanoma phenotypic heterogeneity. In this project we developed an online tool that allows us to predict the phenotype of a melanoma cell line by correlating its gene expression signature to previously defined standards of proliferative and invasive phenotype cell lines (Widmer et al., 2012). We found a close correlation of the computationally predicted phenotypes to the classically defined phenotypes using *in vitro* experimentation. This gave us confidence that our heuristic online phenotype prediction (HOPP) tool had both theoretical and practical utility. Previous to this work, the proportion of proliferative and invasive phenotype cell lines was unknown. Furthermore, it was unclear if many intermediate steps are required for

the switch or if the phenotype correlates with other characteristics of the cell lines, such as the mutation status of certain genes. We were able to answer all of these questions, and made our tool publicly available, in the hope that it will become a more standard technique for classification of the heterogeneity of new melanoma cell lines.

One unanticipated, but very interesting result of this project was the finding that the switch between the phenotypes appears to be rather fast, at least *in vitro*. In addition, the switch seems to be, for the most part, a binary one defined by two mutually exclusive states. This conclusion is strengthened by the finding that there were only very few cell lines that do not fall into one of these two states. For untreated cell cultures this might be expected, but we also looked at treated cell lines that experienced all kinds of different experimental perturbations. A somewhat troubling observation was that independent replicates of commonly used cell lines exhibited a high variance in gene expression, whereas replicates of other cell lines were very homogenous in their expression patterns. This may be due to inconsistencies in the labeling, sharing, and experimental use of many commonly studied cell lines. In melanoma research, cell lines are the most standard tool for understanding melanoma progression. Many of them have been used for several decades and shipped around between many labs. The implication of our work here is that early passage melanoma cell cultures might be a much better tool to study human melanoma than standard cell lines. Finally, the heuristic approach that we developed here could be adapted to easily and quickly discriminate between cell lines or cultures in which the expression of a set of genes discriminates between two states.

Originally we were also interested in a clinical application of this tool. For this reason we tested hundreds of samples derived from tumors instead of cell lines or cultures. It turned out that many of them show intermediate expression signatures. Furthermore, the predicted phenotype did not correlate to any clinical factor we tested. We believe that this is due to the fact that melanoma tumors comprise a mixture of the two phenotypes, resulting in intermediate gene expression signatures. Results presented in this thesis support the hypothesis that melanoma tumors are typically made up of mixtures of invasive and proliferative phenotype cells. Thus the binary phenotypic states we observe *in vitro* represent two forms of heterogeneous variables present in most melanoma tumors.

In the future, microarrays will probably be replaced by sequencing methods like RNA-sequencing, which will allow for a much more comprehensive analysis of gene expression. Already now a lot of studies use these new techniques, and as soon as the prices come down further the use of microarrays will diminish. Although the techniques change, the bioinformatics approach will stay largely the same. Another technique that is gaining attention is high throughput qRT-PCR. Instead of observing one gene at a time, new methods allow the analysis of hundreds of genes in one run. We are currently developing a phenotype prediction method based on a qRT-PCR array, which was custom made but is commercially available. This method is faster, less costly and easier to interpret than microarrays.

Unfortunately, some questions cannot be answered by the use of *in vitro* models, which is why animal models are still essential to study certain aspects of cancer research. Melanoma models have been developed in hamster (DELLA PORTA et al., 1956), Xiphophorus hybrid fish, South American opossum (Dlugosz et al., 2002; Kusewitt and Ley, 1996; Ley, 2002), guinea pig (Pawlowski et al., 1980), Sinclair swine (Hook et al., 1982), Camargue horses (Fleury et al., 2000), Angora goat (Green et al., 1996), dogs and cats (MacEwen, 1990), and in the most widely employed model organism, - the mouse (Benjamin et al., 2007; Larue and Beermann, 2007; Zaidi et al., 2008). All of these models have the disadvantage that the resulting tumors do not fully resemble human cutaneous melanoma. Therefore, we developed a fully orthotopic humanized *in vivo* model for melanoma that recapitulates human disease initiation and progression as closely as possible. Based on a system that was developed to reconstitute human skin *in vitro* (Braziulis et al., 2012; Pontiggia et al., 2008), this project was a collaboration of two groups doing research in melanoma and a laboratory of the University of Zurich Children's Hospital (Kiowski et al., 2012). The rat as a host animal for the engrafted skin constructs has the advantage of an increased available area compared to mice. In addition, it is a fully humanized microenvironment. The major cell types used to construct the skin as well as the melanoma cells can be manipulated. The environment of the melanoma cells very closely resembles the situation of a cutaneous melanoma in the human patient compared to, for instance, a subcutaneous injection of melanoma cells into a mouse. With this

model, all stages from disease initiation to progression, also the very early steps of melanoma development, can be observed. The type of animal model that is used in a particular project can be critical for the outcome of a study. This could nicely be seen in two studies that both identified BHLHE40 as the factor being responsible for a HIF1α-mediated down-regulation of MITF in melanoma. Both studies showed very similar results, but because of a different *in vivo* method, their conclusions were oppositional. Feige et al. treated mice with DMOG, which is stabilizing HIF1α, and observed a downregulation of MITF followed by a decrease in melanoma growth. Thus, they suggested a MITF-targeted melanoma therapy to treat melanoma. Cheli et al. on the other hand found that hypoxia treated cells produce larger tumors and more metastases, leading to the conclusion that the downregulation of MITF was a pro-metastatic event. Treating the mice with a HIF1α stabilizing compound lead to an increase in tumor growth, whereas treating the melanoma cells with hypoxia prior to injection of the tumor cells decreased tumor growth.
The rat model we developed still lacks some important characteristics: the formation of distant metastasis and the interaction with the host immune system are as yet not possible to investigate with this method.

The loss of melanocytic markers during the switch of proliferative to invasive phenotype melanoma cells is considered a critical event in melanoma progression (Goodall et al., 2008; Javelaud et al., 2011; Roesch et al., 2010). Originally the hypothesis was that the downregulation of melanocytic genes in the switch from proliferative to invasive melanoma cells is caused by a reduction of β-catenin through interruption of canonical WNT signaling. The study presented in this work showed that β-catenin is not altered, but two of its co-factors are differentially and inversely expressed in the proliferative and invasive phenotype (Eichhoff et al., 2011). Knocking down these factors changed the expression of proliferative and invasive marker genes independently of β-catenin. In the invasive phenotype, TCF4 is upregulated, increasing cell invasiveness and WNT5A expression independent of β-catenin. WNT5A expression inhibits LEF1 expression, leading to a down-regulation of melanocytic markers and an increase in invasiveness. It also leads to the formation of stress fibers, a reorganization of the actin filaments in invasive cell cultures, and when overexpressed in the proliferative cell cultures to

increased cell motility and invasion. This is caused by a dissociation of β-catenin from the cell membrane to a cytosolic localization of β-catenin. The exact mechanisms that induce this process are unknown. We speculate that microenvironmental factors like hypoxia induce TGFβ signaling, which activates WNT5A, leading to suppression of LEF1 and thereby a switch to the invasive phenotype.

Microphthalmia-associated transcription factor (MITF) is probably the most discussed gene/protein in melanoma research. Due to the obviously very important role of MITF in melanoma cell phenotypes and thus in disease progression, we performed a study based on microarray data to find new potential targets of the transcription factor MITF. Since the publication of this study, several potential targets have been confirmed by other groups.

MITF is critical for melanoblast survival and differentiation (Bharti et al., 2006; Hodgkinson et al., 1993). In melanocytes, this transcription factor and its target genes are not only important for development and survival, but also for melanosome biogenesis, melanin production, the transport of pigment to the keratinocytes, and for dendritogenesis (Cheli et al., 2010; Steingrímsson et al., 2004; Vance and Goding, 2004). MITF is also a key transcription factor controlling various aspects of melanoma cell biology, including pigment production, cell cycle regulation, migration and survival (Steingrímsson et al., 2004). MITF seems to have a dual role in melanoma. It is implicated in activating the expression of differentiation genes and of induction of cell cycle arrest by upregulation of p16 (CDKN2A) and p21 (CDKN1A) (Carreira et al., 2005; Du et al., 2004; Loercher et al., 2005). Furthermore, the *MITF* gene is amplified in melanoma, which is associated with poor patient survival. Since it can enhance cell division and suppress invasiveness it is called a “lineage-addiction oncogene” (Garraway et al., 2005). Based on these observations Carreira et al. proposed a rheostat model in which low levels of MITF induce a G1 arrested stem-like state, whereas MITF positive cells proliferate and differentiate (Carreira et al., 2006). We found that MITF and many of its targets are highly expressed in the proliferative phenotype, but completely down-regulated in the invasive phenotype melanoma cells (Eichhoff et al., 2011; Eichhoff et al., 2010; Hoek et al., 2008; Hoek et al., 2006; Widmer et al., 2012; Zipser et al., 2011). In every treatment, which induces a

switch to a more invasive phenotype, we found a decrease in MITF expression. For instance, in hypoxia treated cells, MITF and several known and potential targets are sharply down-regulated. This suggests a crucial role for the loss of MITF in phenotype switching.

A down-regulation of MITF could also be observed when proliferative melanoma cells were treated with two unspecific tyrosine kinase inhibitors. These two drugs are used for melanoma therapy, because they target the MAPK pathway, which is frequently activated in melanoma by *RAF/RAS* mutations. This pathway has been shown to be important in melanoma proliferation, survival and migration (Fecher et al., 2008). A treatment of proliferative melanoma cells resulted in a change in phenotype, independent of mutation status of the cell culture. Invasive melanoma cell cultures were significantly more resistant than proliferative cells. This might explain the frequently observed resistance to these treatments. The proliferative cells are targeted and die, which leads to shrinkage of the tumor mass, but the surviving invasive cells subsequently induce a relapse. Since this article was published, new promising drugs have been presented that specifically target mutated BRAF. Unfortunately, also in these treatments, relapses are very common and currently subject of many studies.

The hunt for a predictive marker that is correlated with the response of a patient to a certain treatment has been going on for many years. In addition, researchers have tried to identify markers common to all melanoma cells to make them more universally targetable. So far, no protein expressed by melanoma cells appears to be useful for immunotherapy. It is widely accepted that melanoma comprises different subsets of cells with different progression potential. Over time multiple genes with a potential role in melanoma heterogeneity have been identified.
The first study to describe subsets of melanoma cells based on gene expression analysis was Bittner et al. in the year 2000 (Bittner et al., 2000). They classified melanoma cell lines and biopsies by performing DNA microarray experiments resulting in clusters very similar to the proliferative and invasive phenotypes described by our lab. The set of genes discriminating between the two subsets of melanoma cells is similar to the MPSE-list described in our study (Widmer et al., 2012). Among them are *MELANA* and *WNT5A*, which best define the clusters.

Bittner et al. (2000) found that these two subsets of melanoma cells also differ in cell motility and in their ability to form primitive tubular networks. A similar assay is also used in our laboratory to distinguish between the two phenotypes. Microarrays turned out to be a good method to find melanoma subsets with differential gene expression patterns. Freedman et al. conducted a study purely based on microarray data in which they described the heterogeneity of melanoma. By performing extended clustering experiments, gene set enrichment analysis, and pathway analysis of primary and metastatic tissue samples as well as cell lines they found multiple subgroups of primary and metastatic melanoma (Freedman et al., 2011). These data were also analyzed by us with the heuristic online phenotype prediction tool (HOPP) (Widmer et al., 2012). When reduced to cell lines, two of their cohorts corresponded to the proliferative and invasive phenotypes, respectively. Next to gene signatures, single genes could also be found to characterize melanoma subsets important for melanoma progression. One of them is *KDM5B* (*JARID1B*), described by Roesch et al. (Roesch et al., 2010). They showed that this H3K4 demethylase is expressed in a small subpopulation of slow-cycling melanoma cells and is necessary for continuous tumor growth. Knocking down *KDM5B* resulted in the attenuation of tumor growth, thus suggesting an essential role for this gene in tumor maintenance. KDM5B seems to have all the characteristics of a typical cancer stem cell (CSC) marker, but the results of this study show that this model is much more plastic than the CSC model. KDM5B-negative cells are able to become positive for the marker and even single cells are able to induce a tumor. Jane Goodall and coworkers described a subpopulation of melanoma cells that is positive for POU3F2 (BRN2), which is upregulated by MAPK and β-catenin (Goodall et al., 2004a; Goodall et al., 2004b). In this subgroup MITF expression is repressed by BRN2 and invasiveness is increased (Goodall et al., 2008). A subsequent study by Pinner et al. identified a less differentiated BRN2-high population of non-pigmented cells among the melanoma cells, which are motile and capable of intravasation. In a secondary, metastatic site, the population included again more differentiated and pigmented cells, suggesting a reversible switch between two different subgroups of melanoma cells during metastasis *in vivo*. A closer analysis of the less differentiated cells revealed an increase in TGFβ signaling (Pinner et al., 2009). In many of these studies, MITF was only found in one of the two populations. Also in

a recently published study by Cheli et al., a slow growing, MITF-low subpopulation was discovered in melanoma. These MITF-low cells can be found in melanoma cell lines expressing MITF and have a demonstrated increase in tumorigenic potential. They showed that knocking down MITF leads to increased tumor formation in mice (Cheli et al., 2011). In a subsequent study they confirmed and strengthened the pro-metastatic role of the MITF-low melanoma cell population (Cheli et al., 2012). In agreement with our own research, Javelaud et al. found the transcription factor GLI2 to be upregulated in a non-pigmented subgroup of melanoma cells (Javelaud et al., 2011). GLI2, a TGFβ/SMAD target, is an important mediator of the Hedgehog pathway and is associated with increased invasiveness and metastatic potential (Alexaki et al., 2010). This study concludes that GLI2 and MITF antagonize each other and are exclusively expressed in two subgroups of melanoma cells. In contrast to the previously mentioned studies from Goodall and Cheli et al., in this study they do not differentiate between cells within a cell line, but rather between cell lines. A meta-analysis by our laboratory showed that GLI2-high cell lines belong to the invasive phenotype melanoma cell lines, whereas the GLI2-low cell lines comprise the proliferative phenotype melanoma cell lines.

Taken together, these results suggest that MITF-low cells might represent a fraction of melanoma cells with increased tumorigenicity necessary for tumor maintenance *in vivo*. Other important work in identifying important markers in the process of dedifferentiating melanoma cells was published by the laboratory of Mary JC Hendrix. They have shown in many publications that aggressive melanoma tumor cells exhibit a plastic, multipotent phenotype, very similar to embryonic stem cells (Hendrix et al., 2007). Specifically, the ability to form a growth pattern resembling an endothelial network called vasculogenic mimicry is considered a characteristics of aggressive melanoma cells (Hendrix et al., 2003). Postovit et al. published a study where they reprogrammed melanoma cells by the microenvironment of human embryonic stem cells (hESCs). They found that in aggressive melanoma cells, Nodal is often upregulated and the reprogramming by hESCs leads to a suppression of Nodal with subsequent reduction of proliferation, clonogenic potential and tumorigenicity (Postovit et al., 2008). Mihic-Probst et al. recently provided evidence for a contribution of melanoma cells to neovascularisation and vasculogenic mimicry (Mihic-Probst et al., 2012). The term

“vasculogenic mimicry” is somewhat misleading, since it often does not imply a morphological or topological resemblance to blood vessels, but only the formation of a network-like growth pattern of the melanoma cells.
Thus, studies from many laboratories and our own recent results suggest that melanoma tumors are heterogeneous for cell phenotypes which have different progression potential Not all of these models are completely compatible with our results or with each other, but it is clear that in order to develop a therapy for metastatic melanoma it is important to understand these different subgroups.

An important question that was not addressed in this thesis is what maintains the melanoma cells in a particular phenotypic state. The culture conditions for both phenotypes *in vitro* are identical and there is no factor in the environment necessary to maintain any of the two phenotypes. Also, so far we did not see a spontaneous switch of melanoma cells in culture. This system of adaptation seems to be very plastic and flexible *in vivo*, but *in vitro* it takes a severe intervention to push the cells into another phenotype. We think that a possible mechanism for this could be epigenetic reprogramming, as DNA methylation provides a stable yet reversible gene silencing mechanism involved in regulating gene expression and chromatin architecture (Bird, 2002).
In melanoma, promoter hypermethylation as well as global hypomethylation has been reported (Sigalotti et al., 2002b). Genes encoding factors involved in several signaling pathways critical to tumor progression were shown to have hypermethylated promoters, including the *APC* (Worm et al., 2004), *PTEN* (Mirmohammadsadegh et al., 2006), *CDKN2A* (Gonzalgo et al., 1997) and *RASS1FA* (Spugnardi et al., 2003) genes.

Although genome-wide hypomethylation has been observed in melanoma, little is known about its role in tumor initiation and progression (Sigalotti et al., 2002a). It has been postulated that hypomethylation in cancer contributes to genome instability via the demethylation of transposons and pericentromeric repeats and also by inducing the expression of oncogenes (Nishigaki et al., 2005). Recently, Deng et al. demonstrated that the *de novo* methyltransferase, DNMT3a, was essential for melanoma growth and metastasis *in vivo* (Deng et al., 2009). The results from their study suggest that *de novo* methylation is required by the tumor cells to adapt to the microenvironment and to invade to secondary locations, thus

raising the possibility that DNA methylation could play a role in allowing the melanoma cells to switch phenotype during melanoma progression. Interestingly, hypoxia has been shown to induce a loss of global methylation in melanoma (Shahrzad et al., 2007). Thus, the transcriptional signatures we have identified to be predictive of the phenotypic state of melanoma cells may result from large-scale epigenetic modifications in the genome, which themselves are responses to variations in microenvironmental cues that trigger intratumor melanoma heterogeneity. We are currently investigating the role of methylation in the phenotype switching model.

6.1 References

Alexaki, V. I., Javelaud, D., Van Kempen, L. C., Mohammad, K. S., Dennler, S., Luciani, F., Hoek, K. S., Juàrez, P., Goydos, J. S., Fournier, P. J*., et al.* (2010). GLI2-mediated melanoma invasion and metastasis. J Natl Cancer Inst *102*, 1148-1159.

Balch, C. M., Gershenwald, J. E., Soong, S. J., Thompson, J. F., Atkins, M. B., Byrd, D. R., Buzaid, A. C., Cochran, A. J., Coit, D. G., Ding, S*., et al.* (2009). Final version of 2009 AJCC melanoma staging and classification. J Clin Oncol *27*, 6199-6206.

Benjamin, C. L., Melnikova, V. O., and Ananthaswamy, H. N. (2007). Models and mechanisms in malignant melanoma. Mol Carcinog *46*, 671-678.

Bennett, J. P., and Hall, P. (1994). Moles and melanoma: a history. Ann R Coll Surg Engl *76*, 373-380.

Bharti, K., Nguyen, M. T., Skuntz, S., Bertuzzi, S., and Arnheiter, H. (2006). The other pigment cell: specification and development of the pigmented epithelium of the vertebrate eye. Pigment Cell Res *19*, 380-394.

Bird, A. (2002). DNA methylation patterns and epigenetic memory. Genes Dev *16*, 6-21.

Bittner, M., Meltzer, P., Chen, Y., Jiang, Y., Seftor, E., Hendrix, M., Radmacher, M., Simon, R., Yakhini, Z., Ben-Dor, A*., et al.* (2000). Molecular classification of cutaneous malignant melanoma by gene expression profiling. Nature *406*, 536-540.

Bollag, G., Hirth, P., Tsai, J., Zhang, J., Ibrahim, P. N., Cho, H., Spevak, W., Zhang, C., Zhang, Y., Habets, G*., et al.* (2010). Clinical efficacy of a RAF inhibitor needs broad target blockade in BRAF-mutant melanoma. Nature *467*, 596-599.

Braziulis, E., Diezi, M., Biedermann, T., Pontiggia, L., Schmucki, M., Hartmann-Fritsch, F., Luginbühl, J., Schiestl, C., Meuli, M., and Reichmann, E. (2012). Modified Plastic Compression of Collagen Hydrogels Provides an Ideal Matrix for Clinically Applicable Skin Substitutes. Tissue Eng Part C Methods.

Carreira, S., Goodall, J., Aksan, I., La Rocca, S. A., Galibert, M. D., Denat, L., Larue, L., and Goding, C. R. (2005). Mitf cooperates with Rb1 and activates p21Cip1 expression to regulate cell cycle progression. Nature *433*, 764-769.

Carreira, S., Goodall, J., Denat, L., Rodriguez, M., Nuciforo, P., Hoek, K. S., Testori, A., Larue, L., and Goding, C. R. (2006). Mitf regulation of Dia1 controls melanoma proliferation and invasiveness. Genes Dev *20*, 3426-3439.

Cheli, Y., Giuliano, S., Fenouille, N., Allegra, M., Hofman, V., Hofman, P., Bahadoran, P., Lacour, J. P., Tartare-Deckert, S., Bertolotto, C., and Ballotti, R. (2012). Hypoxia and MITF control metastatic behaviour in mouse and human melanoma cells. Oncogene *31*, 2461-2470.

Cheli, Y., Giuliano, S., Guiliano, S., Botton, T., Rocchi, S., Hofman, V., Hofman, P., Bahadoran, P., Bertolotto, C., and Ballotti, R. (2011). Mitf is the key molecular switch between mouse or human melanoma initiating cells and their differentiated progeny. Oncogene *30*, 2307-2318.

Cheli, Y., Ohanna, M., Ballotti, R., and Bertolotto, C. (2010). Fifteen-year quest for microphthalmia-associated transcription factor target genes. Pigment Cell Melanoma Res *23*, 27-40.

DELLA PORTA, G., RAPPAPORT, H., SAFFIOTTI, U., and SHUBIK, P. (1956). Induction of melanotic lesions during skin carcinogenesis in hamsters. AMA Arch Pathol *61*, 305-313.

Deng, T., Kuang, Y., Wang, L., Li, J., Wang, Z., and Fei, J. (2009). An essential role for DNA methyltransferase 3a in melanoma tumorigenesis. Biochem Biophys Res Commun *387*, 611-616.

Dlugosz, A., Merlino, G., and Yuspa, S. H. (2002). Progress in cutaneous cancer research. J Investig Dermatol Symp Proc *7*, 17-26.

Du, J., Widlund, H. R., Horstmann, M. A., Ramaswamy, S., Ross, K., Huber, W. E., Nishimura, E. K., Golub, T. R., and Fisher, D. E. (2004). Critical role of CDK2 for melanoma growth linked to its melanocyte-specific transcriptional regulation by MITF. Cancer Cell *6*, 565-576.

Eichhoff, O. M., Weeraratna, A., Zipser, M. C., Denat, L., Widmer, D. S., Xu, M., Kriegl, L., Kirchner, T., Larue, L., Dummer, R., and Hoek, K. S. (2011). Differential LEF1 and TCF4 expression is involved in melanoma cell phenotype switching. Pigment Cell Melanoma Res *24*, 631-642.
Eichhoff, O. M., Zipser, M. C., Xu, M., Weeraratna, A. T., Mihic, D., Dummer, R., and Hoek, K. S. (2010). The immunohistochemistry of invasive and proliferative phenotype switching in melanoma: a case report. Melanoma Res *20*, 349-355.
Fecher, L. A., Amaravadi, R. K., and Flaherty, K. T. (2008). The MAPK pathway in melanoma. Curr Opin Oncol *20*, 183-189.
Feige, E., Yokoyama, S., Levy, C., Khaled, M., Igras, V., Lin, R. J., Lee, S., Widlund, H. R., Granter, S. R., Kung, A. L., and Fisher, D. E. (2011). Hypoxia-induced transcriptional repression of the melanoma-associated oncogene MITF. Proc Natl Acad Sci U S A *108*, E924-933.
Flaherty, K. T., and Fisher, D. E. (2011). New strategies in metastatic melanoma: oncogene-defined taxonomy leads to therapeutic advances. Clin Cancer Res *17*, 4922-4928.
Fleury, C., Bérard, F., Leblond, A., Faure, C., Ganem, N., and Thomas, L. (2000). The study of cutaneous melanomas in Camargue-type gray-skinned horses (2): epidemiological survey. Pigment Cell Res *13*, 47-51.
Freedman, J. A., Tyler, D. S., Nevins, J. R., and Augustine, C. K. (2011). Use of gene expression and pathway signatures to characterize the complexity of human melanoma. Am J Pathol *178*, 2513-2522.
Garraway, L. A., Widlund, H. R., Rubin, M. A., Getz, G., Berger, A. J., Ramaswamy, S., Beroukhim, R., Milner, D. A., Granter, S. R., Du, J.*, et al.* (2005). Integrative genomic analyses identify MITF as a lineage survival oncogene amplified in malignant melanoma. Nature *436*, 117-122.
Gonzalgo, M. L., Bender, C. M., You, E. H., Glendening, J. M., Flores, J. F., Walker, G. J., Hayward, N. K., Jones, P. A., and Fountain, J. W. (1997). Low frequency of p16/CDKN2A methylation in sporadic melanoma: comparative approaches for methylation analysis of primary tumors. Cancer Res *57*, 5336-5347.
Goodall, J., Carreira, S., Denat, L., Kobi, D., Davidson, I., Nuciforo, P., Sturm, R. A., Larue, L., and Goding, C. R. (2008). Brn-2 represses microphthalmia-associated transcription factor expression and marks a distinct subpopulation of microphthalmia-associated transcription factor-negative melanoma cells. Cancer Res *68*, 7788-7794.
Goodall, J., Martinozzi, S., Dexter, T. J., Champeval, D., Carreira, S., Larue, L., and Goding, C. R. (2004a). Brn-2 expression controls melanoma proliferation and is directly regulated by beta-catenin. Mol Cell Biol *24*, 2915-2922.
Goodall, J., Wellbrock, C., Dexter, T. J., Roberts, K., Marais, R., and Goding, C. R. (2004b). The Brn-2 transcription factor links activated BRAF to melanoma proliferation. Mol Cell Biol *24*, 2923-2931.
Green, A., Neale, R., Kelly, R., Smith, I., Ablett, E., Meyers, B., and Parsons, P. (1996). An animal model for human melanoma. Photochem Photobiol *64*, 577-580.
Hendrix, M. J., Seftor, E. A., Hess, A. R., and Seftor, R. E. (2003). Vasculogenic mimicry and tumour-cell plasticity: lessons from melanoma. Nat Rev Cancer *3*, 411-421.
Hendrix, M. J., Seftor, E. A., Seftor, R. E., Kasemeier-Kulesa, J., Kulesa, P. M., and Postovit, L. M. (2007). Reprogramming metastatic tumour cells with embryonic microenvironments. Nat Rev Cancer *7*, 246-255.
Hodgkinson, C. A., Moore, K. J., Nakayama, A., Steingrímsson, E., Copeland, N. G., Jenkins, N. A., and Arnheiter, H. (1993). Mutations at the mouse microphthalmia locus are associated with defects in a gene encoding a novel basic-helix-loop-helix-zipper protein. Cell *74*, 395-404.
Hoek, K. S., Eichhoff, O. M., Schlegel, N. C., Dobbeling, U., Kobert, N., Schaerer, L., Hemmi, S., and Dummer, R. (2008). In vivo switching of human melanoma cells between proliferative and invasive states. Cancer Res *68*, 650-656.
Hoek, K. S., Schlegel, N. C., Brafford, P., Sucker, A., Ugurel, S., Kumar, R., Weber, B. L., Nathanson, K. L., Phillips, D. J., Herlyn, M.*, et al.* (2006). Metastatic potential of melanomas defined by specific gene expression profiles with no BRAF signature. Pigment Cell Res *19*, 290-302.

Hook, R. R., Berkelhammer, J., and Oxenhandler, R. W. (1982). Melanoma: Sinclair swine melanoma. Am J Pathol *108*, 130-133.
Javelaud, D., Alexaki, V. I., Pierrat, M. J., Hoek, K. S., Dennler, S., Van Kempen, L., Bertolotto, C., Ballotti, R., Saule, S., Delmas, V., and Mauviel, A. (2011). GLI2 and M-MITF transcription factors control exclusive gene expression programs and inversely regulate invasion in human melanoma cells. Pigment Cell Melanoma Res *24*, 932-943.
Kiowski, G., Biedermann, T., Widmer, D. S., Civenni, G., Burger, C., Dummer, R., Sommer, L., and Reichmann, E. (2012). Engineering melanoma progression in a humanized environment in vivo. J Invest Dermatol *132*, 144-153.
Kusewitt, D. F., and Ley, R. D. (1996). Animal models of melanoma. Cancer Surv *26*, 35-70.
Laennec, R. (1812). Extrait au Memoire de M Laennec, sur les
melanoses. In, (Bulletins de L'Ecole et de la Socidtd de Medicine,
Paris).
Larue, L., and Beermann, F. (2007). Cutaneous melanoma in genetically modified animals. Pigment Cell Res *20*, 485-497.
Ley, R. D. (2002). Animal models of ultraviolet radiation (UVR)-induced cutaneous melanoma. Front Biosci *7*, d1531-1534.
Loercher, A. E., Tank, E. M., Delston, R. B., and Harbour, J. W. (2005). MITF links differentiation with cell cycle arrest in melanocytes by transcriptional activation of INK4A. J Cell Biol *168*, 35-40.
MacEwen, E. G. (1990). Spontaneous tumors in dogs and cats: models for the study of cancer biology and treatment. Cancer Metastasis Rev *9*, 125-136.
Mihic-Probst, D., Ikenberg, K., Tinguely, M., Schraml, P., Behnke, S., Seifert, B., Civenni, G., Sommer, L., Moch, H., and Dummer, R. (2012). Tumor cell plasticity and angiogenesis in human melanomas. PLoS One *7*, e33571.
Mirmohammadsadegh, A., Marini, A., Nambiar, S., Hassan, M., Tannapfel, A., Ruzicka, T., and Hengge, U. R. (2006). Epigenetic silencing of the PTEN gene in melanoma. Cancer Res *66*, 6546-6552.
Nishigaki, M., Aoyagi, K., Danjoh, I., Fukaya, M., Yanagihara, K., Sakamoto, H., Yoshida, T., and Sasaki, H. (2005). Discovery of aberrant expression of R-RAS by cancer-linked DNA hypomethylation in gastric cancer using microarrays. Cancer Res *65*, 2115-2124.
Pawlowski, A., Haberman, H. F., and Menon, I. A. (1980). Skin melanoma induced by 7,12-dimethylbenzanthracene in albino guinea pigs and its similarities to skin melanoma of humans. Cancer Res *40*, 3652-3660.
Pinner, S., Jordan, P., Sharrock, K., Bazley, L., Collinson, L., Marais, R., Bonvin, E., Goding, C., and Sahai, E. (2009). Intravital imaging reveals transient changes in pigment production and Brn2 expression during metastatic melanoma dissemination. Cancer Res *69*, 7969-7977.
Pontiggia, L., Biedermann, T., Meuli, M., Widmer, D., Bottcher-Haberzeth, S., Schiestl, C., Schneider, J., Braziulis, E., Montano, I., Meuli-Simmen, C., and Reichmann, E. (2008). Markers to Evaluate the Quality and Self-Renewing Potential of Engineered Human Skin Substitutes In Vitro and after Transplantation. J Invest Dermatol.
Postovit, L. M., Margaryan, N. V., Seftor, E. A., Kirschmann, D. A., Lipavsky, A., Wheaton, W. W., Abbott, D. E., Seftor, R. E., and Hendrix, M. J. (2008). Human embryonic stem cell microenvironment suppresses the tumorigenic phenotype of aggressive cancer cells. Proc Natl Acad Sci U S A *105*, 4329-4334.
Robert, C., Thomas, L., Bondarenko, I., O'Day, S., M, D. J., Garbe, C., Lebbe, C., Baurain, J. F., Testori, A., Grob, J. J*., et al.* (2011). Ipilimumab plus dacarbazine for previously untreated metastatic melanoma. N Engl J Med *364*, 2517-2526.
Roesch, A., Fukunaga-Kalabis, M., Schmidt, E. C., Zabierowski, S. E., Brafford, P. A., Vultur, A., Basu, D., Gimotty, P., Vogt, T., and Herlyn, M. (2010). A temporarily distinct subpopulation of slow-cycling melanoma cells is required for continuous tumor growth. Cell *141*, 583-594.
Saunders, R. (1671). Physiognomie and Chiromancie, Metoposcopie,

The Symmetrical Proportions and signal Moles of the Body. In, (Printed by H Brugie for Nathaniel Brook, at the sign of the
Angel in Cornhill).
Shahrzad, S., Bertrand, K., Minhas, K., and Coomber, B. L. (2007). Induction of DNA hypomethylation by tumor hypoxia. Epigenetics *2*, 119-125.
Sigalotti, L., Coral, S., Nardi, G., Spessotto, A., Cortini, E., Cattarossi, I., Colizzi, F., Altomonte, M., and Maio, M. (2002a). Promoter methylation controls the expression of MAGE2, 3 and 4 genes in human cutaneous melanoma. J Immunother *25*, 16-26.
Sigalotti, L., Coral, S., Nardi, G., Spessotto, A., Cortini, E., Cattarossi, I., Colizzi, F., Altomonte, M., and Maio, M. (2002b). Promoter methylation controls the expression of MAGE2, 3 and 4 genes in human cutaneous melanoma. J Immunother *25*, 16-26.
Spugnardi, M., Tommasi, S., Dammann, R., Pfeifer, G. P., and Hoon, D. S. (2003). Epigenetic inactivation of RAS association domain family protein 1 (RASSF1A) in malignant cutaneous melanoma. Cancer Res *63*, 1639-1643.
Steingrímsson, E., Copeland, N. G., and Jenkins, N. A. (2004). Melanocytes and the microphthalmia transcription factor network. Annu Rev Genet *38*, 365-411.
Urteaga, O., and Pack, G. T. (1966). On the antiquity of melanoma. Cancer *19*, 607-610.
Vance, K. W., and Goding, C. R. (2004). The transcription network regulating melanocyte development and melanoma. Pigment Cell Res *17*, 318-325.
Widmer, D. S., Cheng, P. F., Eichhoff, O. M., Belloni, B. C., Zipser, M. C., Schlegel, N. C., Javelaud, D., Mauviel, A., Dummer, R., and Hoek, K. S. (2012). Systematic classification of melanoma cells by phenotype-specific gene expression mapping. Pigment Cell Melanoma Res.
Worm, J., Christensen, C., Gronbaek, K., Tulchinsky, E., and Guldberg, P. (2004). Genetic and epigenetic alterations of the APC gene in malignant melanoma. Oncogene *23*, 5215-5226.
Zaidi, M. R., Day, C. P., and Merlino, G. (2008). From UVs to metastases: modeling melanoma initiation and progression in the mouse. J Invest Dermatol *128*, 2381-2391.
Zipser, M. C., Eichhoff, O. M., Widmer, D. S., Schlegel, N. C., Schoenewolf, N. L., Stuart, D., Liu, W., Gardner, H., Smith, P. D., Nuciforo, P.*, et al.* (2011). A proliferative melanoma cell phenotype is responsive to RAF/MEK inhibition independent of BRAF mutation status. Pigment Cell Melanoma Res *24*, 326-333.

7. List of Abbreviations

°C	Degree centigrade
ABCB	ATP-binding cassette
ADAM12	ADAM metallopeptidase domain 12
AKT	Protein kinase B
ALM	Acral lentiginous melanoma
ANGPT2	Angiopoietin 2
ANGPTL4	Angiopoietin-like 4
ANOVA	Analysis of variance
ARAF	V-raf murine sarcoma 3611 viral oncogene homolog
aRNA	Amplified ribonucleic acid
ARNT	Aryl hydrocarbon receptor nuclear translocator
AXL	AXL receptor tyrosine kinase
B2M	Beta-2-microglobulin
BHLH	Basic helix-loop-helix
BIRC3	Baculoviral IAP repeat containing 3
BMP	Bone morphogenic protein
Bp	Base pair
BRAF	V-raf murine sarcoma viral oncogene homolog B1
BSA	Bovine serum albumin
CA9	Carbonic anhydrase IX
CAPN3	Calpain 3
CDH1	Epithelial-cadherin
CDH2	Neuronal-cadherin
CDKN2A	Cyclin-dependent kinase inhibitor 2A
CDKN2B	Cyclin-dependent kinase inhibitor 2B
cDNA	Complementary deoxyribonucleic acid
CNS	Central nervous system
COL13A1	Collagen, type XIII, alpha 1
CRAF	V-raf-1 murine leukemia viral oncogene homolog 1
CRIM1	cysteine rich trans-membrane BMP regulator 1
CSC	Cancer stem cell
CTGF	Connective tissue growth factor
CTLA4	cytotoxic T-lymphocyte-associated protein 4
DAPK1	Death associated protein kinase 1
DKK1	Dickkopf 1 homolog
DMEM	Dulbecco's modified eagle medium
DMOG	Dimethyloxalylglycine
DNA	Deoxyribonucleic acid
dNTP	Deoxyribonucleotide triphosphate
DMSO	Dimethylsulfoxid
DNMT	DNA methyltransferase
DSP	Desmoplakin
DTIC	Dacarbazine
ECL	Electrochemiluminescence
ECM	Extracellular matrix
EDTA	Ethylenediamine tetraacetic acid
EGF	Epidermal growth factor
ELISA	Enzyme-linked immunosorbent assay
EMT	Epithelial to mesenchymal transition
ER	Estrogen receptor
ERK	Extracellular signal-regulated kinase
FBS	Fetal bovine serum
FC	Fold change
FDA	Food and Drug Administration
FDR	False discovery rate
FGF	Fibroblast growth factor
FIH	Factor inhibiting HIF
FLNB	Filamin B, beta

FN1	Fibronectin 1
g	Relative centrifugal force
GALNT3	Polypeptide N-acetylgalactosaminyltransferase 3
GAPDH	Glyceraldehyde-3-phospate dehydrogenase
GEO	Gene Expression Omnibus
GFP	Green fluorescent protein
GNA11	Guanine nucleotide binding protein, alpha 11
GNAQ	Guanine nucleotide binding protein, q polypeptide
GPM6B	Glycoprotein M6B
GSEA	Gene set enrichment analysis
H	Hour
HDAC	Histone deacetylase
HEPES	4-(2-hydroxyethyl)-1-piperazineethanesulfonic acid
HGF	Hepatocyte growth factor
HIF	Hypoxia inducible factor
HOPP	Heuristic online phenotype prediction
HRAS	V-Ha-ras Harvey rat sarcoma viral oncogene homolog
HRE	Hypoxia responsive element
HRP	Horseradish peroxidase
HS3ST3A1	Heparan sulfate 3-O-sulfotransferase 3A1
IGF	Insulin growth factor
IgG	Immunoglobulin G
IL	interleukin
IPAS	Hypoxia inducible factor 3A
IRF4	Interferon regulatory factor 4
ITGA3	Integrin, alpha 3
JUP	Junction plakoglobin
KCNMA1	Potassium large conductance calcium-activated channel, subfamily M, alpha member 1
kDA	Kilodalton
KIT	V-kit Hardy-Zuckerman 4 feline sarcoma viral oncogene homolog
KRAS	V-Ki-ras2 Kirsten rat sarcoma viral oncogene homolog
LEF1	Lymphoid enhancer-binding factor 1
LM	Lentigo maligna
LMM	Lentigo maligna melanoma
LOX	Lysyl oxidase
LOXL2	Lysyl oxidase like 2
MAPK	Mitogen activated-protein kinase
MEK	Mitogen activated protein kinase kinase
MITF	Microphthalmia-associated transcription factor
Min	Minute
ml	Mililiter
mM	Milimolar
mm	Millimeter
MMP	Matrix metalloproteinase
MPSE	Melanoma phenotype specific expression
MTT	(3-(4,5-Dimethylthiazol-2-yl)-2,5-diphenyltetrazolium bromide
MYO1D	Myosin 1D
ng	Nanogram
nm	Nanometer
nM	Nanomolar
NMM	Nodular malignant melanoma
NRAS	neuroblastoma RAS viral oncogene homolog
P53	Tumor protein 53
PBS	Phosphate-buffered saline
PDGF	Platelet-derived growth factor
PHD	Prolyl hydroxylase
PI3K	Phosphatidylinositide 3-kinase
PKC	Protein kinase C
PPAR	Peroxisome proliferators-activated receptor
PPIA	Peptidylpropyl isomerase A

PTEN	Phosphatase and tensin homolog
qRT-PCR	Quantitative reverse transcription-polymerase chain reaction
R	Correlation coefficient
RAF	Rat fibrosarcoma
RAS	Rat sarcoma
RNA	Ribonucleic acid
ROS	Reactive oxygen species
RPMI	Roswell Park Memorial Institute
RPL28	Ribosomal protein L28
RPM	Revolutions per minute
RPS13	Ribosomal protein S13
RT	Room temperature
RTK	Receptor tyrosine kinase
S	Second
SCC	Squamous cell carcinoma
SDS	Sodium dodecyl sulfate
SERPINE1	serpin peptidase inhibitor, clade E, member 1
SLC2A1	Glucose transporter type 1
siRNA	Small interfering RNA
SNAIL1	Snail homolog 1
SNAIL2	Snail homolog 2
SPAG4	Sperm associated antigen 4
SRC	V-src sarcoma viral oncogene homolog
SSM	Superficial spreading melanoma
STAT3	Signal transducer and activator of transcription 3
TAE	Tris-acetate-EDTA
TAM	Tumor associated macrophages
TBE	Tris-borate-EDTA
TBS	Tris-buffered saline
TBST	Tris-buffered saline with Tween
TCF	T-cell factor
TF	Transcription factor
TGF-β	Transforming growth factor beta
TNFRSF14	Tumor necrosis factor receptor superfamily, member 14
TUBB	Tubulin, beta class 1
TWIST1	Twist homolog 1
TYR	Tyrosinase
µl	Microliter
µm	Micrometer
µM	Micromolar
UPAR	Plasmin activator, urokinase receptor (PLAUR)
UV	Ultraviolet
V	Volt
VEGF	Vascular endothelial growth factor
VHL	Von Hippel-Lindau tumor suppressor, E3 ubiquitin protein ligase
VIM	Vimentin
W	Watt
Wnt	Wingless-type MMTV integration site family
WT	Wildtype
ZEB1	Zinc finger E-box binding homeobox 1
ZEB2	Zinc finger E-box binding homeobox 2

8. Acknowledgements

I would like to thank everybody who helped me and supported me on the way to my doctoral thesis. Especially I would like to thank:

Prof. Sabine Werner for the opportunity to perform my research under her supervision and to participate in the labseminars of her group where I got a lot of input and suggestions for my research.

Prof. Reinhard Dummer for having me in his research group and for giving me this interesting project. The strong connection of the basic research to the clinics in this laboratory was motivating and challenging at the same time. I also would like to thank Reinhard for the opportunity to visit international conferences where I met many other researchers and collaborators.

Prof. Michael Detmar for being part of my committee and his input and supervision.

Dr. Keith Hoek, who supported me as my boss and friend for many years. Thank you for introducing me into the digital world of melanoma research.

Dr. Mitchell Levesque, who helped me a lot during the last part of my time as a PhD-student. I hope that we can continue to work together on his exciting ideas.

Dr. Ossia Eichhoff for being a great teacher and colleague but also friend over many years.

All my former and current colleagues in the dermatology for the great working atmosphere, especially the F14-crew: Antonia Fettelschoss, Phil Cheng, Sandra Freiberger, Deepa Mohanan, Dr. Marieke Raaijmakers, Franziska Zabel, Niki Kobert.

All the PhD students and postdocs of other labs who became my friends, especially: Sabine Dütsch, Michèle Telorack, Franziska Lieder and Frank Rolfs.

Special thanks also to Micheal Walser for his continuous support and friendship since the day we started to study biology ten years ago.

The Cancer Biology PhD program for providing an excellent research environment and for the opportunity to exchange ideas and start collaborations with other PhD-students of the program.

Thomas Biedermann for the countless discussions and collaborations in interesting projects. I hope we will continue to work together on exciting projects in the future.

Finally it is very important to me to thank my friends and family, especially my parents for all the support I received from them.

9. Curriculum Vitae

Daniel Widmer

Date of birth: 26.02.1982
Hometown: Gränichen AG (CH)
Marital state: single
Nationality: Swiss
E-mail: daniel.widmer@usz.ch
Home phone: +41 79 354 23 33
Home address: Verena-Conzett-Strasse 22, CH-8004 Zürich, Switzerland

Education

Since March 2008: **Ph.D. student; ETH Zürich**, Life Science Zürich Graduate School, Cancer Network Zürich, Department of Dermatology University Hospital of Zürich in the research group of Prof. Reinhard Dummer.
PhD thesis: The role of hypoxia in melanoma phenotype switching.

2005 – 2007 **Master of Science UZH in Human biology (medical biology)**, tissue biology research unit, University Children's Hospital Zurich.
Master's Thesis: "Developing a transplantable dermo-epidermal substitute and testing markers to monitor epidermal stemness, differentiation and homeostasis".

2002 – 2005 **Bachelor of Science in Biology, University of Zurich**

1998 – 2002 **Matura Typus E** (economy), Kantonsschule Wohlen AG, Switzerland

Publications

Widmer, D.S., Hoek, K. S., Cheng, P. F., Eichhoff, O. M., Biedermann, T., Raijmaakers, M., Dummer, R. and Levesque, M.P.
Hypoxia contributes to melanoma heterogeneity by triggering phenotype switching.
(In preparation)

Widmer, D. S., Cheng, P. F., Eichhoff, O. M., Belloni, B. C., Zipser, M. C., Schlegel, N. C., Javelaud, D., Mauviel, A., Dummer, R. and Hoek, K. S.
Systematic classification of melanoma cells by phenotype-specific gene expression mapping.
Pigment Cell & Melanoma Research. doi: 10.1111/j.1755-148X.2012.00986.x (2012)

Kiowski, G*., Biedermann, T*., Widmer, D. S., Civenni, G., Burger, C., Dummer, R., Sommer, L. and Reichmann, E.
Engineering Melanoma Progression in a Humanized Environment in Vivo
Journal of Investigative Dermatology. doi: 10.1038/jid.2011.275 (2011)

Eichhoff, O.M., Weeraratna, A., Zipser, M.C., Denat, L., Widmer, D.S., Xu, M., Kriegl, L., Kirchner, T., Larue, L., Dummer, R., Hoek, K.S.
Differential LEF1 and TCF4 expression is involved in melanoma cell phenotype switching.
Pigment Cell & Melanoma Research. doi: 10.1111/j.1755-148X.2011.00871.x. (2011)

Zipser, M.C*., Eichhoff*, O.M., Widmer, D.S., Schlegel, N.C., Schoenewolf, N.L., Stuart, D., Liu, W., Gardner, H., Smith, P.D., Nuciforo, P., Dummer, R., Hoek, K.S.
A proliferative melanoma cell phenotype is responsive to RAF/MEK inhibition independent of BRAF mutation status.
Pigment Cell & Melanoma Research. doi: 10.1111/j.1755-148X.2010.00823.x (2011)

Pontiggia, L., Biedermann, T., Meuli, M., Widmer, D.S., Böttcher-Haberzeth, S., Schiestl, C., Schneider, J., Braziulis, E., Montano, I., Meuli-Simmen, C. and Reichmann, E.
Markers to evaluate the quality and self-renewing potential of engineered human skin substitutes in vitro and after transplantation.
Journal of Investigative Dermatology. doi:10.1038/jid.2008.254 (2009)

Schneider, J., Biedermann, T., Widmer, D.S., Montano, I., Meuli, M., Reichmann, E. and Schiestl, C.
Matriderm versus Integra: An experimental Comparative Study
Burns. doi.org/10.1016/j.burns.2008.07.018, (2009)

Hoek, K.S., Eichhoff, O.M., Widmer, D.S. and Dummer, R.
Stemming the flood
Pigment Cell & Melanoma Research. doi: 10.1111/j.1755-148X.2008.00539.x. (2009)

Hoek, K.S., Schlegel, N.C., Eichhoff, O.M., Widmer, D.S., Praetorius, C., Einarsson, S.O., Valgeirsdottir, S., Bergsteinsdottir, K., Schepsky, A., Dummer, R., Steingrimsson, E.
Novel MITF targets identified using a two-step DNA microarray strategy.
Pigment Cell & Melanoma Research. doi: 10.1111/j.1755-148X.2008.00505. (2008)

Invited talks

3rd Melanoma Workshop IFOM-IEO Campus Milan, Italy 2011
Widmer, D.S., Eichhoff, O.M., Zipser, M.C., Cheng, P.F., Dummer, R. and Hoek, K.S.
The role of hypoxia in melanoma phenotype switching

XXIst International Pigment Cell Conference in Bordeaux, France 2011
Widmer, D.S., Eichhoff, O.M., Zipser, M.C., Cheng, P.F., Dummer, R. and Hoek, K.S.
The role of hypoxia in melanoma phenotype switching

15th Meeting of the European Society for Pigment Cell Research in Münster, Germany 2009
The Phenotype Switching Model for Melanoma Progression
Widmer, D.S., Eichhoff, O.M., Zipser, Dummer, R. and Hoek, K.S.

Cancer Biology PhD Program retreat Wilderswil, Switzerland
Widmer, D.S., Eichhoff, O.M., Zipser, M.C., Cheng, P.F., Dummer, R. and Hoek, K.S.
The role of hypoxia in melanoma phenotype switching

Presented posters

16th Meeting of the European Society for Pigment Cell Research in Hinxton, Cambridge, UK 2010
Widmer, D.S., Eichhoff, O.M., Zipser, M.C., Cheng, P.F., Dummer, R. and Hoek, K.S.
The role of hypoxia in melanoma phenotype switching
(Funded by a travel grant of the European Society for Pigment Cell Research)

Society for Melanoma Research in Sydney, Australia 2010
Widmer, D.S., Eichhoff, O.M., Zipser, M.C., Cheng, P.F., Dummer, R. and Hoek, K.S.
The role of hypoxia in melanoma phenotype switching
(Funded by a travel grant of the Cancer Biology Ph.D. program)

World Congress on Melanoma in Vienna, Austria 2009
Widmer, D.S., Eichhoff, O.M., Dummer, R. and Hoek, K.S.
The role of hypoxia in melanoma cell phenotype switching

Society for Melanoma Research in Boston, USA 2009
Widmer, D.S., Eichhoff, O.M., Zipser, Dummer, R. and Hoek, K.S.
The role of hypoxia in melanoma cell phenotype switching

Brupbacher Symposium in Zürich, Switzerland 2011
Widmer, D.S., Eichhoff, O.M., Zipser, M.C., Cheng, P.F., Dummer, R. and Hoek, K.S.
The role of hypoxia in melanoma phenotype switching

SGDV Congress in Zürich, Switzerland 2010
Widmer, D.S., Eichhoff, O.M., Zipser, Dummer, R. and Hoek, K.S.
The role of hypoxia in melanoma phenotype switching

Cancer Biology PhD Program retreat Château de Bossey, Switzerland
Widmer, D.S., Eichhoff, O.M., Zipser, Dummer, R. and Hoek, K.S.
The role of hypoxia in melanoma cell phenotype switching

Cancer Biology PhD Program retreat Interlaken, Switzerland
Widmer, D.S., Cheng, P.F., Eichhoff, O.M., Belloni, B.C., Zipser, M.C., Schlegel, N.C., Javelaud, D., Mauviel, L., Dummer, R. and Hoek, K.S.
Systematic classification of melanoma cells by phenotype-specific gene expression mapping.